

A KNOWLEDGE-BASED APPROACH TO MAPPING ROADS FROM AERIAL IMAGERY USING A GIS DATABASE

by

Ali Forghani, B.Eng (UM, Iran), M.Eng (UNSW, Australia).

A thesis submitted in partial fulfilment of the requirements for the degree of

Doctor of Philosophy

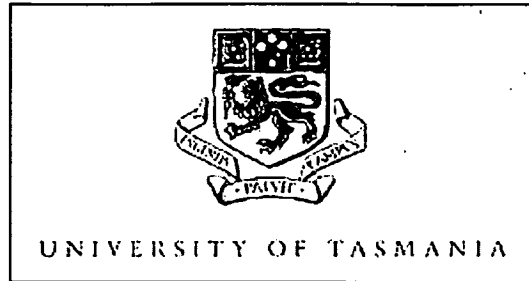
in

Surveying and Spatial Information Science

Faculty of Engineering & Surveying

The University of Tasmania

November 1997

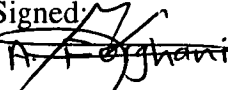


Surveying & Spatial Information Science
Faculty of Engineering & Surveying
University of Tasmania
GPO Box 252-76
Hobart Tasmania 7001
Australia
Fax: +61-3-62240282
Telephone: +61-3-62262134

DECLARATION

Except as stated herein, this thesis does not contain any material which has been accepted for the award of any other degree or diploma in any university nor, to the best of my knowledge and belief, does it contain any copy or paraphrase of material previously published or written by another person, except where due reference is made in the text of this thesis.

I *Ali Forghani*, hereby given consent that my thesis *A Knowledge-Based Approach to Mapping Roads from Aerial Imagery Using a GIS Database* to be made available for loan at the discretion of the Head of Department, and the University of Tasmania shall be authorised to allow a copy of all or part of the thesis for the purpose of study or research.

Signed: 

Date: 18/6/98

Ali Forghani

Surveying & Spatial Information Science

ABSTRACT

Conventional image classification approaches may be inadequate for extraction of complex and spectrally heterogeneous land use classes from remotely sensed imagery. The integration of spatial data with remotely sensed data has the potential to improve significantly the reliability of feature classification. Thus it is informative to use contextual and textural information in the classification process.

This thesis describes a methodology developed to integrate GIS and aerial imagery in a manner that allows it to be used in a knowledge-based analysis system. Using a trial site and aerial photography, the methodology was implemented and tests indicate the technique works well in mapping of roads when roads pass through a rural area where the contrast is high, but fails in urban areas where the roads are confused with man-made structures.

Also, a supervised multispectral image classification of the trial site using colour aerial photography was carried out to compare the performance of a supervised multispectral image analysis with the decision tree analysis to map out roads over the trial site. A classification accuracy assessment shows that the overall classification accuracy was marginally lower than the decision tree analysis.

The GIS data used in the knowledge-base included a DTM and land use covers. For this research, part of the data was already available in digital format. In practice, it may be that a DTM and land use classification would need to be created from aerial photography or satellite imagery. It is in this context that the methodology developed here is most likely to improve significantly attribute-based classification.

The GIS database included geometrically rectified aerial photography, roads, land use, drainage pattern, field and vegetation boundaries, DTM, and edge detection data. A program was developed for semi-automatic linear feature detection using different edge detectors, in which the process is followed by morphological operations. The extracted edges (lines) were used as a GIS layer in a later step of the methodology. Grid raster-based processing was undertaken to build a multi-source database in the GIS to be used for knowledge-based analysis.

The multi-layer database was interfaced with decision tree software for creation of a classification tree. The independent data set comprised six variables, representing the contextual, textural, and geometrical characteristics of the knowledge-based data. In the process of decision tree analysis, the input data was recursively partitioned into mutually clustered, exhaustive subsets which define the best response variable. The resulting classification tree was used to generate generic rules for implementation of an expert system.

The developed expert system was used to map out the spatial distribution of the grid data to show areas with roads (presence) and their background (absence). The output of this model is encouraging when applied over homogeneous rural scenes, but there are difficulties over heterogeneous urban areas. The results show that a framework of roads in a rural site mapped by this knowledge-based technique closely concurred with visual interpretation.

This research devised a general approach to solving problems of road identification. This approach can serve as a model for practitioners who are trying to do practical work in this field. By generating a hybrid system which locates many different databases and integrates many different sources of knowledge in attempting to identify a specific (man-made) geographic feature, and by utilising current artificial intelligence (AI) techniques to perform the classification, this research provides an early example of the techniques which will be in more general use in the areas of GIS and remote sensing in the future.

The methodology developed here is costly and data-intensive. Since the technique investigated in this research requires a large number of data sets to be built, construction of the data is relatively expensive over large areas. The initial costs involved in configuring a knowledge-base, such as the methodology developed in this study, are high, and this may not be justifiable in a production environment.

For my family; Mum & Dad, and especially Farzaneh.

ACKNOWLEDGMENTS

This thesis is the result of the efforts, guidance, and patience of many people over the past three years. Although it would be impossible to acknowledge all who have supported this research, I would like to express my special gratitude to the following individuals:

My supervisors: Dr Anthony Sprent who provided constant support, constructive and valuable advice throughout this research, and Dr Jon Osborn for his close guidance, and encouragement throughout the long period of experimentation and analysis in the course of the research.

Associate Professor Richard Coleman, Dr Peter Zwart, and Dr Michael Roach contributed to the early stages of this research.

I should also express my appreciation to all staff and postgraduate students in the Department, especially Mr Robert Anders, Mr John Catell, Mrs Margaret Stafford, Mr Antonius Wijanarto, Mr Ngoc Lau Nguyen, and Mr Matthew King who contributed in their own way to my student life in the Department.

I would also like to thank Mr Phil Collier at the Department of Computer Science & Electrical Engineering, University of Tasmania; Mr Ross Lincolne at the Space Image Unit of the Central Science Laboratory, University of Tasmania; and Mr Lee Belbin at Antarctic Data Centre Australian Antarctic Division, Tasmania, who provided support and advice.

The data provided by the Land Information Bureau of Tasmania for this research is gratefully appreciated.

In addition, the financial support of the Ministry of Culture & Higher Education of the I. R. of Iran is gratefully acknowledged.

Last, but definitely not least, I would like to extend my deep appreciation to my parents, brothers, sister, and my family: Farzaneh my wife, Pedram and Payam my beautiful children, relatives and friends, because this work owes much to their love,

patience, support and encouragement. Words are insufficient to express my gratitude to Farzaneh for her unfailing moral support and for the sacrifices this research required of her!

TABLE OF CONTENTS

DECLARATION	ii
ABSTRACT	iii
ACKNOWLEDGMENTS	iv
TABLE OF CONTENTS.....	viii
LIST OF FIGURES	xiii
LIST OF TABLES.....	xvi
ACRONYMS.....	xvii

CHAPTER 1

INTRODUCTION	1
1.1 General	1
1.2 Prior Work	5
1.3 Hypothesis and Proposed Approach	6
1.3.1 Stages of Research	8
1.4 Contribution of the Research.....	8
1.5 Organisational Outline of the Dissertation	9

CHAPTER 2

BACKGROUND: CLASSIFICATION AND FEATURE DETECTION.....

2.1 Image Analysis.....	11
2.1.1 Texture.....	15
2.1.2 Context	15
2.2 Machine Learning in Remote Sensing and GIS.....	16
2.3 Approaches in Linear Feature Detection	19
2.4 Expert Systems in Remote Sensing and GIS	22
2.5 Summary and Remarks.....	25

CHAPTER 3

DIGITAL IMAGE AND GIS DATA PROCESSING

3.1 Image Rectification and Registration	26
3.1.1 Geometric transformations	27
3.1.2 Orthophotography	31
3.1.3 Affine Transformation and Rubber Sheeting	33

3.2 Image Enhancement	35
3.2.1 Edge Detection.....	35
3.2.2 Thresholding	39
3.2.3 Mathematical Morphology	40
3.4 Integration of GIS and Remote Sensing	42
3.4.1 Data Acquisition for GIS	42
3.4.2 Data Structure for GIS	43
3.4.3 Data Conversion.....	46
3.4.4 Error Sources from Integration of RS and GIS Data	51
3.5 Summary	53
 CHAPTER 4	 54
BACKGROUND: EXPERT SYSTEMS CONSTRUCTION AND KNOWLEDGE-BASED INDUCTION	 54
4.1 Artificial Intelligence and Expert Systems Implementation	54
4.1.1 Definition and Background.....	54
4.1.2 Components of an Expert System	56
4.1.2.1 Knowledge Acquisition	56
4.1.2.2 Knowledge Representation	58
4.1.2.3 Inference Engine.....	59
4.2 Extracting and Representing Knowledge with Decision Trees	61
4.2.1 Background.....	61
4.2.2 Inductive Learning.....	62
4.2.3 Decision Trees.....	62
4.2.3.1 Induction of Decision Trees Algorithms.....	64
4.2.3.2 Decision Tree-Pruning and Accuracy of the Classification Tree	68
4.3 Summary	71
 CHAPTER 5	 73
STUDY AREA AND DATA SETS	73
5.1 Study Area.....	73
5.2 Available Data.....	88
5.2.3 Base Maps.....	92
5.3 Computer Facilities	93
5.4 Summary	96

CHAPTER 6	97
IMAGE REGISTRATION AND LINEAR FEATURE DETECTION	97
6.1 Geocoding of Images	97
6.1.1 Polynomial Transformations	98
(i) Technique Adopted	98
(ii) Experimental Results	100
6.1.2 Orthophotography	101
(a) Technique Adopted	103
(b) Examining the Corrections	111
6.1.3 Affine Transformation and Rubber Sheetting	111
6.1.4 Discussion	113
6.2 Remarks for Image Registration	114
6.3 Linear Feature Detection and Analysis	115
6.3.1 Pre-Processing of Images	117
6.3.2 Image Segmentation	119
6.3.3 Analysis	122
6.3.4 Discussion	136
6.4 Remarks for Image Segmentation	141
 CHAPTER 7	142
SPATIAL DATA PROCESSING: CONSTRUCTION OF A DATABASE FOR A KNOWLEDGE BASED ENVIRONMENT	142
7.1 Spatial Data Construction	142
7.1.1 Data Entry	144
7.1.2 Database Development	144
7.1.2.1 Editing Road and Stream Coverages	145
7.1.2.2 Land Use Delineation	147
7.1.2.3 Rasterization and Resampling	149
7.1.2.4 Creation of Surface Data	149
7.1.2.5 Processing and Manipulating Raster Grid Data	150
7.1.2.6 Conversion of Raster Grid Data to ASCII Files	150
7.2 Summary	152
 CHAPTER 8	153
EXPERT SYSTEMS DEVELOPMENT: DECISION TREES	153
8.1 Introduction	153
8.2 Developing a Knowledge-Based System	154
8.2.1 Basic methodology	154
1. Spatial Attributes Data (Data Layers)	156

2. Rule Induction	161
3. Inferencing	161
8.2.2 Input Data for Decision Tree Analysis.....	162
8.2.3 Decision Tree Environment and Interfacing a GIS Database.....	163
8.2.4 Generation of Decision Tree: Tree Growing and Analysing.....	163
8.2.5 Expert System Construction: Storage of Output of the Induction Rules.....	169
8.2.6 Analysis of Results	173
8.3 Discussion	180
8.4 Summary	183
 CHAPTER 9	 184
MULTISPECTRAL IMAGE CLASSIFICATION.....	184
9.1 Introduction.....	184
9.2 Supervised Classification Method.....	185
9.2.1 Background.....	185
9.2.2 Image Classification.....	185
9.3 Discussion	187
9.4 Concluding Remarks	189
 CHAPTER 10	 190
SUMMARY.....	190
10.1 Background	190
10.2 Methodology	192
10.3 Results.....	196
10.4 Concluding Remarks	198
 REFERENCES	 199

APPENDIX.....	223
APPENDIX A: DATA SETS INFORMATION.....	224
APPENDIX B: MATLAB CODE FOR PLOTTING THE COMPONENTS OF RELIEF DISPLACEMENT.	225
APPENDIX C: MATLAB CODE FOR BUILDING DATA FOR A KNOWLEDGE-BASED SYSTEM, USING EDGE ENHANCEMENT OPERATORS, EDGE DETECTION FILTERS AND MORPHOLOGICAL OPERATIONS METHODS.	228
APPENDIX D: FORTRAN 77 CODE FOR GENERATING A TABULAR ASCII FILE FROM THE ARC/INFO GRID ASCII FILES.	237
APPENDIX E: MATLAB CODE FOR DEVELOPMENT OF A DECISION TREE PROCESSING EXPERT SYSTEM (DTPES) TO MAP OUT THE SPATIAL DISTRIBUTION OF ROADS AND THEIR BACKGROUND FROM THE GIS DATABASE.....	238
APPENDIX F: CROSS-TABULATION OF THE CLASSIFICATION TREE.....	250
APPENDIX G: GENERATED CLASSIFICATION DECISION TREE.....	299

LIST OF FIGURES

Figure 2.1 Image interpretation techniques classified according to segmentation level....	14
Figure 3.1 Illustrates a rubber sheeting by using links and adjusting position.....	34
Figure 5.1a Topographic map of the study area (approximately 1:25,000).....	74
Figure 5.1b Location of the study area in Hobart (Scale approximately 1:500,000).....	75
Figure 5.2 Aerial photographs of the study area.....	77
Figure 5.3 Native Eucalyptus within the study area.....	79
Figure 5.4 Lake in the study area.....	79
Figure 5.5 Land used for pasture in the study area.....	80
Figure 5.6 Golf course in the study area.....	80
Figure 5.7 Beach and ocean nearby the study area.....	81
Figure 5.8 Urban land use enclosed by rural land use.....	82
Figure 5.9 Semi-rural and urban development.....	82
Figure 5.10 Urban development for residential housing.....	83
Figure 5.11 Development of (a) industrial and (b) commercial areas in the study area.....	84
Figure 5.12 Major access road in a rural area.....	85
Figure 5.13 Major access road in a semi-rural area.....	85
Figure 5.14 Major road in an urban area.....	86
Figure 5.15 Local road in an urban area.....	86
Figure 5.16 Asphalt road in a rural area with shadow from overhanging trees.....	87
Figure 6.1 Components of relief displacement.....	99
Figure 6.2 The vectors representing relief displacement for 1982 image plotted.....	99
Figure 6.3 Illustration of differences between the actual terrain and the maximum error in Z coordinates (DEM).....	102
Figure 6.4 Illustrates the DEM of the area as a grey scale image which was produced by applying ARC/INFO TOPOGRID tool.....	103
Figure 6.5 The camera calibration report for the 1982 and 1991 photography.....	105
Figure 6.6 Contour plot of the test area superimposed with streams coverage.....	107
Figure 6.7 Represents generated TIN boundaries of the study area.....	108

Figure 6.8 The geometrically corrected image using the affine transformations and a rubber sheeting.....	112
Figure 6.9 Schematic of interactive linear feature interpretation of test area.....	116
Figure 6.10 Test images; sub-sections of the 1982 image.....	117
Figure 6.11 Application of a median filtering.....	118
Figures 6.12 Represents application of Sobel filter with different threshold over a rural site (a, b, c) and an urban site (d, e, f).....	123
Figure 6.13 Mathematical morphology operations applied to the Sobel filtered data over a rural site (a, b, c) and an urban site (d, e, f).....	124
Figures 6.14 The result of Canny filtering for different threshold values with a filter of 7 by 7 over a rural site (a, b, c) and an urban site (d, e, f).....	126
Figure 6.15 Morphological operation on detected edges from Canny filtering over a rural site (a, b, c) and an urban site (d, e, f).....	127
Figure 6.16 The result of the Deriche filtering approach for different threshold values and $\alpha = 0.5, \alpha = 1, \alpha = 2$, over a rural site (a, b, c).....	130
Figure 6.17 The result of the Deriche filtering approach for different threshold values and $\alpha = 0.5, \alpha = 1, \alpha = 2$, over an urban site (a, b, c).....	131
Figure 6.18 Morphological operations over the produced Deriche filter edges over a rural site (a, b, c) and an urban site (d, e, f).....	132
Figure 6.19 The result of Canny filtering for different threshold values with a filter of 7 by 7.....	134
Figure 6.20 Morphological operation on detected edges from Canny filtering.....	134
Figure 6.21 The result of the Deriche filtering approach for a threshold value of 40% and, $\alpha = 2$	135
Figure 6.22 Morphological operations over the produced Deriche filter edges.....	135
Figure 7.1 Schematic of the data preparation.....	143
Figure 7.2 The study area.....	144
Figure 7.3 Road networks in a line form overlaid on the georeferenced image for a subset of the study area.....	146
Figure 7.4 Road networks in a buffer form overlaid on the georeferenced image for a subset of the study area.....	146

Figure 7.5 Map of land use/cover of the area generated by manual interpretation of the 1982 air photo.....	148
Figure 7.6 A perceptive view of the synthetic surface of the area.....	149
Figure 8.1 Flow diagram of the expert system construction in this study.....	155
Figure 8.2 Part of a 65-rule model shows as a simple decision tree.....	165
Figure 8.3 Illustrates the end node for rule_17.....	170
Figure 8.3; (a) Displays the results from the clustering classifications for Case 1.....	174
Figure 8.3; (b) Represents the road reference map of Case 1 in a grid, and (c) shows the aerial image of Case 1.....	174
Figure 8.4; (a) Displays the results from the clustering classifications for Case 2.....	176
Figure 8.4; (b) Represents the road reference map of Case 2 in a grid, and (c) shows the aerial image of Case 2.....	176
Figure 8.5; (a) Displays the results from the clustering classifications for Case 3.....	177
Figure 8.5; (b) Represents the road reference map of Case 3 in a grid.....	178
Figure 8.5; (c) Shows the aerial image of Case 3.....	178
Figure 9.1 A subset of the colour aerial photograph of the study area.....	184
Figure 9.2 Represents the classified image with 9 classes.	186
Figure 9.3 Final supervised classification after merging of similar classes	187
Figure 1 (Appendix G) Shows a generated classification decision tree using clustering method.....	299

LIST OF TABLES

Table 5.1 Computer facilities information.....	95
Table 6.1 A summary of results of rectification and registration of the aerial images using polynomial transformations.....	100
Table 6.2 Representations of the DEMs and the maximum error in X and Y coordinates due to DEM discrepancies in mm at photo scale.....	102
Table 6.3 Results of registering fiducial marks on the photo coverage.....	106
Table 6.4 Resection results.....	110
Table 6.5 Accuracy evaluation based on coincidence computations between the existing road map and the classified edge detection map for the rural site.....	137
Table 6.6 Accuracy evaluation based on coincidence computations between the existing road map and the classified edge detection map for the urban site.....	138
Table 6.7 A summary of the results of edge detection.....	139
Table 6.8 Accuracy evaluation based on coincidence computations between the existing road map and the classified edge detection map for 1982 imagery.....	139
Table 7.1 Buffer distances and road class.....	147
Table 7.2 Land use/cover classification scheme for visual classification of B/W photography.....	148
Table 7.3 Subset of a sample database for input into KS.....	151
Table 8.1 The seven variables or attributes (layers) existing in the database.....	160
Table 8.2 Sample of GIS data used for Decision Tree Analysis.....	163
Table 8.3 Classification summary statistics.....	179
Table 9.1 Selected signatures from the aerial image.....	186
Table 9.2 Image classification accuracy.....	188
Table 1 (Appendix A) Data sets information.....	224
Table 1 (Appendix B) Components of relief displacement for 1982 imagery.....	226,227

ACRONYMS

AI	Artificial Intelligence
AID	Automatic Interaction Detector
AMG	Australian Map Grid
B/W	Black and White
B/W	Binary
CART	Classification And Regression Trees
CGIS	Canada Geographic Information System
CIR	Colour Infrared
DEM	Digital Elevation Model
DEMs	Digital Elevation Models
DGN	Integraph Design Files
DN	Digital Number
DPI	Dot Per Inche
DTM	Digital Terrain Modelling
DTPES	Decision Tree Processing Expert Systems
ES	Expert Systems
ERI	Environmental Systems Research Institute
GC	Ground Control Point
GCPs	Ground Control Points
GIS	Geographic Information Systems
GPS	Global Positioning Systems
HMSDS	Hybrid Model of Spatial Data Structure
ID3	Interactive Dichotomizer
IFOV	Instantaneous-Field-Of-View
ILFDP	Interactive Linear Feature Detection Program
KS	KnowledgeSEEKER
KB	Knowledge-Based
KBS	Knowledge-Based Systems
KBR	Knowledge-Based Rule

LBS	Learning Base System
LFC	Large Format Camera
m	Metre
MLC	Maximum Likelihood Classifier
mm	Millimeter
MO	Morphological Operations
MSS	Landsat Multispectral Scanner
NDVI	Normalized Difference Vegetation Index
PAN	Panchromatic
PCA	Principle Component Analysis
PPA	Principal Point of Autocollimation
RS	Remote Sensing
RMS	Root Mean Square
T	Threshold
TDIDT	Top-Down Induction of Decision Trees
TIN	Triangular Irregular Network
TM	Landsat Thematic Mapper
XS	Multispectral
α	Filter Size
2D	Two Dimensional
3D	Three Dimensional

Chapter 1

INTRODUCTION

1.1 General

Historically, land use/cover mapping has been undertaken using aerial photography. Urban areas are a heterogeneous and complex environment which occupy less than one percent of exposed land on the earth's surface. These areas represent both natural and artificial human activities and contain both natural and man-made elements. Consequently, urban land use patterns consist of objects with regular and irregular shapes. Use of remote sensing (RS), in the form of aerial photography, in an historical sequence in urban studies, dates back to 1858 when Tournachon (later named "Nadar") used a camera set on a balloon to study parts of the city of Paris. Since World War II increased consideration has been paid to the potential role of aircraft and satellite remotely sensed data in the study of man-made and natural scenes. These studies have produced classification accuracies ranging from 50-98% (eg Coleman, 1992).

Land cover mapping using airphoto interpretation has proven to be rapid, efficient, and economical. There has been considerable effort given to its application in the acquisition of data for resource management and civil engineering applications throughout the world. Despite proven advantages of employing aerial imagery in urban investigation, there are disadvantages in using this imagery. For example, manual interpretation of aerial photography for a large area may be tedious and time-consuming. In addition, the risk of different interpretations by various interpreters is a concern, as well as the infrequency of data acquisition.

Aerial photography has been used for a wide variety of urban and rural studies, and it provides the most effective method for the study of urban expansion and urban growth analysis. The application areas include analysis of urban housing problems (Hathout, 1988), spatial location of waste disposal sites (Mack et al 1995), town planning (Mirsa, 1986), population estimation using 1:12,000 b/w photography (Lo, 1992), detection of residential areas (Oliveria, 1986), updating urban planning maps (Patmios, 1986), and

analysis of urban spatial structure (Hsu and Wu, 1990). Using colour infrared (CIR) imagery (Gong and Chen, 1988) the overall discrimination accuracy for urban expansion is 94.6%.

Mapping of land use and rural to urban conversions are topics of interest to both GIS and remote sensing communities. Specifically, mapping of road networks is a major research area in image and spatial data processing in order to update digital road network files. The problem of keeping road network files up to date is most acute in the urban fringe of major urban areas where development processes are most concentrated.

Medium level image segmentation operators such as edge detectors have been applied widely to extract linear features from remote sensed data (eg Boggess, 1994). The performance of the medium level operators is satisfactory (Forghani, 1997; Forghani et al 1997). The interface of contextual information by means of incorporation of GIS data and human knowledge-base leads to better quantitative accuracy. The interface of GIS and remote sensing data for classification and feature extraction by machine learning¹ methods (ie decision trees and artificial neural networks) and expert systems (ES) is a major area of research in a knowledge-based (KB) integration of image and spatial data. The results obtained from any single analysis can be subjected to error and are imprecise.

Multispectral image classification approaches have been shown to be inadequate for extraction of complex and spectrally heterogeneous land use classes from high resolution remotely sensed imagery (Barnsley and Barr, 1996). However, in spite of the large body of previous research in this area and a number of comparative studies, the choice of algorithms suitable for complex imagery is not clear. The way forward appears to be to use both contextual and textural information in the classification process (eg Johnsson, 1994).

¹ Machine learning is described as the study and modelling of the learning process. It attempts to develop methods that can automatically construct rules (or other forms of knowledge representation) from a set of examples. This field tries to make the knowledge acquisition paths of knowledge-based system development simpler, more productive, more efficient and user-friendly.

Integration of image understanding techniques within a GIS database have been modelled to govern feature extraction problems, eg Gahegan and Flack (1996). Integrating different analyses of feature extraction improves the results, particularly in complex scenes like urban areas. Little interest has been shown concerning feature extraction (ie roads) using non-parametric methods, eg decision trees. Extension of ES has been successfully presented in combining image processing techniques with a GIS data base for extraction of roads (eg Van Cleynenbregel et al 1990).

Decision trees² have been developed both by the statistical community (Hunt, 1962) and artificial intelligence community (Quinlan, 1983, and 1986). The main limitation of these learning systems is that extrapolation is unreliable, but they can provide reasonable interpolation within the learning example (Lees, 1994). In this research the KnowledgeSEEKER (KS) software was used because it is a simple and widely used symbolic algorithm for learning examples. It has been comprehensively examined on a large number of data sets (De Ville, 1990) and is the basis of several commercial rule induction systems. Moreover, KS has been improved with methods for handling numerically-valued features, noisy and incomplete data, and missing information (ANGOSS, 1994).

A technique has been developed to integrate the information obtained from the different sources. To integrate the aerial photographs into a GIS the images, were geometrically corrected using an affine transformation and rubber sheeting. The rectified images were used for identifying linear features by edge detection and mathematical morphology. In the development of the methodology of this research, an Interactive Linear Feature Detection Program (ILFDP) was developed for semi-automatic linear feature detection using different edge detectors, followed by morphological operations (Forghani et al 1997; Forghani and Osborn, 1998b). The extracted edges were used as a GIS layer in a later step of the methodology A knowledge-based data set which locates spatial and spectral attributes was created using ARC/INFO GIS software.

² Decision tree is one method of knowledge extraction in which knowledge is represented as a series of rules which can be used for the construction of expert systems.

Grid raster-based processing was undertaken to construct the multi-source database. After the gridding process, seven principal map features (layers) were created, namely land use/cover, DEM, grey image, roads, field boundaries, streams, and edge detection data. To input the data into KS it was necessary to convert multiple ASCII files using sources such as land use/cover hydrographic maps, aerial imagery, and digital elevation model (DTM) as well as the medium level image segmentation product (ie extracted edges) held in a GIS to be used in a knowledge-based environment to predict distribution of roads using decision trees.

The data file was interfaced with a decision tree environment (KS software) for creation of a classification tree. The independent data set comprised six fields (variables) that attempt to represent contextual, textural, and geometrical characteristics of the knowledge-based data. The integrated multi-source database includes a priori knowledge of geometry of road networks (eg width), edge detection data, intensity (air photo), terrain type (landuse), streams, field and vegetation boundaries, and scene elevation (DEM). In the process of decision tree analysis, the input data was recessively partitioned into mutually exclusive exhaustive subsets which defined the best response variable. The resulting classification tree was used to generate generic rules for implementation of an expert system called "Decision Tree Processing Expert Systems" (DTPES). The knowledge-based system thus developed consisted of three major components: a database which stores image and spatial data, rule induction which uses decision trees classification and user interface, and an inference engine. In the development of this expert system a forward-chaining process was considered in order to evaluate all rules for a given pixel for mapping spatial distribution of the grid data to show areas with roads and their background. The computation time linearly increases as the number of grid cells increase. This rule-based system was applied to perform road mapping from aerial imagery over an urban/rural scene. After classification, the system computed the overall accuracy of the mapped roads based on the reference road map to maintain consistency and reliability of the performance of the decision trees in feature recognition.

1.2 Prior Work

In the last decade there has been a rapid increase in the development and application of the machine learning approach. Civil engineers, mapping specialists, computer scientists, natural resource managers and environmental science experts are involved, with increased use of machine learning for data analysis, modelling and mapping (Moore et al 1991; Aspinall, 1991 and 1992; Skidmore et al 1996a) employing GIS and remote sensing imagery.

The application of decision trees in the use of remotely sensed images and GIS data for environmental applications has been widely discussed. Key references are, Walker and Moore (1988) for mapping of wildlife distributions, Reddy and Bonham-Carter (1991) for mapping of spatial distribution of mineral occurrence, Lees and Ritman (1991), Moore et al (1991) for vegetation mapping, and recently Skidmore et al (1996b) for classification of kangaroo habitat distribution.

Knowledge-based approaches to road detection and feature extraction are discussed, for example by Van Cleynenbreugel et al (1990), Bogges (1993, and 1994), Geman and Jedynak (1996), and Gaheagan and Flack (1996). It was found that detection of roads over built-up areas was confused with other man-made structures, but the approach was shown to work well for extracting major roads over homogeneous areas.

1.3 Hypothesis and Proposed Approach

This thesis describes a methodology developed to integrate GIS data and aerial imagery in a manner that allows it to be used in a knowledge-based analysis system for detecting and mapping linear topographic objects, particularly road networks. The research uses photometry (ie spectral) or textural³, spatial and contextual information (contextual-based⁴ attributes) within a knowledge-based model using decision trees.

Geometric, spectral, and spatial characteristics are applied to distinguish roads from other linear features (eg rivers, field boundaries). The above information is located in a multi-source spatial dataset (layers) which includes land use/cover, DEM, grey level image, roads, field and vegetation boundaries, streams, and edge detection data. Incorporation of this dataset into a decision tree analysis system was attempted.

This research devised a general approach to solving problems of road identification. This approach can serve as a model for practitioners who are attempting to do practical work in this field. By creating a hybrid system which includes many different databases and combines many different sources of knowledge in trying to identify a specific (man-made) geographic feature, and by utilising current artificial intelligence (AI) techniques to perform the classification, this research provides an early example of the techniques which will be in more general use in the areas of GIS and remote sensing in the future.

The methodology was implemented for a trial site that contained a mix of urban and rural land uses. The study site is located on the southern fringe of Hobart, Tasmania, Australia. The trial site has a number of settlement types including suburban fringes, farms, residential, and commercial areas.

³ Textural attributes in this research include edge detection data and intensity.

⁴ Contextual information for undertaken study refers to spatial attributes such as land use, DEM, drainage patterns, field and vegetation boundaries.

Experiments show the technique works well when mapping roads within rural areas where the contrast is high, but fails in urban areas where the roads are confused with man-made structures.

In addition, a supervised multispectral image classification of the trial site using colour aerial photography was undertaken to compare the performance of a supervised multispectral image analysis with the decision tree analysis to map out roads over the trial site. A classification accuracy assessment shows that the overall classification accuracy was marginally lower than the decision tree analysis.

During the development of the methodology, several issues have been considered. These are:

- Defining the dataset.

What are the most appropriate spatial data layers to use in the dataset?

- Building the spatial dataset:

How can a dataset that recognises knowledge-based attributes (data layers) such as intensity, elevation etc. be built for a decision tree environment in order to distinguish roads from other linear features?

Which geometric correction method may produce better accuracy?

Which type of spatial data structure can be employed in order to manipulate and organise the vector and raster GIS data to build a dataset for KS software?

What cell size should be chosen to meet the requirements of the knowledge-based data?

- Interfacing GIS data with the decision tree program:

What is the best way to transfer GIS datasets into the decision tree software?

- Converting results of the classification tree into a classified image, since the decision tree software gives the results of classification tree both in generic rules and in graphic form:

How can this information be applied to produce a classified image?

1.3.1 Stages of Research

The following steps have been undertaken in this research:

1. Definition of the goal which deals with the development of the methodology and its implementation for a trial site for mapping roads.
2. Selection of suitable hardware and software to do the processing.
3. Selection of an appropriate study area.
4. Selection and acquisition of the datasets and georeferencing of the aerial imagery.
5. Definition of the dataset.
6. Spatial data processing and construction of a database for a knowledge-based analysis system.
7. Transferring of the data with a decision tree environment.
8. Decision tree analysis; generation of a classification tree and rules collection and encoding to develop an expert system.
9. Expert systems construction and testing of the expert system over trial sites.
10. Multispectral image analysis.

1.4 Contribution of the Research

Updating maps of roads in any region of the world is required for a wide range of civil engineering and environmental planning purposes. This research describes a methodology developed to integrate spatial data and aerial imagery in a manner that allows it to be used in a knowledge-based analysis system.

This research contributes to the field of knowledge in this area as follows:

- It provides a clear demonstration of the problems associated with georeferencing aerial imagery to suit an integrated spatial data model for delineation of linear features in rural and urban areas.
- It provides an assessment of low-level image segmentation operators such as edge enhancement and edge detection methods as a means of extraction of roads edges. It describes the development of an interactive optimal linear feature detection program, which incorporates different image enhancement filters (eg median) for noise removal, edge detection (eg Sobel, Canny, and Deriche) for primitives extraction, and

morphological operations (eg dilation) to aid geometric structuring of edge segments. This was implemented as a first step in building data for a knowledge-based environment.

- It implements an integrated GIS (vector data) and RS (raster image) data model to construct a dataset for a decision tree environment, particularly one that recognises knowledge-based attributes such as spectral and spatial information in order to distinguish roads from other linear features.
- It describes the interfacing of GIS data with a machine learning environment to construct a classification tree. This phase is important in deriving knowledge from classification trees. Development and construction of an expert system for mapping road networks using generated decision rules was attempted. Evaluation of the decision tree performance both over urban and rural sites was undertaken.
- It provides a comparison of a standard supervised multispectral image classification techniques with the decision tree analysis to map out roads over a trial site.

1.5 Organisational Outline of the Dissertation

This thesis is organised into 10 chapters. In this first chapter, the research has been placed in a general context, the basic hypothesis and proposed approach have been demonstrated, and the original contribution of the research presented.

Chapter 2 introduces the major concepts which form the basis for this project, and includes a brief review of image segmentation and classification in the context of feature detection with special emphasis on road extraction using machine learning and expert systems.

Chapter 3 presents solutions for geometric correction errors of aerial imagery, image enhancement and classification methods including edge detection, thresholding, and morphological operations. It then provides an overview of integrated GIS and RS.

Chapters 4 introduces the theory of expert systems construction, and the basic concepts involved with decision trees that are associated with this research.

Chapter 5 describes the study area, the available data including GIS data and aerial imagery, and the hardware and software which was used.

Chapter 6 deals with digital image processing; pre-processing of the data sets such as georeferencing of the aerial photography, and processing of the data such as image segmentation via developing a computer program for primitives extraction.

Chapter 7 describes the process used to construct a database for knowledge-based software. The integration of GIS data and remote sensed imagery is considered. A grid raster-based processing was undertaken, and then the grid data were preprocessed by writing a computer program to generate a tabular ASCII file.

Chapter 8 demonstrates the decision tree analysis, and consequent rules collection from the generated classification tree to develop a decision tree processing expert system. In this chapter, two routines are implemented: (1) the first program translates the generated generic decision trees rules to MATLAB programming statements, and prints them in a file, and (2) the second program executes the rules against the datasets to map out the roads and their background, and finally computes the overall classification accuracy based on the reference data.

Chapter 9 describes a supervised multispectral image classification of the trial site using colour aerial photography. The aim was to compare the performance of a standard technique image classification technique (supervised multispectral image analysis) with a decision tree analysis to map out roads over the trial site.

Chapter 10 provides a summary of the thesis, the conclusions reached in the study, and recommendations for future research on this topic

Chapter 2

BACKGROUND: CLASSIFICATION AND FEATURE DETECTION

This chapter reviews image segmentation, using textural and contextual information, machine learning techniques and expert systems (ES) in geographic information systems (GIS) and remote sensing (RS) for feature extraction and classification. The main emphasis is on road detection incorporating decision trees.

2.1 Image Analysis

In the design of an image understanding system, a distinction must be made between different levels of image processing and their impacts. There are two major types of image analysis in the classification of remote sensed imagery (Moller-Jensen, 1990). (1) Synthesizing: its aim is to retrieve overall information about the main spatial trends in the data such as the extension of industrial areas (eg Forghani, 1994). (2) Analytical: the objective is to register information about the smallest elements in the data set such as housing units (eg Forster, 1993). Artificial intelligence methods of information extraction, knowledge representation, and symbolic reasoning can be applied to achieve this aim (Wang and Newkirk, 1988). The spatial resolution of input image plays an important role in the process of feature extraction. For example SPOT data may be suited to the analytical approach because it shows detailed information, whereas Landsat TM data is more appropriate for the synthesizing approach.

Image segmentation has been defined as *“the process of partitioning or synthesizing an image into its constituent objects”* (Rosenfeld and Kak, 1982). Segmentation techniques can be classified based upon the level of representation of resulting images. Many segmentation algorithms have been discussed in the literature (eg Marr, 1982; Haralick and Shapiro, 1985; Gonzalez and Wintz, 1987; Argialas and Harlow, 1990; Domenikiotis, 1994). There are no standard criteria for isolation of the levels of image segmentation. Each research project uses different strategies to assign the image analysis tasks into a favoured segmentation level. However, the segmentation techniques are divided into three levels (Figure 2.1).

I) Low Level; requiring no intelligence on the part of image interpretation. Low level image segmentation methods can be grouped into two phases:

1. Image acquisition which requires two elements, namely a physical device and a digitizer to convert the electrical output of the physical device into digital form.
2. Pre-processing; this phase can be divided into radiometric processing eg histogram equalization, and geometric processing eg polynomial transformation. A number of transformed data sets such as principle component analysis (PCA), normalized difference vegetation index (NDVI) have been used in multispectral image analysis eg for change detection (ie Fung, 1992). Since this thesis will not consider multispectral image analysis in depth, these techniques are not discussed here. Detailed discussion of these techniques is provided in (eg Richards, 1986; ERDAS 1994b; Forghani, 1993). Geometric processing is discussed in Chapter 3.

II) Medium Level; the intermediate level deals with extraction and characterization of the constituent components of an image such as scene description. The medium level process is described as simple aggregation of the basic primitives such as edges and lines. Image primitives do not have any semantic information, but can be meaningful and sufficiently incorporated in high level of representation by using meaningful objects to allow image representation in terms of the aims of the analysis. A prime example of this algorithm is neighbourhood operators which examine the value of a small neighbourhood of pixels around a given pixel and generate a resultant value that is a function of all pixel values in the neighbourhood (Argialas and Harlow, 1990). The image primitives (Marr, 1980) such as edges, lines, and regions extracted by medium-level image operators are subject to error. In reality, the output of these medium-level operators is not perfect (Van Cleynenbreugel et al 1990). Therefore, higher level segmentation tools which involve the human expert interface have to be applied. The major drawback with the human image interpretation process is the lack of speed and poor quantitative accuracy. Despite the fact that the process works efficiently on mixed data, applying a machine-assisted approach may lead to better results (Sirinivinsan and Richards, 1993). Some medium-level segmentation techniques include line and curve detection, line and edge linking, mathematical morphology, and image classification. Multispectral image classification can be classified into two main categories, based on whether they require supervision

(based on a priori knowledge) from the operator or not (based on similarity assumption). These techniques have been widely discussed in remote sensing texts (eg Richards, 1993).

III) High Level; involves intelligent recognition, description, and interpretation using whatever domain-specific knowledge is available about the class of scenes. This stage consists of identifying the important objects in an image and their relationships for subsequent description, and well-defined knowledge structures for the reasoning component using a knowledge-base. For example, a knowledge-based rule was used to link road seeds and extend them by a series of image intensity tests (Zhu and Yeh, 1986). In the high level road processing stage, more global information such as width and length may be considered. In this situation expert systems play a critical role in labelling road segments (Ton et al 1991; Domenikiotis, 1994). Recognition assigns a label to an object based on the information provided by its descriptors. For example, road-like structures may be falsely identified as road segments. Contextual information may be used to solve these ambiguities. Domain specific knowledge can be in many forms such as descriptive definitions of entities, objects and their relationship to each other and criteria for making definitions. Examples of high-level techniques as a knowledge-based approach for image segmentation are fuzzy sets theorem, decision trees, neural networks, frames and rules, and expert systems.

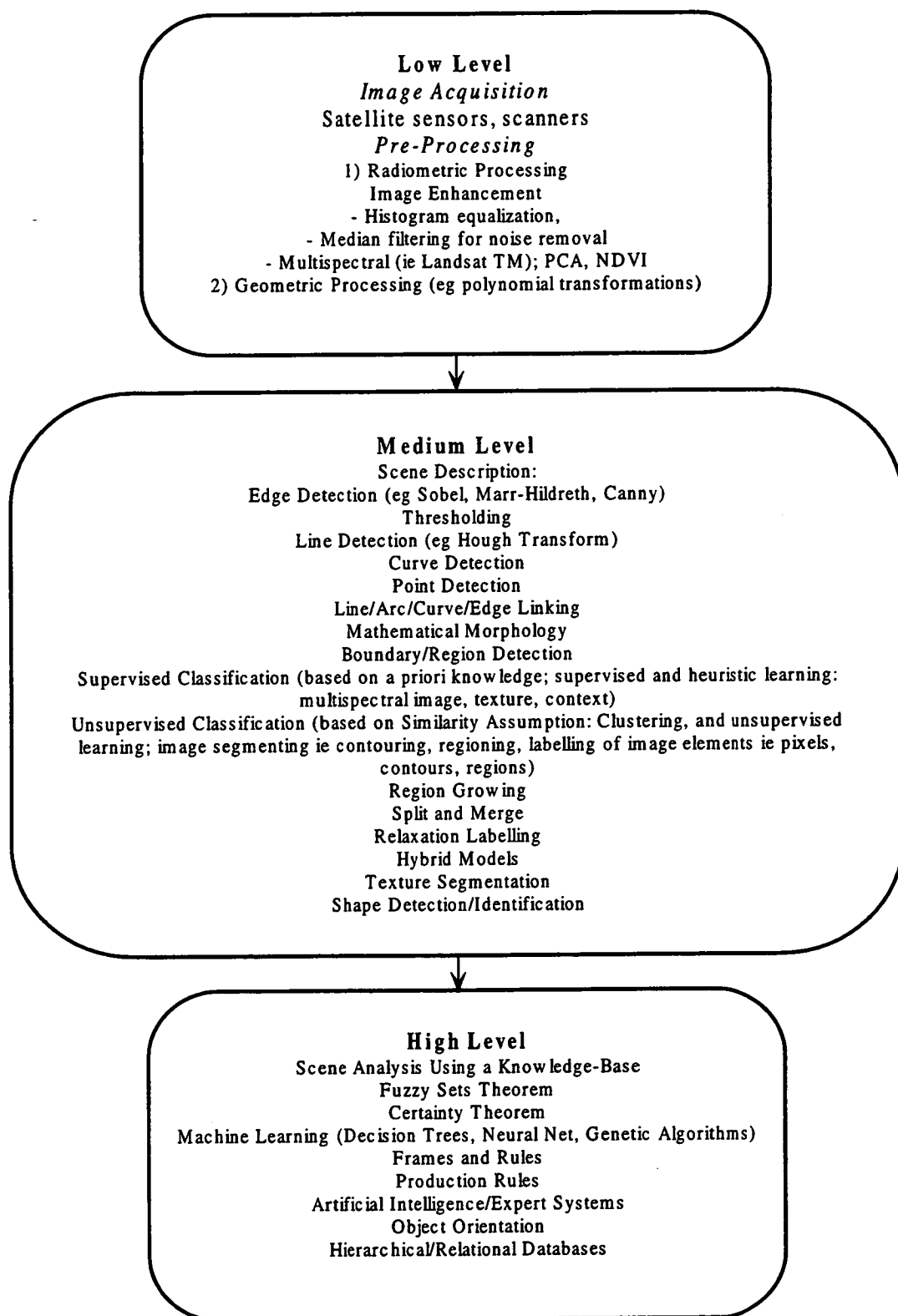


Figure 2.1 Image interpretation techniques classified according to segmentation level.

2.1.1 Texture

Texture describes the smoothness of an object or a part of an image. Also it can be described as structure composed of large numbers of more or less ordered similar objects or patterns without these drawing particular consideration (Van Gool et al 1985). Texture can be used to delineate regions, boundaries in image segmentation, object identification, and to characterize the tonal or grey level variation in an image (Wang and He, 1990). There are many approaches and models for texture analysis in image processing. Algorithms for texture analysis have been developed by many authors including Haralick (1979); Harlow et al (1986); Franklin and Peddle (1990). These include statistical approaches such as autocorrelation (Haralick, 1979), optical transforms, digital transforms, textural edge operators, structural elements (eg Haralick and Shapiro, 1985; Frankline and Peddle, 1990), grey tone occurrence (eg Gong et al 1992), run lengths, and autoregressive models (Haralick, 1979). Reed and Du-Buf (1993) provide a comprehensive review of the literature in this field.

2.1.2 Context

Context utilizes a variety of information types such as tone, size, shape and geometry, shadow, patterns, and association (spatial) characteristics. In general it considers interrelationship between objects or their spatial relationships with pixels in the remainder of the scene. Contextual information is important in human visual interpretation and human decision making and in those conditions where a classifier is used to emulate human abilities (Harris 1985). The application of a contextual model, such as the probabilistic relaxation model has been widely discussed eg by Gurney and Townshend (1983), Harris (1985). Human analysts in interpretation and classification of visual images consider the contextual information (Avery and Berlin, 1992), whereas, these spatial attributes are not entirely considered in conventional per-pixel procedures for pattern recognition (Civco, 1993). Contextual image analysis does not simply consider discrete pixels during classification, but rather interprets whole regions based upon consideration of a variety of characteristics.

The main objective of using context in linear feature extraction is to improve the accuracy of image classification results. Considerable efforts have been made by Wang and He (1990), Johnsson (1994) and Ko (1995) to develop and improve classification of image data using contextual information.

2.2 Machine Learning in Remote Sensing and GIS

Machine learning methods such as non-parametric methods have been used to integrate analysis of GIS and remote sensing data. They can be grouped into three distinct areas:

- artificial neural networks,
- genetic algorithms, and
- decision trees.

This research will deal with decision trees. Neural networks are used to recreate biological information processing methods in software. The paradigm of artificial neural systems is based on the way the brain processes information. A simple model of a neural network consists of (i) input layer where values are applied to the inputs, changed, based on some mathematical rule and then accumulated at the nodes; (ii) output layer where the inputs are processed and classified. The sum can then be functioned mathematically again before it is applied to the output. Each dendrite in the brain acts as an input to the neuron; and a hidden layer. The nodes (neurons) are connected with weights that are adjustable during the learning process, and adjustment takes place to improve the performance of the neural network. The neurons and weighted links between these neurons simulate synaptic activities. One of the most common neural network models is the back-propagation that has been under experiment in land cover classification problems. The model neurons can be connected into networks in widely varied ways. Michie et al (1994) provide a detailed discussion of the theoretical viewpoints on this technique.

Artificial neural networks have been applied to a wide range of image classifications such as the classification of multispectral imagery (Turner, 1994; Foody et al 1995), feature identification (Ryan et al 1991; Wolfer et al 1994; Cote and Tatnall,

1995), signalized point recognition in aerial photographs (Kepuska and Mason, 1995). More importantly, Boggess (1993, 1994) and Ko (1995) applied artificial neural networks for identification of roads from Landsat TM imagery. Artificial neural networks have drawbacks in the slow learning process that is initially related to a back-propagation training scheme. However, solutions can be found by developing a dynamic learning neural network to perform classification (Chen et al 1995).

Decision trees use a contextually-based approach which incorporates decision rules and spatial relationships of attributes (if they are input to the process) to classify objects (Walker and Belbin, 1990). The authors conclude that incorporating more spatial relationships into a GIS is more effective using clustering methods. The decision tree facilitates grouping large numbers of observations and subsequently translates group membership into classification rules which provides effective analytical tools for the GIS user.

A number of authors have developed algorithms to generate decision trees including Classification And Regression Trees (CART by Breiman et al. 1984), Interactive Dichotomizer (ID3 by Quinlan, 1986), and KnowledgeSEEKER (KS by ANGROSS, 1994). Decision trees have been applied for land cover classification by prime researchers, for example, Walker and Moore (1988), Lees and Ritman (1991), Reddy and Bonham-Carter (1991), Evans et al (1996) and Skidmore et al (1996b). Induction is most suitable for analysis of problems where knowledge of the underlying process is either non-existent or incomplete (Walker and Moore, 1988). The major component of a GIS required to enable inductive modelling is a technique for systematically identifying relationships between spatial objects. GIS is the beginning point for developing the spatial objects. GIS contains data definition patterns such as distribution of roads and location attributes. Classification trees can describe these relationships by assigning a set of rules (eg Quinlan, 1986; Williams, 1987).

Decision tree analysis has been applied for mapping mineralisation based on a GIS multi-map overlay using cluster and exhaustive partitioning¹. It was reported that the exhaustive method provided better results over the cluster model (Reddy and Bonham-Carter, 1991). Also, Moore et al (1991) have applied decision trees with a GIS data base for prediction of vegetation distribution. They confirmed the value of decision tree analysis and cartographic modelling for environmental mapping.

An inductive modelling technique has been applied for analysis of wildlife patterns in spatial data (Landsat TM data and DTM) and employs a Bayesian statistical approach to develop a GIS for habitat mapping (Aspinall, 1991). The research used a spatial modelling procedure operating within GIS and introduced a significant learning capacity. Aspinall (1992) concluded that this modelling technique offers significant potential in mapping and management of the environment. Also Stockwell (1993) developed a learning base system (LBS) classifier for the purpose of automatic mapping in a GIS such as automatic mapping of wildlife distribution, and diagnosis of diseases by acquisition of knowledge from an expert. The Bayesian algorithm proved to be a flexible method for conducting an extensive variety of knowledge-based tasks (Stockwell, 1993).

In addition, two techniques of machine learning including decision trees (ID3 and CART) and genetic algorithms² were conducted for analysis of natural resource data in terms of investigation of lake acidification. The result of the survey showed that both the decision tree and genetic algorithm approach seemed to be appropriate methods for identification of lake acidification (Liepins et al 1990). Recently, Skidmore et al (1996) attempted to compare three methods for mapping wildlife, so-called BIOCLIM, CART (decision trees) and a non-parametric classification technique employing a GIS dataset.

¹ Cluster method refers to two-way partitioning or pair-wise merging (binary tree) which clusters values of partitioning variables together and finds the maximum similarity within the groups and dissimilarity between the groups. Exhaustive method refers to a multi-branch technique which identifies the codes that form the nodes and branches of the classification tree. These choices generate a split for each potential partitioning variable. Further details can be found in De Ville (1990).

² A genetic algorithm is a computational method that transforms a set (population) of individual mathematical objects which are usually fixed length character or binary strings, each with an associated fitness value, into a new population (next generation) applying operations patterned after Darwinian theory of reproduction and survival of the fittest and after naturally occurring genetic operations [sexual recombination, mutation] (Koza, 1992).

Among these techniques, the decision tree provided the most accurate result, but was costly to implement.

Apart from the above discussed areas, fuzzy set theory to image classification and accuracy assessment of thematic maps (eg Gopal and Woodcock, 1994) have been applied. An algebraic approximation to the generating appropriate classification with fuzzy attributes has been provided in Gisolfi and Nunez (1993). The fuzzy set theory emerged in the 1960s to describe the imprecision that is characteristic of much human reasoning, particularly in domains such as pattern recognition and information abstraction. It has been successfully applied to pixel or subpixel classification (Wilkinson and Megier, 1990). In addition, applying the theory of evidence is reported by (Shafer, 1976) for classification purposes. The theory of evidence relies on a numerical integration function to add to the evidence and has been performed in some problems of mixed spatial data. However, due to its numerical basis, it has limitations for use in some situations which would not themselves simply to the incorporation of non-numerical map-like data in terms of being subjective and inconsistent in generating the prerequisite evidence (Sirinvinsan and Richards, 1993; Peddle, 1995). This problem can be overcome by applying a more subjective approach for deriving evidence from histogram bin transformations of supervised training data frequency distributions (Peddle, 1995).

2.3 Approaches in Linear Feature Detection

Linear features in remote sensing imagery include roads, rivers, bridges, vegetation alignments, field boundaries, shorelines, and geologically significant features such as faults and joints. Fundamentally, there are two techniques used to detect these linear features.

- 1) Line detection and line tracking algorithms have been used to identify road networks directly rather than identify boundaries of road features. Line detection algorithms incorporate a method that takes into account the size of the kernel that can be used to filter the data, then adjusts the size of the kernel in the template in order to match the width of the roads. The idea is based on applying a model in the form of a mask

which is shifted over a region and compared to the corresponding grey levels (eg Domenikiotis, 1994). The Hough Transform is a line detection method used by various researchers (Wang and Liu, 1994; Aghajan and Kailath, 1994) to detect roads and lines. Line tracking algorithms track roads by using seeds from an image. Papers dealing with road tracking models include those by Fischler et al (1981); McKeown and Zlotnick (1990); Geman and Jedynek (1996). Although these models vary in their detail, all assume prior knowledge of the location of linear structures and are based on that domain knowledge, and generate more information on the road networks.

2) An edge detection approach may be fruitful if the user is concerned with representing the exact size of the road. If roads have significant width (ie 2 or more pixels width), it may well be more useful to employ an edge detector in order to derive edges of roads rather than the centre line (Domenikiotis et al 1995). Edge detection and filtering (eg Nevatia and Babu, 1980; Schanzer et al 1990), contextual filtering (eg Vanderbrug and Rosenfeld, 1978; Gurney and Townshend, 1983) and mathematical morphology (eg Destival, 1986) have been discussed and applied for feature extraction (eg Destival, 1986).

The use of GIS and knowledge-based rule (KBR) algorithms (eg Van Cleynebreugel et al 1990; Stilla, 1995), and dynamic programming (Grune and Li 1995) are other approaches for delineation of linear features. Knowledge-based interpretation of remote sensed data constitutes an active research area. Examples include the analysis of aerial photos (McKeown, 1987), radar imagery (Pai et al 1986), Landsat data (Bogges 1993, and 1994; Wolfer et al 1994), and SPOT images (Geman and Jedynek, 1996) to road network extraction. Different sorts of knowledge sources have been used: domain knowledge (about features and their structural and geometrical relationship); respective relationships (eg tangential direction at the end of a line, collinearity, adjacency, parallelism, anti-parallelism, orthogonality); incidence, proximity, relation, and position of features. Shorter reports and reviews include those by McKeown (1987), Ton (1989), Zelek (1990), Schanzer et al (1990), Zlotnick, and Carmine (1993), and others.

Employing knowledge sources such as photometry and perceptual grouping (eg Tavakoli and Bajcy, 1976; Van Cleynenbreugel et al 1990; Domenikiotis, 1994), global land cover classification (ie Ehlers et al 1990; Stadelmann and Lodwick, 1993), existing roadmaps, drainage networks maps and a digital terrain model (ie D'Agostino et al 1993; Skidmore et al 1996) can be expected to improve the reliability of road detection and classification routines. Two main types of knowledge sources have been used: photometry and perceptual grouping rules (eg. Pai et al 1986; Wang and Newkirk, 1988; McKeown and Zlotnick, 1990; Van Cleynenbreugel et al 1990).

To delineate a road, an image interpreter may apply structural, spectral, and contextual knowledge (Swain et al 1980). Structural knowledge of roads has been examined with incorporation of computer systems, and by a GIS-guided technique (Van Cleynenbreugel et al 1990). Researchers are using the following properties to aid road detection:

- spectral characteristics,
- geometric shape, and
- spatial properties.

Previous attempts have been made to find roads from remote sensing imagery using machine learning and expert systems. For example, Bogges (1993) used a back-propagation artificial neural network technique for the identification of roads. It was pointed out that this analysis technique is insufficient for an accurate classification of whether or not a pixel represents road, and that a back-propagation neural network may not be able to provide a complete solution. This uses low level image segmentation, which relies perceptually on the spectral reflectance properties of land cover types. The use of context or other domain-specific data for successful classification was recommended. Furthermore, Ko (1995) followed a hybrid road detection method using edge detection in a back-propagation neural network. The hybrid road detection technique in this context refers to employing both spectral and spatial information in a back-propagation neural network. The technique was found to be superior to previous techniques due in part to its ability to incorporate not only spectral information but also contextual information which applies domain-specific knowledge of spectral and spatial

information as an intermediate image segmentation level. It would appear that this method has difficulties in accurate detection of roads over a mixture of man-made structures. A more comprehensive discussion of road detection applying neural networks for combining multi-source evidence is provided by Boggress (1993 and 1994) and Ko (1995). In addition, genetic algorithms have been applied to classify roads in satellite imagery, and the results have been compared with a neural network technique (Boggress, 1990).

Recently, Geman and Jedynak (1996) presented a new method for tracking roads from SPOT images. The approach was related to the recent work in active vision on where to look next and associated with the divide and conquer method of parlour games. The general methodology dealt with decision trees and the role of entropy in pattern recognition. In this approach intensity and geometry are considered in the process of road detection. Implicit in Geman and Jedynak's approach (1996) was the concept of the decision trees. The approach was shown to work well for tracking major highways, but it had difficulty tracking the smaller roads due to the fact that roads were confused with other man-made structures.

2.4 Expert Systems in Remote Sensing and GIS

In remote sensing, image processing and spatial data manipulation, expert systems (ES) are playing a critical role in development of automated knowledge-based systems. The application of ES and Knowledge-Based-Systems (KBS) has been mainly made in four areas: geographic feature extraction (McKeown et al 1985; Taib and Trinder, 1992; Stadelmann and Lodwick, 1993), geographic database systems (Frank, 1988), geographic decision making (Karimi et al 1987), and map design or production (Muller, 1991; Hartog et al 1996). Feature extraction is the main emphasis of this research. Low level image segmentation techniques have some shortcomings due to the huge amount of information in each image, ambiguous and contradictory information present in the images, object scale and resolution, geometric and radiometric effects (Robinson et al 1987). These shortcomings lead to building ES for feature detection. Several papers reported that automatic methods have been developed in the area of feature recognition (eg Gruen and Li, 1995; Stilla, 1995).

A number of applications of Knowledge-Based Systems (KBS) are concerned with analysis and processing to develop rule-based techniques. Several systems have been designed in artificial intelligence (AI) and ES to provide support for integration of GIS and remotely sensed data (eg Pai et al 1986; Stadelmann and Lodwick, 1993; Skidmore et al 1996a). Application of ES techniques in the domain dealing with spatial data has been widespread. For example, Skidmore et al (1996) conducted an expert system approach for mapping forest soils by utilizing a DTM, vegetation map, and knowledge provided by a soil scientist. This technique provides an accuracy of 70% which competes with a map drawn by the soil scientist.

The use of knowledge-based methods in current applications of GIS seems a little more than ad-hoc application of strategies initiated in the area of AI (Smith and Yiang, 1991). There is a wide variety of contemporary literature that deals with knowledge-based approaches such as the theory of evidence, machine learning methods, fuzzy logic for GIS and RS applications. An idea of how the scope of GIS can be developed by employing techniques from an AI context that can resolve the constraints and problems in user interfaces mainly by data representation and its visualization in the process of integration of remotely sensed imagery and GIS data, has been illustrated in many articles (McKeown, 1987). Image processing techniques alone are inadequate if in a situation where specific information or prior knowledge about the scene in question is required.

The KBS applications did not concentrate on the promotion of the computational efficiency of GIS. Current application of knowledge-based approaches is typically associated with employing rules in relation to GIS modelling. Loose coupling between the rule based ES and the geographic database (Smith and Yiang, 1991), in particular the construction of applications of KBS, provides a user-friendly interface to GIS. Most KBS applications associated with analysis and processing have dealt with ES approaches to provide an environment for a system loosely coupled to the spatial database component of a GIS. The use of KBS is involved in many sub-components and components of GIS. The major application areas are acquisition, storage, access, analyzing and processing, conversion, and interfaces. The adoption of applications of KBS in GIS components has

been identified as a facilitative tool which enhances the power of GIS. These parameters are related to the following areas (Smith and Yiang, 1991):

1. KBS, defined in terms of languages that support knowledge representation and deduction, will not add any new expressive or computation power to the current languages employed in GIS.
2. In connection to the acquisition, KBS enhances the construction of applications in the context of automization of procedural knowledge capture.
3. KBS techniques for storage of GIS databases have been employed.
4. KBS made an easy mechanism to use GIS in the process of access such as query optimization and the use of metadata. The query optimization is extremely significant for large-scale GIS modelling involving complex multi-component and nested spatial objects in which features may be implicitly represented in a multi-layer data model.
5. KBS facilitate the building of natural language interfaces, and these languages provide an easy way to use GIS in the process of interfaces.

The topics of data acquisition, data structures, and problems of data conversion will be discussed in Chapters 3 and 7. The interface of GIS and RS in a KBS model for methodology developed in this research will be elaborated in Chapter 8.

The rule-based expert systems approach is another attractive method of road extraction. Pai et al (1986) contributed to rule-based approaches using a real-world model which was generated from a road network map of the terrain. The starting point for searching roads is a key road technique. Once the key road is selected, the rest of the roads in the network are represented relative to the key road, and relationships between the model roads are indicated by properties (ie branch of, branched from, cross, and others) in accordance to defining x and y coordinates. Furthermore, a low level image segmentation technique (line detection) is incorporated into building a backward chaining expert system for extraction of road networks in a forested area. This study used brightness values, length, and shape characteristics to refine the image using moment invariants. Overall, the research shows that effective road reconstruction is possible even though preliminary results from edge detection algorithms are poor (Domenikiotis, 1994).

2.5 Summary and Remarks

A number of image segmentation approaches have been discussed, starting with image analysis, segmentation methods, using textural and contextual information, extension of machine learning and ES into feature extraction, and knowledge-based approaches to road detection. Consequently a review of classification (segmentation) methods leads to identification of four basic operations:

- 1) Incorporating radiometric and geometric enhancement for image interpretation
- 2) Applying contextual information
- 3) Incorporating textural information
- 4) Employing semi-automatic and automatic approaches using artificial intelligence and machine learning techniques, particularly artificial neural networks, decision trees, genetic algorithms, fuzzy logic, theory of evidence, and expert systems.

A number of reviews have supported this conclusion (eg Richards, 1993; Lees, 1994). Many systems using different levels and methods of segmentation have been used for aerial and satellite scenes analysis. There is a common reliance based on medium level segmentation and low level image cues which are extractable, eg by edge detectors and thresholding. It is crucial to have intermediate operators which do not have to depend only on medium-level image cues. It is appropriate to use this information to reflect perceptual similarity in order not to have too severe errors in labelling classes.

Chapter 3

DIGITAL IMAGE AND GIS DATA PROCESSING

This chapter provides a review on integration GIS datasets and RS imagery, giving emphasis to data conversion problems, particularly the problems associated with geometric distortions of digital aerial photographs. These later problems are discussed and standard methods for their geometrical correction are presented. The subject of image enhancement using edge detection and mathematical morphology is reviewed.

3.1 Image Rectification and Registration

Image registration is the process of spatially best aligning two views of a scene captured using similar or dissimilar sensors (Pratt, 1978; Kanal et al 1981; Ton, 1989). Georeferencing is the process of establishing a best fit between an image (row, column) coordinate system and a map (x,y) coordinate system (ERSI, 1992d). This involves warping the geometry of the image in order to establish the same relationship between the image and map coordinates.

Image rectification is the process of geometrically correcting systematic and random distortions in an image to fit ground control (Lillesand and Kiefer, 1987; Goshtasby, 1987 and 1988). Image rectification is a common problem arising in digital image processing and GIS applications whenever the image and the ancillary data of the same scene have to be compared pixel by pixel.

Distortions in aerial photographs are caused by changes in ground elevation, camera (sensor) position and orientation, lens distortion, earth curvature, film distortions, and atmospheric refraction (Wolf, 1988; Zhizhuo, 1990; Frost, 1995). These distortions need to be corrected before an image can be used for remote sensing and GIS applications. The aim is to provide a photo as free from errors as possible.

Image rectification and image registration are crucial when undertaking the following:

- (a) mapping and map revision (eg Coloveoresses, 1990; Torlegard, 1992; Mather, 1995)

- (b) change detection (eg Milne, 1988; Forghani, 1993; ERDAS 1994a)
- (c) scene classification and analysis (eg Silfer, 1988; Della Ventura et al 1990)
- (d) image or feature enhancement (eg Ford et al 1983; Goshtasby, 1987; Ehlers et al 1990)
- (e) depth perception (Goshtasby, 1987)
- (f) GIS data entry (eg Johnson, 1989; ESRI, 1992d).

For topographic map production, reliable spatial data is produced from aerial photographs using stereo-photogrammetric techniques. For GIS applications there are three common types of geometric rectification applied to digital images:

- 1) Geometric (polynomial) transformations are applied when image distortions are highly systematic and relief displacement is not significant.
- 2) Digital orthophotography, which is applied when there is significant relief displacement. A Digital Elevation Model (DEM) is used to resample an image and produce an orthographic projection of the terrain.
- 3) Affine transformation and rubber sheeting which is based on point matching of the two sets of points by applying a rubber sheeting process.

3.1.1 Geometric transformations

(i) Ground Control Points Selection

Image features commonly used as GCP include points on roads, rivers, field boundaries, shorelines, and power lines sometimes, using a visual fit of curved tracings to sections of the physical features in the image and referenced map. The use of GCP's to register remote sensed images to a georeferenced map is described by, for example, Welch and Usery, (1984); Labovtiz and Marvin, (1986); Marvin et al (1987).

Polynomial transformations use a set of GCP's to establish the relationship between a map and an image based on interpolation techniques. The principal considerations when applying polynomial transformation methods are the choice of ground control points (GCP) and the order of the polynomial. There are two common methods of control point selection:

- (1) Manual selection of GCP which depends on the visibility of invariant physical features such as line intersections and points. Numerous researchers have addressed the problem of control point selection (eg Welch, 1985; Marvin et al 1987; Mather, 1995).
- (2) Semi-automatic and automatic methods such as point and line matching, relaxation labelling schemes (eg Goshtasby, 1988; Ton, 1989; Li et al 1993)

The number of GCP's used and their position in the image depends upon the type of terrain and a variety of other factors. It has been shown elsewhere that polynomials are an effective way of correcting different types of image geometric distortions in digital images (Van Wie and Stein, 1977; Usery and Welch, 1989). There is a relational formula for the number of required GCP and the order of transformation (Labovtiz and Marvin, 1986). A minimum practical number of GCP's is required to calculate a transformation (Welch, 1985). A useful formulation is shown below (ERDAS, 1994b):

$$\text{GCP} = \frac{(t_1 + 1)(t + 2)}{2} \quad (3.1)$$

where t is the order of transformation.

Provided that sufficient accuracy is obtained, a low order transformation is preferable due to the fact that few GCP are required to register the image on to a map. The number of GCP required is dependent on terrain type, scale, and the required level of accuracy.

An image with low spatial variation, often a low order bivariate polynomial ($m = 2$ or 3) is a good approximation to the actual situation. Larger geometric variations need higher order polynomials to gain a given error tolerance. Generally, the coefficients associated with higher order in the polynomial are sensitive to the location of the GCP, which has to be uniformly distributed throughout the image. This problem can be avoided by employing orthogonal polynomials ie Legendre or Hermit polynomials. Coordinate transformations are an approximation of the true values.

Root Mean Square (RMS) errors can be used to evaluate the performance of least squares fitting routines. The root-mean-square error (RMS) is a measure of accuracy for each GCP in the image and can be written (Domenikiotis, 1994):

$$\text{RMS} = \sqrt{(x - x_{\text{original}})^2 + (y - y_{\text{original}})^2} \quad (3.2)$$

Once the transformation for a given GCP is performed, the suspect points from the total RMS error, the X and Y residual, and contribution table can be examined and errors detected and eliminated. The pair point distances¹ are then computed and the RMS difference values identified. The RMS errors reflect the reliability of GCP's, and are an index of the internal geometric fidelity of the image data.

Lincolne (1995) and Forster (1995) report if the GCP come from a 1:25,000 scale map, it can be expected that the GCP will be accurate to 0.5 mm (obtaining error values of about ± 12.5 m on a 1:25,000 scale topographic map). Della Ventura et al (1990) gained an accuracy of 2.57 RMS error pixel and 2.68 RMS error pixel using 8 automatically detected GCP and 11 manually detected GCP's respectively.

(ii) Resampling

Resampling can be described as the process of adjusting the location of pixel centres for generating an image (grid) at a predetermined scale and with attribute values derived from the original data. Three common methods of polynomial transformation are cited in the literature, and these techniques have been applied in image (grid) data which are available in GIS (eg ARC/INFO) and remote image processing software (eg ERDAS IMAGINE):

1. Nearest-neighbour
2. Bilinear-interpolation
3. Cubic-convolution

In addition, interpolation techniques such as bilinear interpolation and weighted Brownian interpolation² have been extended to digital elevation models (DEM) (eg Ungar et al 1988; Polidori and Chorowicz, 1993).

¹ Pair point distances are a comparison of map and scaled photo distance between all alternative combinations of point-pairs.

² Brownian interpolation refers to a Random Midpoint Displacement algorithm, described by Polidori and Chorowicz (1993).

A nearest-neighbour assignment is computationally the fastest and easiest method to use of the three methods of interpolation. Primarily it is applied for categorical data such as land use classification, since it preserves the exact value of pixels in the original dataset values without averaging them, and therefore does not introduce new grey values. This is an important issue when discriminating between vegetation classes, locating an edge associated with lineament, or identifying different levels of turbidity or temperatures in a lake (Jensen, 1986). It suffers from some disadvantages as follows:

- it introduces spatial shift errors such that local geometry can be inaccurate by up to $\frac{\sqrt{2}}{2}$ of ground grid size (Lodwick and Pain, 1986), so that the maximum spatial error will be one half the cellsize of the grid.
- in resampling a larger to smaller grid size, there is usually a "stair stepped" effect around diagonal lines and curves.
- also some data values may fall, while other values may be duplicated.
- in addition, on linear thematic data (ie roads, streams) gaps or breaks in a network of the linear features may result.

A bilinear-interpolation determines the new value of a cell based on a weighted distance average of the four nearest input cell centres. This method tends to give more natural looking images, without the blockiness of nearest-neighbour or the over smoothing of the cubic convolution option, although there is a risk of information loss for high frequency data (Mather, 1987). It is useful for continuous data or thematic files, which may have data file values according to a qualitative (nominal or ordinal) system or a quantitative (interval or ratio) system. The bilinear-interpolation is not appropriate for a qualitative class value system. When using this method for continuous data, it will cause some smoothing of the data.(ERDAS, 1994b).

A cubic convolution calculates the new pixel value employing third degree polynomials and the 16 nearest pixel values from the original data. It increases the high frequency component of data and has poor frequency characteristics. This type of tranformation also distorts the original data significantly. Cubic convolution is not appropriate for image processing calculations (ER Mapper, 1993). Further information

can be found in ESRI (1992e), ERDAS (1994b) and other photogrammetry and GIS texts.

Using Global Positioning Systems (GPS) to obtain GCP coordinates rather than scaling coordinates from a map will increase the reliability of the GCP's (eg Clavet et al 1993; Adkins and Merry, 1994; August et al 1994). If GPS is used then planimetric accuracy to centimetre level can be obtained. In general, DTM are within 5 to 10 m of surveyed ground control (Tudor and Sugarbaker, 1993; Jensen, 1995), and an accuracy of about 5.5 ± 3 metres can be gained. This degree of accuracy is well suited to some planimetric applications.

3.1.2 Orthophotography

Historically, errors in aerial photography have been corrected using photogrammetric stereo plotters. Tall buildings, hills and valleys can be displaced from their true position depending upon whether these objects are below or above a given datum, sea level being the usual datum for mapping. The relief displacement is a function of the change in height and the distance away from the centre of the photo. Further information on this topic can be found in Wolf (1988).

It has also been shown that polynomial methods may not efficiently remove relief displacement in areas of gentle relief (smooth terrain) and rugged terrain (eg Steiner, 1992). Recent developments in vector-based spatial data technology have enhanced efficiency in managing terrain information and facilitated high accuracy mathematical computations and analysis in 3-dimensional surface (3D) modelling (Burrough, 1986). The Triangular Irregular Network (TIN) surface representation is a clear example of how a surface may be stored, manipulated, and displayed. TINs are applicable for continuous surface data such as elevation. Basically, these data can be represented as a continuous surface; commonly the transition between possible values on a continuous surface is without sharp changes. The attribute of this data is stored as a Z value, a single variable in the vertical direction associated with an X, Y position. Continuous data are described in a large body of literature (eg Burrough, 1986; ESRI, 1992e). Continuous surface data can be divided into two categories; one represents features where each location is measured

from a conformed registration point such as elevation and aspect, and another includes phenomena which progressively vary with their movement across a surface from a source such as contamination of water from a nuclear reactor.

The DTM derived from existing topographic maps by digitizing will not be as accurate as a map, since some errors can occur in processing data. Moreover, human map compilation and the process of capturing the elevation data is subject to errors. In the process of capturing the elevation data in the field, using high quality and quantity instruments, and a well skilled crew, the risk of occurrence of errors can also be taken into consideration. Surveyors may ensure that DTM created from surveying fieldwork sufficiently represents the surface observed. The accuracy of an orthophoto is affected by the quality of a DEM, and the distribution and accuracy of the GCP's. GPS technology makes it possible to capture accurate ground control points (GCP) information X, Y, Z root-mean-square-error of about 15cm when the data are differentially correct (Jensen, 1995). It depends on many parameters such as the type of instruments and required accuracy.

Continuous data are described in a large body of literature (eg Burrough, 1986; ESRI, 1992e) and in Section 3.4.2. Comparisons of continuous field data and the vector and raster data models are widely discussed in the literature. Continuous surface data can be divided into two categories; one represents features where each location is measured from a fixed registration point such as elevation and aspect, and the other includes phenomena which progressively vary with their movement across a surface from a source eg contamination of water from a nuclear reactor.

The DTM has been used extensively in a large number of diverse applications in GIS (Tsai, 1993). Prime examples are land use change detection (Forghani, 1994 and 1995), feature extraction (Forghani and Zwart, 1995; Forghani and Osborn, 1996), digital analysis of viewshed inclusion and topographic features (Lee, 1994), hydrological applications (Skidmore, 1990), and others. Application of DTM's to create orthophoto rectification (Numan et al 1992; Forghani and Zwart, 1997; Forghani and Osborn, 1998a) is another area, described later in this study.

Surface elevation information can be obtained in five common ways: from map contours (Forghani and Osborn, 1996), a TIN (Skidmore, 1990), stereo-correlated aerial photos or other images and x,y,z photogrammetric ASCII files, (ESRI, 1992e), field surveys and GPS or global positioning systems (Clavet, 1993; Adkins and Merry, 1994), and from gridded matrices of elevations (Skidmore, 1990). It is not within the scope of this research to deal with the above-mentioned methods in full. The principal consideration is extracting DTM from digital contours by building a TIN model.

Conventional methods produce sufficiently accurate results; however, there are some disadvantages with using the photographic methods of orthophoto production (Steiner, 1992).

- the produced ortho-negative is at one scale,
- the image produced cannot be enhanced and manipulated further for a particular application,
- the orthophoto has to be converted to digital form for use with a GIS.

3.1.3 Affine Transformation and Rubber Sheeting

Affine transformation, and polynomials of two and three degrees, and image matching³ have been used to correct image distortions (eg Ton, 1989; Goshtasby, 1987). A rubber sheeting process is one solution to the precise determination of correspondence between man-made features (roads) in an image and the GIS data (digital roads). A number of researchers have tried to overlay images with relief distortions. Prime examples are Bajcy and Briot (1982), and Goshtasby and Stockman (1986) who applied a rubber sheeting approach to register and overlay two sets of images. This approach attempts to overlay images with local geometric distortions with an elastic sheet and then to apply external forces to the image to be overlaid with the GIS data. When applying this force which deforms the digital image, the required corresponding points in the image and the map overlay can be obtained.

³ Matching is one of the basic processes in pattern recognition. The aim is to find the mapping between a proposed model and a set of data. It requires two steps to execute the process; (1) a model and the data have to be in the same representational form, (2) a similarity relationship has to exist between the model and the data. Further details can be found in Della Ventura et al (1990), Li et al (1993).

Rubber sheeting removes the flaws through the geometric adjustment of coordinates. The surface is literally stretched, moving other features using a piece-wise transformation⁴ that maintains the straightness of lines (ESRI, 1992b). To do rubber sheeting, a series of deformation vectors, so-called links, are required in which every link indicates where the coordinates have to be shifted (Figure 3.1).

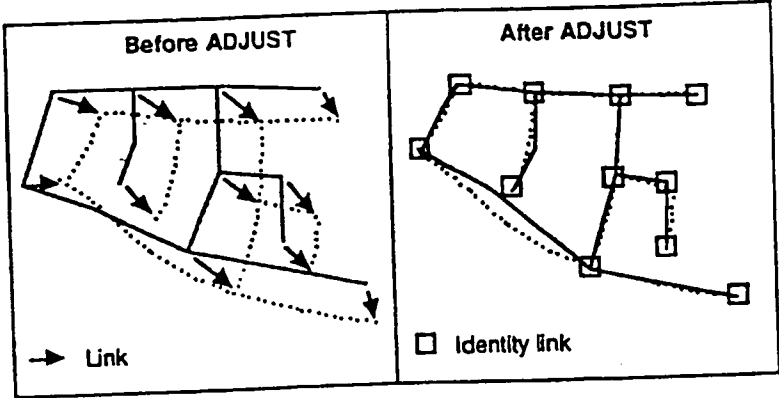


Figure 3.1 Illustrates a rubber sheeting by using links and adjusting position (ESRI, 1992b).

The rubber sheeting process often consists of a series of repetitive steps of adding links, modifying links and adjusting the coverage. It is important to have the links spread systematically over the whole coverage or grid including the outer edges in order to set the adjustment systematically with distribution of equal weight to the adjustment of all parts of the grid or coverage. The adjustment may have to be modified by deletion and addition of links (Figure 3.1).

⁴ This is described in ESRI (1992c).

3.2 Image Enhancement

(i) Filtering

Spatial filtering is a context-dependent operation in which the digital value of a pixel is changed, based on its relationship with the digital values of other pixels in the neighbourhood. Image enhancement techniques suppress or emphasise selected elements of an image to make the image more acceptable and more efficient for its users. For a linear feature which is wider than one pixel, a modal filter (template) may be implemented and linear features can be delineated but the results interpreted in a different way (Domenikiotis, 1994; Ko, 1995; Domenikiotis et al 1995). The extraction of different objects needs to apply different filtering functions with different kernel sizes. For instance, a 3x3 pixel sized filter will result in less blurring of the boundaries, while a 5x5 filter will reduce the amount of variance and therefore smooth out more scene noise and class boundaries. Care should be taken when the window size is larger than 5x5 (Cushnie and Atkinson, 1985). According to practical experiments (eg Cushnie, 1987; Walsh et al 1990), a 3x3 sized filter is more generally applicable than the larger neighbourhood windows for edge enhancement. Jazouli et al (1994) found that a 3x3 kernel size is the best filter for image enhancement in order to detect roads compared with testing 5 x 5 and 7 x 7 kernels.

Median filtering of 3x3 is commonly used to reduce the noise and remove outlying noise in order to get a smoother image for edge detection (Solberg et al 1990). This filter replaces the digital number (DN) of each pixel by the median of DN in the neighbourhood of that pixel. It uses sliding neighbourhoods to process an image to determine the value for each output pixel by testing an m x n neighbourhood around the corresponding original pixel input (Mathworks, 1995).

3.2.1 Edge Detection

Edge detection refers to the identification of edges in an image such as object boundaries, abrupt changes in surface orientation and material characteristics (Van Der Heijden, 1995). Trade-offs between edge detectability, noise sensitivity and computational efficiency are often involved in selecting a suitable edge detector for a

given application. Edge detectors generally suffer from weaknesses not only in sensitivity to noise, but also in poor performance near corners of structures (McKeown and Zlotnick, 1990). A successful edge detector for image segmentation depends upon a number of criteria. These include edge continuity, minimal width (sharpness), accurate location, and completeness in terms of discriminating all relevant edges. The literature describes many edge detectors. Typical examples are Sobel, Roberts, Canny, and Deriche edge detectors. There is, of course, no shortage of literature dealing with the edge detection problem. Numerous authors, among them Pratt (1978); Fischler et al (1981); Canny (1986); Deriche (1987 and 1990); Gonzalez and Wintz (1987); Argialas and Harlow (1990); Monga et al (1991); Mason and Wong (1992); Faugeras (1993); Abramson and Schowengredt (1993); Petrou (1993); Domenikiotis (1994); Aghajan and Kailath (1994); Forghani (1995 and 1997) have surveyed and applied edge operators. Classically, there are two types of edge enhancement technique:

i) First Derivative Operators or Gradient Enhancement Operators (ie Sobel, Roberts Cross, Kirsch, Prewitt)

These operators are limited to a particular edge orientation, and for linear features with higher and lower values on both sides, the gradient will be negative for one side and positive on the other. These shortcomings prevent the discrimination of edges by a simple amplitude thresholding technique. Thus these characteristics are not consistent with an ideal segmentation criterion. Most edge detection filters such as Sobel look for the edge of line in one direction at a time (Schanzer et al 1990). Roberts and Sobel filters have been widely used to suppress low frequency information in the image data and highlight high-frequency objects like roads. Due to the fact that roads are generally lighter or darker than immediately adjacent terrain, the Sobel edge operator can compute a direction which is aligned with the direction of maximal intensity change and a magnitude defining the amount of this change.

ii) Second Derivative Operators or High Pass Spatial Frequent Enhancement Filters (eg Laplacian, Canny, Deriche, Marr Hildreth etc.)

Using this approach, the Laplacian of a two-dimensional Gaussian distribution can be convolved with the image for detection of edges. Convolution with Laplacian filters approximates calculation of the second derivative only if the inflection points of the grey levels are aligned with non zero values (Rosenfeld and Kak, 1982). Whereas directional filters enhance digital number gradients with particular orientations, maximum output values can be generated by convolution over grey level variations in the associated direction (Pratt, 1978).

Two-Dimensional Edge Detection

In two-dimensional edge detection, an edge is defined by the maxima (its position) and the gradient magnitude (its direction) in which the image intensity is constant. In directions 0° and 90° , the edge map can be detected more precisely than other directions. In 45° and 35° directions edges will be more smooth in comparison to the directions of 0° and 90° . Thus maximum confusion will occur in 45° and 135° . It has been shown (Faugeras, 1993) that if one-dimensional edge detectors are used, an edge may not be detected by convolution of the intensity distribution perpendicular to its direction. In this situation, the error propagation will be distributed systematically. Thus, the two dimensional (2D) case seems to be more useful. Using 2D edge detectors can also give a misleading response for ramp-like variations (Domenikiotis, 1994).

(a) 2D Canny Edge Detector

The Canny edge detector reduces noise, locates the edge points, and minimises false response to edges in an image. It uses two thresholding values called hysteresis to avoid streaking. The threshold can be tuned based on the image content. It has been reported that there are three basic problems associated with identification of an edge location, namely, missing true edge points, the lack of complete ability to localise edge points and discrimination of noise signals from real edge points (Pratt, 1978). Most early edge detectors tried to handle the problems of computing some derivatives of the image

intensity and to find an ideal threshold to make the distinction between edge and no-edge (Faugeras, 1993). Canny's algorithm improved these errors by establishing three basic criteria for an ideal convolution filter:

- 1) Good signal to noise ratio
- 2) Good localization
- 3) Single response to one edge or minimal false response (uniqueness of response).

Like other edge detection algorithms based on the step-edge assumption, the Canny edge algorithm cannot perform well at non-step-edges, edge corners, and edge junctions (Mason and Wong, 1992). Petrou (1993) claims that *"It is impossible to choose a convolution filter which will maximize all three of these quantities"*. However, he combined them to maximize this measure. The implementation of feature extraction by Canny in conjunction with the use of optimal filters from remote sensing images, applying knowledge-based systems to identify roads, canals, hedges, and rivers is reported by Petrou (1993). A number of modifications to Canny's work are given (eg Deriche, 1987; Petrou, 1993).

(b) 2D Deriche's Approach

Deriche developed an optimal edge detection algorithm that can preserve Canny's criteria. Deriche reports that Canny's algorithm was implemented for an antisymmetric filter⁵. The size of the edge detector of the Deriche can control the amount of noise suppression without repetition of the iterations per output. To get rid of the false edge points, it is possible to perform some thresholding by applying a gradient magnitude. Canny's hysteresis⁶ thresholding uses two thresholds T_1 and T_2 where $T_2 > T_1$. Suppose a chain of connected edge points is characterised by the topological property of a contour, then if for one point (pixel) in the chain the gradient norm is higher than the

⁵ An antisymmetric (odd) filter has been designed to detect antisymmetric features such as step edges, whereas a symmetric filter has been implemented for symmetric features such as line edges. Further information can be found in Nalwa and Binford (1986), Petrou (1993).

⁶ Hysteresis thresholding refers to the identification of edges of all extremes whose magnitude is higher than a low threshold. Hysteresis thresholding allows local gradient extrema with low gradient magnitude to be removed (Monga et al 1991).

T_1 , a connected path of extremes must be maintained where the gradient magnitude is higher than T_2 by selecting the local maxima.

Two important parameters defined in the Deriche operators are local maxima α (controls the width of the impulse response), and T (threshold). The value of Deriche's approach is that by adjusting the local maxima α , the size of the kernel can be effectively controlled, and the amount of noise is suppressed without repeating the number of iterations per output. Deriche (1990) convolved an image in three step edges recessively to detect a noise by applying $\alpha = 1, \alpha = 0.5, \alpha = 0.25$. It was pointed out by Faugeras (1993) that to tackle the thresholding at the right level, only the edge pixels whose gradient norm is higher than some T can be kept. The hysteresis thresholding of Canny (1986) attempts to keep the edge pixels continuous as much as possible. Full algorithmic details of Deriche's and Canny's approaches can be found in Deriche (1990) and Faugeras (1993).

3.2.2 Thresholding

After applying an edge detector, the result produced is noisy. Thresholding is one of the most frequently encountered processes for classifying a pixel as an edge or non-edge (background) pixel from filtered images. Thresholding is based on the selection of a gradient percentage, which ideally could discard noise and keep the true edges. Fine tuning of the threshold is crucial in order to optimise the display of edge features. However, it is a tedious task. The basic question remains as to what is the best threshold. Faugeras (1993) says *"there is no good answer to this question, and the [threshold value] must be guided by application and the lighting conditions of the scene"*. The threshold (T) value depends mostly on image content, image quality, image geometry, and the amount of noise present in the data (Rosenfeld and Kak, 1982).

Hysteresis thresholding of Canny's edge detector provides one solution to this problem. As mentioned, if the threshold is set too low, there would be many dominant edges, points, and lines; while if the threshold is set too high, there would be some dominant features from which much useful information is removed. For example, the optimal threshold for Canny's operator has been reported as 70 to 80 percent (eg Canny,

1986; Gustari, 1996) using hysteresis thresholding. Experience has shown that the output of edge and line algorithms decreases significantly if the line or edge detectors are applied to imagery of urban scenes in comparison to rural areas (eg Forghani, 1995 and 1997; Geman and Jedynak, 1996; Forghani and Osborn, 1998b).

3.2.3 Mathematical Morphology

Geometric shape detection is an especially significant aspect of pattern recognition, finding many applications in machine vision, medicine, etc. Furthermore, the rule-based knowledge of shapes present in an image is a useful parameter as contextual information. In mathematical morphology, images are tested applying a structural element which is a small set. The points of the structuring element can be compared to the region surrounding a pixel in an image. A modification in pixels can be implemented in order to see how the points match and what operation was conducted. The structuring element is performed for every pixel of the whole area of the image. The traditional approach of mask convolution was combined with mathematical morphology by Destival (1986). It has been reported that the result of this approach is fragmentary and error-prone (Wang and Liu, 1994).

A considerable effort has been made to examine mathematical morphology as a tool for delineating linear structures from remotely sensed data (Asana and Yokoya, 1981; Destival, 1986; O'Brein, 1987). Destival (1986) pointed out that difficulties may arise when applying mathematical morphology due to the number of human interpretations required for rejoining and reconstructing line segments. As mentioned earlier, the linear features and urban area are very complex, and the use of mathematical morphology can be affected by the complexity of scene because of noise in the data. To overcome these ambiguities, the use of domain knowledge, and global information about roads and surrounding areas, improves the accuracy of the output. Noise edge responses may be mainly removed by discarding all responses that do not rely on either near or edge borders. Simultaneously, gaps in the lines can be filled by joining line pixels into continuous features to discard redundant information applying morphological transformations. Edge linking is a well known technique. The basic hypothesis is to find

local edge pixels using some low-level process, and to join them into contours on the basis of proximity and orientation.

The transformation of a binary image by mathematical morphology introduces the geometric structure and texture of line features using the concept of structuring elements. Possible tools for morphological operation (hit and miss transformations) are: bottom hatting, bridging, cleaning, closing, diagonal filling, dilation, erosion, gating, filling, horizontal breaking, majority, opening, removing, shrinking, skeletonization, spurring, thickening, thinning, and top hatting (Mathworks, 1995). Further details on the principles of mathematical morphology are presented by Serra (1988 and 1996).

3.4 Integration of GIS and Remote Sensing

3.4.1 Data Acquisition for GIS

Data capture refers to a digitizing or scanning process from existing maps, field surveys, direct input from digital cartographic database, CADs, photogrammetric records, aerial photographs and manual interpretations data from sensors into GIS compatible form. Remotely sensed imagery is a common data source for GIS. The RS data can be categorised into two major groups:

1. Raw data (eg satellite and airborne imagery)
2. Classified images

Classified images and existing maps are the major sources of data for GIS. There are many methods to meet this aim. Some of the important ones are listed below (Burrough, 1986; Stadelmann and Lodwick, 1993):

- manual input to a vector-based system
- manual input to a grid-based system
- digitization
- automated and semi-automated electromechanical scanning including raster scanners, vector scanners, video digitizers, and analytical stereo plotters.

Hardcopy maps and images must be scanned for use in a GIS environment. Researchers agree that to scan an image, 300-600 DPI (42-84 mm/pixel) is sufficient for many mapping applications (eg Steiner, 1992). A 300-500 DPI is a common range of resolution of raster images which can be binary (B/W) or full grey level image of 256 DN (digital number) or more. The achievable level of accuracy, detail, and production costs, depends largely on the type of scanner. The utilisation of low-cost desktop scanners is more common, and high resolution images need substantially more resources for data processing and storage (Pries, 1995). The relationship between digitizer instantaneous-field-of-view (IFOV) both in dots per inches and metres, and the pixel ground resolution at different scales of photography is provided in Cowen et al (1995).

The application, funds, and type of data being input will mainly determine the choice of data input. These data are existing maps, field sheets and hand-drawn maps,

aerial and radar images, satellite scanner images, point sample data (eg geological profile), census data, and other spatial surveys. To digitize the maps, they can be classified into two categories:

- types of map (point, line, area) and
- complexity (very simple, eg a map containing few lines; intermediate maps eg polygon maps and drainage maps, dense maps, eg dense road maps).

There are two basic manual digitizing methods; using tablet digitizing, and using interactive (vector over raster digitizing) editing. There are two common techniques for digitizing vector data from existing maps into a computer format.

- *spaghetti digitizing*, digitizing predominant straight lines such as roads and land use
- *discrete digitizing*, eg digitizing contour lines.

A hybrid vector and raster GIS software allows the user to capture the data manually by "overlay digitizing" for vector editing (drafting). The map data acts as a passive background frame of reference, to proceed in the establishing of vector map data (Jackson and Woodsford, 1991). The accuracy of this method of data capture is largely dependent on the skill of the operator and the availability of high magnification or resolution. A high speed graphics work station is critical in using interactive editing. This approach is superior to the first in respect of accuracy and speed.

3.4.2 Data Structure for GIS

The data structures can be classified into three major categories (Ehlers et al 1991):

(a) Raster Data

Satellite data and Digital Elevation Models (DEMs) are general forms of raster (grid) format. The raster input for GIS includes provision of remote sensing image analysis-maps, rasterized versions of cartographic data, interpreted point and profile measurements, and scanned maps (Ehlers et al 1991). Fidelity and accuracy of the output from employing the exiting representations of spatial data sources has mainly related directly to the quality of the course, geometric and radiometric accuracy of the scanner,

and the capabilities of the associated software. In a raster model an object can be given locations and attributes in an object model (Ehlers et al 1989).

(b) Vector Data

Vector data models differ in the level of topological information inherent in the data system, ranging from a simple data structure (eg spaghetti), in which there is no topological information except for the coordinates of points which form a polygon, to the more sophisticated models where topological information (eg the left and right polygons adjacent to a line) is recorded. For representation of geographic data in a raster-based system, the ability to specify a location in space will be limited by the size of the elements, due to the fact that the analyst will not know anything about the different locations within the raster cell. In contrast to the raster data systems, vector data models are constructed based on elemental points whose locations are defined to arbitrary precision. With geographic data in most GISs the coordinate data is encoded, and after processing, it will be stored as points, lines, and polygons or as a series of these combinations (Pequet, 1979). Burrough (1986) has provided a full definition and comparison of the forms of vector data structures such as whole polygon structure, arc-node structure, relational structure, and digital line graph.

The GIS data type can be classified as raster and non-raster dichotomy (Ehler et al 1991). Flowerdew (1991) classified the spatial data into five major types:

1. Dichotomous; this type is useful when the analyst is dealing with presence or absence of an interest object, eg presence or absence of kangaroos.
2. Categorical; this class scale is used when a region is classified into one or more classes, eg soil type, forest type, and national park.
3. Ranked; these data can be either naturally ordered eg suitability of agricultural lands for crops; or artificially ranked, eg the price of urban land in an urban area.
4. Count; eg population of a country, the number of male workers in a factory.
5. Continuous; eg average annual temperature.

Continuous surface data can be divided into two categories; one which represents features where each location is measured from a conform registration point such as elevation and aspect, and another which includes phenomena which progressively vary

with their movement across a surface from a source such as contamination of water from a nuclear reactor. Continuous data (eg slope, contour interpolations) in a grid are represented as a matrix of evenly spaced points called a lattice.

Jackson and Woodsford (1991) believe that vector graphics-based cartography and mapping data required for GIS applications based on data formats can be classified into three major categories:

- vector data in layers,
- vector data in feature coded form, and
- structured data.

For GIS and RS data to be stored in a simple access form, they should be allocated in specific data structures (Ehlers et al 1991). Specific data structures for GIS and RS may include (Frank and Barrea, 1990):

- Kinds of geographic phenomena (point vs area)
- Object handling (non-fragmenting vs fragmenting)
- Division of space vs data determined, and
- Retrieval (direct vs hierarchical)

(c) Hybrid Structure

Hybrid models of spatial data structure may provide an explicit integration between raster and vector data for many GIS applications. A classification based on a hybrid model may consist of location-based and attribute-based data models (Vanzuella and Cabay, 1988). The strength of a hybrid spatial data structure is that the model allows classification of most existing spatial data. This data model corresponds to the two major spatial data representations of vector and tessellation models. These authors pointed out that this model can be a superior empirical alternative choice for representation of very large thematic data in GIS applications. The CGIS (Canada Geographic Information System) which partitions the vector data (chaincode) represents a theme by applying tiles of fixed area. However, it is in spirit similar to a HMSDS (Hybrid Model of Spatial Data Structure). Ehlers et al (1991) provided a detailed discussion on the hybrid topic.

Current GIS deals mainly with digital map data, which are two-dimensional (2D), and which are static in time. Much environmental modelling requires data with additional dimensions, normally the vertical spatial dimension and the time dimension. For example, to predict the movement of ocean water masses in 3D space, and time under different forcing agencies of ocean currents and tidal flows, wind and pressure, 4-dimensional capabilities are required to satisfy the model in question. The need for handling four-dimensional (4D) georeferenced datasets has been addressed and implemented (Mason et al 1994).

3.4.3 Data Conversion

Processing of spatial data in image processing and GIS generally contains some types of data conversion. Geographic data may be represented in three varied formats, vectors, raster, and mathematical modeling. The last format has proved to be not significantly efficient in GIS applications (Zhou, 1991). Conversion of vector to raster formats (and vice versa) has been widely discussed in the computer literature, and the data conversion problem has been addressed (eg Peuquet, 1981a and 1981b, Piwowar et al 1990).

The task of vector to raster conversion is not as difficult as conversion of raster to vector (Lunetta et al 1991). For this reason, a grid format is used as the major data structure of the incorporated GIS vector-based data (Wang and Newkirk, 1988). The difficulty in transferring vector to raster lies in the large number of polygons generated if the data are directly transferred to vector format. In the worst case condition, each pixel in the image becomes a polygon which requires a huge disk space for storage. Furthermore, in many situations the required result of image classification may not be a pixel map and tends to be a polygon map of areas of similar characteristics. In these situations, it is a good idea to resize (reduce) the pixel by pixel classification to some smaller number of polygons such as simplifying the image.

Two common approaches have been reported: the *Image Strip Frame Buffer* algorithms, and the *Scan Line* technique (Piwowar et al 1990). The first method will keep a feature by representing it with at least one pixel without considering the size of

feature. The latter approach will eliminate the features which are smaller than the cell size.

Grid is an implementation of a generic raster data structure. According to ESRI (1992e) *"the term raster data structure refers to a matrix composed of distinct units called pixels or cells. Each pixel stores a numeric value. The pixel in a raster image usually consists of continuous brightness values represented as digital numbers. A raster image may be converted into a raster map by using image processing techniques to label each pixel with a numeric value indicating its category or surface type.....It [GRID] uses blocks and tiles for spatial indexing and an adaptive run-length compression technique for reducing storage. Hence, both raster images and raster maps can be stored in GRID"*.

(i) Choice of Cell Size

The cell size is a parameter that can be determined by its usage. Deciding what cell size is to be applied is a crucial decision to be taken when using cell-based GIS modelling. Important parameters influence the decision regarding raster cell size such as the resolution of the input (original) data eg vector database, the disk space requirements or storage overheads, the processing speeds or time, precision and positional accuracy requirements of the analysis, and the application and type of analysis to be implemented (Burrough, 1986; ESRI, 1992e; Carver and Brunsdon, 1994). It should be kept in mind that a cell size finer than the input resolution will not produce more accurate data than the original data. As a general rule, the cell size of a grid should be equal to or coarser than the input data. Cell sizes vary from square kilometres to a centimetre. The selection of the cell size of a grid can have a critical effect on the results of the conversion. If the cell size of the pixels is large in regard to the dimensions of the objects in an image, some generalisations have to be made. Storing vector-based GIS data in a raster form demands significantly more storage space, otherwise very fine resolution (pixels sizes) is in place. If it is, there is a loss of accuracy in sampling to coarser resolution raster grid (Aronoff et al 1987). It was noted that raster size is the major obvious control on rasterizing error (Carver and Brundson, 1994), and several empirical pieces of research have shown that increased raster size has an extensive effect in reducing map accuracy.

(ii) Raster-to-Vector and Vector-to-Raster Conversion

There are two types of conversion algorithms:

1) Vector to Raster

Two basic steps are involved. Firstly, the polygon boundaries in the form of vector files have to be transferred to the raster image by establishing the correspondence pixels to the value of the polygon. Secondly, the interior of the pixel outline is then filled with the classification value. The task of converting vector-based cartographic data into raster-based formatted images may be categorised into major components, namely rasterization or scan conversion, and line thickening. These components have been widely described in mathematical morphology in image processing literature (eg Serra, 1996) and GIS papers (eg Pequet, 1981).

(a) Advantages of Data Encoding and Handling in Raster Format:

The raster structure is suitable for a very large database. A large proportion of the data required for a GIS are being collected directly from aerial and satellite imagery. Experience has shown that there is a number of advantages if the data are encoded and managed in raster format:

- there is a highly accurate interpretational element on the image,
- partitioning is easier in multi-tasking aims,
- it is useful in resource management applications such as forestry, soils inventory,
- most image processing software being developed for the RS field is cheap and developing rapidly,
- storing data in raster (eg a classified image) is easy,
- many input and output hardware devices are compatible with the raster data structures,
- it is a simpler and cheaper data structure for establishing GIS data,
- handling raster data is suited to some programming languages eg FORTRAN because of the ease with which arrays can be stored and manipulated.

(b) Disadvantages of Data Encoding and Handling in Raster Format

There are a number of disadvantages:

- it requires extensive knowledge of photointerpretation,
- the risk of losing information within the data is high, for example, to detect boundaries of regions in terms of edges,
- the lack of high spatial accuracy,
- the lack of radial symmetry in grids, resulting in network analysis being hard to perform (Peuquet, 1983),
- most operational GIS software is designed for vector-based methods,
- in the case of using compaction methods such as quadrees, chain, run-length codes, and block codes the risk of loss of implicit topological information is a concern; due to the limitation of hardware memory; thus more processing overhead is needed as compensation (Burrough, 1986).
- a major drawback is the need for large memory space because of data redundancy (Burrough, 1986). However, to remedy this problem, compact forms of data storage and data structure such as quatees have been adopted in raster-based GIS.
- conversion of data from raster data (eg classified satellite data) to vector is difficult.

2) Raster to Vector

This refers to both the batch process and the interactive process of extracting pixels which represent lines or graphics, and isolating these pixels from the background to be converted into a connected vector representation. An adequate resolution must be provided by the source of raster image for the geometry in order to be accurately delineated by vectorization algorithms (Jackson and Woodsford, 1991). Generally, a minimum of 2-3 pixels is required in the finest lines to maintain a cartographically acceptable vector representation. In contrast, an optimal number of points is required to prevent cluttering up the GIS databases. There are three major steps involved; boundary extraction, topology reconstruction, and boundary smoothing. Also, to convert a raster-formatted map into vector format, three basic operations have been reported, namely skeletonization or line thinning, line extraction or vectorization, and topology

reconstruction. These topics have been widely discussed in mathematical morphology in image processing texts (eg Serra, 1996) and GIS papers (eg Pequet, 1981).

(a) Advantages of Data Encoding and Handling in Vector Format:

Experience has shown that there are a number of advantages if data is encoded and managed in vector format including:

- in representation of a contiguous area it is very difficult to locate the vector polygon which best represents it,
- vectors well work in accurate representation of real world spatial conditions such as lines, edges,
- capturing important topological information is problematic if a raster approach is undertaken,
- vectorization is highly effective in some application areas such as property and utilities mapping,
- the CPU processing burden for image processing is sufficiently high that grid data structures are the only possible alternative on low speed systems,
- it seems that raster processing is more natural due to the fact that detectors operate to capture raster digital information directly, although vector processing has been used in some applications,
- a great deal of information on the earth's surface has already been captured; almost all of the generated maps, as well as photointerpretation maps are available in vector format,
- vector data keep the real geometry of a polygon using a series of vertices linked by straight lines,
- generally vector data are a preferable method of display and visualization for the majority of GIS thematic maps, due to the fact that lines and edges will appear smoother.

(b) Disadvantages of Data Encoding and Handling in Vector Format:

In spite of the elaborated advantages of data encoding and handling in vector format, there are a number of key disadvantages:

- transforming highly accurate interpretative pixels into data is sometimes misleading. Suppose that there is an image of an area, many phenomena can be seen without sharp boundaries, If one wishes to impose lines (vectors) on the image to aggregate such phenomena, then a problem of false conception occurs.
- it is difficult to implement for multiple attributes.
- data structures in vector data systems are complex and the technology is expensive to establish (Skidmore, 1990), Also for polygon overlay, the vector approach is difficult and tedious.
- Drawing of the transitional spatial phenomena by different image interpreters in different seasons is subjective due to overhanging and overlapping of trees and their canopies in a wooded area.
- Boolean and overlay operations on different layers are relatively difficult.

3.4.4 Error Sources from Integration of RS and GIS Data

To perform spatial analysis in a vector GIS, boundaries of relevant feature maps eg land use, forests, are effectively imposed on a base map of common scale. In the same manner, in a raster based GIS analysis, cell to cell correspondence has to be identified and the output cell has to be labelled according to corresponding cells of each feature map (Lowell, 1994).

GIS analysts should consider the accuracy of produced maps before decision making. Error is a major issue in any integration of RS and GIS data when using integrated ancillary and collateral datasets (Estes, 1992).

Errors come from many sources, for example Lowell (1994) noted that (1) Errors in map registration, especially in a vector GIS, may cause an excessive number of seemingly aberrant silver polygons. Since remote sensed images are increasingly being employed as a data source in GIS, georeferencing of these images may introduce errors as well. (2) Errors associated with each map layer can be so serious as to invalidate the results entirely. (3) Spatial distribution of such errors cannot be random leading to high variability over a variety of locations.

Chapter 4

BACKGROUND: EXPERT SYSTEMS CONSTRUCTION AND KNOWLEDGE-BASED INDUCTION

Expert systems are composed of a knowledge base, knowledge representation, and inference engine. Since the decision tree is one way of knowledge representation, knowledge in the form of rules can be formulated for development of expert systems. In this chapter the main components of an expert system will be described. The chapter will also provide an introduction to decision tree algorithms. Construction of an ideal decision tree in the context of tree growing, tree pruning, and methods of accuracy estimation is discussed.

4.1 Artificial Intelligence and Expert Systems Implementation

4.1.1 Definition and Background

An Expert System (ES) is defined as "a system of software or combined software and hardware capable of competently executing a specific task usually performed by a human expert. ES are highly specialised computer systems capable of simulating the element of a human specialist's knowledge and reasoning that can be formulated into knowledge chunks characterised by a set of facts and heuristic rules" (Bowerman and Glover, 1988). "Better" can mean more accuracy, more speed, more economy, and more consistency. There are several definitions for ES in the basic texts.

The implementation side of artificial intelligence (AI) is the use of expert systems (eg Domenikiotis, 1994). AI can be grouped into three major categories, namely robotics, ES, and natural language processing. AI began in earnest with the emergence of modern computers during the 1940s and 1950s with one of its goals being to make machines more intelligent and thus useful. ES represent by far the most mature area of AI research and development. The science of AI from the early 1950s has focused into two main streams consisting of 1) psychological or cognitive modelling and 2) search methods.

Following the incremental progress in the AI field, ES were initiated from the AI community in the late 1960s involving a shift in focus from formal reasoning techniques

to a focus on knowledge itself, and interacted with many applications in engineering and medical science disciplines. Likewise many AI terms, ES is loaded with extensively more implied intelligence than is warranted by their real level of complexity (Mason, 1995). The AI community has devoted considerable effort towards development of highly complex search strategies and inference engines. An example of typical problem solving is the development of ES in computer chess games (Bielawski and Lewand, 1988). Apart from the AI community challenges, many contributions have been made from non-specialists of the AI in other groups who developed extremely robust ES interfaces.

In the early 1970s the knowledge base was separated from the inference engine. This isolation was an indication of the successful maturing of ES. By 1980, however, it became clear to many AI developers that ES architecture is built on structured knowledge. Thus, knowledge-based-systems became an apt definition for many ES designers. The new knowledge-based-systems (KBS) terminology is often used rather than the more popular term ES (Bielawski and Lewand, 1988). Since the 1970s production systems and knowledge representation emerged into a well-organised structure.

ES are computer systems that use knowledge and inference procedures for solving problems that are difficult enough to require significant human expertise for their solution (Karimi and Lodwick, 1987). In comparison with conventional computer programming methods, ES are designed to associate a large amount of fragmentary, judgemental interpretation, and heuristic knowledge. This assists experts in decision-making, even if human expertise may not be available at the given time, and will speed up the operation of problem solving (Stadelmann and Lodwick, 1993).

Computers require human reasoning for decision making. Such decision making may be made by applying probabilistic rules that reflect a given knowledge-base corresponding to a specific condition or conditions. Every rule depending on its degree of correlation to the given circumstance, is given a different weight when finding a conclusion to a problem. Rule-based systems are currently used in image analysis tasks such as road detection from remote sensed imagery (eg Pai et al 1986; Ton et al 1991;

Domenikiotis et al 1995). AI provides an alternative to human expert interpretation by associating a degree of intelligence into the image analysis system to enhance the human interpretation of an image (Domenikiotis, 1994).

There are two principle approaches to build an ES. One may employ a programming language and write original code from the beginning for the system. There are specialised languages for development of ES such as LISP and PROLOG. The other approach relies on the tools developed (shells) to assist in building of ES. The shells facilitate the development of ES and require only minimal knowledge of any high level programming.

An ES may be composed of three knowledge levels, namely facts, rules and inference engine. There are three major operations involved in construction of ES.

4.1.2 Components of an Expert System

4.1.2.1 Knowledge Acquisition

Knowledge acquisition is the process of collection and formation of knowledge content of ES. This step is associated with the entire life cycle of the system from design to maintenance. It deals with transfer and transformation of problem solving expertise from knowledge source to software systems. Knowledge acquisition is the extraction of rules to solve problems from an expert and human expertise in an area and its representation, in a form commensurate for machine intelligence processing. The process of transferring knowledge for example from teachers to students, and from parents to children is a knowledge transfer form which is a natural process, whereas in transferring knowledge from an expert to a computer, the naturalness disappears.

Computers have a limited ability to handle the information held. There are several phases in the knowledge acquisition process including knowledge elicitation¹, knowledge extraction from the knowledge sources, knowledge encoding into symbolic form,

¹ The term knowledge elicitation refers to the process of extracting and capturing knowledge from an expert or other sources in such a manner that it is comprehensible to people. It compasses the collection of all information that knowledge engineers need to build an ES.

knowledge based organising, and modifying to gain the best performance (Marshall 1990).

Primary sources of knowledge for an ES can be books or manuals, case studies or test cases, human experts, technical articles, learning from examples, discovery, and the like. Rules may be produced from the knowledge base. The process of knowledge rule extraction may occur through an interviewing mechanism with the expert, where he or she attempts to find the basis on which the decisions can be made. Alternatively it can be done through testing of a quite large and different set of primary input states, and decisions can be made by the expert. Machine Learning is an area that deals with the automation of this process of knowledge acquisition.

The process of building knowledge in the ES is defined as knowledge engineering. It is the process where knowledge from the expert can be captured with all the elements of heuristic experience. To structure the ES, the knowledge has to be collected from appropriate knowledge sources either manually or automatically. In the AI field the manual method is often used as a standard technique in which knowledge from a domain expert and other ancillary sources is acquired, and more specifically, people are the source of gaining knowledge.

A major bottleneck in developing knowledge-intensive AI systems is the derivation of knowledge (Bielawski and Lewand, 1988; 1993; Al-Garni, 1995). In interpretation of an image the key elements such as shape, shadow, pattern, size, association and tone, are the major attributes in the system. A more advanced interpretation of elements such as landuse, geology, etc. can provide knowledge for building a system. Often, the knowledge is not organised in a proper form, and experts use knowledge which is clear to them, but not to others, and the expert has to compile the knowledge. In designing an ES, it is critical to assign the number of subjects required to assist the problem solving capabilities of a given system. In addition, it is important to gauge the depth of knowledge in order to determine an ideal amount of required knowledge. Decision trees are examples of the induction method for generating knowledge or rules from a set of examples. To make the ES more powerful, the expert may add some learning abilities to the system.

4.1.2.2 Knowledge Representation

In the early 1970s knowledge representation was recognised as a critical step and a unique research area (Lucas and Van Der Gaag, 1991). Acquired knowledge may be encoded to solve problems. The result of collected knowledge has to be presented in forms suitable for the approaches of AI problem solving. Up to now, many diverse algorithms have been developed to derive information. Broadly speaking, these methods are not only different in the actual algorithms but also different in the form of knowledge representation that they apply. For example, De Ville (1990) has developed an algorithm (KnowledgeSEEKER) that produces the knowledge from example data and represents it in decision trees.

Several knowledge representation schemes exist and more are being developed as research becomes more sophisticated. Decision trees and rules are the most common methods in this context, although it is possible to extract the rules from a decision tree. Some machine learning software can represent the knowledge in a decision tree form, and then if the user wishes to have the knowledge in rules, the software can automatically generate rules as both generic rules and programming statements (eg PROLOG). For example KS which is a decision tree based software offers this capability. ES tools such as KS, and 1st-Class offer induction learning by which they accept sets of examples and automatically generate rules.

To design an ES, development shell tools (eg inductive shells) are required. Inductive shells use the concept of machine induction to facilitate the process of knowledge acquisition. Some ES development tools may provide an alternative to clearly formulating and entering IF ... THEN rules or IF-AND-THEN statements into a knowledge base. Thus, rules in the knowledge base contain separate CONDITION and ACTION parts. The CONDITION may contain Boolean operators such as AND, OR, and inequalities such as >, <, =. The conditional part is taken into account as a pattern, and the statement part may characterise an action to be carried out on a successful match with the pattern. The ACTION part of the rule represents: IF the condition is satisfied, THEN the relevant rule is invoked. Rules consist of premise-action pairs, for example:

IF R1 & ... & Rn,
THEN C1 & ... & Cn.

with reading IF premises R_1 and ... and R_n are true, then actions C_1 and ... C_n , are performed. The R_i and C_i are "condition", and "conclusions" respectively.

Neural networks are another form of knowledge extraction and representation. The neural net represents their knowledge at the lower level, while knowledge-based systems use higher knowledge representations.

4.1.2.2.1 Inference Methods

The approaches to knowledge representation were discussed in earlier sections. There is a wide range of approaches employed in AI for information extraction from knowledge. These approaches of so-called methods of inference include deduction, induction, intuition, heuristic, generate and test, abduction, default, autoepistemic, nonmonotonic, and analogy (Giarrantano and Riley, 1989). Expert knowledge, or commonsense knowledge, may be an association of all mentioned inference methods. Explicitly, the method of inference for ES is based on the method undertaken to represent knowledge. Since this research is more interested in the induction approach which will be discussed later, the other methods are not discussed.

4.1.2.3 Inference Engine

The inference mechanism can be divided into two chaining methods:

- 1) Forward chaining or data-driven chaining to reach a conclusion (bottom-up reasoning) where reasoning starts as the original state of problems from the evidence, facts, to the top-level conclusions that are based on facts. In forward processing, the inference mechanism will compare the information in the goal data base not with the THEN part of a rule in the knowledge base, but rather with its IF part (Bielawski and Lewand, 1988). In the forward method if all the premises are satisfied, then the conclusion is gained, a fact is changed, a new rule can be examined and so forth. A group of inferences joined to give a solution to a problem is a so-called chain (Giarrantano and Riley, 1989). The elementary technique of forward chaining arbitrarily begins with the first rule in the knowledge base and an attempt to use it. This rule or any other rule, requires all of its premises to be known to be true ahead of time. The process is called

"true list" on which are stored all the things found to be true. The true list will be employed at the beginning of every decision, and filled in as the decision process progresses. The forward approach can be used in maintenance circumstances with all required information existing at the starting point (Wang and Newkirk, 1987).

2) Backward chaining or goal-driven chaining or sub-goaling (top-down inference) is where processing starts from the higher level evidence (hypotheses) down to the lower level facts that can support the hypotheses. The processing starts with a conclusion and proves that conclusion by providing the truth of each premise in a left to right, or top to bottom, order. It differs from forward chaining in that the operator begins by assuming a conclusion to be true and then applies the rules to try to prove it. Backward chaining is often well organised (Giarrantano and Riley, 1989). In the backward strategy the inference guesses at a conclusion and then tries to prove that its guess is correct by finding a rule whose THEN part is the same as its guess, and setting up the condition (s) exited in the IF part of the rule. The backward technique is more applicable for interactive problem solving. Primarily a goal is established which should match with the conclusion of one of the rules. PROLOG is an explicit example of a backward chaining inference engine (due to backtracking functions) with considerably more power than most commercial shells that utilise the same method. The goal defines a hypothesis, and the system tries to identify evidence, as facts are named in backward inference, which support this conclusion. Backward processing may be a good inference approach when the operator is able to reasonably guess what the conclusion will be.

The heart of the ES is often an inference engine used to decide which rules have to be satisfied, leaving them in a priority list, and executing those with the highest priority. The facts or rules are stored separately and employed by the knowledge-base for the firing of the conditional part of the rule. It is intended to undertake a forward chaining strategy to the execute the decision rules against the spatial database to perform road mapping, which will be implemented in Chapter 8.

4.2 Extracting and Representing Knowledge with Decision Trees

4.2.1 Background

A common approach to supervised classification and prediction among the Artificial Intelligence and Statistical Pattern Recognition community is the use of decision trees. Classification trees (decision trees) may not be the most accurate approach, but they are user friendly to interpret. A number of algorithms have been developed to build decision rules from examples of decisions made by an artificial intelligence system.

In this section some aspects of decision trees will be discussed. While no attempt is made to provide a comprehensive survey, other relevant work will be pointed out in this area. Techniques for the construction of an automated decision tree have been described in the contemporary literature. The use of trees in regression dates back to the AID (Automatic Interaction Detector) program which was developed by Morgan and Sonquist in the early 1960s. The ancestry classification program is THAID and was developed by Morgan and Messenger in the early 1970s. Indeed, there have been many independent inventions of the decision tree methodology, which dates back to the 1960s. In particular Quinlan's C4.5 is a descendent of his 1979/1983 ID3 (Interactive Dichotomizer). In an improved AID, more information can be found in Kass (1980) for more improvements in the technique called CHAID, also the technique by Quinlan (1986). Standard decision tree algorithms are CART (Classification And Regression Tree) by Breiman et al (1984) and its successor C4 and ID3 (Quinlan, 1986). There have been many algorithms proposed since the creation of CART methodology. Others have created their own original algorithms eg Quinlan's C4.5. Meanwhile, other descendants of AID, CHAID, and THAID, are still in use. More recently, De Ville (1990) developed an AID-based algorithm called KS which was employed for this research.

Quinlan et al (1986) have achieved some success in using these methods to assist in the induction of a knowledge base for use in knowledge-based systems. The ID3 algorithm and its relatives are primarily designed for categorical variables. The CART algorithm is suited to continuous independent variables and categorical dependent

variables. In systematic classification tree construction, past experience is summarised by a learning sample. Historically, ordinal variables are referred to as monotonic, while categorical variables are free. Ratio and interval scale fields are treated as monotonic. KS, which is based on the AID approach, accommodates both categorical and continuous types of variables.

4.2.2 Inductive Learning

Broadly speaking, the induction task is to find general rules in order to generate, classify, or define a training set of particular examples and correctly predict new examples. Learning is the ability to perform new functions that may not have been performed before and is essential for any intelligent behaviour. Any system which is intended to be intelligent should include a learning procedure. Inductive learning particularly is suitable when there exists no strong background knowledge. Researchers have suggested a number of approaches to induction mechanisms, such as the use of decision trees and production rules.

There has been considerable research on the learning concept in which objects, defined in terms of a fixed collection of attributes, belong to one of a small number of mutually conclusive and exhaustive classes. The learning function may be defined as given a training sample object whose classes are known, find a rule for forecasting the class of an unseen (underlying knowledge) object as a function of its attribute values (Quinlan, 1990). Learning from examples is a special case of inductive learning from which, given a set of examples and counter-examples of a concept, the learner induces a common concept definition which defines all of the positive examples and none of the counter-examples. This method has been widely applied and investigated in artificial intelligence. It has been studied since the early 1950s by many researchers.

4.2.3 Decision Trees

Decision trees are a sequential data analysis. They have been widely used in many areas for decades, for example, in pattern recognition, taxonomy, decision programming and switching theory, medical domains, more recently in environmental modelling and mapping of land use/cover using remote sensing imagery and GIS data. Industrial

applications include systems for diagnosing faults in printed circuit boards, assessing space shuttle engine performance, dealing with problems associated with nuclear fuels, and assessing credit card applications (Gray, 1990). The decision tree can be regarded as a type of automatic taxonomic key.

The decision tree classifier is an important and efficient technique for separating samples (observations) into categories or for predicting the highest output to a given situation. Decision tree methodology is nowadays recognised to be a generally non-parametric method, able to produce classifiers in order to evaluate new, unseen circumstances (Quinlan, 1986, Wehenkel and Pavella, 1991). In the area of decision tree induction, empirical comparisons have been implemented by Breiman et al (1984), Quinlan (1986 and 1990), and De Ville (1990) to guide the development of these learning systems. The decision tree approach appears to be an alternative that allows a selection of techniques and also acts as a tool in describing the most appropriate techniques and data sets (Lees and Ritman, 1991).

Most work has been focused on recursive partitioning with the partitioning driven by some optimisation procedure. Classification and segmentation is implemented through a series of splits (decisions) in the different fields. Zhou and Dillon (1991) have indicated extensive research on the use of decision trees. They stated that four parameters are essential in a decision tree algorithm:

- 1) a set of features,
- 2) a feature selection criterion,
- 3) a stop-splitting rule, and
- 4) a central role in the quality of the decision tree as a classifier and its complexity or simplicity.

(a) Advantages of Decision Trees

There are a number of advantages with using decision trees including:

1. Utilisation of contextual information; the major powerful aspect of a classification trees is the use of contextual information as the result of isolation of local interactions in relationships. Every decision rule will reflect the characteristics of a particular subset of all available observations of each class.

2. It is inexpensive to use; each decision rule may not need to be considered for all ambiguities in that particular class (Walker, 1991).
3. Lack of complexity and simplicity of interpretation and understandability; it is easy for people with minimal knowledge of statistics to use (Walker, 1991).

Inductive learning has some limitations which should be taken into account when using these algorithms.

(b) Disadvantages of Decision Trees

There are a number of disadvantages with employing decision trees such as:

1. Lack of high sensitivity if a minor change happens in the composition of learning samples (Walker, 1990).
2. Lack of a good extrapolation (Lees, 1994; Walker, 1988) and absence of justification (Khoshnevis and Parisay, 1993). For instance, it is possible to gain a rule which, in the context of its domain knowledge does not make sense. This may take place due to inappropriate control feature engineering or improper experiment design.
3. Difficulties in selection of a "right sized" tree or "better" tree (Walker, 1988) and the existence of probable noises² (Khoshnevis and Parisay, 1993) in training instances. The use of neural networks is one solution to a noisy domain. A neural network effectively filters out noise and enables production of the correct rules defining the domain.

In particular, the inductive modelling in GIS suffers from such as number of examples required, lack of efficient algorithms and the problem of noisiness of data.

4.2.3.1 Induction of Decision Trees Algorithms

(1) ID3

Induce is a common-purpose inductive program that transforms definitions of examples into general definitions of the concepts of which the examples are instances (Gemello et al 1991). Several commercial packages use ID3 algorithmic derivatives to

² Noise is referred to as errors such as misclassification of instances, incorrect values of control features, and unknown (missing) control feature values.

discover unseen knowledge inductively from large data sets. Most of the proposed inductive inference techniques have been released from the ID3 algorithm (Quinlan, 1986), from which, however, it departs in some essential aspects. ID3 is an inductive learning technique for categorical data that maximises homogeneity at the leaf nodes through use of an information theoretic measure. It has performed well in various medical diagnostic and other engineering applications and has shown empirically to be relatively powerful in the presence of moderate amounts of noise (Liepins et al 1990).

The ID3, originally intended to handle mostly symbolic and deterministic learning problems, is characterised by very large (almost complete) learning sets composed of objects defined by discrete (or qualitative) attributes only. Therefore it was necessarily designed to handle large sets of data in order to compress rather than extrapolate their information (Quinlan, 1983). ID3 uses the training data to construct a decision tree for determining the category of an example. At any step, a new node is added to the decision tree by partitioning the training examples. Empirical comparisons can be taken into account as an important part of machine learning research.

Quinlan (1983) created a top-down induction of decision trees (TDIDT) technique for encoding the knowledge which is required for direct play in chess end games. The ID3 algorithm, which handles a principal version of TDIDT, has been widely adopted and extended. Most of the typical decision tree induction procedures belong to the family of TDIDT algorithms (Quinlan, 1986). Gray (1990) applied the TDIDT to capture knowledge through top-down induction of decision trees. The TDIDT approach restricts search by using a heuristic measure, considering combinations of attributes appearing to have a high information content. Evans et al (1994) followed the idea of Quinlan (1986) who used weather observation in order to apply the TDIDT. They categorised new observations by examining the tree from the top down. According to its value for the attribute at the root of the tree, an observation was classified into one of the three classes at the next lower level.

The learning principle of the algorithm ID3 induction of decision trees (Quinlan, 1986) can be briefly explained as follows: Find the best attribute with the highest information content and locate it at the root of the tree. The set of examples can then be

divided into subsets. Any subset has examples belonging to one and only one class. Consequently make the subset a leaf of the tree and choose for it the label of the special class. Alternatively, find in each of the subsets the best attributes, splitting the subsets into subsubsets and so on until both the remaining subsets are empty and assigned a label, until there is no unused attribute. In other words, the process continues until a terminal node or leaf is reached; the class that labels the leaf is predicted as the class of the new observation.

The ID3 stops splitting at a node only if the corresponding learning subset is entirely included in one of the classes of the goal partition. ID3s stop splitting criterion amounts to building decision trees which classify the learning set as correctly as possible, which is the best policy if the latter is almost complete. ID3 considers the best test to be the one providing the largest apparent information gain. It has been stated that this measure is biased in favour of those having the largest number of successors, particularly in the context of randomness (Wehenkel and Pavella, 1991). They compared the ID3 technique and a proposed method for building a decision tree. If the training set is large and the data noisy, pruning can be implemented. Trees are included in a two stage process often referred to as growing and pruning. A great deal of effort has been made in developing decision trees for induction, generally in the form of pruning strategies. These techniques have been discussed widely (Breiman et al 1984; Quinlan, 1990; Walker and Moore, 1988; Lees and Ritman, 1991).

(2) CART

CART is a method of producing a set of decision rules to explain an observed pattern. This technique is described in detail in Breiman et al (1984). Trees are built by splitting a set of observations into two partitions (Walker and Moore, 1988). Splitting can be continued as long as impurity can be decreased. All splits in CART are binary. CART offers two options: least squares and least absolute deviation from the median. Least squares is well suited to data that satisfy ideal circumstances and faulty outliers (Liepins et al 1990), while least deviation may be considered to be a more powerful analysis approach (Liepins, 1990). CART is an appropriate choice for real attributes with dependent variables (Liepins et al 1990).

(3) KS

KS is an AID-type algorithm which works on multiway partitions (k-way) as well as binary tree (two-way splits). A multiway partition for classification and decision tree was revealed to remedy the shortcomings of the cluster method. Because, in exhaustive splitting, all possible combinations of variable values are taken into account, this approach will be more costly. In KS the integration of the two methods is implemented and can be used for classification trees. Bonferroni adjustment in KS tries to minimise the discovery of chance relationships or bad effects. It also employs validation, cross-validation or tree pruning at every stage of the decision tree growing. Normally, this will cause the tree to stop growing before actual significance is exhausted.

KS uses two methods of split search, namely cluster and exhaustive to grow the classification tree. If the cluster method is applied to a categorical dependent field it is often referred to as the CHAID approach, while if it is applied to continuous dependent variables, it is similar to the CART algorithm. The cluster method utilises a method of pair-wise merging and partitioning that was originated by Kass (1975 and 1980). Statistically speaking, the disadvantage of the cluster method is that it is overly conservative and some significant relationships may be missed (ANGOSS, 1994). Biggs et al (1991) described the Monte-Carlo experiments which prove that the exhaustive method is not overly conservative and will not generate misleading relationships. The exhaustive method (multiway partitioning technique) tends to produce a tree with more branches in comparison with the cluster (heuristic method) technique. The major shortcoming of the exhaustive technique is that it is a more time-consuming process, while in contrast the splits formed are empirically stronger than heuristically derived splits (ANGOSS, 1994).

In relation to tree growing and pruning, one approach is to look at the problem from the opposite side of how to prune a tree to build a best set of rules. This involves checking the growth "at the pass". KS may generate a 4-branch split, say, below a given node, but semantically 3 is all that is needed. For instance, if a variable refers to a quality test result, the regions corresponding to "pass", "too low", and "too high" are all that are really relevant. Without knowing this, KS may find an apparent sub-distinction in the

too-high region. If this happens, the operator can "force" a split, specify the three ranges and see if the threshold (p) value remains acceptable. Clearly, removing a branch near the top of the tree can save dozens of nodes below. It may be possible to use an integrated pruning algorithm that links the two approaches.

4.2.3.2 Decision Tree-Pruning and Accuracy of the Classification Tree

The question remains as to what is the best way to prune a decision tree in order to construct a "better" tree and to end up with a proper number of rules for the available learning examples. The major difficulty researchers have encountered, is how to choose the size of the tree. Researchers believe that it is complex and difficult (and may be impossible) to define a theoretically "best" tree for a set of data. This is a real problem, with no satisfactory answer. In general, the best tree is the one that makes most sense from a theory, and theory development.

Two leading authors of decision tree algorithms have used different strategies to generate an ideal decision tree. Use of purity measures to stop the tree from growing is sometimes called forward pruning (Quinlan, 1986). Alternatively, a tree that is much too large is pruned upward, so called backward pruning (Breiman et al 1984). In general, the accuracy of the classification tree increases with the number of terminal nodes. However, a bushy tree may contain splits consisting of just one object, and may present a false impression of the accuracy of the tree. On the other hand, a tree with few partitions may result in unacceptably high impurity. It should be stated that tree pruning results in a progressive decrease in prediction accuracy, because there is really no "right" way to prune or remove decisions in the tree. Different proposals may differ significantly and dramatically in the right size of the tree. The induction methods are limited to splitting the original number of categories of the predictor variable for partitioning. Thus, the resultant decision trees contain redundant rules which cause the result to be less comprehensible (Quinlan, 1986).

Generally there is no explicit way of telling if the error rate of a decision tree is near optimal. Indeed the entire question of what is to be optimised is a very open one (Michie et al 1994). In reality, balance should be struck between conflicting criteria. One

way of handling the tree is the use of cost-complexity as a criterion, as suggested by Breiman et al (1984). As a rule of thumb, if a tree is over-pruned, it has too high an error rate due to that fact that the decision tree will not represent the full structure of the database, and the tree is biased. In contrast, a bushy tree which is not pruned will have too much random variation in the allocation of examples. Thus in extremes, there is an optimal pruning in between. This can be achieved by trying different values of the pruning factor, and the error rate is examined against an independent test set. By plotting the error rate against a pruning parameter the optimal amount of pruning can be gained. Accordingly, the error rate can be plotted against the number of end nodes. Generally the error rate falls dramatically to its minimum value as the number of nodes is increased, increasing slowly as the nodes increase beyond the optimal value (Brazdil and Henery, 1994). It is a time consuming process.

The concept of a "better" tree or right size means a tree with smallest error in the classification of previously unknown objects. Breiman et al (1984) declared that a better misclassification rate is often obtained if the decision tree used is incomplete and smaller than a tree that fully classifies all known objects. A heuristic approach that minimises the error of new object classification can be undertaken. The approach is a TDDT construction that is complete for given examples followed by erasing of branches up to a selected measure. This is utilised in order to minimise errors of the classification tree. Quinlan (1986) stated that empirically a pruned tree or a set of production rules is expected to be more comprehensible than the original classification tree although it must not be comprehensibly less accurate for classification of unseen cases.

1. Validation methods

A major problem with decision trees is the accurate identification of unreliable rules or nodes. However, the problem can be handled in the following ways (De Ville, 1990):

- i. By validating and pruning of the classification tree methods that may verify the classification tree. The benefit of this method is that it relies on empirical characteristics, although it is tedious to perform and presents difficulties to non-specialists.

The cross-validation procedure gives the human expert a test and guides the accuracy and realism of the structure and the size of the decision tree. Using classification tree-pruning, the expert has the option to grow a larger tree than is justified by the data but may remove it back to a more realistic or conservative size by testing the performance of predictions on the different splits of the decision tree (De Ville, 1990). This approach is preferable when the sample size is not large (eg less than 1000). Further information on this topic can be found in Walker and Moore (1988).

ii. By using hypothesis experimentation techniques based on statistical theory and experience. Where the branch falls below a desired level of significance it may be rejected.

2. Test sample estimate

With the test case method, normally 33% of all data is chosen randomly as a test sample and the remainder will form the new learning sample (Walker and Moore, 1988). The use of test sample estimates may comprehensively underestimate the accuracy of samples and the variance of the measure can be high. Growing the tree has a direct relation with the increment of observation and the computation time. Further insights on the theory of this topic are provided in Stone (1974), Breiman et al (1984), Walker and Moore (1988).

4.3 Summary

The principles of expert systems, namely knowledge acquisition, knowledge representation, and inference engine were described. Knowledge acquisition is the most difficult task in expert systems development. This and the inference engine are the main components of an expert system. The use of decision trees is a typical method of knowledge extraction and it represents knowledge in order to construct expert systems. Undertaking inference strategy is mainly determined by the application. In this research a system that will use the induction method with a forward chaining inference engine has been constructed.

Decision tree induction algorithms have achieved some success and widespread popularity. These algorithms produce decision trees by first setting the root node to be the set for all training sets and then partitioning the samples in the root node. This generates child nodes that are then recursively partitioned to obtain the nodes of the next levels in the trees which specify attributes to be used to partition the samples of a node. It will be used as an information entropy measure to choose the best attribute with the least randomness in the distribution of classes. In a decision tree, the nodes correspond to selected object attributes, and the edges correspond to predetermined alternative values for these attributes. Leaves of the tree correspond to sets of objects with a particular categorisation. Among different probability-based induction systems, the KS seems to be more user-friendly and handles more sophisticated models.

The induction methods are limited to splitting the original number of categories of the predictor variable for partitioning. Thus, the resultant decision trees contain redundant rules which cause the result to be less comprehensible. The KS software handles both these approaches. Its potential is concentrating on the speed of data analysis, comprehensiveness, user-friendliness and the ability of summarisation. These are offered by the concept of statistical knowledge that is implemented by virtue of a statistical significance hypothesis experimentation circle. Inductive deviation of rules from an expert supplied set of examples is one of the most attractive applications of machine learning to knowledge acquisition as implemented by such programs as KS. The inductive method is especially helpful when the developer is not experienced in building

an ES or when the knowledge that is being collected resists simple expression as a collection of IF ... THEN rules, and where knowledge of underlying processes is either unavailable or incomplete.

In previous chapters, aspects of image (spatial data) processing and expert systems were shown. Upon this theoretical knowledge, it is now appropriate to shift into implementation of the methods mentioned for identification, classification and mapping of a road network from aerial photography, aided by spatial data.

Chapter 5

STUDY AREA AND DATA SETS

This chapter covers the description of the study area and the available data. The study site measuring 3 km x 2 km contains urban and rural areas and is located on the southern fringe of Hobart, Tasmania, Australia (Figures 5.1a and 5.1b). The study site was chosen because it provided a mix of rural and urban land use, and urban development has been relatively rapid over the past 10 years. In particular, one would want to detect roads in the area. This chapter describes the study area and the data sets employed. The chapter also indicates the hardware and software utilized in this research, consequently outlining the implemented computer program for the development and testing of the developed methodology. Special emphasis has been placed on the resolution of the data that are associated with the choosing B/W aerial photography for this research.

5.1 Study Area

5.1.1 Location

The selection of the area to be studied in this project was an important task, given that it was considered important to experiment with the model over a mixed urban and rural area, since characteristics of each of these scenes are different.

The municipality of Kingborough is one of the fastest growing municipalities in Tasmania and is typical of many expanding suburban communities in terms of dwelling characteristics and land cover mix. The community is characterised by a small core of older residential neighbourhoods with houses of 35 years or more in age, aligned in a modified grid road pattern. These are in the middle of the study site. Two commercial locations exist along the north west and middle thoroughfares. Surrounding the established core are more recent residential subdivisions composed mainly of detached single family houses and pastoral land uses. The recent residential subdivisions, built within the last 15 years, are typified by curvilinear roads and rural land uses. Large areas of new development are located in the southern and mid-western portion of the study

area. Mature trees are generally located along the local roads. The site provides a complex mix of rural land uses and residential, commercial buildings.



Figure 5.1a Topographic map of the study area (approximately 1:25,000).



Figure 5.1b Location of the study area in Hobart (Scale approximately 1:500,000).

The following reasons indicate why the site was chosen for this research.

- A mix of urban and rural land use:

The site contains a wide range of land uses. The selected area incorporates a range of features, from natural to man-made. Based on the field visitation and manual land use classification, there are 12 land use classes which will be shown later. A high density of residential roads is suited within the site, most of these roads are more than 20 years old, but some are less than 10 years old.

- Significant land uses conversion:

Land use and land cover changes are occurring in this region because of outward migration from the city. As a result, farmland and natural land at the fringe are being changed to residential, commercial, and industrial uses. The site is representative of the changing environment within the region and has undergone significant changes over the 11 years of the multirate imagery from vegetation in 1982 image to man-made features in 1991, such as new residential land in the southern and eastern parts of the site which can be easily observed when comparing the two images (Figure 5.2).



(b) 1982 imagery (1:42000)



(b) 1991 imagery (1:42000)

Figure 5.2 Aerial photographs of the study area.

5.1.2 Land cover

The landscape is typical for the region around Hobart. The study area is composed of urban and rural land uses. The test area is close to Hobart and therefore it is subject to intensive development. Approximately 35% of the area is built-up land. Most parts are residential. Correspondence between the land use categories used by the author based on Anderson et al (1976) land use classification scheme, shows there are 12 major land cover/use types include residential, commercial, industrial, recreational, educational, utilities, clearing and developing areas, forest, grassland, rivers, lakes.

The predominant natural vegetation of the rural area is native Eucalyptus. Extensive recent forest degradation has been undertaken for urban development. Figure 5.3 illustrates native Eucalyptus. Figure 5.4 shows the lake which consists of an expanse of water and natural shrubland. It is placed near to recreational land use categories. Figures 5.5, 5.6, and 5.7 demonstrate the land use for pasture and different recreational purposes. Figures 5.8 demonstrates the type of semi-rural and urban development which has taken place on the edge of the study area. The rapid transition from pastoral land use to urban development can be seen when Figures 5.8 and 5.5 are compared. Figures 5.9, 5.10, and 5.11 show the urban development for residential housing, commercial and industrial purposes.

Roads in the study area have varying width. Four major road classes can be distinguished. Major roads (eg highways) are located in the northern and southern of the study area. The width of these roads are 10 to 16 metres. Local roads (eg urban main roads) can be seen extending in two directions, starting from north to south east to south west. The width of these is between 6 to 10 metres. Urban streets are concentrated mainly in the central part of the study area. The width of these streets is 3 to 6 metres. Minor roads which are located mostly in the rural areas. These roads include rural roads, access roads, unpaved tracks. The width of these roads is 2 to 3 metres. Figures 5.12, 5.13, 5.14, and 5.15 illustrate the different roads in the study area. As can be seen in Figure 5.16 the extent of shadow overhanging the roads varies significantly due to the time of data capture, season and orientation of the roads. It is interesting to evaluate the technique for detection of these line features from the given imagery.



Figure 5.3 Native Eucalyptus within the study area.



Figure 5.4 Lake in the study area.



Figure 5.5 Land used for pasture in the study area.



Figure 5.6 Golf course in the study area.



(a)



(b)

Figure 5.7 Beach and ocean nearby the study area.



Figure 5.8 Urban land use enclosed by rural land use.

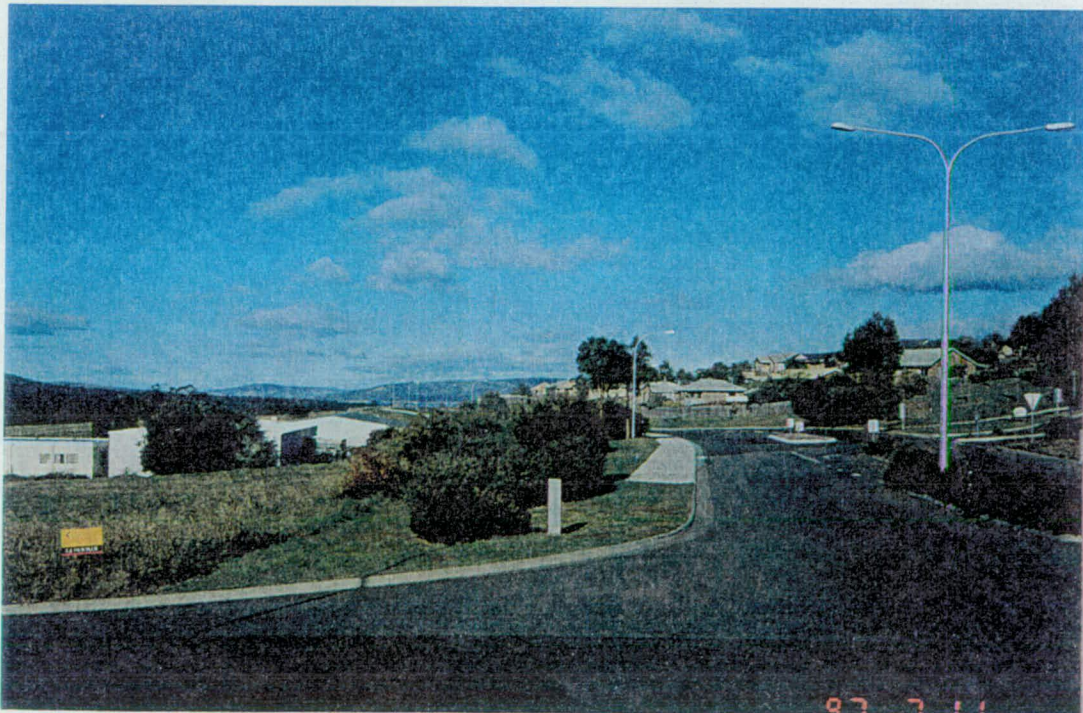
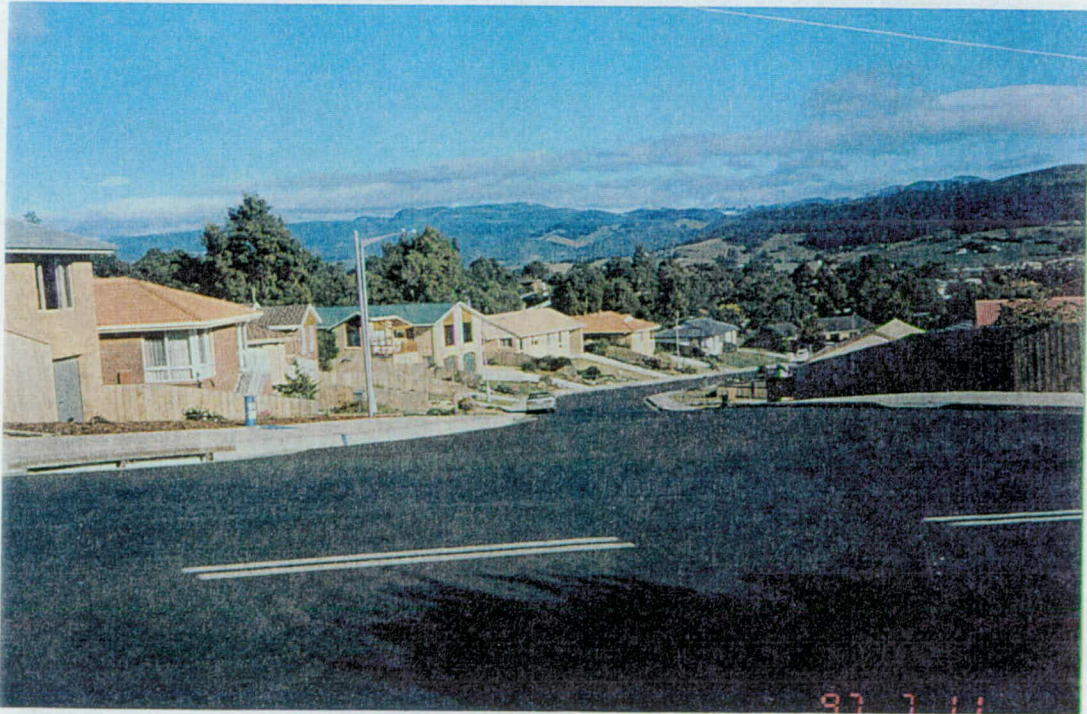


Figure 5.9 Semi-rural and urban development.

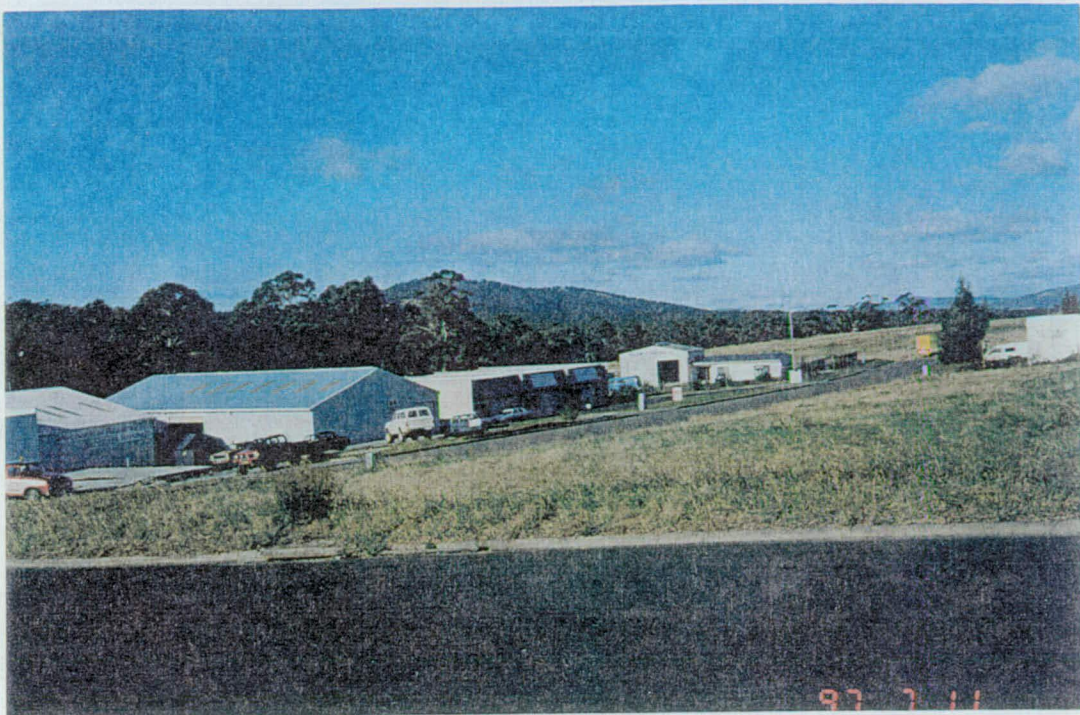


(a)

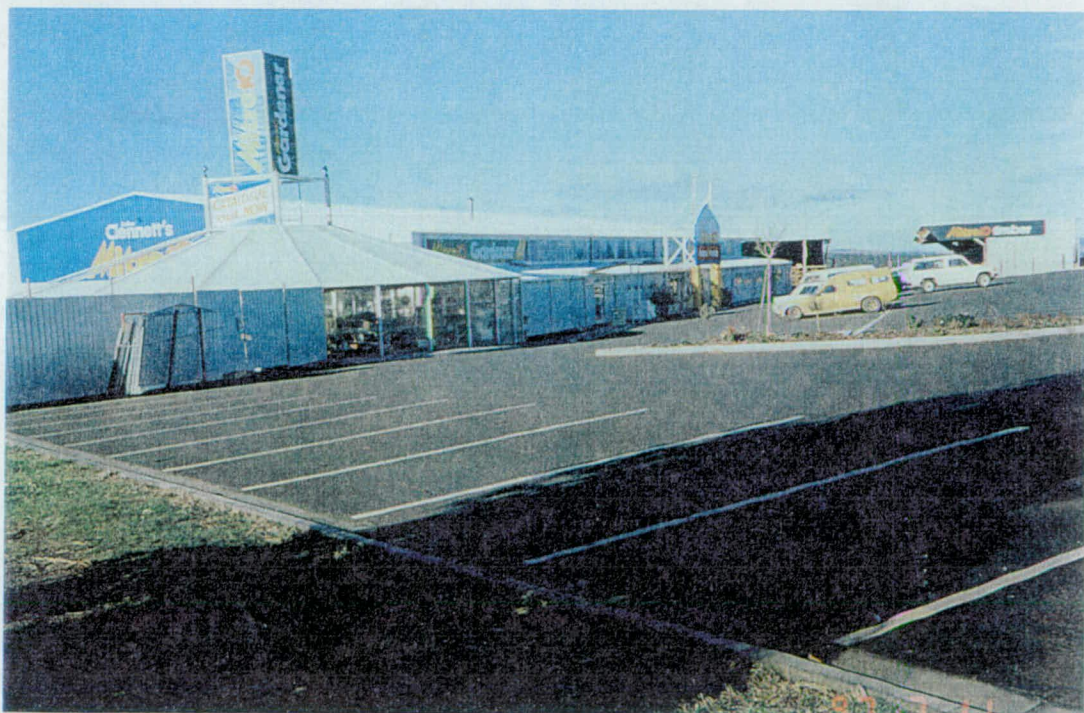


(b)

Figure 5.10 Urban development for residential housing.



(a)



(b)

Figure 5.11 Development of (a) industrial and (b) commercial areas in the study area.



Figure 5.12 Major access road in a rural area.



Figure 5.13 Major access road in a semi-rural area.



Figure 5.14 Major road in an urban area.



Figure 5.15 Local road in an urban area.



Figure 5.16 Asphalt road in a rural area with shadow from overhanging trees.

5.2 Available Data

The following digital and hardcopy data was provided by the Land Information Bureau, Department of Environment and Land Management, Tasmania (More details are included in Table 1; Appendix A):

1. Digital coverage of road networks
2. Digital coverage of drainage networks
3. Digital coverage of contours
4. Two sets of B/W aerial photographs at 1:42,000 scale for 1982 and 1991
5. Two sets of colour aerial photographs at 1:22,500 scale and 12,500 for 1984 and 1995 respectively
6. Hard-copy topographic map of the area at 1:25,000 scale

The main raster data source was B/W airphotos acquired over the study area in 1982 and 1991 (Figure 5.2). The nominal area coverage of the geocoded aerial imagery encompasses eastern and northern ranges 5,240,000 mN to 5,242,000 mN and 523,000 mE to 526,000 mE respectively of Zone 55 Australian Map Grid (AMG) coordinates.

5.2.1 Imagery Comparison - 1982 vs 1991

A comparison of the 1982 aerial photograph and 1991 aerial images was conducted. Aerial photography at the given scale and resolution is the most suitable imagery for the task of road mapping in this research. Visual examination of the aerial images indicated that delineation of residential roads within subdivisions would not be possible for many urban neighbourhoods. On both images roads, buildings, and clearing area from vegetation to urban were clearly visible on cursory examination.

Due to the high spatial resolution of the images, buildings are the most prominent man-made features with a similar contrast to roads. This makes the image analysis more difficult. Line features in aerial photography are very complex as their spectral and spatial characteristics often vary along their extent. For example, the contrast between the roads and natural land cover (background) in the rural scene is significant. Whereas, the contrast along roads against their background in an urban area generally is not as high as the rural area. Experiments have shown that detection of roads over this area would be

more easy than an urban scene due to the spectral characteristics of the roads and vegetation.

5.2.2 Criteria for Selecting Aerial Imagery

One of the major reasons for selecting aerial photography for a particular application is the high resolution and low cost of the data compared with alternative satellite data. Since the spatial resolution of high resolution satellite imagery may be insufficient for detection of road and track networks, it was decided to use medium scale aerial photography (1:42000) combined with spatial information data through a GIS for the purpose of this research. Associated with roads are point and line features such as overpasses, underpasses, bridges, and tunnels which are important for many road networks mapping applications. As discussed earlier, within the study area the road and track network varies from 2 to 16 m in width. The feature of prime importance is roads in the images. The mapping of roads in urban areas and the urban fringe necessitates the use of high spatial resolution imagery in order to resolve the component objects in this landscape.

Spatial resolution may be especially important in the scene analysis of urban-suburban features because of the inordinate amount of dependence on geometric and spatial relationships and on detailed shapes of features as well as on convergent and associated evidence for discrimination of features in urban industrial settings (Colwell and Poulton, 1985). For example, road delineation depends heavily on resolution of the image data. Generally a resolution of 10 m or less may satisfy undertaking most urban monitoring programs (Welch 1982, and 1985).

Different urban applications will require different spatial resolution. For instance, experience has shown that a resolution of 5 m or better is necessary to carry out urban mapping in developing countries (Welch, 1982) due to the fact that cities in developing countries are intensely populated and the housing sizes are often smaller than developed countries. Fundamentally, both cartographic and thematic mapping requires different resolution levels. Landsat MSS imagery is sufficient to extract class I (urban: eg residential, commercial) whereas to extract classes II (urban: eg low density residential), III (eg medium/high density residential), and IV (eg single family housing) requires the

use of high, medium, and low altitude aerial imagery (Welch, 1982). Welch (1982) also indicates that a spatial resolution ranging from 0.5 to 3 m is required for urban land use mapping for levels II and III of the classification theme of Anderson et al (1976). This idea was supported by Konecny et al (1982 cited by Welch, 1982) who illustrated that a ground resolution of 5 m or less is required for urban cartographic mapping, whereas for these types of resolution perhaps it is not necessary for thematic mapping, due to the fact that change detection is more important than feature identification (Forster, 1985). This may require a sensor system with an instantaneous field of view (IFOV) of nearly 20 m. SPOT and Landsat imagery provide the ability to resolve rural based problems. It should be kept in mind that it is not often necessary, however, to obtain this level of spatial resolution for thematic mapping which is associated with cartographic/GIS mapping such as extraction of roads, streams, and so on where change detection is more critical than identification. In the urban environment, road pattern provides a degree of complexity to the scene in context of occurring change. The claim has been made that *"experience has indicated that use areas with dimension of less than 2 mm x 2 mm at the map scale should not be included on the final product. For 1:50,000 scale mapping this represents a dimension of 100 x 100 m, requiring a sensor with an IFOV of 50 m, assuming a minimum of 4 pixels are required for identification"* (Forster, 1985). In the meantime, the classification accuracy result may improve urban classification up to a limit, owing to the reduction of noise at a given scene which may be considered as the land cover variation within a land type. The larger IFOV is proven to average the noise effects out, thus reducing between pixel variance. The different mapping purpose will determine the spatial resolution levels (Forster, 1986; Barr, 1992).

Based on practical exercise, some have asserted that SPOT Pan and large format camera (LFC) can be applied in topographic mapping at 1:50,000 scale due to its stereo capability (Torlegard, 1992). Torlegard examinations show that for detectibility the required size of the pixels can be 2 m for buildings and footpaths, 5 m for local roads and finer hydrography, and 10 m for major roads and building blocks. Using SPOT Pan and XS data was problematic to delineate older subdivisions with well treed streets and industrial-commercial developments (Li et al 1989). On the other hand, arterial roads and subdivisional collectors have been successfully delineated. Similarly, at a ground

resolution of 3 m to 4m of an aerial photograph, the road surface has high contrast with the background (Zhu and Yeh, 1986). Road segments commonly maintain high contrast as they pass through urban infrastructures and mountainous terrain. Roads in agricultural land have commonly lower contrast than roads elsewhere (Thirlwall et al 1988).

According to these statements, Landsat MSS, TM, and SPOT XS may not be adequate for an analytical classification in urban scenes, and these data are more applicable to urban monitoring (Treitz et al 1992). However, improved spatial resolution satellite data may not lead to improvements in classification accuracy (Gurney and Townshend, 1983). Cushnie (1987) stated that the greater the proportion of scene noise to begin with, the greater the reduction afforded by coarsening the resolution. But, in general, higher spatial resolution data provide details that aid detection, identification and image positioning of objects (Thirlwall et al 1988). However, it should be clarified that it does not always provide the best detection and identification of all elements. It should be kept in mind that in spite of high performance of high resolution satellite images, researchers (Gurney and Townshend, 1983) believe that the highly resolved data may be problematic in terms of information extraction.

At ground resolution of 2 m to 5 m for the scanned aerial photography, the road surface can be distinguished by human eye with the background. The 1:42,000 photograph, was scanned at 500 DPI, providing a resolution of 2.1. At this resolution delineation of features from 1.5 to 4.5 m should be possible. On the B/W imagery all major access road and tracks are clearly visible, although the occurrence of vegetation within some access roads results in them appearing as non-contiguous lines of pixels. Minor access tracks are mainly obscured by overhanging vegetation. The pixel size for the captured data mode is small enough to discriminate the smaller tracks.

The two sets of B/W air photos were used in the knowledge-based database. These include a summer data set acquired on 10 February 1982, and a spring data set acquired on 2 December 1991 (Table 1 in Appendix A). The visual interpretation of B/W aerial photos was supported by two sets of colour air photographs, which cover the study area. They were acquired on 1st November 1984, 2 years after the first B/W photo was taken, and 3rd November 1995, 4 years after the second B/W air photo was taken. The original

colour photo was acquired in 1984 at 1:22,500, and it was used for a supervised classification in order to compare with the decision tree analysis. The colour photography of the study site was used to provide ground truth data.

5.2.3 Base Maps

Image registration and rectification was accomplished using ARC/INFO rubber sheeting and an affine transformation (Chapter 6). Ground control points were selected from hardcopy maps produced by the Department of Lands, Division of Mapping, Hobart, Tasmania (dated July 1987). The horizontal accuracy of the maps is such that not less than 90% of well defined points fall within 12.5 metres of their true positions at map scale. The vertical map accuracy is such that not less than 90% of elevations fall within 5 metres of their true elevation. All of the GIS and RS data was registered onto a Universal Transver Mercator (UTM) projection, Australian Map Grid Zone 55. The topographic maps for Kingston served as reference bases for creation of georeferenced images for image interpretation and mapping of roads.

5.3 Computer Facilities

The computer facilities are available in the Surveying and Spatial Information Science and Centre for Spatial Information Science, University of Tasmania. Major software included ERDAS IMAGINE¹, MATLAB², ARC/INFO³, PhotoGIS⁴ and Ortho-PhotoGIS, and KnowledgeSEEKER (KS)⁵.

5.3.1 KS Software

Machine Learning Software KnowledgeSEEKER (KS) version 3.0 was used for decision tree analysis. KS is an automatic data analysis software package using decision trees. It is a well-known decision tree algorithm which explores contextual information, and displays the information in a decision tree form, as well as generating rules to allow construction of an expert system. This software was used to construct decision rules from the GIS database. The generated rules (knowledge) were employed for the construction of an expert system to map out the road distribution.

5.3.2 Computer programs

1. Columns.f pre-process the constructed GIS database to be imported into KS software.
2. Expert Systems Implementation: The MATLAB software forms one component of a developed expert system called "Decision Tree Processing Expert Systems" (DTPES) to interface KS with GIS data. The DTPES was programmed in

¹ The ERDAS IMAGINE software is manufactured by ERDAS, Inc. 2801 Buford Highway, NE, Suite 300, Atlanta, Georgia 30329-2137 USA.

² The MATLAB software is a product of the MathWorks, Inc. 24 Prime Park Way, Natick, Mass. 01760-1500, USA.

³ The ARC/INFO software is manufactured by Environmental Systems Research Institute, Inc. (ESRI) 380 New York St. Redlands, CA 92373, USA.

⁴ The PhotoGIS software and the Ortho-PhotoGIS addendum were developed by Salamanca Software Pty Ltd, PO Box 844, Sandy Bay, Tasmania 7006, Australia.

⁵ The KnowledgeSEEKER algorithm is the property of ANGOSS Software International Limited, Suite 201, 430 King Street West, Toronto, Canada M5V 1J5.

MATLAB language under the MATLAB environment. The DTPES consists of two subroutines, namely `ks2mat.m`, and `dtpes.m`. The `ks2mat.m` converter converts the generated rules (knowledge) from KS into MATLAB rules form, and stores results in a file called `matrules.m`. The `dtpes.m` program maps the roads distribution from the rules through dataset, and then calculates the overall classification accuracy based on the roads data.

The MATLAB software was selected for its user-friendliness, flexibility, interface capabilities, high level programming language, and the familiarity of the author with this language.

FTP was used for transferring the required files from a PC to the UNIX machines and vice versa.

Computer Facilities	Type	Name and Model	Comments
Hardware	Unix Workstation	SUN	All spatial and image processing was primarily undertaken using SUN SPARC workstation with 32 Mbytes RAM, SUNOS 4.1, a SUN SPARC workstation with 64 Mbytes RAM, SUNOS 4.1, and recently SUN ULTRA SPARC workstation with 64 Mbytes RAM, SOLARIS 2.5.
	IBM PC	486	An IBM compatible PC with 812 Mbytes disk space was used mainly for decision tree analysis, and writing the documents.
Software	Image Processing	ERDAS IMAGINE Version 8.1	This software was used for part of the image processing for this project.
		MATLAB Version 4.0	MATLAB image processing toolbox was used mainly for implementation of an edge detection program.
		PaintShopPro Version 3.01	This software was run on a PC. It was used mainly for image format conversion purposes.
	GIS	ARC/INFO Version 7.0.2	ARC/INFO was used to create, manipulate, and display GIS data in digital format. This software was principally used for construction of a database for a knowledge-based environment. ARC/INFO is a well-known GIS produced by ESRI that organizes geographic data using a relational DBMS (INFO) and topological model (ARC).
		PhotoGIS version 2.2	PhotoGIS is fully integrated with ARC/INFO software. It was used for image rectification.
		Ortho-PhotoGIS	Ortho-PhotoGIS is associated with PhotoGIS version 2.2. Ortho-PhotoGIS is a raster-based software, and PhotoGIS is a vector-based algorithm.
	KBS	KS Version 3.0	Refer to Section 5.3.1.
	Developed Computer codes and an Expert System (DTPES)	MATLAB Version 4.0, and Fortran 77	MATLAB environment was used for construction of a rule-based expert system program as part of decision tree implementation. Also refer to Section 5.3.2, Chapter 7.

Table 5.1 Computer facilities information.

5.4 Summary

This chapter described the study area and the data sets employed. A study site in the urban fringe of Hobart was chosen because of its mix of rural and urban land use, and urban development. The spatial data sets assembled for the project included digital coverage of road networks, digital coverage of drainage networks, digital coverage of contours, two sets of B/W aerial photographs at 1:42,000 scale (for 1982 and 1991), a colour aerial photograph at 1:22,500 scale (for 1984), and hard-copy topographic map of the area (at 1:25,000 scale).

Chapter 6

IMAGE REGISTRATION AND LINEAR FEATURE DETECTION

To integrate the aerial photographs into the GIS, it was necessary for the images to be geometrically corrected. It was necessary to overlay the road coverage to an accuracy of about 2 pixels (4 metres). Standard image rectification techniques were adopted to correct the data geometrically: (1) polynomial transformations, (2) digital orthophotography, (3) affine transformations and rubber sheeting. Neither the polynomial transformations nor the digital orthophotography provided the required accuracy. Affine transformation and rubber sheeting using a series of links produced a result which was satisfactory for the aim of this project.

The rectified images were used for identifying linear features by edge detection and mathematical morphology. The Interactive Linear Feature Detection Program (ILFDP) was developed for semi-automatic linear feature detection using different edge detectors, followed by morphological operations. The main aim of this program was to build data for a GIS database. By specifying different edge enhancement, noise removing filters, edge detectors and filters, and morphological tools it is possible to produce a variety of different results. The aerial images were processed using ILFDP implemented in the MATLAB program. The extracted edges were used as a GIS layer in a later step for delineation of roads by implementation of decision tree analysis.

6.1 Geocoding of Images

Standard software, ERDAS IMAGINE, PhotoGIS and ARC/INFO were used to correct the imagery.

Two black and white images from different dates (1982 and 1991) were used. Both were 1:42,000 photoscale (9" format, 6" lens). The photographs were scanned at 500 DPI and stored in a 25MB TIFF File.

A sub-region for each image was selected and rectified using each of the following methods: polynomial rectification, digital orthophotography, affine transformation and rubber sheeting. The methods employed are explained in the following sections.

6.1.1 Polynomial Transformations

This section describes the application of manual GCP selection, a polynomial transformation and image-to-image registration.

(i) Technique Adopted

Relief displacement was calculated (Wolf, 1988). The effects of terrain were estimated by plotting relief displacement in the two aerial photographs. For example, for the 1982 imagery, height variation in the terrain resulted in a maximum relief displacement of 6.3 pixels (13.2 m). The relief displacement at the closest point to the principal point (height = 120 m) on the ground pixels was 0.55 pixels. The relief displacement on the furthest point (height = 125 m) from the principal point of the image on the ground was 6.3 pixels. The photo scale used 1 pixel equal to 2.1 m on the ground. Relief displacement is therefore significant.

The effect of relief displacement at the edge of the image, near to the principal point, and at the furthest point from the principle point of the image, was 37 m, 4 m, and 38 m respectively. The amount of relief displacement in pixels from the principal point of the photo in both X and Y directions was calculated (refer to Equation 6.1, and Figure 6.1), and the dx and dy components of the relief displacement plotted. Equation 6.1 was used to calculate dy and dx of components of the relief displacement in order to present the effects of terrain relief displacement for 1982 imagery. Further information can be found in Appendix B. The results are presented in diagrammatic form in Figure 6.2.

$$\theta = \arctan\left(\frac{Y}{X}\right) \quad (6.1)$$

$dx = d \cos \theta$, and $dy = d \sin \theta$

where

d is the relief displacement in pixels

X is the x displacement from principal components ($P.P$)

Y is the y displacement from $P.P$, and

Δx , Δy are components of relief displacement measured in pixels.

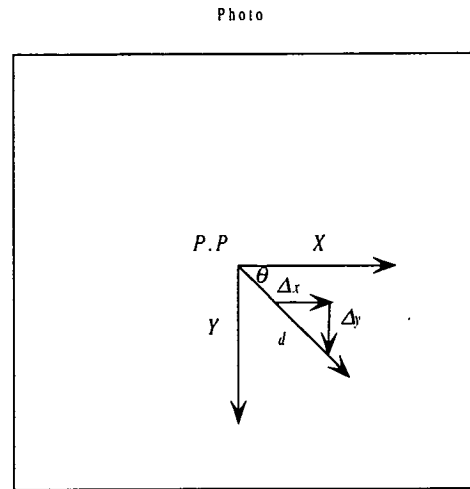


Figure 6.1 Components of relief displacement.

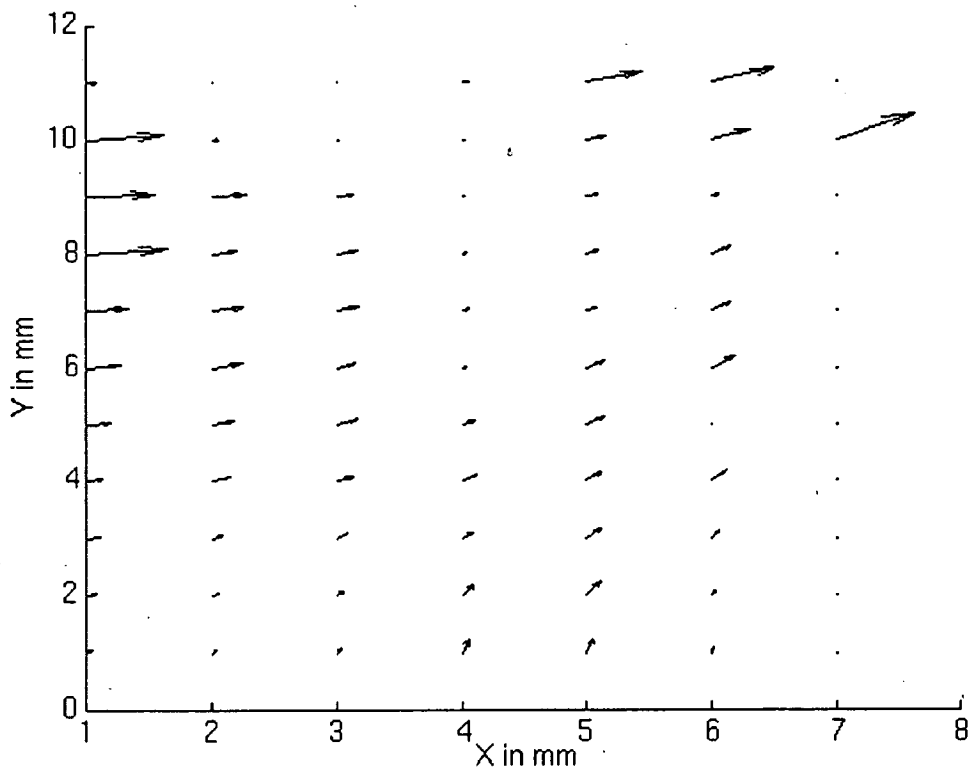


Figure 6.2 The vectors representing relief displacement for the 1982 image plotted. These were shown only for a portion (subset) of the aerial photograph where the study site is located.

The first photograph (1982) was registered to the digital road and drainage pattern maps using ground control points identified on the digital data and the second

photograph (1991) was registered to the georeferenced photograph (1982) using points appearing in both images. For the registration of the 1982 photography 8 GCP and for the registration of 1991 imagery 10 GCP were used. The distribution of GCP throughout the scene, and having an adequate control point near the edges, are very crucial functions. The choice of GCP has been elaborated by Welch (1985); Labovtiz and Marvin (1986); ERDAS (1994b). In this work a second order transformation using bilinear interpolation was used.

(ii) Experimental Results

Table 6.1 summarises the experimental results of image rectification and registration using two polynomial transformation functions (first order and second order). The selection and matching of control points was implemented manually. Both water path regions and road networks were used as ground control, with coordinates derived from 1:25,000 topographic maps.

The total RMS error for the 1982 image and 1991 image was found to be 6.3 and 1.88 pixels respectively. The photo registered image (1991) has a much lower RMS error than the map rectified image (1982) in this study.

First Order Transformation	GCP #	X RMS Error in Pixel	Y RMS Error in Pixel	Total RMS in Pixel
Subset_1982	8	5.27	3.44	6.30
Subset_1991	10	0.76	0.94	1.21
Second Order Transformation	GCP #	X RMS Error in Pixel	Y RMS Error in Pixel	Total RMS in Pixel
Subset_1982	8	3.40	1.67	6.30
Subset_1991	10	0.98	1.61	1.88

Table 6.1 A summary of results of rectification and registration of the aerial images using polynomial transformations.

Three major sources of error placed limits on the accuracy to which the 1982 aerial photo could be fitted to map coordinates using a polynomial rectification:

- (1) the principal limitation is the process itself. A second order polynomial transformation cannot match the complexity of the relief displacement which was shown in Figure 6.2.

(2) location errors due to the scale of aerial photographs (1:42,000) because of inadequate resolution.

(3) map errors attributable to the scale and quality.

A vector overlay for both corrected images was performed in order to provide a comparison between the geometric quality of the polynomial methods used. Visual inspection confirmed that the polynomial methods failed to provide adequate accuracy. The range of error was about 4 to 13 metres (2 to 6.5 pixels). For the purpose of this research this accuracy is not satisfactory, since about 2-2.5 pixel accuracy is required.

6.1.2 Orthophotography

Recently, researchers (eg Abramson and Schowengredt, 1993; Forghani and Osborn, 1998a) have used digital orthoimagery and digital elevation models in the integration of remotely sensed data and a GIS database. As mentioned earlier, polynomial methods may not efficiently remove relief displacement in areas of gentle relief (smooth terrain) and rugged terrain. Photogrammetric approaches for differential rectification to eliminate the effects caused by terrain have led to orthophotography algorithms which are now well accepted for GIS applications (Jensen, 1995).

The PhotoGIS orthophotography software used in this research requires at least four GCP on a given image in order that the camera position and orientation at the moment of exposure can be determined. These points should surround the area that needs to be corrected. The accuracy of the DEM affects the accuracy of the orthophoto.

The likely error in planimetric coordinates based on residual DEM errors and photo scale is shown in Table 6.2. Maximum error in X and Y coordinates of a point at the edge of the useable area of a standard photo for different scales for eight values from r_1 to r_2 is represented in Figure 6.3. An optimum mapping range appropriate for topographic mapping is highlighted.

Photo Scale	1:3000	1:5000	1:10000	1:25000	1:50000
Flying height (metres)	450	750	1500	3750	7500
Residual DEM Error					
0.2m	0.04 mm	0.02	0.01		
0.5	0.10	0.06	0.03	0.01	
1.0	0.20	0.12	0.06	0.02	0.01
2.0	0.41	0.25	0.12	0.05	0.02
5.0	1.03	0.62	0.31	0.12	0.06
10.0		1.24	0.62	0.25	0.12
20.0			1.24	0.50	0.25
30.0m				0.74	0.37 mm

Table 6.2 Representations of the DEMs and the maximum error in X and Y coordinates due to DEM discrepancies in mm at photo scale (PhotoGIS, 1994).

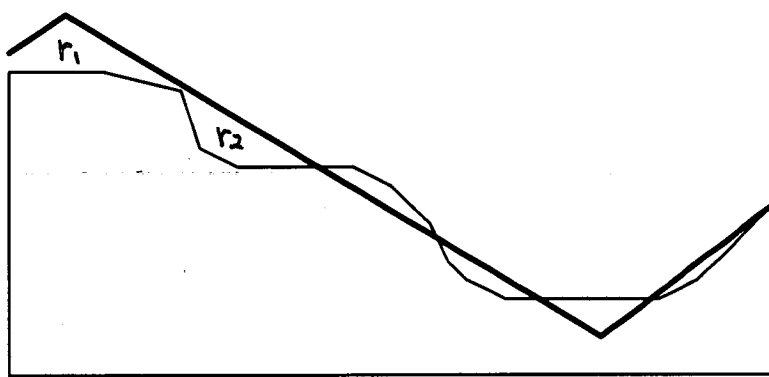


Figure 6.3 Illustration of differences between the actual terrain and the maximum error in Z coordinates (DEM) (PhotoGIS, 1994). PhotoGIS uses the DEM to map the geometry of the terrain accurately. However, there are two differences between the real world and the DEM. These are differences due to the heights used to construct the DEM (r_1), and the separation between the actual terrain and its representations because of the resolution of the DEM (r_2). The effects of these residual errors on PhotoGIS corrected points are the same, eg they cause a residual relief displacement error which has been presented in the above table (PhotoGIS, 1994).

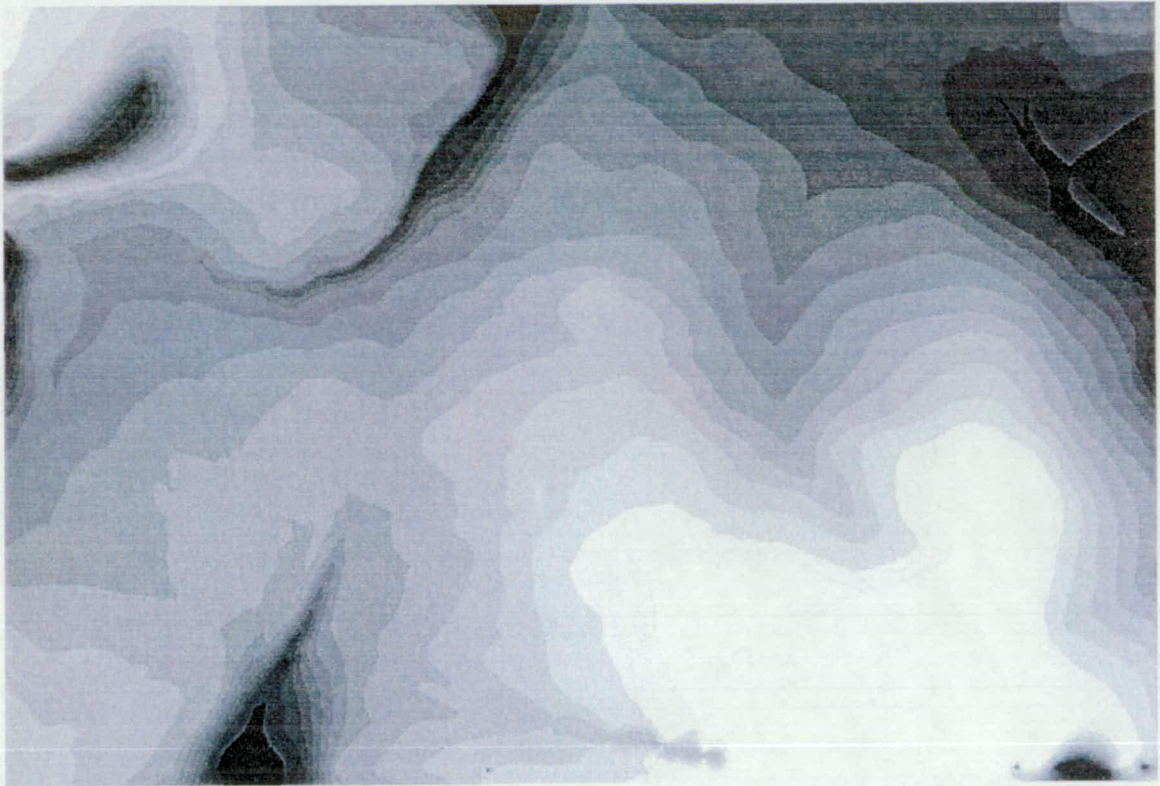


Figure 6.4 Illustrates the DEM of the area as a grey scale image which was produced by applying ARC/INFO TOPOGRID tool. Digital contours with a 10 metres interval, and stream networks were used to construct a DEM for the study area.

(a) Technique Adopted

In order to produce an orthophoto, the following steps were taken.

1) Examining the Image

Due to the fact the fiducial marks were not clear in the digitised photos, the histogram equalisation algorithm of IMAGINE ERDAS was used for contrast enhancement of the aerial photographs.

2) Creating a Photo Coverage and Registering the Image

The photo coverage contains the fiducial ties (marks) to establish the photo coordinate system for the photo coverage. Fiducial marks establish the relationship between the photo and the camera lens. The camera calibration report was available to

set up the photo template coverage. The digitising of fiducial marks was performed. The magnification facility assists digitisation of the tics directly off the screen more accurately. The images are registered on the photo coverages by using ARC/INFO's REGISTER module to link the four fiducial tics in the template photo coverage with their corresponding image points. The camera calibration report of the captured photographs was used to create the template ARC/INFO coverage based on these coordinates (Figure 6.5). This information was also required for performing resection which will be discussed later.

Visual Goniometer Camera Calibration				
Camera	Tasmania Lands	Zeiss RMKA	No. 118418	Date: 19/4/1988
				Photo: 1982
No filter used during calibration				
Coordinates of Principal Point of Autocollimation (PPA) with respect to Fiducial Centre in millimeters				
X = 0.01, Y = 0.00				
The uncertainty associated with these values does not exceed 0.010 millimeters				
coordinates of fiducial marks				
	N	S	E	W
Xmm	-79.85	79.88	79.89	-79.98
Ymm	-79.85	79.88	-79.88	79.87
The coordinates of fiducial marks are in millimeters				
The uncertainty associated with these values does not exceed 0.020 millimeters				
Calibrated Focal Length in mm 152.963				
The uncertainty associated with these values does not exceed 0.010 millimeters				
The calibrated Focal Length has been determined such that the sum of squares of the distortions is a minimum				
The temperature at the time of calibration was approximately 20 C° .				

Figure 6.5 The camera calibration report for the 1982 and 1991 photography.

The results of registering fiducial marks (82.img) to the photo coverage.

(a)

Link Id	Calculated X in mm	Calculated Y in mm	True X in mm	True Y in mm	Distance in mm
1	-79.821	-79.906	-79.850	-79.850	0.063
2	79.909	79.824	79.880	79.880	0.063
3	79.861	-79.824	79.890	79.880	0.063
4	-79.919	79.926	-79.890	79.870	0.063

Scale (X,Y) = (0.052,0.052) Rotation = 44.707 degrees, RMS error (image, cover) = (1.225 pixels, 0.063 mm)

The results of registering fiducial marks (91.img) on the photo coverage.

(b)

Link Id	Calculated X in mm	Calculated Y in mm	True X in mm	True Y in mm	Distance in mm
1	-79.810	-79.908	-79.850	-79.850	0.070
2	79.920	79.822	79.880	79.880	0.070
3	79.850	-79.822	79.890	-79.880	0.070
4	-79.930	79.928	-79.890	79.870	0.070

Scale (X,Y) = (0.052,0.052) Rotation = 45.282 degrees, RMS error (image, cover) = (1.359 pixels, 0.070 mm)

Table 6.3 Results of registering fiducial marks on the photo coverage. ARC/INFO TRANSFORM tool generates and displays the above report. This represents comparisons between the input and output coverage tics, the parameters applied for the transformation, and measures how accurately the photo coverage and the photo coordinate system from the camera lens fit together. The RMS error describes the deviation between the tic location in the input coverage and those in the output coverage. However, it never occurs with real-world data, perfect transformation should produce an RMS error of 0.000.

3) *Building a TIN in ARC/INFO*

Surface feature type (SFTYPE) information including mass points (eg from contours), hard replace (eg lake and ocean) polygon, and hardclip (eg shoreline) associated with each feature are applied to create a TIN model. Interpolation methods within a GIS can be used to estimate values for other points and to build a surface. For this research, contours with an interval of 10 metre were available in digital form (Figure 6.6). Finally, the TIN coverage was generated by using the ARCTIN tool in ARC/INFO package.

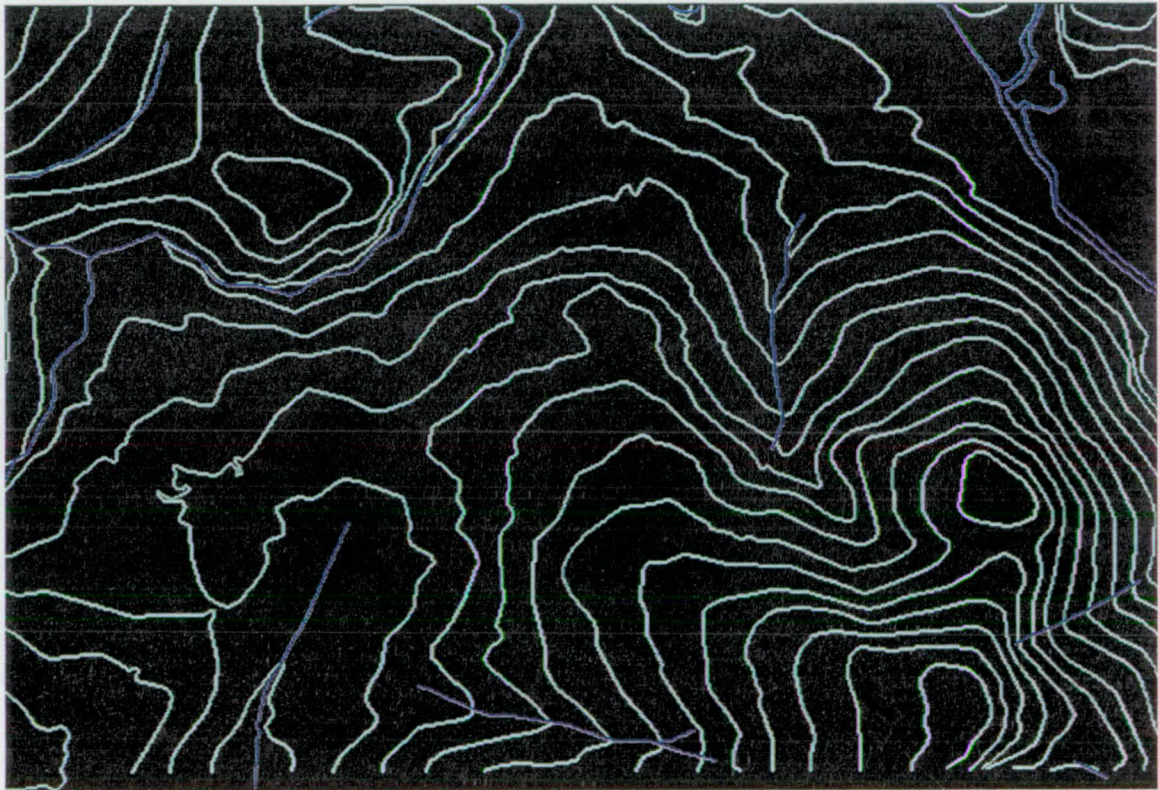


Figure 6.6 Contour plot of the test area superimposed with streams coverage. The interval of the contours is 10 metres. The contours are shown in green and streams represented in blue.

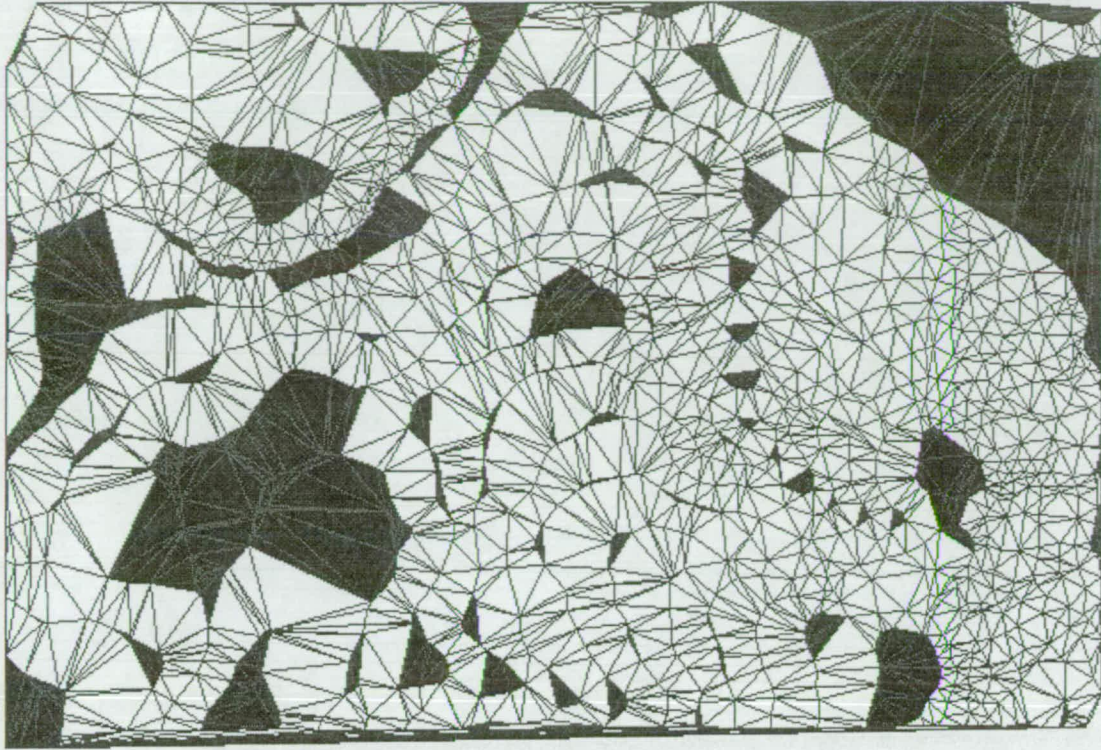


Figure 6.7 Represents generated TIN boundaries of the study area. The contour data file was converted to a regular grid or elevations (DEM) at 2-m spacing using the ARC/INFO TOPOGRID command.

4) *Identifying GCP and Interpolation of Z Coordinates of the GCP*

The X and Y coordinates were derived from the digital data in ARC/INFO. As was cited earlier, the distribution of GCP throughout the scene and the presence of control points near the edges was crucial. A total of 6 unambiguous GCP for correction of the 1991 and 1982 images were determined from the digital topographic data based on the 1:25,000 topographic map sheets. The Z value was interpolated from a DTM using the coordinates and a TIN coverage. As has been discussed, the X, Y and Z coordinates of the GCP should be at least twice as accurate as those achieved from digitising at the scale of photography (eg: 1:20,000 map data is appropriate for 1:42,000 photography).

5) *Performing the Resection*

The resection determines the position and orientation (X,Y,Z, Omega, Phi, Kappa) of the camera in space (X,Y and Z) at the time the photo was captured and the camera's orientation in context of rotation about the axes (Omega, Phi, and Kappa). The resection process was repeated until the residual values were within the tolerance. Given that the control points came from a 1:25,000 digital map it can be expected (given best circumstances) that those points are accurate to 0.5 mm on the map (PhotoGIS, 1994). Thus, in units of the map database this is about 12 meters. Consequently, a tolerance of 10 m was determined. This tolerance (10 m) was the largest residual that can be accepted. For example, the maximum residual error for the 1982 and 1991 images was 0.05 m (Xdiff), -9.90 m (Ydiff), and 7.96 m (Xdiff), -3.98 (Ydiff) respectively. Also, the minimum residual error for the 1982 and 1991 images was 1.19 m (Xdiff), 1.19 m (Ydiff), and -0.22 m (Xdiff), -0.48 (Ydiff) respectively (Table 6.4).

As soon as a satisfactory resection result was obtained the photo was then corrected to remove the tilt and relief distortion, using the orientation parameters (X,Y, Z, Omega, Phi, Kappa) determined in the resection and a TIN.

Resection results for 1982 image (a)

TicID	Xgcp	Ygcp	Xcalc	Ycalc	Xdiff	Ydiff
1	526015.70	5240272.68	526014.44	5240274.90	1.26	-2.23
2	522373.33	5240264.24	522376.66	5240261.25	-3.33	3.00
3	523358.40	5237952.80	523349.58	5237948.86	8.82	3.95
4	524849.12	5242669.61	524847.93	5242670.12	1.19	1.19
5	526216.64	5241048.48	526216.59	5242670.12	0.05	-9.90
6	523607.27	5242493.93	523615.44	5242488.79	-8.17	5.14
Resection successful because the most recent differences between actual control coordinates (per GCP file) and the calculated coordinates (per this resection) are within the resection tolerance of 10.0000 terrain units. Final Estimates:						
XL	YL	ZL	Omega	Phi	Kappa	
522375.596	5240240.583	6706.766	0.0288338	-3.1605873	2.3469597	

Resection Results for 1991 image (b)

TicID	Xgcp	Ygcp	Xcalc	Ycalc	Xdiff	Ydiff
1	524849.05	5242669.48	524855.53	5242663.87	-6.48	5.61
2	522386.74	5238272.51	525971.35	5238270.92	-3.32	1.59
3	522372.93	5240264.41	522364.97	5242797.91	7.96	-3.98
4	522386.74	5238679.89	522390.79	5238678.57	-4.06	1.32
5	526492.35	5241188.23	526486.23	5238270.92	6.12	-4.06
6	523168.84	5242797.43	524855.53	5242797.91	-0.22	-0.48
Resection successful because the most recent differences between actual control coordinates (per GCP file) and the calculated coordinates (per this resection) are within the resection tolerance of 10.0000 terrain units. Final Estimates:						
XL	YL	ZL	Omega	Phi	Kappa	
522611.278	5252547.465	6704.840	-0.0347410	0.0101401	-0.0489147	

Table 6.4 Resection results

(b) Examining the Corrections

To provide a comparison between the numeric results of resection and visual inspection of the corrected data, the digital roads were overlaid on the corrected data in order to quantitatively assess the accuracy for different parts of the image. There were significant discrepancies on the precise overlaying of the digital roads to the roads of the images. An error of approximately 2.5 pixels (4.2 m) is acceptable for this study. The range of error was from 3 to 10 metres. Because higher accuracy was required, it was necessary to try an alternative method to solve this problem (gain required accuracy).

6.1.3 Affine Transformation and Rubber Sheeting

Affine transformation and polynomials attempt to overlay images with local geometric distortions using a network of relative displacement or links. The affine transformation uses an interpolation algorithm, and rubber sheeting applies a triangulation method to divide the adjustment region into transformation segments. A digital georeferenced image with ± 4.2 m accuracy must be produced. A minimum of 60 links was defined for each image. This image correction approach has been successful on restricted relief distortions (eg Goshtasby, 1987; Forghani and Osborn, 1998a) and also for the purpose of this work. As a general rule of thumb, the more links, or GCP's, the better the fit. This approach was implemented using ARC/INFO software and consists of three stages:

1. An initial affine transformation was applied, using ARC/INFO REGISTER RECTIFY commands to register the image approximately into map coordinates. Links between the image and the digital road network were created interactively to define the local geometric distortion.
2. In theory the program works on three GCP (links), and up to sixty links can be added. In fact, for the purpose of this research these links were not sufficient to accurately overlay the digital road coverage on the roads in the photographs. To add more than sixty links, the rectified image was converted to a grid through the IMAGEGRID tool. Then, a link coverage was created which contained the added links.
3. Rubber sheeting of the image was then accomplished using the ARC/INFO ADJUST command. The ADJUST command applies a triangulation method to divide the

adjustment region into transformation segments. It is important to have the links spread systematically over the whole coverage or grid including the outer edges in order to set the adjustment systematically with distribution of equal weight to the adjustment of all parts of the grid or coverage. The adjustment was modified by deletion and adding of links. The corrected image with digital road network superimposed is shown in Figure 6.8.

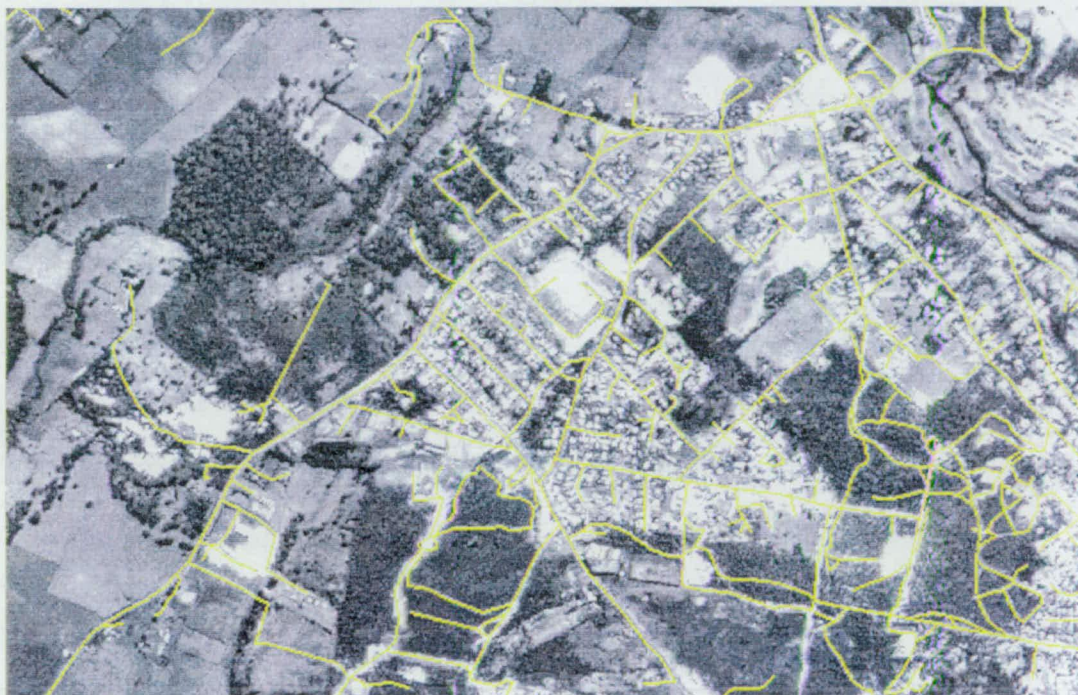


Figure 6.8 The geometrically corrected image using the affine transformations and a rubber sheeting. The road networks (yellow) were overlaid onto the georeferenced image.

A qualitative (visual inspection) assessment of the results of image rectification was undertaken. The digital road networks were overlaid on the corrected images. There was good correlation between overlaid digital roads and the roads of the corrected image. In addition, a quantitative evaluation of the results of image rectification was attempted. The errors were measured in map unit (metres) on different sections of the image. The range of errors was 2 to 4.2 metres.

6.1.4 Discussion

The digital road networks were overlaid onto the corrected images to quantitatively assess the residuals (eg Figure 6.8). In order to compare three methods, the errors were measured in map unit (metres) on different parts of the image. An error of approximately 2.5 pixels (4.2 m) is acceptable for this study.

The polynomial transformations provided the lowest accuracy. The major sources of error include the complexity of the relief displacement, location errors due to the scale of aerial photographs and consequently inadequate resolution, map errors attributable to the scale and quality.

The errors in the orthoimage were attributed to uncertainty in the DEM as digital topographic data was based on the 1:25,000 topographic map sheets.

An affine transformation and rubber sheeting provided the highest accuracy. An accuracy of 2.5 pixels or about 4.2 meters was gained. The corrected images will be used for mapping roads using a GIS database and knowledge-based approach.

6.2 Remarks for Image Registration

When registering images on to a GIS using topographic map data at 1:25,000, more precise image rectification may be obtained from a rubber sheeting procedure than can be obtained from a polynomial adjustment or orthophotography algorithm.

For a typical data set (eg 1:42,000 photography), typical software (eg ARC/INFO), and an available topographic map (1:25,000), an affine transformation and rubber sheeting method may be the best approach to carry out image registration. This method is very useful when relief displacement is significant. This is particularly productive when there is a large amount of detail available from a map which provides more GCPs to fit image on the map features.

In the case of orthophotography, the reliability of the DTM is the key consideration.

6.3 Linear Feature Detection and Analysis

Image processing techniques include certain types of image segmentation such as edge detection (eg Sobel filter), edge enhancement (eg median filter) and mathematical morphology (eg dilation). As mentioned in Chapter 3, principally there are two linear feature detection approaches:

- line detection or tracking, and
- edge detection.

The edge detection process was considered the most fruitful approach for the purposes of this study since the roads appear as multiple pixels when using edge enhancement. Hence the concern is to define (extract) both sides, and to delineate other linear features (eg field boundaries, rivers). It may well be more useful to use an edge detector in order to obtain the edges of roads and other line features.

Three different spatial filters were employed in the ILFDP program:

- a) noise removal filters
- b) edge detectors (Canny and Deriche) and thresholding, and
- c) mathematical morphologic transformations.

The routines of ILFDA program are listed in Appendix C.

A 180 by 160 pixel window of a rural site, and 185 by 235 pixel window of a built-up site was selected from the study area for image segmentation analysis (Figure 6.10). The processing chain to extract edges of linear features from the original image is as illustrated in Figure 6.9.

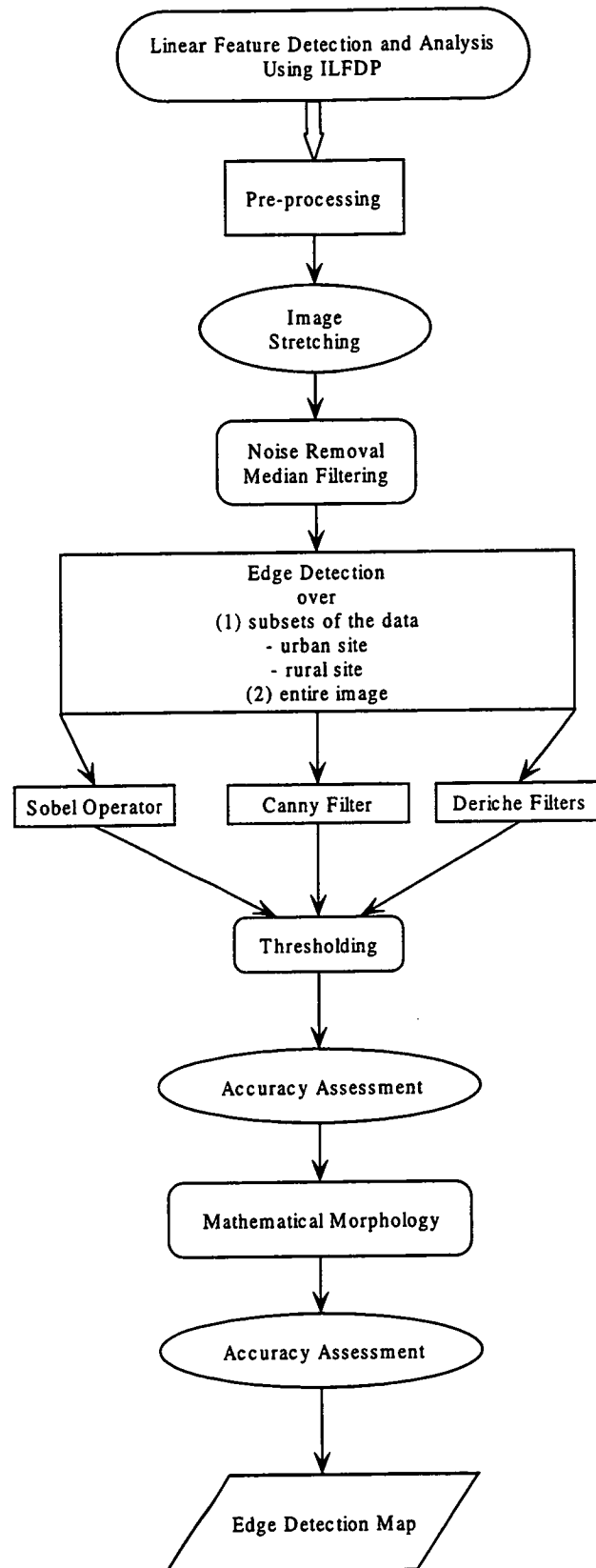


Figure 6.9 Schematic of interactive linear feature interpretation of test area.



(a) 180x160 pixel window of a rural site



(b) 185 by 235 pixel window of a built-up area

Figure 6.10 Test images; sub-sections of the 1982 image.

6.3.1 Pre-Processing of Images

6.3.1.1 Image Stretching

Primary processing of the data was undertaken including standard image histogram stretching (Imadjust tool) and median filtering techniques. The image histogram stretching function in the ILFDP transforms the values in intensity image (I) to values in output image (J) by mapping values between low and high to values between bottom and top using the stretching function. Values below the lower limit of the range map to 0 and values above the upper limit of the range map to 1 (256).

6.3.1.2 Median Filtering

The effects of noise on the responses of different operators can be suppressed by smoothing the image with a low pass filter before applying an edge operator. Median filtering with a 3x3 nonlinear kernel was used to reduce “salt and pepper” type noise, remove outlying extreme pixel values (Figure 6.11). Thus it minimised the influence of noise, and produced a smoother image. Too large a filter eg bigger than 7x7 may cause fuzzy images which are not appropriate for edge detection. This especially occurs where edge density is high and complex such as urban areas. Using median filtering the digital number (DN) of each pixel was replaced by the median of DN in the neighbourhood of that pixel. If image smoothing and noise removal is not employed on the image, problems may occur in edge detection.



(a)



(b)

Figure 6.11 Application of a median filtering.

6.3.2 Image Segmentation

6.3.2.1 Edge Detection

An edge may be defined as any extended edge in an image which can be approximated by short linear segments characterised by a position and angle. The grey value of one linear feature against its background may differ from one location to another. Edges correspond to local discontinuities of various order in the intensity surface of a scene. Thus, edges are those places in an image where the intensity changes rapidly. Since roads are line features which have narrow grey level plateaus of constant width, after edge detection they appeared as closely-spaced, parallel chains of edge pixels. Edge detection enhances the presence of edges in the original intensity image, thus generating a new image where edges are more conspicuous.

Edge detection is the best way to tackle the problem of edge feature detection. ILFDP offers several standard edge detectors including, Sobel, Canny, and Deriche. Directional edge detection is not a new concept. If the presence of noise in images is ignored, the edge detection is primarily based on intensity gradient and subsequent thresholding of its magnitude.

6.3.2.2 Thresholding

Thresholding makes an edge/no-edge decision by transforming a gray level representation of an image, yielding a binary edge map (binary representation of the image). By thresholding, some information loss may occur. The response of image features (pixels) to edge detection filters depends primarily on the contrast of linear features with the background, and the orientation of features relative to the edge mask operator.

To decide how much information to lose in order to retain useful information is a difficult task in image edge or line filtering. Indeed, it is very difficult to set a threshold so that there is small probability of enhancing noise while retaining high sensitivity. If the threshold is set too low, portions of edges or lines are removed. In contrast, if the threshold is set too high, some false information or edges/points are presented. The best compromise was found by experimentation. To facilitate the thresholding task a colorbar

was added to the program to select an approximate threshold. This tool appends a vertical bar to the current axes, resizing the axes to make room for the color bar which can be used with both 2D and 3D plots. An ad hoc procedure has to be taken to find an optimal threshold level.

The Sobel, Canny, and Deriche filters were compared at different threshold values. Using the Canny and Deriche edge detectors requires higher threshold values for built-up areas in comparison to rural areas. To satisfy this objective, three thresholds T_1 , T_2 and T_3 were used. The performance of different thresholds is compared in Figures 6.12-6.15. By increasing the threshold values, it can be seen that the roads begin to disconnect, and significant aggregation of distinct features (eg adjacent houses) remains. A greedy (low) threshold causes better road connectivity but blurs houses into roads. More conservative thresholds produce neater road segments, but leave gaps, eliminate small roads, and still some building and driveways are attached. It was found that the Canny edge detector (with a filter size of 7) and Deriche operator (with an a filter size of $\alpha = 2$) using a threshold value of 40% yielded more road boundaries, and tended to trace closed contours around houses.

The very clear edges on both sides of major roads, and many edges of agricultural field boundaries and vegetation alignments, streams, buildings, and other terrain features may be observed (Figures 6.19 and 6.21). A road is composed of two edges, one on either side. Additionally, an edge may not be the edge of a road; any sharp change in the grey value of adjacent pixels can be judged to be an edge. Even if all the edges in an image are extracted, it is difficult to interpret the result. In a complex scene like urban areas which are full of man-made features, many parallel edges can be detected. Consequently it is unclear which two edges can be considered to form a road. This shows the limit of low level image analysis techniques. They can only use brightness values in the image rather than spatial and contextual information available from both from humans and GIS data.

6.3.2.3 Mathematical Morphology

Morphological transformation was considered for extraction of boundaries, connected components, and the thinning of the line features by skeletonisation. Dilation and erosion tools may be described as neighbourhood transformations. To clarify the functions of mathematical tools, the results of these operations are illustrated in a subset of the extracted line features in Figures 6.13, 6.15, and 6.18. The mathematical morphology tools are exploited after edge detection and thresholding to improve the edge detection output.

The ILFDP allows the user to apply the mathematical operations for the binary data using the "bwmorph" function. This function (filter) has 512 possible results, one for each possible configuration in a 3x3 neighbourhood. It uses the white pixels for hit and black pixels for miss configurations respectively. The morphological operators applied to the Sobel, Canny, and Deriche filtered output images are shown (Figures 6.13, 6.15, and 6.18)

Five basic transformations of binary image are used in this process, namely dilation, skeletonisation, bridge, fill, and close. The order of operations and parameters used for each operation are as follows: bridge, fill, close, dilation, and skeletonization. A single tolerance was used for each operation. Bridge was used to bridge previously unconnected pixels. Fill, isolated interior pixels, that is, black pixels that are surrounded by white pixels. Close, performed binary closure in the data. Dilation was used to add 8-connected pixels to the boundary of binary objects. It helps to join edge segments within the binary image. A thinning (eg skeletonization) algorithm keeps the connectivity of the lines on an image. These operations help increase accuracy of linear feature detection.

Application of the morphological operations (MO) over the produced Sobel filter, Canny, and Deriche edges with three different thresholds (10%, 20%, 30%) over a rural test area, and (30%, 40%, 50%) over a built-up is represented (Figures 6.13, 6.15, and 6.18). The performance of morphological transformation on the enhanced edges from the Canny and Deriche filters over the entire 1982 image of the study area is presented in Figures 6.20 and 6.22.

6.3.3 Analysis

(a) Sobel Filtering

Non-linear edge enhancement algorithms are based on gradient operators. A conventional technique is then to estimate two components of the intensity gradient vector using the Sobel edge masks. Sobel filtering is one of the better edge detection algorithms which represent the spatial derivative edge detectors. The Sobel operator is a non-linear edge detection operator, which can be applied to separately estimate the discrete gradient both in vertical and horizontal directions in the following matrix form:

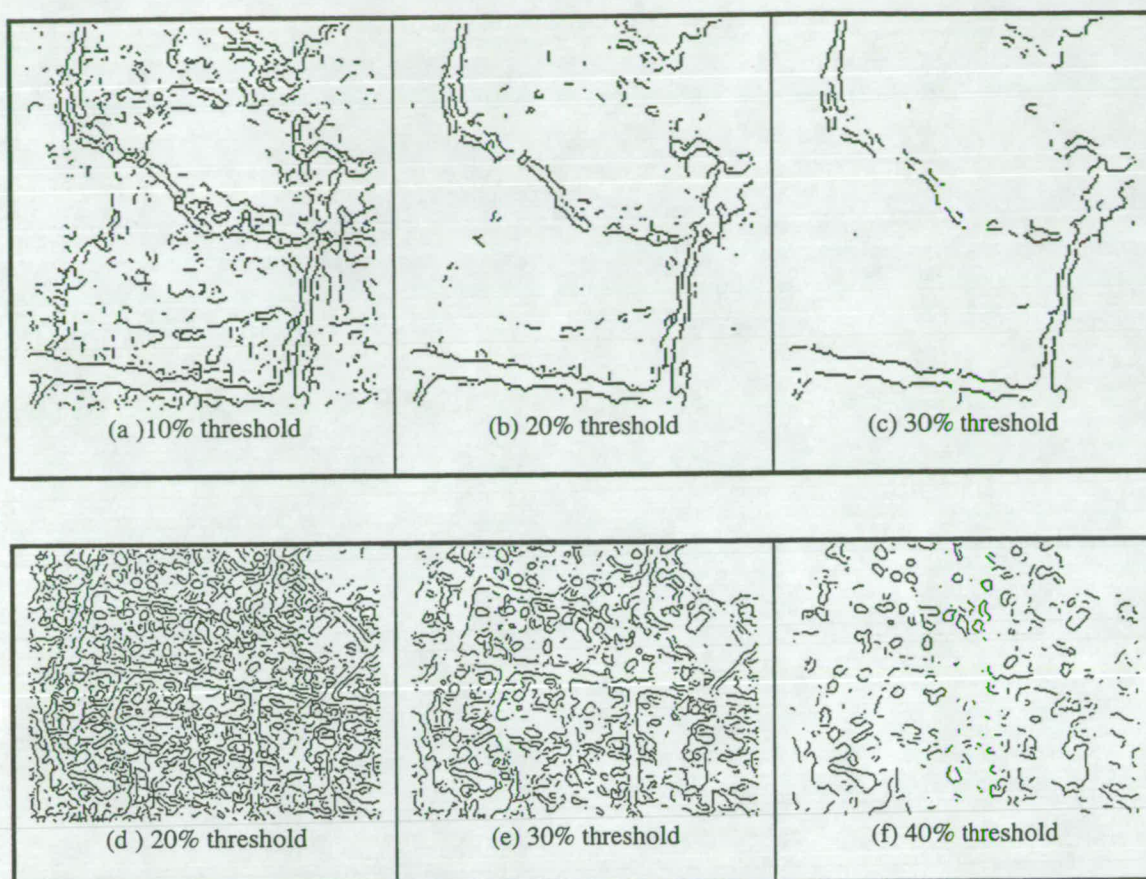
$$H_x = \begin{bmatrix} -1 & 0 & 1 \\ -2 & 0 & 2 \\ -1 & 0 & 1 \end{bmatrix}, H_y = \begin{bmatrix} -1 & -2 & -1 \\ 0 & 0 & 0 \\ 1 & 2 & 1 \end{bmatrix}$$

where H_x and H_y are obtained by convoluting the 3 by 3 neighbourhoods in both vertical and horizontal directions respectively. The combination of kernels is shown below.

-1	0	1
-2	0	2
-1	0	1

-1	-2	-1
0	0	0
1	2	1

These masks were used to detect the horizontal and vertical edges within the image. The Sobel operator allows the user to define edges as places where the first derivative of the intensity is larger in magnitude than some thresholds, and places where the second derivative of the intensity has a zero crossing. The Sobel edge finding method in the ILFDP uses a default estimator that produces consistently good results. The regions obtained at 3 threshold values were shown in Figures 6.12.



Figures 6.12 Represents application of Sobel filter with different threshold over a rural site (a, b, c) and an urban site (d, e, f).

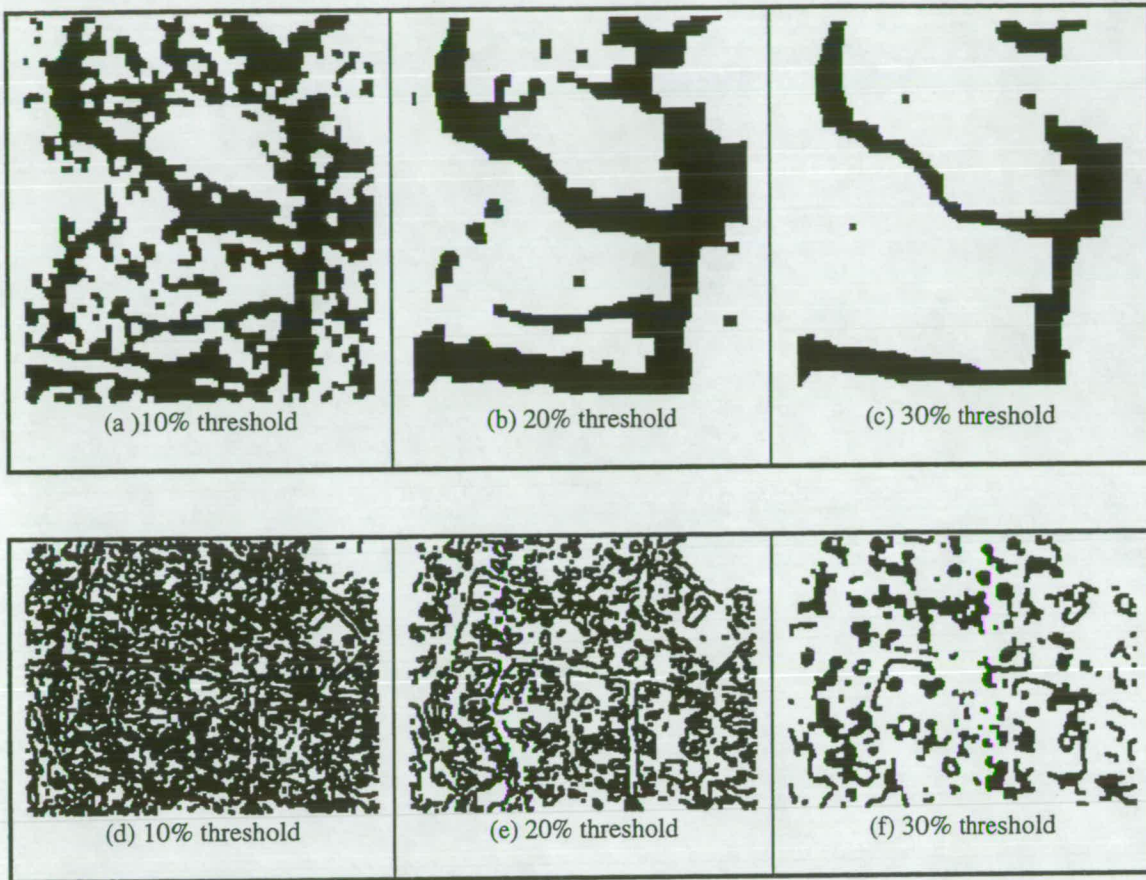
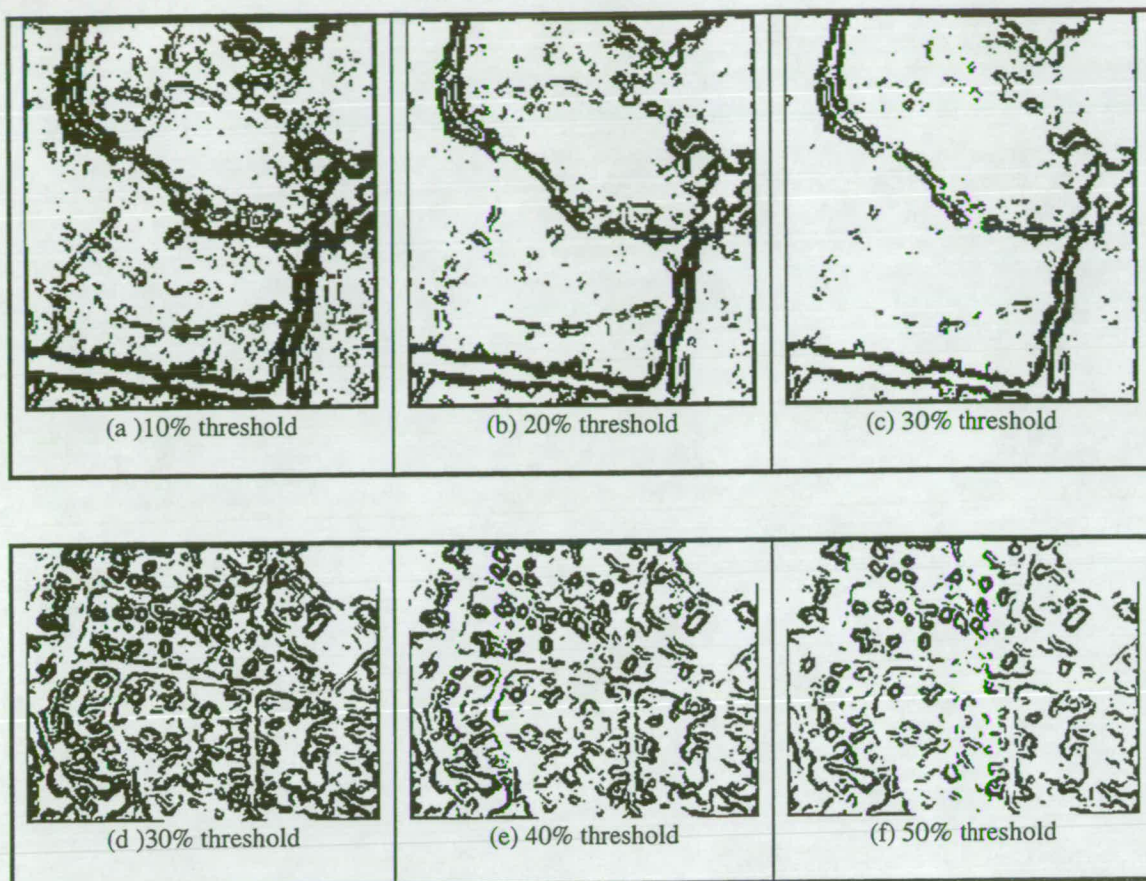


Figure 6.13 Mathematical morphology operations applied to the Sobel filtered data over a rural site (a, b, c) and an urban site (d, e, f).

(b) Canny Edge Detector

Canny's model distributes the edge and non-edge response with a Gaussian distribution in order to separate the signal and noise amplitude distribution of the filter response from noise and real edges. The optimal threshold for a Canny's operator was reported to be 70 to 80 percent by other researchers using hysteresis thresholding; however, this may be too high for the imagery used in this research. The hysteresis thresholding of Canny tries to keep the edge pixels as continuous as possible. The above threshold (70% to 80%) may lead to unconnected edges and may remove very useful information. It was necessary to try different threshold values for a homogeneous test site (eg the rural site), and a heterogeneous area (eg the built-up area).

After empirical testing, it was found that thresholding of between 20 to 30 percent over a rural site, and 40-50 percent over a built-up area produce edges which most closely correspond to real road boundaries. Based upon qualitative and quantitative assessment of edge detection results, a threshold value of 40% was chosen to apply over the entire image of the study area.



Figures 6.14 The result of Canny filtering for different threshold values with a filter of 7 by 7 over a rural site (a, b, c) and an urban site (d, e, f).

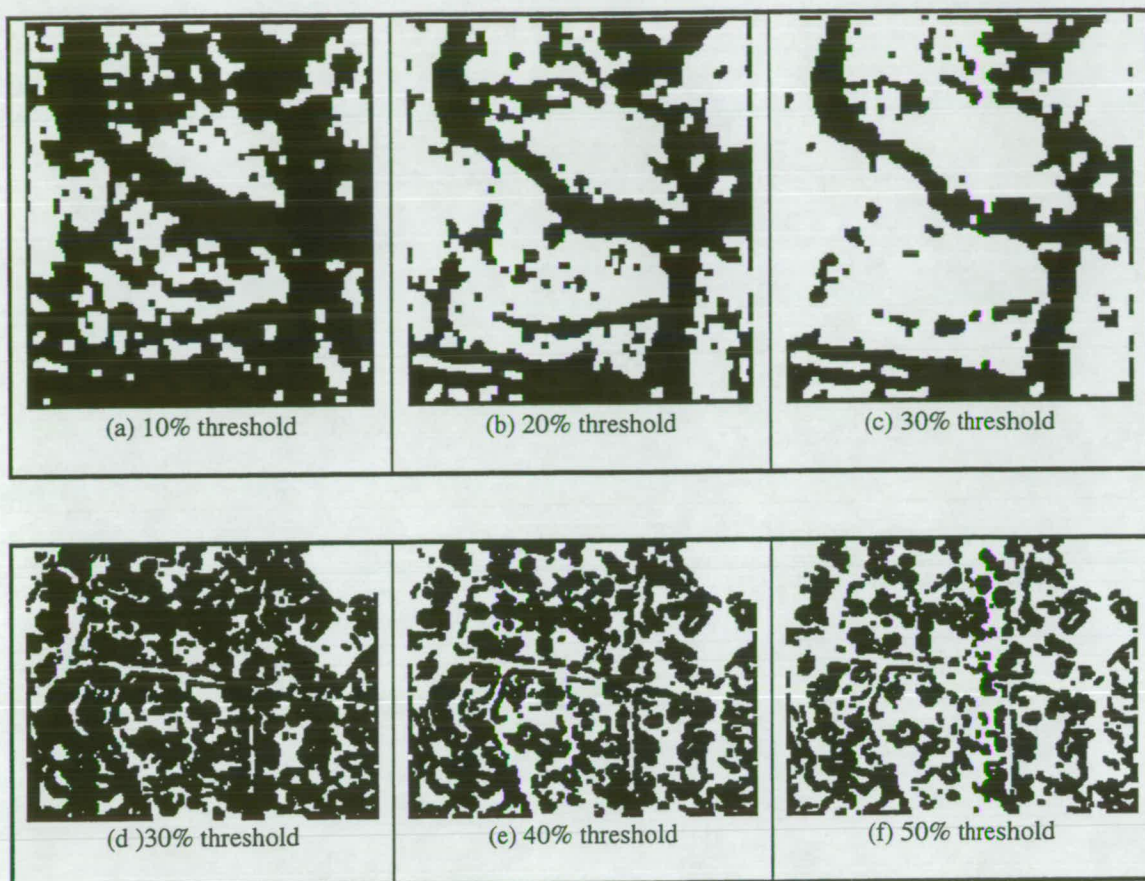


Figure 6.15 Morphological operation on detected edges from Canny filtering over a rural site (a, b, c) and an urban site (d, e f).

Morphological operations over the rural site eg using $T = 40\%$ decreased the commission errors significantly (Table 6.5). The classification accuracy before and after morphologic transformation (at $T = 40\%$) was 81% and 71% respectively, and the commission errors before and after morphologic transformation (at $T = 40\%$) were 58% and 21% respectively. In the same manner, morphological operations over the urban site eg using $T = 40\%$ decreased the commission errors moderately when compared with the rural site. The classification accuracy before and after morphologic transformation (at $T = 40\%$) was 63% and 37% respectively, and the commission errors before and after morphologic transformation (at $T = 40\%$) were 78% and 54% respectively. This occurs because there are two land cover classes in the rural site, roads and vegetation where the contrast is high, while in the urban site there are more than two classes such as buildings, cleared land, and construction. Thus, the commission errors after morphological transformation was decreased rapidly, and the classification accuracy after morphological transformation decreased slightly.

(c) Deriche's Approach

In the ILFDA program, the user has three options for the size of the filter or local maxima (α) in which $\alpha = 2$ has the best performance over images here. The Deriche operator applied to variety of images with different values of the parameter α controlling the width of the impulse response. It is evident that too many edge points are being detected, particularly in regions where the contrast is low. Lower threshold values present too many pixels which are not true edges. Higher threshold values cause breaking connected chains of edge pixels into chains, which is not highly desirable.

Based upon the study of the literature in this field, the Deriche filter has not yet been experimented with for remote sensing imagery. Therefore, there is no evidence that benefit can be gained from those filters which were applied with different thresholds. The results of the Deriche approach have been applied to the test area with a range of threshold (T) (Figures 6.17 and 6.18). It was found that lower thresholds will produce too many edges, particularly in the eastern and central portions of image where the contrast is fairly low. For example, the best threshold values for the rural site was 20-40 percent, and for the urban site was 30-50 percent using Deriche filter. It was pointed out

by Faugeras (1993) that to tackle the thresholding at the right level, one can keep only the edge pixels whose gradient norm is higher than T . Threshold values of 35, 40, 45 percent were applied to evaluate the edge detection result for the whole image (Table 6.8). Consequently a 40% threshold obtained reasonable results to carry out morphological transformation in order to a generate final classification edge detection map.



Figure 6.16 The result of the Deriche filtering approach for different threshold values and $\alpha = 0.5$, $\alpha = 1$, $\alpha = 2$, over a rural site (a, b, c).

The classification accuracy assessment showed that the Deriche filter using $\alpha = 2$ produced the best result among the above filter sizes ($\alpha = 0.5$, $\alpha = 1$, $\alpha = 2$) for the rural site.

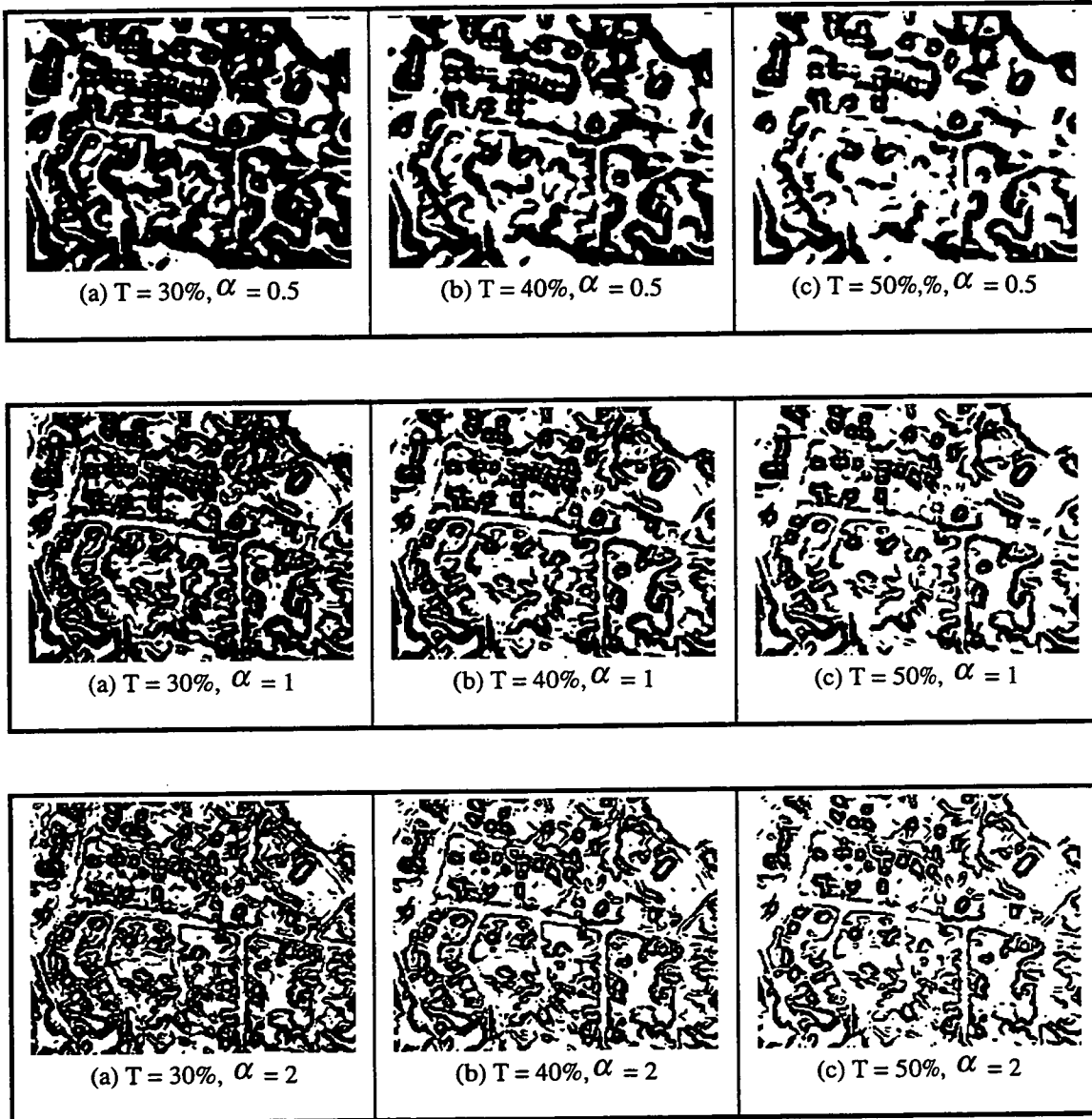


Figure 6.17 The result of the Deriche filtering approach for different threshold values and $\alpha = 0.5$, $\alpha = 1$, $\alpha = 2$, over an urban site (a, b, c).

The classification accuracy assessment showed that the Deriche filter using $\alpha = 2$ produced the best result from the above filter sizes ($\alpha = 0.5$, $\alpha = 1$, $\alpha = 2$) for both rural and urban sites (Tables 6.5 and 6.6). It can be seen that the classification accuracy

increases directly if α increases. The $\alpha = 2$ produced neater edges in respect to noise compared with other values of α . For example, if $\alpha = 0.5$ and the threshold value is 30 percent, the classification accuracy is 64 percent, and commission error is 46 percent whereas if $\alpha = 2$ and the threshold value is 30 percent, the classification accuracy is 83 percent, and commission error is 50 percent. In addition, by increasing the threshold values, it can be observed that the commission errors increase. This trend is similar in both urban and rural test sites. In short, classification accuracy evaluation demonstrated that the Deriche filter using an $\alpha = 2$ produced the most accurate result from the above filter sizes ($\alpha = 0.5, \alpha = 1, \alpha = 2$) for the built-up site.

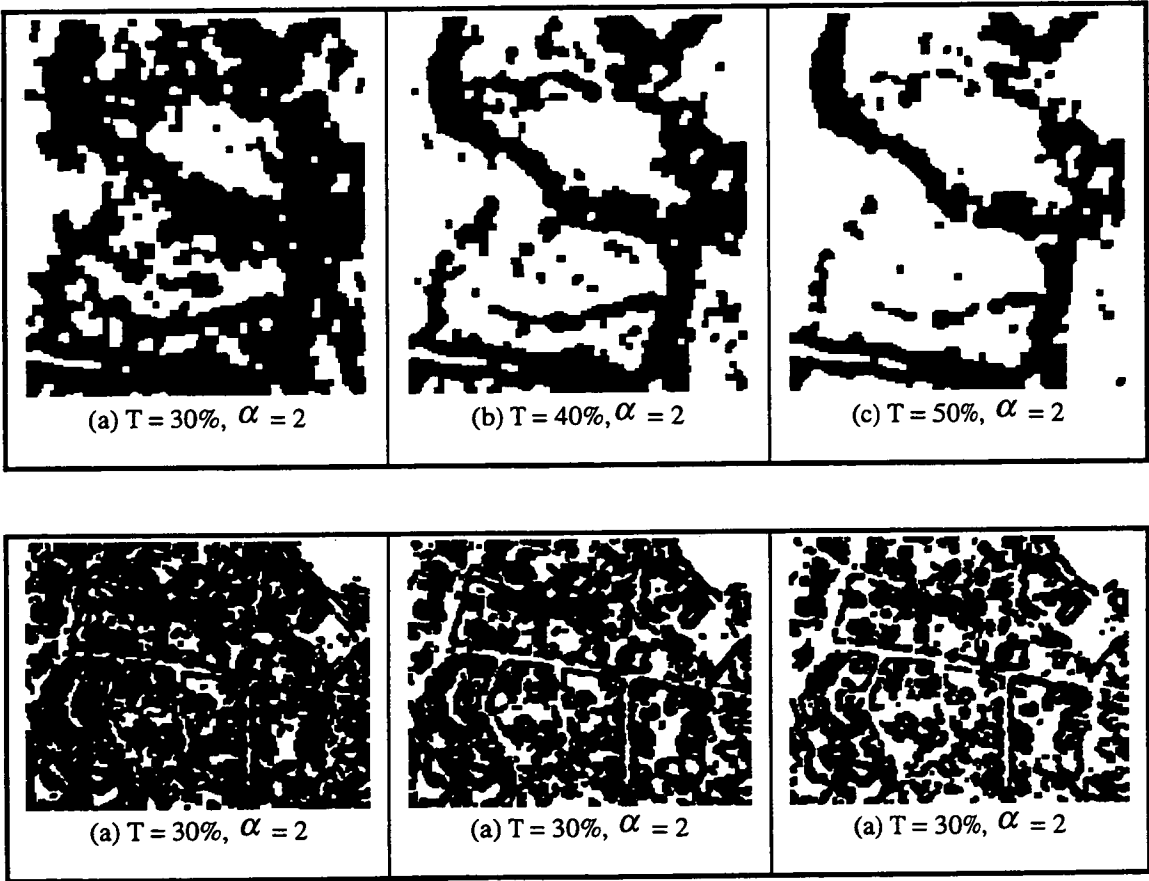


Figure 6.18 Morphological operations over the produced Deriche filter edges over a rural site (a, b, c) and an urban site (d, e, f).

As with Canny, using Deriche filter edges, the morphological operations over the rural site (eg using $T = 30\%$, and $\alpha = 2$) decreased the commission errors (Table 6.1). The classification accuracy and commission errors before morphologic transformation (at $T = 30\%, \alpha = 2$) were 83% and 50% respectively, and the classification accuracy and commission errors after morphologic transformation (at $T = 30\%, \alpha = 2$) were 64% and 17% respectively. Similarly, morphological operations over the urban site (at $T = 30\%, \alpha = 2$) decreased the commission errors. The classification accuracy and commission errors before morphologic transformation were 45% and 65% respectively, and the classification accuracy and commission errors after morphologic transformation were 19% and 32% respectively. This happens because the rural site contains two classes, namely roads and vegetation where the contrast is high, while in the urban site there are more than two classes such as buildings, cleared land, and construction. Therefore, the commission errors after morphological transformation decreased significantly. Classification accuracy evaluation demonstrated that the Deriche filter using $\alpha = 2$ produced the most accurate result from the above filter sizes ($\alpha = 0.5, \alpha = 1, \alpha = 2$) for the built-up site.

The traditional approach of mask convolution has been combined with mathematical morphology operations (eg Destival, 1986). The result of this approach is fragmentary and error-prone. To overcome these ambiguities, domain knowledge and global information about roads and surrounding areas should be used. A qualitative (visual assessment/inspection) of the results of image segmentation is presented in Table 6.7, and a quantitative summary of the results is given in Table 6.8.



Figure 6.19 The result of Canny filtering for different threshold values with a filter of 7 by 7.



Figure 6.20 Morphological operation on detected edges from Canny filtering.



Figure 6.21 The result of the Deriche filtering approach for a threshold value of 40% and, $\alpha = 2$.



Figure 6.22 Morphological operations over the produced Deriche filter edges.

6.3.4 Discussion

Three edge detectors namely Sobel, Canny, and Deriche were tested on subsets of the aerial image. The performance of the Sobel filter was generally lower than the Canny and Deriche filters. Based upon this, the analysis over the entire image was undertaken on the Canny and Deriche edge detectors. Results showed that Canny was marginally better than the Deriche operator. In respect to thresholding values, if threshold = 10% is used, many isolated spots are also picked out, because the threshold is too low. However when a higher threshold (eg threshold = 20), was chosen, there was much less noise, but similar roads are missing too.

In order to demonstrate the quantitative assessment of image segmentation, the classification accuracy for each edge detector, threshold value, and morphological operations for both rural and urban test sites were computed (Table 6.5-6.8). This type of approach for image segmentation accuracy evaluation is widely used (eg O'Brien, 1991; Ton et al 1991; Treitz et al 1992; Harris and Ventura, 1995). The omission error of a land-cover type is described as the number of omitted pixels (labelled as the land-cover type by the ground truth data but not by the algorithm) divided by the total number of pixels in the land-cover type. The commission error of a land-cover type is described as the number of commission pixels (labelled as the land-cover type by the algorithm but not by the ground truth data) divided by the total number of pixels in the land-cover type. The classification accuracy of a land cover type is described as the number of correctly classified pixels divided by the total number of pixels in the land-cover type (Ton et al 1991). Therefore, classification accuracy plus the omission error will sum to 100%. The commission error is a separate statistic.

Edge Detectors Data Type	Classified	Edge of Road	Networks
	Overall Classification Accuracy	Omission Errors	Commission Errors
Sobel, T = 10%	0.84	0.16	0.75
Sobel, T = 10% and MO	0.55	0.45	0.18
Sobel, T = 20%	0.86	0.14	0.83
Sobel, T = 20% and MO	0.72	0.28	0.19
Sobel, T = 30%	0.92	0.08	0.89
Sobel, T = 30% and MO	0.86	0.14	0.37
Canny, T = 20%	0.64	0.36	0.35
Canny, T = 20% and MO	0.45	0.55	0.05
Canny, T = 30%	0.76	0.24	0.44
Canny, T = 30% and MO	0.56	0.44	0.14
Canny, T = 40%	0.81	0.19	0.58
Canny, T = 40% and MO	0.70	0.30	0.21
Deriche, T = 20, $\alpha = 0.5$	0.53	0.47	0.31
Deriche, T = 30, $\alpha = 0.5$	0.64	0.36	0.46
Deriche, T = 40, $\alpha = 0.5$	0.73	0.27	0.54
Deriche, T = 20, $\alpha = 1$	0.67	0.33	0.28
Deriche, T = 30, $\alpha = 1$	0.72	0.28	0.45
Deriche, T = 40, $\alpha = 1$	0.77	0.13	0.61
Deriche, T = 20, $\alpha = 2$	0.71	0.29	0.42
Deriche, T = 30, $\alpha = 2$	0.83	0.17	0.50
Deriche, T = 40, $\alpha = 2$	0.85	0.15	0.65
Deriche, T = 20, $\alpha = 2$, and MO	0.45	0.56	0.08
Deriche, T = 30, $\alpha = 2$, and MO	0.64	0.36	0.17
Deriche, T = 40, $\alpha = 2$, and MO	0.76	0.24	0.22

Table 6.5 Accuracy evaluation based on coincidence computations between the existing road map and the classified edge detection map for the rural site.

Edge Detectors Data Type	Classified	Edge of Road	Networks
	Overall Classification Accuracy	Omission Errors	Commission Errors
Sobel, T = 10%	0.75	0.25	0.80
Sobel, T = 10% and MO	0.21	0.79	0.25
Sobel, T = 20%	0.81	0.19	0.87
Sobel, T = 20% and MO	0.42	0.58	0.55
Sobel, T = 30%	0.94	0.06	0.92
Sobel, T = 30% and MO	0.72	0.28	0.85
Canny, T = 30%	0.52	0.48	0.66
Canny, T = 30% and MO	0.21	0.79	0.36
Canny, T = 40%	0.63	0.37	0.78
Canny, T = 40% and MO	0.37	0.63	0.54
Canny, T = 50%	0.71	0.29	0.84
Canny, T = 50% and MO	0.40	0.60	0.63
Deriche, T = 30, $\alpha = 0.5$	0.34	0.66	0.46
Deriche, T = 40, $\alpha = 0.5$	0.50	0.50	0.61
Deriche, T = 50, $\alpha = 0.5$	0.62	0.38	0.71
Deriche, T = 30, $\alpha = 1$	0.39	0.61	0.55
Deriche, T = 40, $\alpha = 1$	0.52	0.48	0.68
Deriche, T = 50, $\alpha = 1$	0.63	0.37	0.79
Deriche, T = 30, $\alpha = 2$	0.45	0.55	0.65
Deriche, T = 40, $\alpha = 2$	0.59	0.41	0.77
Deriche, T = 50, $\alpha = 2$	0.71	0.29	0.81
Deriche, T = 30, $\alpha = 2$, and MO	0.19	0.81	0.32
Deriche, T = 40, $\alpha = 2$, and MO	0.31	0.69	0.43
Deriche, T = 50, $\alpha = 2$, and MO	0.41	0.59	0.54

Table 6.6 Accuracy evaluation based on coincidence computations between the existing road map and the classified edge detection map for the urban site.

Thresholding (%)	Canny filter		Deriche filter	
30	n ++	r1+ + r2++	n ++	r1+ + r2++
	c+ +	d - -	c+ +	d - -
40	n+	r1+ + r2++	n+	r1+ r2- -
	c+	d - -	c+	d+
45	n - -	r1+ r2- -	n - -	r1- r2 -
	c+	d+ +	c - -	d + +

Table 6.7 A summary of the results of edge detection. The +, ++, -, - -, mean high, very high, low, and very low respectively.

Three basic criteria are considered to test the success of each edge detector viz. in this approach and are reported in the above table:

- 1) The amount of noise present (n)
- 2) Which types of roads are well presented (r):
 - roads (r1)
 - tracks (r2)
- 3) Capacity of morphological operation
 - to connect the unconnected edges or lines (c)
 - to remove or connect isolated pixels or dots (d)

Edge Detectors Data Type	Classified	Edge of Road	Networks
	Overall Classification Accuracy (%)	Omission Errors (%)	Commission Errors (%)
Canny, T = 35%	74	26	67
Canny, T = 40%	78	22	70
Canny, T = 45%	80	20	76
Canny, T = 40% and MO	86	34	35
Deriche, T = 35%, $\alpha = 2$	70	30	61
Deriche, T = 40%, $\alpha = 2$	75	25	69
Deriche, T = 45%, $\alpha = 2$	73	27	75
Deriche, T = 40% and MO	77	33	43

Table 6.8 Accuracy evaluation based on coincidence computations between the existing road map and the classified edge detection map for 1982 imagery.

Classification accuracy evaluation helped to choose the best edge detection filter, and threshold parameters. According to the previous experimentation with the test sites, it became possible to optimise the process of linear feature detection by means of edge

detection filter and thresholding. Using Deriche edge detection filter ($\alpha = 2$) and Canny operator employing three different threshold values based on the introductory experiment demonstrated that a threshold of 40% would be the most subjective threshold to be applied for the whole image.

Using Canny and Deriche filters, significant confusion occurred between cleared land, construction, buildings, and other natural line features (eg field boundaries), as evidenced by high classification commission errors (eg if $T = 40\%$ for both Canny and Deriche filters, then the commission errors were 70% and 69% respectively) (Table 6.8). This is not surprising because cleared areas, man-made features and natural line features occur within the spectral make-up of road edges. Both Canny and Deriche filters generated very similar results. However, it is clear that the Canny edge filter has higher classification accuracy compared with the Deriche operator.

Morphological operations over the Canny and Deriche edges (at $T = 40\%$) optimised classification accuracy (Table 6.8). The classification accuracy before morphologic transformation (using Canny with a $T = 40\%$) was 78%, and the classification accuracy after morphologic transformation (using Canny with a $T = 40\%$) was 86%. Similarly, the classification accuracy before and after morphologic transformation (using Deriche with a $T = 40\%$ $\alpha = 2$) was 75% and 77% respectively. Despite the fact that the classification accuracy after morphological operation for Canny and Deriche edges was increased by 12% and 2% respectively, the commission errors after morphological operation for Canny and Deriche edges decreased dramatically (by 45% and 33% respectively). The overall classification accuracy after and before morphological transformation was 86% and 78% respectively (with Canny, and a $T = 40\%$), and 77% and 75% respectively (with Deriche, and $T = 40\%$, $\alpha = 2$). This indicates that the classification accuracy was optimised. The Canny edge detector provided better results in comparison to the Deriche edge detector.

6.4 Remarks for Image Segmentation

It has to be acknowledged that remote sensing images particularly in urban scenes are very complex. The use of spatial filtering can be affected by the complexity of the scene because of noise in the data. Materials along the road with the same intensity as the road are problematic where there are objects with similar intensity as roads. This problem also occurs at intersections where two roads with similar material meet. If the area is a mixture of urban and residential, then the problem of feature detection becomes much more difficult. Edge detection and mathematical morphology have been used; however the output is noisy and incomplete in high density residential areas. The noise effect is a common problem in road detection. Noise causes small isolated blobs of pixels to be recognised as roadlike segments. In the process of removing noise, small segments or real roadlike structures might be missed.

A number of edge detection techniques and morphological operations were examined. The ILFDP algorithm presented here is the first step of a more complex process of pattern recognition in road networks and linear features mapping. A major limitation of line and edge filters is the need for optimal selection of thresholds for feature extraction. The size of filter (in Deriche and the Canny) and the threshold levels play the most important roles in the edge detection process. This program is able to detect edges of roads, field boundaries, and rivers. The processed data (after morphological operations) has been used as an additional GIS layer for decision tree implementation.

Chapter 7

SPATIAL DATA PROCESSING: CONSTRUCTION OF A DATABASE FOR A KNOWLEDGE BASED ENVIRONMENT

Detecting features on remotely sensed imagery is highly dependent upon the type of object, size, association, shape, tone and intensity. This chapter describes the procedures used to construct the knowledge-based data set using a grid raster-based processing approach. It covers the process of data capture, manipulating, integrating, converting, and generating ASCII data files. A cell size of 2 metres was used for the output raster layers to enable integration of this data with the georeferenced air photo data. The multiple ASCII files were converted into a single formatted ASCII file to be interfaced with decision tree software.

7.1 Spatial Data Construction

The process used to prepare data is depicted in Figure 7.1.

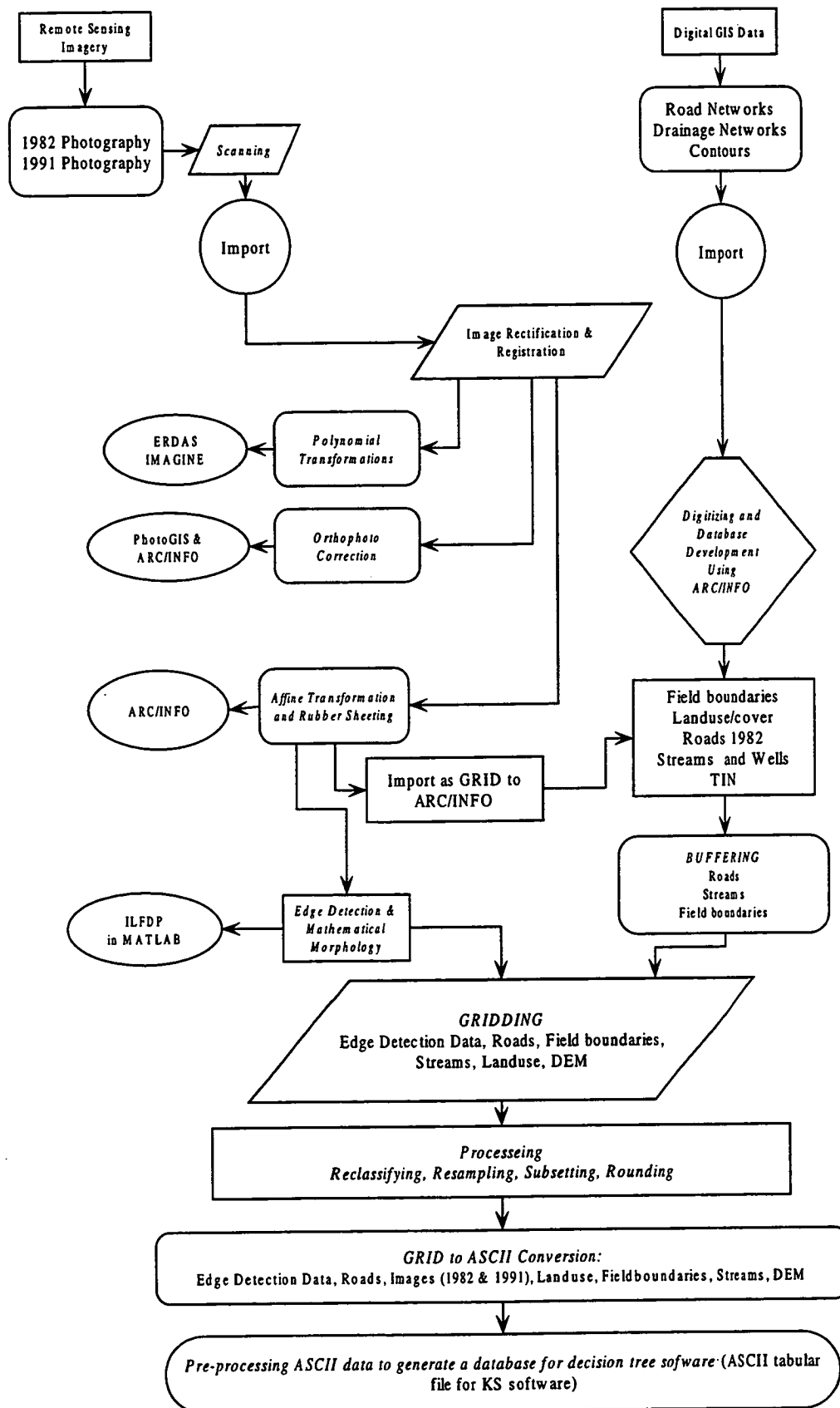


Figure 7.1 Schematic of the data preparation.

The spatial data processing and manipulation can be categorized into the following steps:

7.1.1 Data Entry

The first step in a GIS project is data capture. This phase (data entry in both raster and vector) is one of the most costly, time-consuming and tedious tasks in the development of GIS in any project.

Two sets of aerial images (1982 and 1991) were acquired at a scale of 1:42000. The B/W air photos were scanned with 500 DPI and stored in a 25 MB TIFF format.

The digital vector data was provided by TASMAP in Integrgraph Design Files (DGN) format, and all available vector data layers were converted into ARC/INFO files.

7.1.2 Database Development

A sub-region for each image was separately created for the process of polynomial rectification, affine transformation and rubber sheeting. The test area measured 3 km by 2 km.



Figure 7.2 The study area.

The final geocoded product from the process of rectification and registration in ARC/INFO, was in ARC/INFO grid format files (Chapter 6). All data were registered to a Universal Transverse Mercator (UTM) projection (zone 55).

Additional data was acquired by digitizing from geocoded imagery. All vector and grid processing was undertaken using ARC/INFO software. The following coverages were generated by screen digitizing:

- field and vegetation boundaries
- land use boundaries based on the 1982 image.

An edge matching technique was used to join the map sheets. A rubber sheeting algorithm was used to align features on the edge of coverage (eg Flowerdew, 1991). The coverage was joined by using the EDGEMATCH tool in ARCEDIT. Ultimately each network coverage including road network, streams, and contours maps was precisely edge-matched to form a single output coverage (layer) where these maps were required for creating an orthophoto (Chapter 6).

All digitized data was carefully verified and topologically corrected. This process ensured there was no missing data, no extra data, accurate data, connecting features, each polygon had single label point, and all features were within the outer boundary. BUILD and CLEAN commands were used to create topology of the coverages. Error detection included node errors, unclosed polygons, label errors (missing label and too many labels), dangling nodes (overshoot and undershoot) and pseudo nodes.

7.1.2.1 Editing Road and Stream Coverages

The roads coverage provided by TASMAP was updated based on 1984 map compilation. Since existing digital roads did not correspond with the 1982 imagery, the roads from the roads vector data that were not on the 1982 image, were eliminated. Also, the road segments that did not appear on the available digital data, were digitized and edited into the roads coverage. This step was critical for implementation of decision trees in this research since the roads coverage was used as the training data set. The supplied digital drainage network coverage was not complete. It was updated from the 1982 image and verified by the control points from the topographic map.



Figure 7.3 Road networks in a line form overlaid on the georeferenced image for a subset of the study area.



Figure 7.4 Road networks in a buffer form overlaid on the georeferenced image for a subset of the study area.

Because roads in the study area have different width, the roads vector coverage was overlaid on the geocoded 1982 image, and every road segment was labelled with a specific distance for its width based on visual assessment. The road networks in a line form superimposed on the georeferenced image for a subset of the study area can be seen in Figure 7.3. The roads were classified into eight categories with buffer distances ranging from 1 to 8 metres as shown in Table 7.1. The buffer zones created using this technique are shown superimposed on the subset of georeferenced 1982 image in Figure 7.4.

Record #	Class of roads	Distance for buffering in metres
1	1	8
2	2	7
3	3	6
4	4	5
5	5	4
6	6	3
7	7	2
8	8	1

Table 7.1 Buffer distances and road class.

A constant buffer distance of 1.5 m was used for the stream coverage to provide polygons of the same width. The field boundaries were also buffered with a distance of 1.5 metres.

7.1.2.2 Land Use Delineation

The map of land use/cover was developed from the B/W aerial photographs recorded in 1982, and a topographic map released in 1987 by screen digitizing (Figure 7.5). A supplementary colour air photograph (1984) was used to aid visual interpretation. The photographs were interpreted under high magnification, and each polygon was manually classified based on the type of land use. A vector land use map coverage was produced and digitized from the interpretation of aerial photographs. The following classes were extracted from the 1982 image (Table 7.2).

Class	Abbreviation (the attribute in the PAT table)
1) Urban land	
1-1 Residential	U re
1-2 Commercial	U co
1-3 Industrial	U in
1-4 Recreational	U rec
1-5 Educational	U ed
1-6 Utilities	U ut
2) Clearing and Developing areas	Cl/De
3) Agricultural land	
2-1 Forest (timber lands)	Ag fo
2-2 Grasslands	Ag gr
4) Water	
3-1 Rivers	W ri
3-2 Lakes	W la

Table 7.2 Land use/cover classification scheme for visual classification of B/W photography.



Figure 7.5 Map of land use/cover of the area generated by manual interpretation of the 1982 air photo.

7.1.2.3 Rasterization and Resampling

All the processed vector data layers were converted into raster form (ARC/INFO GRID Format) for incorporation into the KBS. Deciding what cell size should be used, is one of the crucial decisions to be made when using cell based GIS processing. Applying RESAMPL function in GRID prompt, all data were resampled into 2 pixels, which is compatible with the scale and the resolution of the aerial images in order to provide integrity for the database. The categorical data (eg buffered roads, land use/cover) were resampled by the nearest-neighbour technique. The continuous (surface) data (ie DEM) were resampled by bilinear-interpolation.

7.1.2.4 Creation of Surface Data

The TIN coverage was converted into TINLATTICE (DEM) with a 2-metre grid cell resolution. The quality of DEM was not satisfactory. Thus, a second technique which involves using an interpolation method was applied. The TOPOGRID tool was used to generate DEM using stream networks and the contour coverage. Three dimensional (3D) perspective views of terrain were created with ARC/INFO and the area displayed as a viewframe display. A Z-exaggeration factor of one was used to portray subtle change in landscape elevations (Figure 7.6).

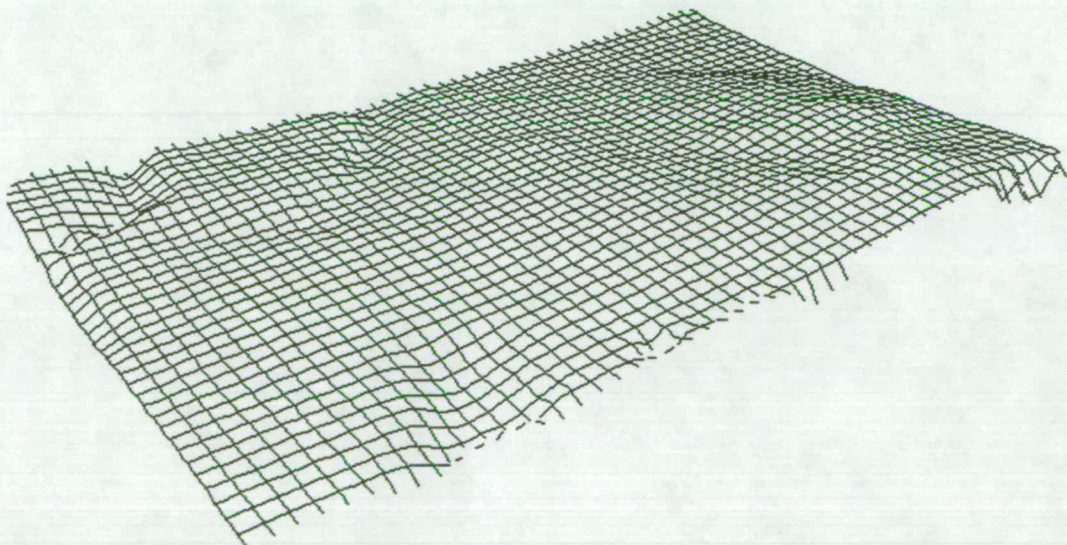


Figure 7.6 A perspective view of the synthetic surface of the area.

After the gridding process, seven principal map features were created, namely land use/cover, DEM, grey level image, roads, field and vegetation boundaries, streams, edge detection data.

7.1.2.5 Processing and Manipulating Raster Grid Data

To reduce the amount of data for later processing by KS, the DEM data was filtered (rounded) through by INT function which converts input floating-point values to integer values through truncation on a cell-by-cell basis within the analysis window.

Initial grid processing included reclassifying (eg land use), and subsetting (eg creating subsets of the data).

7.1.2.6 Conversion of Raster Grid Data to ASCII Files

KnowledgeSEEKER (KS) provides users with an import format file to predefine the field names and field locations when importing many similar data files, or processing data with many fields. KS software reads dBase (dbf) compatible files, Lotus 1-2-3 (wk1), Lotus compatible files, Paradox files in their native format, and Delimited ASCII files. In addition, SPSS files stored in binary format can be imported into KS.

All of the remote sensing and geographic information systems data should be in the same format files in order to make the process of data conversion to knowledge based system practical. Accordingly, a database was constructed to be employed for feature recognition. The database was composed of seven fields or variables.

7.1.2.6.1 Pre-Processing of ARC/INFO ASCII Data for KS Software

The mechanism of data importation from ARC/INFO to KS is not straightforward. Since ARC/INFO ASCII files are not compatible with KS, a program was written to create a tabular ASCII file for direct input to KS. One way of structuring this data for KS is to import files as tabular ASCII format. Thus, the data must be in attribute tabular format to be imported into KS. The data from ARC/INFO was in the form:

```
layer1 pixels1, pixels2, pixel3, ...pixelm
layer2 pixels1, pixels2, pixel3, ...pixelm
```

.

.

```
layerm pixels1, pixels2, pixel3, ...pixelm
```

Those layers must be structured to look like this:

```
Index_No field1 field2 field3, ...fieldn
```

.

m

Where Index_No refers to the sequential location of the observation in the original table (data).

In order to load the grid ASCII data from ARC/INFO into KS, a FORTRAN 77 program was written (Appendix D) to independently generate tabular ASCII data (eg Table 7.3) from the input files.

Roads	Edge	Photo	Streams	Fieldb	Land use	DEM
-9999.00	-9999.00	23.0000	-9999.00	-9999.00	7.00000	8.00000
-9999.00	-9999.00	23.0000	-9999.00	-9999.00	3.00000	8.00000
1.00000	1.00000	56.0000	-9999.00	-9999.00	6.00000	27.0000
1.00000	1.00000	56.0000	-9999.00	-9999.00	6.00000	27.0000
1.00000	-9999.00	64.0000	-9999.00	-9999.00	4.00000	31.0000
-9999.00	-9999.00	12.0000	1.00000	-9999.00	11.0000	1.00000

Table 7.3 Subset of a sample database for input into KS.

7.2 Summary

This chapter described the procedures used to prepare GIS data for input into the KnowledgeSEEKER program for decision tree analysis.

Chapter 8

EXPERT SYSTEMS DEVELOPMENT: DECISION TREES

The Decision Tree Processing Expert System (DTPES) was used to map out road distributions over an urban to rural area. A multi-source database was employed using Geographic Information System (GIS) data and remote sensing imagery. The independent data set comprised six fields (variables) which attempted to represent contextual, textural and geometrical characteristics of the knowledge-based data. A tabular ASCII data file was interfaced with a knowledge-based environment for creation of a classification tree. In the process of decision tree analysis, the input data was recursively partitioned into mutually exclusive exhaustive subsets which would define the best response variable. The resulting classification tree was used to generate generic rules for implementation of DTPES. Each rule is a representation of each node in the tree that describes a class (the presence and absence road pixels) or pixels of the grid data. The spatial distribution of these pixels was mapped out to show areas with roads and their background. The program computes the overall classification accuracy based on the reference data. Finally, the produced image was imported into a GIS environment for overlaying the road reference map on the predicted roads for visual interpretation.

8.1 Introduction

Currently, researchers are using knowledge-based rule image analysis techniques to encode rules used by human interpreters which can be used by a computer for feature extraction. To solve a spatial image recognition problem such as the detection of linear features and extraction of roads from image data, human analysts rely on their expertise in combining external data sets such as topographic maps and land-cover classification. Such data are currently stored in GIS. A specific rule-relation such as KS reveals would usually show up as IF AND THEN or two in-contexts determined by the field of interest. The rules can have some measure of uncertainty associated with them. It is necessary to filter out of the knowledge base biases that are imparted by the unique views and values of the experts who are the resource of the knowledge that constitutes knowledge bases.

This chapter explores the role and capability of an integrated GIS approach using a decision tree method for recognition of roads from aerial photography. The input for the decision tree is a set of data from remote sensing imagery and a database from spatial information systems. A decision tree was generated and processed by KS software. The GIS layer is used as the knowledge source to map out roads, using an inductive approach. Predicted values are required for each of the observations in the dataset. These are then converted into an image format. The simplified KS-generated rules which are the key rules for implementation of a "rule-based expert system", namely the DTPES program which derives prediction of roads distribution over an urban to rural area. Decision rules from the output files were programmed, and the program was run through the database to obtain predicted values. MATLAB environment was used as a shell tool for constructing the DTPES program. The DTPES consists of two subroutines, namely `ks2mat.m` and `dtpes.m` which can be seen in Appendix E.

Previous research on road delineation, including detection and tracking using non-machine and machine learning techniques was reviewed in Chapter 2. The technique of this research works well in prediction and mapping of roads when roads pass through a rural area where the contrast is high, but fails in urban areas where the roads are confused with man-made structures.

8.2 Developing a Knowledge-Based System

8.2.1 Basic methodology

A database was created using GIS and RS datasets employing ARC/INFO software. The knowledge-based system uses a decision tree approach and involves developing an expert system to predict roads from the database. The methodology for the use of decision trees for this study involves several steps:

1. Geometric correction of the aerial images (Chapter 6),
2. Construction of a data set for a knowledge-based software (Chapter 7),
3. Spatial data interfacing with a decision tree environment,
4. Generation of decision tree or a learning set,

5. Tree-pruning procedure; a test case is performed down through the tree and the rules simplified,
6. Rules collection and encoding in MATLAB language to construct an expert system,
7. The expert-rule-based system is tested over any set of new examples,
8. Displaying of the output of rules induction,
9. Computing the overall classification accuracy,
10. Overlaying the output of DTPES on the referenced roads map.

A model of a knowledge based system approach (an expert system development) undertaken in relation to remote sensing and GIS is shown in Figure 8.1.

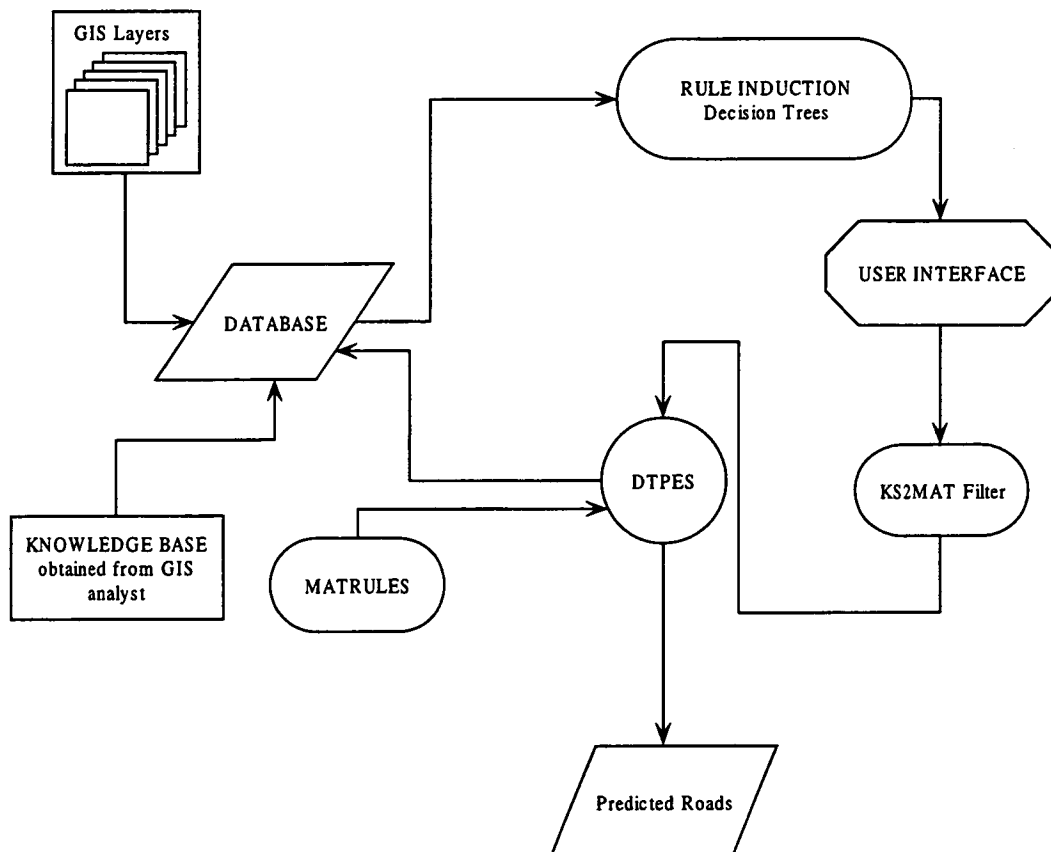


Figure 8.1 Flow diagram of the expert system construction in this study.

In the above model, the interface of GIS and remote sensing data was conducted to develop feature recognition using rule-based techniques and a decision structure. The model consists of three main functions namely, spatial attributes data, rule induction and inferencing.

1. Spatial Attributes Data (Data Layers)

The first component is a database composed of GIS and remotely sensed data both in raster and vector form. The GIS analyst interacts with structuring of this data based on his/her knowledge and experience. This phase of knowledge acquisition was a major issue in the development of the methodology. Gathering information from an expert is a means by which knowledge is to be acquired and represented. The GIS analyst collected evidence from the image and spatial data was inferred from the principal elements of interpretation. To maintain high identification of features, the interpreter relies on the information and the experience obtained from the image, familiarity with the site and field visitation, and any supportive spatial data. To avoid error and inconsistency from the visual based methods caused by differences in the interpreter's knowledge and experience, rigorous procedures and guides can be set out. However, these types of keys may not be available for all land cover types.

Clearly, GIS analysts use their knowledge concerning roads, particularly the relationships of roads to other features such as buildings, parks, rivers, lakes, field boundaries etc to help with the identification of roads. Discrimination of roads between urban and rural areas is also important. Prior knowledge of the topology of road networks (ie width), approximate location, direction, terrain type, and scene elevation was used in this study to assist discrimination of roads from other linear feature.

The knowledge-based attributes data were used in the development of the methodology of this thesis. The GIS data and remote sensing imagery were applied to build a database. The database locates seven attributes (layers) which include: aerial imagery (intensity/contrast), roads, land use/cover, field and vegetation boundaries, edge detection data, streams (drainage patterns), DEM. Geometric, spectral, and spatial characteristics were taken into consideration when building attributes for the knowledge-based analysis. The major knowledge-context data (layers) are as follows:

1. *Contrast or intensity (lightness and darkness) and strength (average contrast).* To support this, spectral data (aerial imagery) was incorporated into the database. Roads against a background (eg vegetation) with high reflectance were easily detectable but became indistinct when they passed areas of similar or low reflectance. For example,

roads between two rows of houses in a dense urban area have a similar grey level. Thus, it was more difficult to recognise the roads in an urban region than a rural area. Other examples are old roads which have high reflectance values and no vegetation cover. New roads in general have less reflectance and are normally partly covered by vegetation. Visibility of roads can be affected by a number of parameters such as sun angle, look angle and surrounding vegetation. The optimal time of year, and optimum look angle for street visibility is a concern. Low sun angle or a large off-nadir view angle can affect the amount of shadow of buildings and trees.

2. *Geometry or topology of roads (eg width, connectivity)*. The geometric shape of roads is an important factor for a contextual classification. Functional requirements, ecological and engineering limitations affect the geometrical and physical form of a road. For example, slope, width, and the local curvature of a road all contain an upper bound. Intersection of roads is another example, as rivers do not intersect one another, rather they join. The existing road-map was added to the knowledge-based data. Referenced road maps contain clues as a guide for the image analyst to recognise analogous roads according to photometry and structural characteristics and other parameters. To maintain a better topology of the roads, it was necessary to use a multi-distance buffer technique in the process of spatial data construction (Section 7.1.2.1). As discussed earlier, road segments were buffered into 8 distances (1-8 metres). Based on the visual interpretation of the image and existing road map, there are three major road classes which can be identified: (1) major roads such as highways or railtracks that are usually long, straight and wide (about 10-16 m wide), (2) local roads: two lane paved roads (about 5-10 m wide) that may have smooth curves and are also long; (3) minor roads; access roads, commonly unpaved and short, (approximately 2-5 m wide). ARC/INFO provides two commands that create topology of a coverage. For example, undershoot errors can be rectified using these functions. This maintains connectivity of road segments in the road coverage (layer).

3. *Land use (location and density)*. An overall land cover classification using visual interpretation was undertaken and the developed data was incorporated into the database. The area was divided into 11 classes on the basis of land cover/use. These heuristic rules imply typical ways to substantiate road network delineation. But this model may not be sufficient for roads which do not exist on maps and extend over

more than one region. Generally, the density of roads is related to the type of land use. For example in a high density urban area, roads are likely to be more complex and dense, while in rural areas and in steep terrain the number of built roads is less than in urban areas. Fundamentally, three dimensions of complexity are involved in road extraction on remote sensing data:

- (a) Image quality: this varies in terms of visibility, resolution, contrast.
- (b) Road density: depending upon the area under investigation (rural, urban, rigorous terrain), different densities exist.
- (c) Road complexity: roads may have very different outlines, from straight lines such as highways and railtracks to sinuous, partially occluded line structures such as mountain roads.

Land-cover/use may be associated with given types of land cover, and to the position and shape of the real world. Different types of land cover can be associated with different types of road network topology. As an example, a road network in an urban area and a network in a rural environment are likely to be structured differently: many crossroads connected to many road segments; one central lane and many branches respectively. This contextual information assists to distinguish roads from other detected features.

4. *Field and vegetation boundaries.* Field and vegetation boundaries in remote sensing imagery appear as line features. When using an edge detector, these features can be misclassified as roads because of their sharp contrast with the background. Thus, it is useful to include field boundaries in the database.
5. *Drainage pattern (streams).* The drainage pattern was also incorporated, and has an effect on the appearance of road structures. Roads normally follow contour lines in valleys and are less curved than channels and rivers. These fundamentals are essential to apply in road construction in order to minimise the number of bridges to be built on road-river crossings. Collinearity and connectivity were considered, and drainage networks were used to avoid confusion of water and bridges as a road segment may be bounded by water.
6. *Edge detection data.* Image segmentation techniques were employed via developing a computer program for primitives extraction (road edges) to generate an additional GIS

layer. Linear structures are made up of two parallel edges and usually represent highways, channels and large rivers using edge detection data.

7. *Digital elevation model (DEM)*. Topography has an effect on the appearance of road structures. As mentioned, roads normally follow contour lines in valleys and are less curved than channels and rivers. The DEM can be used to indicate plausible road tracks in an image. In a mountainous area, a road between locations eg towns and countryside having almost the same altitude commonly follows a line of the same altitude. In an area with high slope (very close contours), a line is unlikely to be a road unless it is approximately parallel to the contours. However, there are exceptions. For example, line elements, like fire lanes in forestry, are known for their slopes perpendicular to the relief. Therefore, a DEM was employed to direct the photometric extraction of a road. Lines can have slope values in a limited interval to be characterised as road candidates.

Table 8.1 summarises the key points made in the above discussion of spatial attributes data (data layers).

Variables (Fields)	Characteristics
Aerial Photography	The image contains grey level information including contrast and strength characteristics.
Road Networks	The roads in the database locate geometric (topology) characteristics such as width and connectivity. For example, to maintain width of the roads, a multi-distance buffer technique which buffered the road segments into 8 distances (1-8 metres) was used. This provides the width characteristic in the database. When using Build and Clean functions in ARC/INFO, connectivity of line (road) segments can be maintained by rectifying undershoot errors.
Edge Detection Data	Roads are made up of two parallel edges. In edge detection data, the characteristic of parallelism partially exists (refer to Section 6.3).
Land Use/Cover	Different types of land cover can be associated with different types of road network topology. As an example, a road network in an urban area and a network in a rural environment are likely to be structured differently: many crossroads connected to many road segments; one central lane and many branches respectively.
Field and Vegetation Boundaries	Field and vegetation boundaries in remote sensing imagery appear as line features. When using an edge detector, these features can be misclassified as roads because of their sharp contrast with the background. Thus, it is useful to include field boundaries in the database.
Drainage Pattern (Streams)	Drainage pattern has an effect on the appearance of road structures. For example, roads normally follow contour lines in valleys and are less curved than channels and rivers. Drainage networks help to avoid confusion of water and bridges as a road segment may be bounded by water.
DEM	Topography has an effect on the appearance of road structures. As mentioned, roads normally follow contour lines in valleys and are less curved than channels and rivers. The DEM can be used to indicate plausible road tracks in an image. In a mountainous area, a road between locations eg towns and countryside having almost the same altitude, commonly follows a line of the same altitude. In an area with high slope (very close contours), a line is unlikely to be a road unless it is approximately parallel to the contours. Therefore, a DEM was employed to direct the photometric extraction of a road. Lines can have slope values in a limited interval to be characterised as road candidates.

Table 8.1 The seven variables or attributes (layers) existing in the database.

2. Rule Induction

The second part is rule induction, which will be explained in Section 8.2.3. This part is concerned with knowledge representation and display production which are driven by decision trees using the spatial database. To date, GIS has generally been deductive rather than inductive. Deductive structures are those in which a known general relationship is employed for particular observations. This allows the users to ask questions requiring the identification of all areas in which a known relationship or desired set of premises are satisfied. On the other hand, inductive structures deal with finding general rules based on the training examples, and then correctly predict or classify new examples.

3. Inferencing

The third component dealing with knowledge inferencing is called the inference mechanism, and uses rules of inference. In this phase, the information generated and collected from the prior phases was aggregated in a rule-based view to maintain consistency and reliability of use of multi-source data in feature recognition.

A forward-chaining process was considered in order to evaluate all rules for a given pixel. The computation time linearly increases as the number of grid cells increases. The forward chaining (bottom-up) search was time consuming since it led to a large number of hypotheses. This is particularly important, if the database is large in terms of number of pixels and the number of rules is great. For example, if there are 7 data files, and the size of every file (grid) is 1000 by 1000 cells or pixels, then a total of 7000,000 pixels has to be processed. In addition, the more rules there are, the more computation time is required. In practice, it is tedious and time-consuming to use such a database since it requires a powerful computer with enough RAM, enough hard drive space, and considerable processing time. Thus, it was necessary to experiment with a small subset of the data.

8.2.2 Input Data for Decision Tree Analysis

A total of seven variables was held in the database. The variables constructed as the raster database that were used in the analysis are as follows:

1. road networks from a topographic map
2. the georeferenced 1982 and 1991 images
3. land use/cover, terrain, digitized from the 1982 aerial photo
4. drainage pattern built from the digital streams, and a topographic map
5. digital terrain model (DTM), built from the digital contour map with 10 m intervals
6. field (vegetation) boundaries and vegetation digitized from the 1982 image.
7. Two sets of detected linear features (from 1991 and 1982 photos) were made, and stored in GIS. Edges were detected by implementation of the ILFDA program under MATLAB environment.

Initially two additional variables, namely slope and aspect, were applied in the analysis. However using these two particular variables caused the classification tree to become very bushy, and made the analysis more difficult. Experience showed that by excluding these two variables the classification accuracy was not increased significantly (only 1%). Therefore, it was decided to exclude slope and aspect from the analysis.

8.2.3 Decision Tree Environment and Interfacing a GIS Database

The input for the KS is a tabular ASCII data file which is defined to KS by the width of each column. In the following example, the field widths of the seven fields are 12, 11, 11, 11, 11, 11, and 11 (78 characters in each record). Once the data is imported into KS, dependent variables can be selected to begin the analysis.

Dependent field (I)	Independent fields (J)					
roads	photo	edge	streams	fieldb	landuse	DEM
1.00000	1.00000	1.00000	-9999.00	-9.0000	8.00000	125.000
1.00000	1.00000	1.00000	-9999.00	-9.0000	8.00000	125.000
1.00000	1.00000	-9999.00	-9999.00	-9.0000	8.00000	125.000

Table 8.2 Sample of GIS data used for Decision Tree Analysis

8.2.4 Generation of Decision Tree: Tree Growing and Analysing

Most decision tree analyses are supplied with a dataset consisting of an I dependent (response) variable or field (eg roads) and N independent (predictor) variables or fields, J1, J2, J3, ...Jn. Decision tree algorithms may produce a binary tree (two-way splits) or multiway partitions (k-way). For example, CART generates only two-way partitioning, while classic AID-type (eg KS) algorithms work on k-way splits. The statistical significance testing employed in the KS algorithm allows the users to gain the clustering method to cluster values of partitioning variables together. In this correspondence, splits in the classification tree establish groups of values in partitioning variables that are statistically the same yet are statistically different from other groups of codes that build the branches of the partition (refer to Section 4.2.3.1). Thus, this effect can be referred to as "k-way" partitioning of the decision tree.

The building of a decision tree is based on training data, composed of a large number of positions together with their corresponding known classification. KS performs the classification in a similar way to other heuristic rule generators such as top-down induction of decision trees (TDIDT) algorithms, which are a more successful form of attribute-based learning. Using KS the spatial data were analysed and classified by finding the best attribute with the highest information content and locating it at the root of the tree. The building procedure in KS was begun at the top node of a tree with a

whole training set, and progressed by recursively creating successor nodes through splitting the training set into subsets of increasing classification purity. The mechanism was terminated when all the newly created nodes were terminal ones, contained sufficiently pure learning subsets.

In the course of this work, a number of classification trees were generated from each learning sample for the analysis sites. Figure 8.2 shows the part of a decision tree that represents the presence (roads) and absence (road background) of road pixels. This is included for illustrative objectives only.

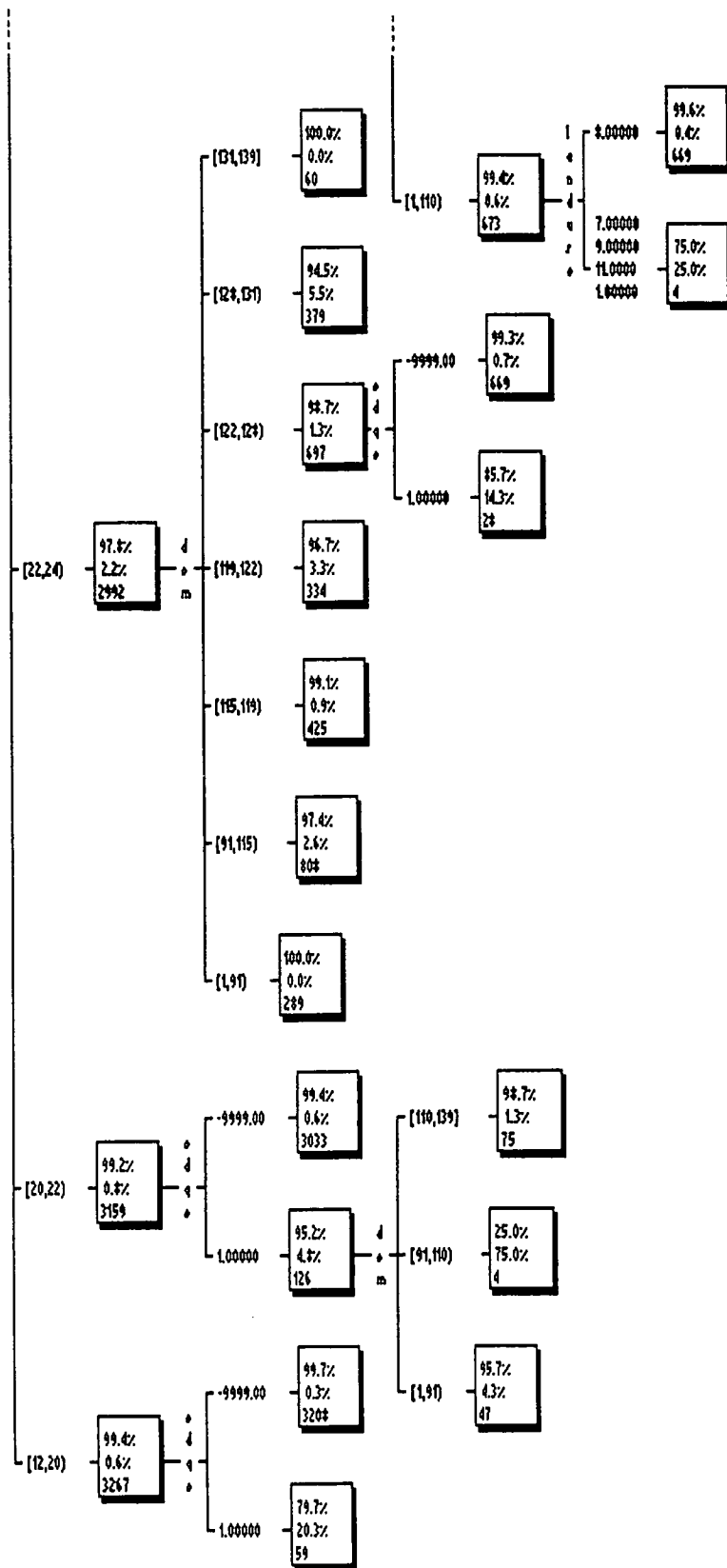


Figure 8.2 Part of a 65-rule model shows as a simple decision tree.

In this example of classification tree, the first rule determines the absence of roads (background) and presence of roads as 79.7% and 20.3% respectively; if the intensity (grey value of photo) is between 12 and 20, and the edge is 1 and -9999, then out of 59 pixels, there is a chance of 79.7% absence of roads and 20.3% presence of roads. By looking at the other branches of the tree, it can be seen that the intensity is the strongest way of characterising roads: the more intensity increases, the more likely roads can be mapped. In the second split from the first level of the tree, the association of elevation appears: if the intensity is between 20 and 22, and the edge is 1 and -9999, and the DEM is 1 to 91, then 97.7% of pixels are classified as non-roads and 4.3% are classified as roads.

It appears that the number of observations in some of the rules are not sufficiently high. It is due to the nature of the dataset used in the decision tree analysis. For example, on the lower part of the classification tree (the third subsets), the DEM is broken down into three branches; in the second branch (rule_4); if DEM is between 91 and 110, there are four pixels in this rule. Among these pixels, 25% of the observations are classified as absence of roads and 75% as presence of roads.

In this research, the classification trees were grown from GIS data using a recursive partitioning algorithm to create decision tree models which give a good prediction of classes on some of the new data. The dependent field was treated as a categorical data type and the independent fields are either ordinal or categorical. Construction and application of the decision tree is separated into two major steps:

- 1) initially all the available records are randomly broken down into learning examples and test examples. A learning set may be applied with heuristic rules to achieve a decision tree. Then a test set is performed through the tree and the rules simplified.
- 2) the tree is employed to classify any new samples.

Tree growing involved applying training sets to build a tree. This stage was overgrown, in the sense that the induced trees were too large. Such trees can be named to track noise in the data. Tree induction performance on training data was found to be a misleading induction of true predictive accuracy. As a complex tree achieves high

accuracy on training data, it often fares worse on fresh data than an uncomplicated tree which performs less spectacularly. This is due to the complicated tree reflecting true underlying relationships and patterns which arise purely by chance.

The next step was a pruning procedure used to avoid overspecialised definition and to remove noise. Pruning includes cutting off those branches that are not statistically grounded. In most applications, the existing mapping data represents a small portion of all possible observations. As a result, input from experts is necessary to ignore over-generalised or over-specialised induction rules. Noise is an essential parameter that was taken into account where attribute and class values were subjected to misclassification. The consideration of noise however, makes it problematic to differentiate a large set of examples from correct special cases.

Automatic tree growth was shown to generate a lot of questionable nodes or rules, in terms of interpretability. Since each field in the database had just one value per record, a rule making reference to two or more range bounds may not always be identical. As the accuracy of a classification tree increases with the number of terminal nodes and a bushy tree will clearly be more accurate than the sequence of subtrees, the tree was often pruned by an erase function at each node. The splits which are borderline or suspect were ignored and this cycle continued through 2nd and 3rd attempts for each node in order to end up with a rule-set that was more manageable. For building expert systems, dependency and simplicity are required. This suggests stopping even before running out of significance; ie about 3-4 levels down in the tree should be considered. This kind of tree is simpler, only showing the very strongest effects, and probably makes most sense from a theoretical point of view. The presence and absence of roads was modelled by the learning sample. It was preferred to grow and then test, grow then test, and so-on. This way growth was stopped when marginal improvements in accuracy started to occur.

Given the input of the database for generating a classification tree for this research, it helped to prune the tree from one node at a time, and the meaning of the variables involved was kept in mind. The KS allows the user to start from a given node and remove the next split. In particular, in a tree generated by automatic growth it may be found that, for a given node, none of the suggested splits are realistic. Either noticing the

absence and presence of roads is getting too small for some branches, or there is no meaningful interpretation for splitting the data that way. This approach gives a terminus for that branch.

8.2.4.1 Cluster and Exhaustive Methods

The KS automatically looks through all variables in the database and detects those associated with the independent variable. It uses the methods of two-way (cluster) and k-way partitioning. To make the analysis, ideally both cluster and exhaustive methods should be applied to identify the codes that form the nodes and branches of the classification tree. These choices generate a split for each potential partitioning variable.

In the first phase, the exhaustive method was used since it is not overly conservative and explores all of the fields that have a statistically significant relationship with the dependent field. The exhaustive method (multi-way partitioning technique) tends to produce a tree with more branches in comparison with the cluster (heuristic method) technique. The major shortcoming of the exhaustive technique is that it is a more time-consuming process. In contrast, the splits formed are empirically stronger than heuristically derived splits. In exhaustive splitting, all possible combinations of variable values are taken into account, making this approach more costly.

The cluster technique was applied to find the maximum similarity within the groups and dissimilarity between the groups. The cluster method utilises pair-wise merging and partitioning. In other words, the cluster method was used to find the most natural patterns of codes for the significant variables. The "prediction filter" which represents the relationships is valid with a 95% certainty rating, as applied to grow the classification tree. This significance setting produces almost no misleading results. However, this setting still generated a bushy tree which made the analysis, interpretation, and communication of the results difficult. To overcome this problem, the significant setting was changed to 0.01 (99%) instead of 0.05 (95%). This setting filters out any relationships that are not at least 99% significant, and produces a less bushy tree. In spite of the previous work in the area of decision trees, the cluster method provided better

accuracy, despite the fact that it has been reported that the cluster method is overly conservative and some significant relationships may be missed.

8.2.5 Expert System Construction: Storage of Output of the Induction Rules

8.2.5.1 Knowledge Acquisition and Representation

The next step in this method is to convert the classification decision tree into a programming set to build a rule-based expert system and develop a procedural code to execute instructions against a database. A rule is a combination of knowledge that represents an antecedent or condition and its immediate consequence or conclusion. Rules in the knowledge base contain separate IF and THEN parts or a more sophisticated form. The examples below demonstrate the representation rules which were used in network design knowledge in the DTPES. Examples of generic rules used in the construction of an expert system are shown below:

```
RULE_16 IF
    photo82 = [24,26)
    edge = -9999.00
    DEM = [1,110)
    landuse = 7.00000, 9.00000, 11.0000 or 1.00000
THEN
    road background = -9999.00 75.0%
    roads = 1.00000 25.0%
```

```
RULE_17 IF
    photo82 = [24,26)
    edge = -9999.00
    DEM = [1,110)
    landuse = 8.00000
THEN
    road background = -9999.00 99.6%
    roads = 1.00000 0.4%
```

```
RULE_25 IF
    photo82 = [26,29)
    edge = 1.00000
    DEM = [131,139)
THEN
    road background = -9999.00 0%
    roads = 1.00000 100%
```

To analyse and interpret the rules, an example (the end node for the rule_17) is shown and can be analysed as below:

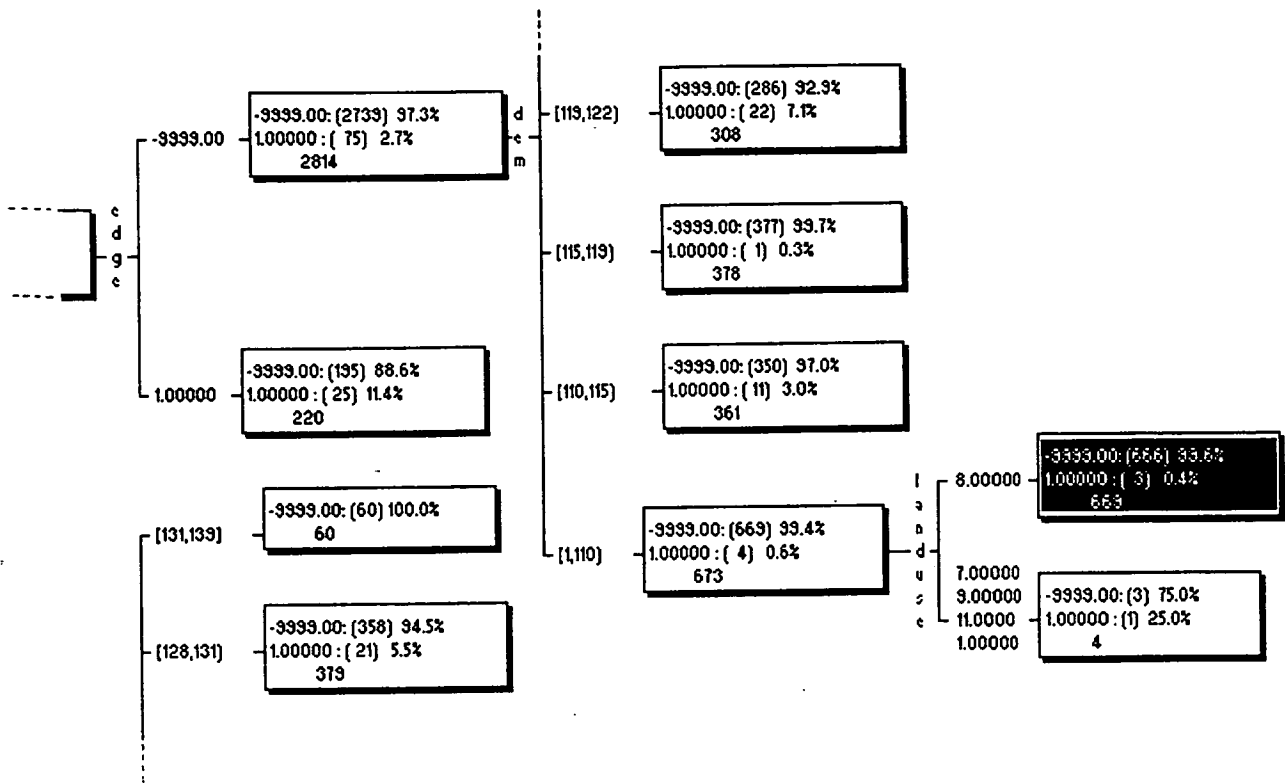


Figure 8.3 Illustration of the end node for rule_17.

Rule_17 indicates there are two categories including road background (-9999) and roads (1). In this rule there are 669 records, or observations. In the landuse analysis, 99.6% fall into the road background category and 0.4% fall into the last category. This node display also tells the GIS analyst that of the 669 observations in the database, 99.6% have road background category (666 records) and approximately 0.6% have road. As seen in this rule and in Figure 1 at Appendix F, the intensity attribute is the strongest way of characterising roads: the larger the DN, the greater the chance of roads.

To design DTPES, MATLAB was used as a shell tool to develop a machine induction program. The above generic rules were clearly formulated by IF... THEN or IF-AND-THEN statements. Thus, the rules in the knowledge base contain separate CONDITION and ACTION parts, where these rules are encoded in MATLAB language to develop DTPES. This symbol [means; > or =, and this] means; <. The CONDITION

contains Boolean operators (eg OR), and inequalities which can be seen in the above rules and in the encoded MATLAB rules (eg greater than [$>$], less than [$<$], equal to [$=$]). As discussed in Chapter 4, the conditional part was taken into account as a pattern, and the statement part was characterised as an action or procedure to be performed on a successful match with the pattern. In the ACTION part of the rule, if the condition was satisfied, then the relevant rule was invoked. Rules consist of premise-action pairs, for instance:

IF C1 & ... & Cn,

THEN T1 & ... & Tn.

with reading IF premises C1 and ... and Cn are true, then actions T1 and ... Tn, are performed. The Ci are so-called "conditions", and Ti are "conclusions".

Originally, the KS rules in PROLOG rules were used due to the fact that KS can convert the decision tree in both generic and PROLOG rules. The PROLOG interpreter was very slow to interpret the KS PROLOG statements. Then the classification tree was converted into generic rules for the purpose of implementation of an expert system. Manually encoding the generic rules into MATLAB rules was error prone and tedious. Therefore, automatic conversion of generic rules into MATLAB rules by implementation of an intelligent filter ks2mat.m was used. The ks2mat.m program converts the generic KS rules to MATLAB rules, and puts them in matrules.m routine. For example, the above generic rules were encoded and generated as follows:

```
%RULE_16
if (photo82(i,j)>=24)&(photo82(i,j)<26) ...
&(edge(i,j)==-9999) ...
&(DEM(i,j)>=1)&(DEM(i,j)<110) ...
&(landuse(i,j)==7) | (landuse(i,j)==9) |
(landuse(i,j)==11) | (landuse(i,j)==1)...
roads_probability(i,j)=roads_probability(i,j)+25;
end;
%RULE_17
if (photo82(i,j)>=24)&(photo82(i,j)<26) ...
&(edge(i,j)==-9999) ...
&(DEM(i,j)>=1)&(DEM(i,j)<110) ...
&(landuse(i,j)==8) ...
roads_probability(i,j)=roads_probability(i,j)+0.4;
end;
%RULE_25
if (photo82(i,j)>=26)&(photo82(i,j)<29) ...
```

```

&(edge(i,j)==1) ...
&(DEM(i,j)>=131)&(DEM(i,j)<=139) ...
roads_probability(i,j)=roads_probability(i,j)+100;
end;

```

For example, rule_16 tells the GIS analyst, if the grey scale attribute data is larger than or equal to 24 DN, or less than 26 DN, the edge detection attribute falls into road background (-9999). Consequently land use type goes from clearing and developing areas to man made structures, or land use is forest, or land use is urban residential. Then out of the total observation under these conditions, there is a 25 percent chance of assigning the particular pixel or pixels as roads.

8.2.5.2 Inference Engine

The rules that meet certain key conditions are used. Generally, the inference engine is the heart of the expert system which decides which of the rules are satisfied, puts them in a priority list, and fires those rules with the most priority. In connection to expert systems implementation here, if the condition is satisfied, then the relevant rule is fired and will assign a probability to the particular pixels as a chance of identification as roads or background. The prediction process is applied to each pixel separately. To form roads, a single label (*a posteriori* probability) must be assigned to each pixel.

The conclusion of each rule is composed of two parts namely the presence (roads = 1) and the absence (background = -9999) of road pixels. For instance, if the presence is 100%, it means that all given pixel (s) in that rule, are identified as roads pixels. In contrast, if the presence is 0%, it means that all given pixel (s) in that rule, are identified as road background.

The dtpes.m in the MATLAB environment predicts the road distributions from the ancillary data. This process was automated by writing a program to map out the decision tree rules and write the matrix into an image file. Once an output has been written, it can be retrieved and put back in image and spatial processing environments. An output of induction rules may be written into any specified file in the matrues.m routine. The combination of ks2mat.m, matrues.m, and dtpes.m sub-routines is called "Decision Tree Processing Expert System" (DTPES).

8.2.6 Analysis of Results

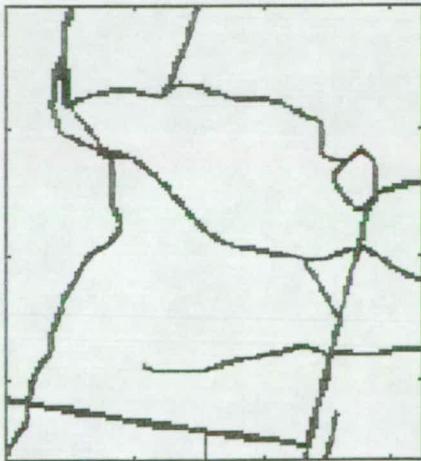
The results of the trials were analysed using the cluster method. A series of classifications was performed to gauge the sensitivity of classification results to the different sites. Classification accuracy comparisons are summarised in Table 8.3. The classification tree over Case 1 performed better than Case 2, and Case 2 performed better than Case 3.



(a)

[Case 1]

Figure 8.3; (a) Displays the results from the clustering classifications for Case 1. A 180 by 160 pixel window of the study area. An extract showing the *a posteriori* probabilities of roads. The brighter the pixel, the greater the probability of roads, and the darker the pixel, the greater the probability of absence (background) of roads.



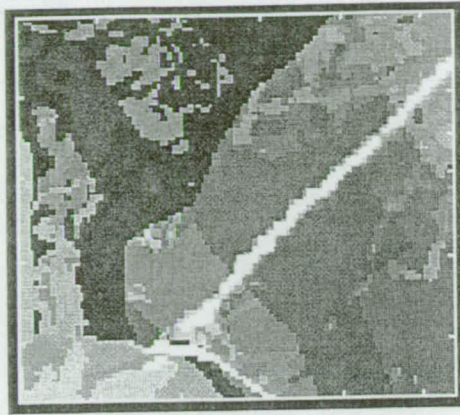
(b)



(c)

Figure 8.3; (b) Represents the road reference map of Case 1 in a grid, and (c) shows the aerial image of Case 1.

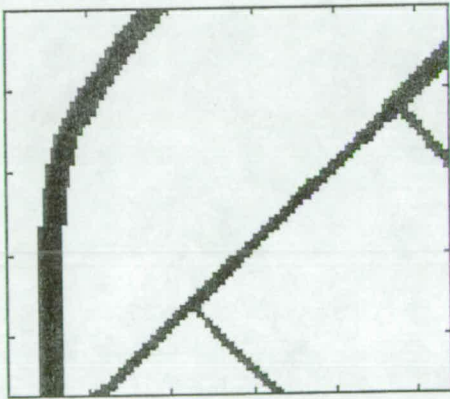
In the first Case (Case_1_1982), the land cover theme which contained vegetation also consists of man-made features (roads). Since the contrast of the roads and the background is high, the decision tree classification produced the highest accuracies. The accuracy obtained was 83%. As can be seen in Figure 8.3 [a, b, c], there are good correlations between the output of DTPES (a), the reference road map (b), and the aerial image (c) of the site. This site is a rural area, with three land use/cover classes, namely agricultural land, lakes, and cleared or developed areas characterised by man made features. Due to the high contrast of the roads with their background, the classification tree provided the better results. The association of roads with other land use classes is high, and roads are dominant features in the generated classification.



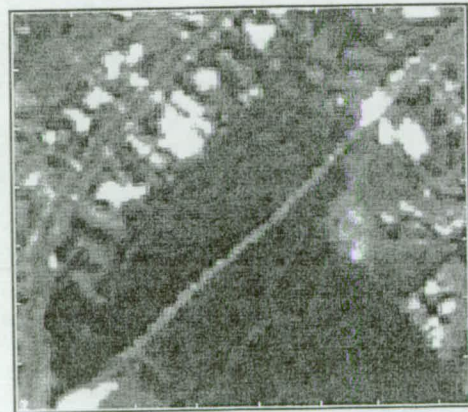
(a)

[Case 2]

Figure 8.4; (a) Displays the results from the clustering classifications for Case 2 (a 95 by 105 pixel window of the study area). An extract showing the *a posteriori* probabilities of roads. The brighter the pixel, the greater the probability of roads, and the darker the pixel, the greater the probability of absence (background) of roads.



(b)



(c)

Figure 8.4; (b) Represents the road reference map of Case 2 in a grid, and (c) shows the aerial image of the Case 2.

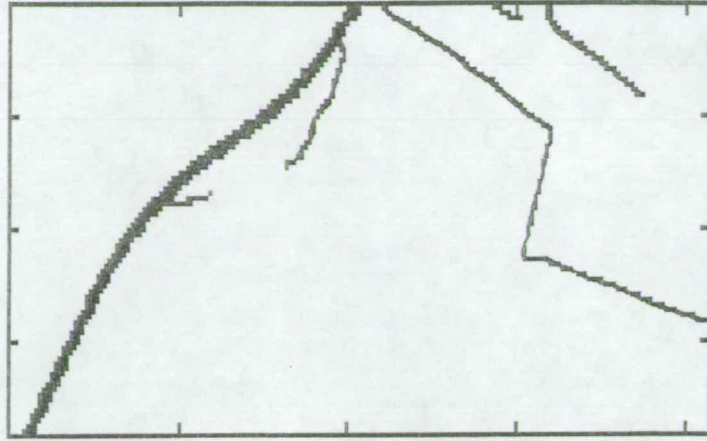
There are four land use/cover classes in the landuse variable in the database. These are urban residential, agricultural land, clearing and developing areas to man made features, and urban recreational. This site is relatively homogeneous. In the eastern part of the classification map, the mapped straight line which is a road segment, can be seen clearly. Confusion of roads with structural man-made features such as buildings, roofs, and to a lesser extent pavements prevented the mapping out of the roads in the western part of the test case. Errors were also partially associated with bare soil or fields; thus interruption of roads occurred. As can be seen in Figure 8.4 [a, b, c], there are relatively good correlations between the output of DTPES (a), the reference road map (b), and the aerial image (c) of the site. As associated classification accuracies were low, roads and man-made features were confused. Note that residential areas are a complicated mix of a variety of land cover/use classes, although there is still a measure of residential structures.



(a)

[Case 3]

Figure 8.5; (a) Displays the results from the clustering classifications for Case 3 (a 190 by 410 pixel window of 1991 image of the study area). An extract showing the *a posteriori* probabilities of roads. The brighter the pixel, the greater the probability of roads, and the darker the pixel, the greater the probability of absence (background) of roads.



(b)

Figure 8.5; (b) Represents the road reference map of Case 3 in a grid.



(c)

Figure 8.5; (c) Shows the aerial image of the Case 3.

In Case 3 most errors were associated with structural man-made features such as buildings, roofs, and pavements. The bright parts are buildings and bare soils which have a high spectral value. With the spatial resolution of the data used here, the roofs and buildings become generalised and increasingly associated with roads. The errors are associated with the bare soil or fields, buildings, roofs, and pavements. For this site, as can be seen in Figure 8.5 [a, b, c], there are not strong correlations between the output of DTPES (a), the reference road map (b), and the aerial image (c) of the site.

In Cases 2 and 3, roads were interrupted by other man-made structures including large building outlines, shadows of buildings intruding on the roads, and parking lots. As in Case 1, roads were interrupted by overhanging trees, shadows and tree canopy. Unsealed roads in poor condition provided limited contrast between the road surface and the surrounding terrain. Residential areas dominated the imagery especially in populated neighbourhoods with small yards. Conventional classifiers share the same problems as those associated with dissimilar features because of similar intensity characteristics (Benjamin and Gaydos, 1986; Barr, 1992). Road network classification was best accomplished in Cases 1 and 2. Resolution of the data caused problems for the texture of the imagery. In this regard, objects within urban sites (houses, trees, parking lots, etc.) were each in different pixel size.

The primary step for inductive learning is a selection of the sample learning which is the set of features of a known class from which the classification rules will be induced. After generation of a classification tree, it is important to gauge the accuracy of the classification tree over the fresh data (test sample). This was done and the results were validated by calculation of the overall accuracy, pixel by pixel, so that the road map of the reference data was converted into a grid file. The certainty and uncertainty of the classified pixels as roads and background were validated for the area. The accuracy for mapping roads increases over rural areas as enough contrast between the roads and other elements is included in the photos. The human eye is subject to error in determination of accuracy of a classification pixel by pixel. Although the estimated overall accuracy of the DTPES's output based on the reference map (road grid coverage) agrees with the overall visual interpretation of the output of the DTPES, the decision rules broadly concur with expert opinion and classification rules (Table 8.3).

Samples	Overall Accuracy (in percent)
Case_1_1982 (Site 1)	83
Case_2_1982 (Site 2)	66
Case_1_1991 (Site 3)	53

Table 8.3 Classification summary statistics. Overall accuracy refers to the total correctly classified pixels (confidence interval is at the 0.01 significance filter level of KS) compared with the reference data.

8.3 Discussion

The main issue with decision trees in general is the lack of ability for interaction of variables. It was noted that decision trees seem to be useful in throwing up some interesting perspectives (Belbin, 1995). To simplify the presentation of the decision tree processing from this study, two test sites (cases) on 1982 imagery were examined. In addition, a test site (case) on 1991 photography was also examined.

There are four levels in the tree (Figure 1 in Appendix F). While the first level is entirely associated with the intensity attribute information of the database, the second, third, and fourth show a mixture of contextual and environmental parameters. Accordingly, two classes of rules in the knowledge system were identified. The first category only deals with the spatial context of image. The second class is concerned mainly with the geographic context of the data. These rules are concerned with the landuse type and elevation. Cross-tabulation of the classification tree was used to facilitate the analysis and interpretation (Appendix G).

In the formulation of road prediction, it is almost impossible to re-compute and keep the whole classification tree: the decision tree is too large with many branches from each node and the depth is too great. This means that significant tests are required to reach a decision. Too many nodes (rules) may give an impression of an accurate classification tree for the test data, although the classification of the original dataset may be poor, particularly if the rules are generated from a small sample observation dataset. Too few rules causes misclassification. It was found that knowledge acquisition was a bottleneck problem in construction of the expert systems in this study. The expert can control this issue by using domain knowledge. The entire tree was grown for the small subsets of the dataset, and the rules produced from the resulting tree were applied to map out the presence and absence of roads.

Not surprisingly, the results of this GIS modelling exercise within test Case 1 were satisfactory. Despite the success of this exercise within Case 1, the demonstrated results for Cases 2 and 3 highlighted the inadequacies of this type of approach. A similar accuracy has been reported using a decision tree for salinity mapping (Evans et al 1996)

who obtained 61% to 78% over the test data. The overall accuracy of Case 1 and 2 is only slightly better than that of Case 3.

It is clear from these numbers (Table 8.3) that while a good deal of roads are extracted eg for Case 1, the results are not good enough to claim that a complete mapping has been conducted eg in Case 3. Perhaps the most significant problem is the error of misclassification, which is typically in the 15%-45% range. Eliminating this error requires re-examining every extracted road segment which would be a tedious and costly solution. The majority of the roads which were not mapped, were well hidden by leaf cover, bare soils, roofs of buildings, or alongside fields with similar spectral characteristics, etc.

Lower classification accuracies were also associated with the following factors:

- The optimal time of year, optimum look angle, low sun angle or a large off nadir view angle, surrounding vegetation and shadow of buildings and trees all affected the visibility of roads in the images.
- A major rate of misclassification of pixels was related to minor geometric misregistration of the images when compared directly with ground truth or maps.
- Even when geometric misregistration was not a problem, discrepancies were largely associated with classifying the man-made features which have very similar grey value to the roads.
- In addition, there is error associated with imprecise location and digitization of the road networks in the process of editing the coverage, as well as the buffering operation.

Potential users may improve decision tree classification by:

1. Incorporating more independent fields as an associative key.

For example, feature attributes such as shape and size can be used as an additional source of evidence.

2. Applying more advanced measures of coping with feature recognition problems.

For example, the combination of geometrical feature recognition algorithms with a decision tree is expected to generally enhance the success of linear feature identification in heterogeneous urban scenes.

3. Employing topographic knowledge-based information in 2D and 3D.

For example, a road is a ridge; generally the ridge drops off on both sides. Residential houses are hills, generally brighter than the road. A road pixel is commonly not a valley. It will cut the road as a result of shadowing or overlap from the neighbourhood. Topography and associated changes in lighting may result in a cut road.

Using the above findings, it should be possible to build a better model for delineation of roads using a spatial database in the future. These knowledge-based rules can be integrated with other attributes such as curvature and connectivity of roads to characterise an individual road segment or whole road network. Collinear and connectivity rules can be used to join road segments. Also, proximity may be employed to describe spatial relationships between features. Thus, for example, the distance between two road intersections can be used in the process of road detection.

8.4 Summary

An expanded GIS has been developed that encompasses an image interpretation system. A rule-based system was applied to perform road prediction from aerial imagery over an urban to a rural scene. The system consisted of three major components: a database which stores image and spatial data; rule induction which uses a decision tree classification and user interface, and inference engine. A multidisciplinary approach using integrated spatially referenced data was used to predict roads. *A priori* knowledge of geometry of road networks (eg width), terrain type, scene elevation, and the field test were taken into account.

Roads against a background of low reflectance fields are easily detectable. They become indistinct when they pass areas with a mixture of man-made structures, since roads between two rows of houses in a dense urban area may have a similar grey level. It can be argued that classically it is more difficult to recognise the roads in an urban region than a rural area. The roads which pass through rural terrain have high contrast. Road surface contrast in urban areas is affected by different surface material and shadows from nearby structures. The ground resolution is an important determinant factor for feature detection including roads. Even though the width of the roads is less than the spatial resolution of the image, the road is extracted whenever its spectral contrast is considerable in relation to its background.

Decision tree and rule-based classifiers, such as KS, can be used to integrate GIS datasets with remotely sensed imagery. The decision trees can be examined to determine relationships between the data, and to find out which spatial data layers are the most important co-operative in prediction of roads. In spite of previous research, decision tree modelling is costly, since this type of modelling process is data-intensive. The investigated technique in this research requires a large number of data sets to be built. Thus, construction of these data is relatively expensive when applied to large areas.

Chapter 9

MULTISPECTRAL IMAGE CLASSIFICATION

This chapter describes a supervised multispectral image classification of the trial site using colour aerial photography. This was carried out to compare its performance with a decision tree analysis to map out roads over the trial site. A classification accuracy assessment shows that an overall accuracy of 63% can be obtained. This accuracy is marginally lower than the decision tree analysis.

9.1 Introduction

The aim of spectral classification is to segment the image into spectrally homogeneous regions. Multispectral image classification can be classified into two main approaches, whether supervision from an operator is required or not.

The image used was a colour aerial photograph, acquired at 1:22500 scale (12", format, 6" lens) in summer 1984. It was scanned with 600 DPI and stored in a 25MB TIFF File. It has three bands corresponding to red, green, and blue (RGB). The data was imported into the ERDAS IMAGINE raster data base. The 22500 scale image data was geometrically corrected using an affine transformation and rubber sheeting, and resampled to 2 m (1 pixel = 2 m) on the ground (Figure 9.1).



Figure 9.1 A subset of the colour aerial photograph of the study area.

9.2 Supervised Classification Method

9.2.1 Background

Supervised classification is closely controlled by the analyst by selecting pixels that represent known land uses. The analyst uses ancillary sources such as ground truth data, and air photos to facilitate the classification. In this process the analyst trains the computer system to determine the similar patterns (pixels) or homogeneous regions that represent each class. It is crucial to have a set of desired classes in mind. The analyst prepares spectral signatures of land cover/use types confirmed by reference to ground information (Martin et al 1988), or the user defines the classes, generally by interactive extraction of training areas on the screen (ERDAS, 1994b). These spectral signatures are used to classify all pixels comprising the study area.

The supervised technique is the most popular classification method for the classification of land-cover/use employing multispectral satellite data (eg Richards, 1986; Michaelis, 1988; Gong and Howarth, 1990; Johnsson, 1991; Forghani, 1994; Barnsley and Barr, 1996).

A maximum likelihood technique estimates the likelihood of a particular pattern belonging to a category. Among the most common supervised classifiers are minimum distance, parallelepiped, and maximum likelihood. The maximum likelihood classifier (MLC) is easy to use and theoretically guarantees that the classification error is minimized. It is the most widely employed classification algorithm in digital classification of land cover data (Swain et al 1980; Harris, 1985; Matther, 1985; Michaelis, 1988; Bolstad and Lillesand, 1991; Trietz et al 1992; Forghani, 1994; Johnssen, 1994).

9.2.2 Image Classification

In this work the training areas were selected with the use of AOI tools and stored in a SIGNATURE EDITOR file. Initially 9 spectral classes were selected as is shown in Table 9.1.

Initial image classification for these classes was performed using a MLC technique. The result of this supervised classification of the aerial image is presented in Figure 9.2. The assigned colours for the classified image are shown in Table 9.1.


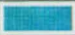

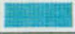





Class #	>	Signature Name	Color
1	>	Remnant Forest	
2		Cut Over Forest	
3		Riparian Vegetation	
4		Improved Pasture	
5		Unimproved Pasture	
6		Bare Soil/Roofs	
7		Main Roads	
8		Local Streets	
9		Tracks	

Table 9.1 Selected signatures from the aerial image.

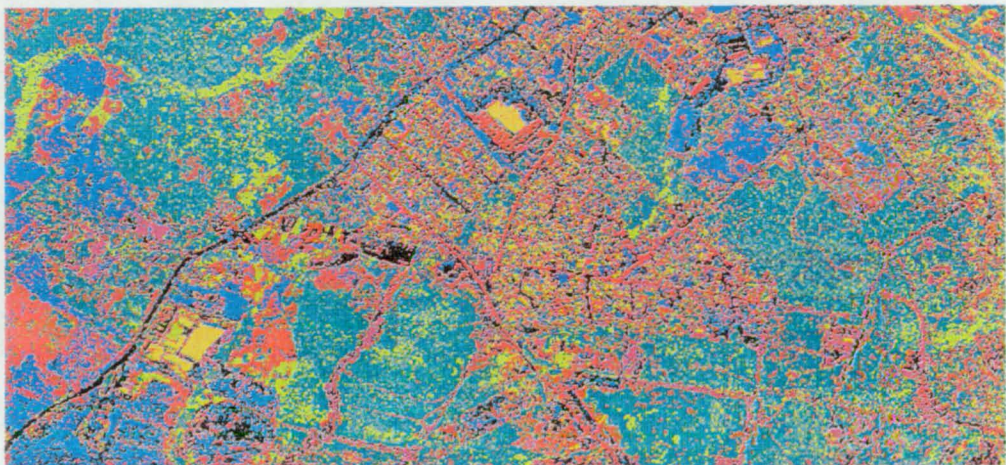


Figure 9.2 Represents the classified image with 9 classes.

Since the concern is to map out roads, two land use classes should be kept in mind. The developed land use map (Chapter 7) was used as control data. The control layer is in raster (grid) format. The classified maps have been compared to the existing roads map to evaluate the classification accuracy. The spectral classes with similar cover types were merged. The two classes used were roads, and non-roads (background) which comprised classes that do not have any association with roads. The resulting modified signature file

was used to perform MLC using a standard deviation of 2 for the image. Finally, a map was produced with only two classes namely roads and non-roads (background) (Figure 9.3).



Figure 9.3 Final supervised classification after merging of similar classes .

9.3 Discussion

The classification result was evaluated visually by superimposing the road layer (in buffer) with the classified image. In addition, the classified image was numerically compared to the original road map by coincidence matrices and accuracy measures.

It should be kept in mind that mapping roads in a heterogeneous land use such as a built-up area can be problematic since the roads and other man-made features such as buildings have similar spectral characteristics. Bare soils, dirt roads/tracks, and building roofs have very similar spectral signatures (Figure 9.1). The confusion of these features with roads can be clearly observed in the classification map (Figures 9.2 and 9.3). An overall classification accuracy was 63%. Using an automated classifier over urban area, errors have been increased considerably (Gurney, 1981).

The classification accuracy assessment was performed for the road class. The classification accuracy is 63 percent, whereas the commission errors are 75 percent. The

commission errors are relatively high (Table 9.2). A similar trend was found when using edge detection algorithms in both urban and rural test sites (Forghani et al 1997).

Classified Feature	Classification Accuracy	Omission Errors	Commission Errors
Roads	63%	37%	75%

Table 9.2 Image classification accuracy

The overall classification accuracy decreased in areas where the roofs of buildings, bare soils, concrete, and tracks roads have very similar spectral characteristics. This problem can be related to increasing noise due to the heterogeneous nature of spectral response of urban areas (Forghani, 1994) and cleared agricultural lands. Similar classification accuracy has been reported using a standard maximum likelihood classification with identification of six broad cover types over a rural/urban area from SPOT and TM data (Toll and Kennard, 1984; Welch, 1985; Nagarathinam et al 1988; Shimoda et al 1988; Barr, 1992). Averaging accuracies may be in the range of 55%-85%.

To refine the supervised classification, thresholding was interactively carried out for each class in the thematic raster layer. It was found that the overall classification accuracy marginally increased, while commission errors dramatically increased. After thresholding (post-classification), the commission errors increased significantly (11%).

9.4 Concluding Remarks

It has been shown that roads in rural portions of the trial site can be extracted with high accuracy using either decision tree analysis or multispectral classification. For built-up land, the multispectral analysis produced a better result in comparison to the decision tree analysis. In the built-up area (central portion of the study area), the main roads and local streets were classified significantly better than were the rural. This is because, the roofs/buildings are not continuous (connected as road pixels) like bare soils (cleared land). The houses and roofs classified as isolated pixels which can be seen in Figures 9.2 and 9.3. For rural land use (eastern portion of the image), multispectral classification did not perform well, as the confusion of roads with bare soils (cleared land and unimproved pasture) can clearly be seen. This is due to the similar spectral properties of these features (Figures 9.2 and 9.3). In areas of low housing density pixels containing mixed land use, or no buildings, considerable road misclassification occurred particularly towards the cleared lands.

The decision tree classification over Case 1 (refer to Figure 8.3 and Section 8.2.7) which is a rural area performed better than Case 2 and Case 3 (refer to Figures 8.4 and 8.5, and Section 8.2.7). The overall classification accuracy was found to be 83% over the rural site, for the semi-urban it was 66%, and for the built-up area it was 53%. It is not surprising that the classification was more accurate using a decision tree analysis over the rural area and decreased over built-up areas. If contextual (spatial) information has been incorporated into the multispectral classification, the decision tree analysis results would have been more comparable. The high spatial resolution of the colour aerial photograph resulted in low overall classification accuracy with respect to typical satellite data. The use of higher spatial resolution data may not always increase classification accuracy (Gurney and Townshend 1983; Toll, 1985; Forster, 1985; Martin et al 1988; Barnsley and Barr, 1996).

It is concluded that both a standard supervised classification and decision trees analysis are insufficient to extract "real world objects" (roads) in a heterogeneous environment.

Chapter 10

SUMMARY

10.1 Background

A review of the current literature demonstrates that:

1. Knowledge-based (KB) methods such as artificial neural networks and decision trees as an associative key in integration of image understanding techniques within a GIS, are increasingly applied.
2. To delineate a road from an image, researchers are using three basic properties namely spectral characteristics, geometric shape, and spatial properties. Experience has shown that low level image segmentation methods such as edge detection are insufficient for an accurate classification of a road pixel. Thus, it is crucial to employ brightness values, length, and shape characteristics for an effective road extraction.
3. There are three common types of geometric rectification applied to digital images: (1) polynomial transformations, (2) digital orthophotography, and (3) image matching using affine transformation and rubber sheeting. It has been shown that image matching will be more applicable if higher accuracy is required. It should be noted that Global Positioning Systems (GPS) can be used to obtain GCP coordinates for polynomial transformations and digital orthophotography if higher accuracy (to centimetre level) is required.
4. Researchers believe that it is impossible to choose a convolution filter which will maximize good signal to noise ratio, good localization, and uniqueness of response when a linear feature has to be extracted particularly in an urban area. The main problem with edge (line) detectors is the association of noise, since noise presents false edges as true edges. In addition, thresholding is a difficult task in order to remove noise edge responses, and the best compromise can be gained by experimentation.
5. To scan images and maps, researchers concur that 300-600 DPI (42-84 mm/pixel) is sufficient for many mapping applications. Commonly, three major types of mapping data are required for GIS applications based on data formats: vector data in layers,

vector data in feature coded form, and structured data. Geographic data is often represented in three varied formats, vectors, raster, and mathematical modelling. A hybrid model of spatial data structure is more effective if users are interested to work in an integrated environment since it provides an explicit integration between raster and vector data for many GIS applications.

6. The task of vector to raster conversion is not as difficult as conversion of raster to vector. For this reason, a grid format is used as the major data structure of the incorporated GIS vector-based data. In relation to choosing of cell size for grid data, it has been reported that raster size is the major obvious control on rasterizing error and research has shown that increased raster size has an extensive effect on reducing map accuracy.
7. To perform spatial analysis in a vector GIS, boundaries of relevant feature maps eg land use, forests, are effectively imposed on a base map of common scale. In the same manner, in a raster based GIS analysis, cell to cell correspondence has to be identified and the output cell has to be labelled according to corresponding cells of each feature map.
8. The major error sources in GIS come from: errors in map registration, errors associated with each map layer, and spatial distribution of such errors cannot be random, leading to high variability over a variety of locations.
9. Knowledge acquisition is the most difficult task in expert systems development. The decision tree is typical of knowledge extraction and it represents knowledge to construct expert systems. The decision tree induction technique is particularly helpful when the developer is not experienced in building an ES or when the knowledge that is being collected resists simple expression as a collection of IF ... THEN rules, and where knowledge of underlying processes is either unavailable or incomplete.
10. The decision tree classifier is an important and efficient technique for separating samples (observations) into categories or for predicting the highest output to a given situation. Fundamentally, four parameters are essential in building a decision tree algorithm: a set of features, a feature selection criterion, a stop-splitting rule, and a central role in the quality of the decision tree as a classifier and its complexity or simplicity. Experience has shown that there are a number of advantages with using decision trees such as utilisation of contextual information, that it is inexpensive to

use, its lack of complexity and simplicity of interpretation and understandability. However, it suffers from a number of disadvantages, for example lack of high sensitivity if a minor change happens in the composition of learning samples, lack of good extrapolation and absence of justification, difficulties in selection of a "right sized" tree or "better" tree and the existence of probable noise in training samples.

10.2 Methodology

In respect of the methodology developed in this research, a GIS database and aerial imagery were integrated in a manner that allowed them to be used in a knowledge-based analysis system for detecting and mapping linear topographic objects, with special reference to road networks. The research used photometry (ie spectral), spatial and contextual information within a knowledge-based model using decision trees to identify roads from other linear features (eg rivers, field boundaries). The above information is located in a multi-source spatial dataset (layers) which includes land use/cover, DEM, grey level image, roads, field and vegetation boundaries, streams, and edge detection data. Incorporation of this dataset into a decision tree analysis system was attempted.

As mentioned earlier, this research devised a general approach to solving problems of road detection. This approach can serve as a model for others who are trying to do practical work in this field. By creating a hybrid system which includes many different databases and combines many different sources of knowledge in trying to identify a specific (man-made) geographic feature, and by utilising current artificial intelligence (AI) techniques to perform the classification, this research provides an early example of the techniques which will be in more general use in the areas of GIS and remote sensing in the future.

As discussed earlier, in the development of the methodology a number of issues emerged:

1. Defining the dataset:

What are the most appropriate and best parameters to use in the dataset?

2. Building the dataset:

How can a dataset be built for a decision tree environment, particularly one that recognises knowledge-based attributes (layers) such as intensity (grey image), landuse, edge detection data etc. in order to distinguish roads from other linear features?

Which geometric correction method produces a better accuracy?

Which type of spatial data structure can be utilised in order to manipulate and organise the GIS data, such as vector processing and raster processing or a hybrid approach?

What cell size should be chosen to meet the requirements of the knowledge-based data?

3. Transferring data from a GIS environment into the decision tree system:

What is the best way to transfer GIS datasets into the decision tree software?

4. Converting a classification tree into a classified image, since the decision trees software gives the results of classification tree both in generic rules and in graphic form.

How can this information be applied to produce a classified image?

10.2.1 Phases of Research

The following steps were undertaken in this research:

- Definition of the goal, which deals with the development of the methodology and its implementation for a trial site to map out roads.
- Provision of suitable hardware and software to do the processing.
- Selecting an appropriate study area.
- Selecting and providing the datasets.
- Defining the dataset.
- Georeferencing of the aerial imagery.
- Spatial data processing and construction of a database for a knowledge-based analysis system.
- Interfacing of the data with a decision tree environment.

- Decision tree analysis in a knowledge-based analysis; generation of a classification tree and rules collection and encoding to develop an expert system.
- Expert systems construction and testing of the expert system over trial sites.
- Calculation of the overall classification accuracy and comparison of the results by overlaying the output of the expert system on the referenced roads data.
- Undertaking a standard supervised multispectral image classification to be compared with the decision tree analysis.

The methodology was developed through a knowledge-based approach using a digital spatial database. A wide range of factors was associated to build a database for the methodology and implementation of the hypothesis. It was necessary to test the proposed model over a mixed urban and rural area, due to the fact that characteristics of each of these scenes are different. The selection of study area was an important task. In this situation, the selected area incorporates a range of features, from natural to man-made structures for developing and testing the hypothesis. Furthermore, the type of remote sensing imagery by means of spatial resolution, availability of imagery, and the interface problems of image to a machine learning software were determinant parameters when choosing aerial photography for this research.

The aerial photography was geometrically corrected using three standard methods: (a) polynomial transformations, (b) digital orthophotography, and (c) affine transformations and a rubber sheeting. The required accuracy ($\pm 4\text{m}$) for the purpose of this study was only gained by employing the affine transformation and rubber sheeting method.

Edge detection as a low level image segmentation was employed to construct data for a GIS database. In this regard, a program for semi-automatic linear feature detection using different edge enhancement, noise removing filters, and edge detectors in which the process is followed by morphological operation, was developed under MATLAB software. The extracted data were used as a GIS layer in a decision tree classification. The use of an edge detection filter can be affected by the complexity of the scene because of noise in the data. For instance, materials along the road with the same intensity as the road are problematic where there is little texture on the road. This problem also occurs at

intersections where two roads with similar material meet. If the area is a mixture of urban and residential, then the problem of feature detection becomes much more difficult. The output of edge detectors is noisy. Thresholding was thus used as a typical solution to remove the false response and isolate the significant edges within the area by using gradient magnitude, since in aerial imagery, a local gradient extreme may not reflect the true response from the real edges. When the threshold is set too low, there are many dominant edges, points, and lines; while if the threshold is set too high, some information loss may occur. Fine tuning of the threshold was used in order to optimise the display of edge features. However, it is a tedious task. Faugeras (1993) says *"there is no good answer to this question, and the choice of threshold must be guided by application and the lighting conditions of the scene"*.

To facilitate the thresholding task a colourbar was added to the program to select an approximate threshold. The best compromise was found by experimentation. Later, morphological operations were applied to resolve part of this problem, in which for example skeletonization and erosion may help in using higher threshold levels, and dilation can assist in using lower threshold levels. Different thresholds and different edge detectors were compared. Researchers agree that the output of edge and line algorithms decreases significantly when the line/edge detectors are employed for imagery of urban areas. The performance of low level image segmentation may be improved by associating spatial and contextual information from both humans and GIS. Therefore, there is increasing interest in applying intelligent image interpretation techniques such as using ES and artificial neural networks.

As a major part of this research, construction of a database which locates spatial and spectral attributes for a knowledge-based environment, using ARC/INFO GIS software was conducted. This involves data capture by means of importing existing data and generating ancillary data by digitising, manipulating in context of processing and analysing, integrating, converting produced data into a grid, and subsequently generating ASCII data files. Grid raster-based processing was undertaken to construct a multi-source database for a decision tree classification. As a requirement of the research database, all the digital layers were resampled to a constant cell size to permit overlaying and registering the coverages to the same pixel size. Finally, the grid data was converted

into ASCII files which were preprocessed by a computer program to generate tabular ASCII data.

The multi-layer file was interfaced with decision tree software (KS) for decision tree analysis. The independent data set comprised 6 variables (fields) that attempt to represent contextual, textural, and geometrical characteristics of the knowledge-based data. The integrated multi-source database included a priori knowledge of geometry of road networks (eg width), edge detection data, intensity (air photo), terrain type (landuse), streams, field boundaries and vegetation alignments and scene elevation (DEM). In the process of decision tree analysis, the input data was recessively partitioned into mutually exclusive exhaustive subsets which define the best response variable. The resulting classification tree was used to generate generic rules for construction of an expert system. The knowledge-based system thus developed comprised three main components: a database, rule induction and user interface, and an inference engine. In the development of this expert system a forward-chaining process was considered in order to evaluate all rules for a given pixel for mapping spatial distribution of the grid data to show areas with roads and their background. The computation time linearly increases as the number of grid cells increase. This rule-based system was used to perform road mapping from aerial imagery over an urban/rural scene. After classification, the system computes the overall accuracy of the mapped roads based on the reference road map to maintain consistency and reliability of the performance of the decision trees in feature recognition.

10.3 Results

Decision tree classification works well for prediction of roads in areas in which the roads and the background have a high contrast, since these areas contain homogeneous cover and the association between land cover/use is significant. On the other hand, the method for heterogeneous areas (urban scenes) has produced low accuracy. Ground resolution is an important determining factor for feature detection including roads. Even though the width of the roads is less than the spatial resolution of the image, the road is mapped whenever its spectral contrast is considerable in relation to its background. Discrimination of roads over urban areas was more difficult than rural areas.

Classification tree methods have been shown to be powerful tools for splitting data into homogenous groups and building and collecting sets of decision rules. The major problem with identification of roads seems to be to find some characteristics that distinguish a road from other line and man-made features that share the spectral characteristics of roads. In particular, feature recognition using the decision trees (DTPES) model over homogeneous areas was most accurate in general, although more time-consuming to implement. The results showed that framework of roads in a rural site mapped by this knowledge-based technique closely concurred with visual interpretation.

Accuracy of the results is highly dependent upon the quality of data in terms of accuracy of input of GIS data eg registration and digitisation errors, and the spectral characteristics of the scene, that is ie in rural areas the accuracy of the output is acceptable since it contains spectrally homogeneous feature types. The skill of the GIS analyst is also of importance. It must be noted that the output from these models has relatively direct relationships with the quality of input GIS layers, since in situations where the accuracy of the overlaid maps is not high, the output from GIS modelling will not be great.

10.4 Concluding Remarks

The findings of this research are consistent with the conclusions drawn by other researchers investigating spectral classification methods based on machine learning techniques. Using neural networks has not produced desirable results if the roads pass from urban areas; the man-made features are mixed with the roads (Boggess, 1993, and 1994). Similar findings were also reported by Geman and Jedynak (1996). The accuracy obtained in this research is similar to that of Evans et al (1996) who applied decision tree classifiers in an integrated GIS for salinity mapping; also to Walker and Moore (1988), Lees and Ritman (1991), Aspinall (1992), and Skidmore et al (1996b) who reported an overall accuracy of 55% to 75% for mapping wildlife and vegetation.

The initial costs involved in configuring a knowledge-base, such as the methodology developed in this study, are high, and this may not be justifiable in a production environment.

The success of decision tree modelling for the application in question may be improved by using high quality spatial data, and incorporating more independent variables such as feature attributes (ie shape and size) as an additional source of evidence. Further research should be concentrated on employing more advanced measures of coping with feature recognition problems such as the combination of geometrical feature recognition algorithms (eg line detection) with a decision tree. This is expected to generally enhance the success of linear feature identification in heterogeneous urban scenes.

REFERENCES

- Abramson, S. B., and R. A. Schowengredt, 1993. *Evaluation of Edge-Preserving Smoothing Filters for Digital Image Mapping*. ISPRS Journal of Photogrammetry and Remote Sensing, Vol. 48, No. 2, pp. 2-17.
- Adkins, K. F., and C. J. Merry, 1994. *Accuracy Assessment of Evaluation Data Sets Using the Global Positioning System*. Photogrammetric Engineering and Remote Sensing, Vol. 60, No. 2, pp. 195-202.
- Aghajan, H. K., and T. Kailath, 1994. *SLIDE: Subspace-Based Line Detection*. IEEE Transactions on Pattern Analysis and Machine Intelligence, Vol. 16, No. 11, pp. 1057-1073.
- Al-Garni, A. M., 1995. *An Expert System for Site Evaluation Using Aerial and Space Imagery*. Photogrammetric Record, Vol. 15, No. 85, pp. 91-105.
- Anderson, J. R., E. E. Hardy, J. T. Roach and R. E. Witmer, 1976. *A Land Use and Land Cover Classification System Use with Remote Sensor Data*. U. S. Geological Survey: Professional Paper, pp. 964, 28.
- ANGOSS., 1994. *KnowledgeSEEKER User's Guide: Version 3.02 for Windows*. ANGROSS Software International Limited.
- Argialas, D. P., and C. A. Harlow, 1990. *Computational Image Interpretation Models: An Overview and a Perspective*. Photogrammetric Engineering and Remote Sensing, Vol. 56, No. 6, pp. 871-886.
- Aronoff, S., R. Mosher, and R. V. Maher, 1987. *Operational Data Integration - Image Processing to Interface Vector GIS and Remotely Sensed Data*. Proceedings of Eleventh Canadian Symposium on Remote Sensing, Waterloo, Ontario, Vol. II, pp. 216-225.
- Asano, T., and N. Yokoya, 1981. *Image Segmentation Schema for Low-Level Computer Vision*. Pattern Recognition, Vol. 14, No. 1-6, pp. 273.
- Aspinall, R.J., 1991. *Use of an Inductive Modelling Procedure Based on Bayes Theorem for Analysis of Pattern in Spatial Data*. Computer Modelling in the Environmental Sciences. (Farmer, D. G. and M. J. Rycroft: Editors), Institute of Mathematics and its Applications Conference Series, No. 28, Oxford University Press, Oxford, pp. 325-339.
- Aspinall, R. J., 1992. *An Inductive Modelling Procedure Based on Bayes Theorem for Analysis of Pattern in Spatial Data*. International Journal of Geographical Information Systems, Vol. 6, No. 2, pp. 105-121.
- August, P., J. Michaud, C. Labash, and C. Smith, 1994. *GPS for Environmental Applications: Accuracy and Precision of Locational Data*. Photogrammetric Engineering and Remote Sensing, Vol. 60, No. 1, pp. 41-45.

Avery, T. E., and Berlin, 1992. *Fundamentals of Remote Sensing and Airphoto Interpretation: Fifth Edition*. Macmillan Publishing Company, New York.

Bajcsy, R., and C. Broit, 1982. *Matching of Deformed Images*. Proceedings of Sixth International Conference on Pattern Recognition, pp. 351-353.

Barr, S. L., 1992. *Object-Based Re-classification of High Resolution Digital Imagery for Urban Land-Use Monitoring*. XVIIth Congress of International Archives of Photogrammetry and Remote Sensing Washington, D. C., Commission VII, Vol. XXIX, pp. 969-976.

Barnsley, M. J., and S. L. Barr, 1996. *Inferring Urban Land Use from Satellite Sensor Images Using Kernel-Based Spatial Reclassification*. Photogrammetric Engineering and Remote Sensing, Vol. 62, No. 8, pp. 949-958.

Belbin, L., 1995 and 1996. *Personal Communication*. Antarctic Data Centre. Australian Antarctic Division, Hobart, Tasmania, Australia.

Benjamin, S. P., and L. Gaydos, 1986. *Processing of Scanned Imagery for Cartographic Feature Extraction*. U.S. Government Work.

Bielawski, L., and R. Lewand, 1988. *Expert Systems Development: Building PC-Based Applications*. QED Information Sciences, Inc. Wellesley, Massachusetts.

Biggs, D., B. De Ville and E. Suen, 1991. *A Method of Choosing Multiway Partitions for Classification and Decision Trees*. Journal of Applied Statistics, Vol. 18, No. 1, pp. 49-62.

Boggess, J. E., 1990. *Using a Genetic Algorithm to Evolve a Set of Rules for Classification of Roads in Satellite Images*. Image Understanding Using Artificial Intelligence Technology: Interim Technical Progress Report, Independent Research and Development Project, Department of Computer Science, College of Engineering, Mississippi State University, USA.

Boggess, J. E., 1993. *Identification of Roads in Satellite Imagery Using Artificial Neural Networks: A Contextual Approach*. Technical Report MSU-930815, Department of Computer Science, College of Engineering, Mississippi State University, USA.

Boggess, J. E., 1994. *Using Artificial Neural Networks to Identify Roads in Satellite Images*. Proceedings of World Congress on Neural Networks San Diego, 1994 International Neural Network Society, Annual Meeting, June 5-9, Vol. 1, pp. 410-414.

Bolstad, P. V., and M. Lillesand, 1991. *Rapid Maximum Likelihood Classification*. Photogrammetric Engineering and Remote Sensing, Vol. 57, No. 1, pp. 67-74.

Bowerman, R. G., and D. Clover, 1988. *Putting Expert Systems into Practice*. Van Nostrand Reinhold Company, New York.

Brazdil, P. B., and R. J. Henery, 1994. *Analysis of Results. Machine Learning, Neural and Statistical Classification (Edited by M. Michie, D. J. Spiegelhalter and C. C. Taylor)*. Department of Computer Science, University College London.

Breiman, L., J. H. Friedman, R. A. Olshen, and C. J. Stone, 1984. *Classification and Regression Trees*. Wadsworth Statistics, Wadsworth, Belmont, California.

Burrough, P. A., 1986. *Principles of Geographic Information Systems for Land Resources Assessment*. Monographs on Soils and Resources Survey, No. 12, Oxford, Oxford University.

CART., 1984. *Classification and Regression Trees*. California Statistical Software, Lafayette.

Canny, J., 1986. *A Computational Approach to Edge Detection*. IEEE Transactions on Pattern Analysis and Machine Intelligence, Vol. PAMI-8, No. 6, pp. 679-699.

Carver, S. J., and C. F. Brunsdon, 1994. *Vector to Raster Conversion Error and Feature Complexity: an Empirical Study Using Simulated Data*. International Journal of Geographic Information Systems, Vol. 8, No. 3, pp. 261-270.

Chanond, C., and C. Leekbhai, 1986. *Small Format Aerial Photography for Analysing Urban Housing Problems (Case Study Metropolitan Region)*. Proceedings of the 7th International Symposium Remote Sensing for Resources Development and Environment Management, Enschede, Netherlands, Vol. 26, pp. 993-1003.

Chen, S. K., Y. C. Tzeng, C. F. Chen, and W. L. Kao, 1995. *Land-Cover Classification of Multispectral Imagery Using a Dynamic Learning Neural Network*. Photogrammetric Engineering and Remote Sensing, Vol. 61, No. 4, pp. 403-408.

Civco, D. L., 1993. *Artificial Neural Networks for Land-Cover Classification and Mapping*. International Journal of Geographical Information Systems, Vol. 7, No. 2, pp. 173-186.

Clavet, D., M. Lasserre, and J. Pouliot, 1993. *GPS Control for 1:50,000-Scale Topographic Mapping from Satellite Images*. Photogrammetric Engineering and Remote Sensing. Vol. 59, No. 1, January, pp. 107-111.

Coleman, T. L., 1992. *Three-Dimensional Modelling of an Image-Based GIS to Aid Land Use Planning*. Geocarto International: A Multidisciplinary Journal of Remote Sensing, Vol. 4, pp. 47-53.

Colvocoresses, A. P., 1990. *An Operational Earth Mapping and Monitoring Satellite System: A Proposal for Landsat 7*. Photogrammetric Engineering and Remote Sensing, Vol. 56, No. 5, PP .569-571.

Colwell, R. N., and C. E. Poulton, 1985. *SPOT Simulation Imagery for Urban Monitoring: A Comparison with Landsat TM and MSS imagery and with High Altitude Colour Infrared Photography*. Photogrammetric Engineering and Remote Sensing, Vol. 51, No. 8, pp. 1093-1101.

Cote, S., and A. R. L. Tantnall, 1995. *Estimation of Ocean Surface Currents from Satellite Imagery Using a Hopfield Neural Network*. Proceedings of the Third Thematic Conference on Remote Sensing for Marine and Coastal Environments, Seattle, 18-20 September, USA, Vol. 1, pp. 538-549.

Cowen, D., J. R. Jensen, P. A. Bresnahan, G. B. Ehler, D. G. Graves, X. Huang, C. Wiesner, and H. E. Mackey, 1995. *The Design and Implementation of an Integrated Geographic Information System for Environmental Applications*. Photogrammetric Engineering and Remote Sensing, Vol. 61, No. 11, pp. 1393-1404.

Cushnie, J. L., and P. Atkinson, 1985. *Effect of Spatial Filtering on Scene Noise and Boundary Detail in Thematic Mapper Imagery*. Photogrammetric Engineering and Remote Sensing, Vol. 51, No. 9, pp. 1485-1493.

Cushnie, J. L., 1987. *The Interactive Effect of Spatial Resolution and Degree of Internal Variability Within Land-cover Types on Classification Accuracies*. International Journal of Remote Sensing, Vol. 8, No. 1, pp. 15-29.

Davis, F. W., D. A. Quatrochi, M. K. Ridd, N. S-N Lam, S. J. Walsh, J. C. Michaelsen, J. Franklin, D. A. Stow, C. J. Johnnsen, and C. A. Johnston, 1991. *Environmental Analysis Using Integrated GIS and Remote Sensing Data: Some Research Needs and Priorities*. Photogrammetric Engineering and Remote Sensing, Vol. 57, No. 6, pp. 689-697.

D'Agostino, V., M. Stanghelini, and G. Trisorio-Liuzzi, 1993. *A Fortran-77 Program for Preliminary Extraction of Drainage Networks Based on a DEM*. Computers of Geosciences, Vol. 19, No. 7, pp. 1006-1019.

Delawar, M. R., E. G. Masters, and B. C. Forster, 1996. *The Development of a Geographic Information Probability System with Particular Reference to Remotely Sensed Information*. Proceedings of the 8th Australian Remote Sensing Conference, 25-29 March, 1996, Canberra, Australia, Vol. 2, pp. 340-346.

Della Ventura, A., A. Rampini, and R. Schettini, 1990. *Image Registration by Recognition of Corresponding Structures*. IEEE Transactions on Geoscience and Remote Sensing, Vol. 28, No. 3, pp. 305-314.

Deriche, R., 1987. *Using Canny's Criteria to Derive a Recursively Implemented Optimal Edge Detector*. International Journal of Computer Vision, Vol. 1, No. 2, pp. 167-187.

Deriche, R., 1990. *Fast Algorithms for Low-Level Vision*. IEEE Transactions on Pattern Analysis and Machine Intelligence, Vol. 12, No. 1, pp. 78-87.

Destival, I., 1986. *Mathematical Morphology Applied to Remote Sensing*. Acta Astronautica, Vol. 13, No. 6/7, pp. 371-385.

De Ville, B., 1990. *Applying Statistical Knowledge to Database Analysis and Knowledge Base Construction*. Proceedings of Sixth IEEE Conference on Artificial Intelligence Applications, IEEE Computer Society, March 5-9, Washington, pp. 30-36.

Domenikiotis, C., 1994. *Knowledge-Based Interpretation of a Forest Road Network Using Remote Sensing Data*. Ph.D Dissertation, School of Surveying and Land Information, Curtin University of Technology, Perth, Western Australia, Australia.

Domenikiotis, C., G. D. Lodwick, and G. L. Wright, 1995. Intelligent Interpretation of SPOT Data for Extraction of a Forest Road Network. *Cartography*, Vol. 24, No. 2, pp. 47-57.

Dowman, I. J., D. G. Gagan, J. P. Moller, and G. Peacegood, 1987. *The Use of SPOT Data for Mapping and DEM Production*. SPOT-1 Image Utilization, Assessment, Results, Paris.

Ehlers, M., G. Edwards and Y. B'edard, 1989. *Integration of Remote Sensing with Geographic Information Systems: A Necessary Evolution*. Photogrammetric Engineering and Remote Sensing. Vol. 55, No. 11, pp. 1619-1627.

Ehlers, M., M. A. Jadkowski, R. R. Howard, and D. E. Brostuen, 1990. *Application of SPOT Data for Regional Growth Analysis and Local Planning*. Photogrammetric Engineering and Remote Sensing, Vol. 56, No. 2, pp. 175-180.

Ehlers, M., 1991. *Multisensor Image Fusion Techniques in Remote Sensing*. ISPRS Journal of Photogrammetry and Remote Sensing, Vol. 46, pp. 19-30.

Ehlers, M., D. Greenlee, T. Smith, and J. Star, 1991. *Integration of Remote Sensing and GIS: Data and Data Access*. Photogrammetric Engineering and Remote Sensing. Vol. 57, No. 6, pp. 669-675.

ERDAS., 1994a. *ERDAS IMAGINE Production Tour Guides*. Erdas Inc., pp. 1-18.

ERDAS., 1994b. *ERDAS IMAGINE Field Guide*. Erdas Inc., pp. 279-318.

ER Mapper., 1993. *ER Mapper Reference*. Version 4.0, Earth Resource Mapping Pty Ltd, San Diego, USA.

ESRI., 1992a. *ARC Command References*. ARC/INFO User's Guide: Version 6, Environmental Systems Research Institute Inc., Redlands, California.

ESRI., 1992b. *ARCEDIT Command References*. ARC/INFO User's Guide: Version 6, Environmental Systems Research Institute Inc., Redlands, California.

ESRI., 1992c. *GRID Command References*. ARC/INFO User's Guide: Version 6, Environmental Systems Research Institute Inc., Redlands, California.

ESRI., 1992d. *Image Integration*. ARC/INFO User's Guide: Version 6, Environmental Systems Research Institute Inc., Redlands, California.

ESRI., 1992e. *Cell-Based Modelling with Grid*. ARC/INFO User's Guide: Version 6, Environmental Systems Research Institute Inc., Redlands, California.

ESRI., 1994. *Understanding GIS: The ARC/INFO*. Environmental Systems Research Institute Inc., Redlands, California.

Estes, J. E., 1992. *Remote Sensing and GIS Integration: Research Needs, Status and Trends*. Journal of ITC. Vol. 1, pp. 2-9.

Evans, B., and D. Fisher, 1994. *Overcoming Process Delays with Decision Tree Induction*. Machine Learning, pp. 60-66.

Evans, H. F., P. Caccetta, and R. Ferdowsian, 1996. *Integrating Remotely Sensed Data with Other Spatial Data Sets to Predict Areas at Risk from Salinity*. Proceedings of the 8th Australian Remote Sensing Conference, 25-29 March, 1996, Canberra, Australia, pp. 18-25.

Faugeras, O., 1993. *Edge Detection*. Three-Dimensional Computer Vision: A Geometric Viewpoint, The MIT Press, Cambridge, Massachusetts, London, England, pp. 4-123.

Fischler, M. A., J. M. Tenenbaum, and H. C. Wolf, 1981. *Detection of Roads and Linear Structures in Low-Resolution Aerial Imagery Using a Multisource Knowledge Integration Technique*. Computer Graphics and Image Processing, Vol. 15, pp. 201-223.

Fisher, P. F., and R. E. and Lindenbergh, 1989. *Distinction among Cartography, Remote Sensing and Geographic Information Systems*. Photogrammetric Engineering and Remote Sensing. Vol. 55, No. 10, pp. 1431-1434.

Flowerdew, R., 1991. *Spatial Data Integration. Geographical Information Systems: Principles and Applications*. (Edited by D. J. Maguire, M. F. Goodchild, and A. W. Rhind). Longman Scientific & Technical Co., Published in the United States and Canada with John Wiley & Sons Inc., New York, pp. 24-375.

Foody, G. M., M. B. McCulloch, and E. B. Yates, 1995. *Classification of Remotely Sensed Data by an Artificial Neural Network: Issues Related to Training Data Characteristics*. Photogrammetric Engineering and Remote Sensing, Vol. 61, No. 4, pp. 391-401.

Ford, G. E., V. R. Algazi, and D. I. Meyer, 1983. *A Noninteractive Procedure for Land Use Determination*. Remote Sensing of Environment, Vol. 13, No. 1, pp. 1-16.

Forghani, A., 1993. *Monitoring Change in Urban Areas Using Satellite Remote Sensing Data with Particular Reference to Developing Countries*. M. Eng. Sc. Thesis, School of Surveying, The University of New South Wales, Sydney, Australia, pp. 1-104.

Forghani, A., 1994. *A New Technique for Map Revision and Change Detection Using Merged Landsat TM and SPOT Data Sets in an Urban Environment*. Asian-Pacific Remote Sensing Journal, Vol. 7, No. 1, July, pp. 119-131.

Forghani, A., 1995. *Linear Feature Detection from Aerial Imagery*. Proceedings of the Third Thematic Conference on Remote Sensing for Marine and Coastal Environments, Seattle, Washington, 18-20 September, 1995, USA, Vol. 2, pp. 689-698.

Forghani, A., 1997. *A Review of Image Segmentation Methods: Integration of Image Analysis and GIS for Intelligent Feature Extraction*. Proceedings of the Twelfth International Conference and Workshops on Applied Geologic Remote Sensing, Denver, Colorado, 17-19 November 1997, USA, pp J-34/1-10.

Forghani, A., and P. Zwart, 1995. *Surveying and Mapping with Space Data*. Proceedings of the 21st National Surveying Conference: Surveyors and Surveying - Today and Tomorrow, Technical Papers, Hobart, 31 August - 3 September, 1995, Australia, pp. 232-240.

Forghani A. and P. Zwart, 1997. *An Investigation to the Use of PhotoGIS for Orthophotography: Does the PhotoGIS Offers Capabilities to Use in Iran?* Proceedings of the Fourth Thematic Conference and Exhibition Geographic Information Systems (GIS), May 1997, Tehran, Iran, pp. 23-34.

Forghani, A., and J. Osborn, 1996. *Detection of Roads Using a GIS Database and a Knowledge-based Approach*. Proceedings of the 8th Australian Remote Sensing Conference, 25-29 March, 1996, Canberra, Australia, Vol. 2, pp. 37.

Forghani A., and J. Osborn, 1998a. *Geometric Registration of Aerial Photography Using Three Image Correction Methods*. International Journal of Geographical Information Systems, March 1998, PP. 1-12 (submitted).

Forghani A., and J. Osborn, 1998b. *Interactive Linear Feature Detection to Support Integration of Image Understanding Techniques within a GIS*. IEEE Transactions on Geoscience and Remote Sensing, March 1998, PP. 1-17 (submitted).

Forghani A., and J. Osborn, 1998c. *Integration of Remotely Sensed Imagery and a GIS Database for Knowledge-Based Analysis*. For Presentation at the Fifth International Conference on Remote Sensing for Marine and Coastal Environments, San Diego, California, 5-7 October 1998, USA, pp. 1-8.

Forghani A., and J. Osborn, 1998d. *A Knowledge-Based Approach for Mapping Road Networks Using GIS Databases*. For Presentation at the 9th Australasian Remote Sensing & Photogrammetry Conference, 20-24 July 1998, Sydney, NSW, Australia, 1-10.

Forghani, A., J. Osborn, and M. Roach., 1997. *An Image Interpretation Model to Support Integration of Image Understanding Techniques within a GIS: Delineation of Road Structures from Aerial Imagery*. Proceedings of the International GIS/GPS'97 Symposium, Istanbul, Turkey, September, 1997, pp 1-10.

Forster, B. C., 1985. *An Examination of Some Problems and Solutions in Monitoring Urban Areas from Satellite Platforms*. International Journal of Remote Sensing, Vol. 6, No. 1, pp. 139-151.

Forster, B. C., 1986. *Evaluation of Combined Multiple Incidence Angle SIR-B Digital Data and Landsat MSS Data over an Urban Complex*. Proceedings of the 7th International Symposium, ISPRS Commission VII, Remote Sensing for Resources Development and Environmental Management, Enschede, pp. 195-303.

Forster, B. C., 1993. *Coefficient of Variation as a Measure of Urban Spatial Attributes, Using SPOT HRV and Landsat TM*. International Journal of Remote Sensing, Vol. 14, No. 12, pp. 2403-2409.

Forster, B. C., 1995. *Personal Communication*. School of Geomatics Engineering, University of New South Wales, Sydney, NSW, Australia.

Frank, A. U., 1988. *Requirements for a Database Management System for a GIS*. Photogrammetric Engineering and Remote Sensing, Vol. 54, No. 11, pp. 1557-1564.

Frank, A. U., and R. Barrea, 1990. *The Fieldtree: A Data Structure for Geographic Information Systems*. Design and Implementation of Large Spatial Databases (Edited by A. Buchmann, O. Gunther, T. R. Smith, and Y. F. Wang), Lecture Notes in Computer Science, Vol. 409, Springer-Verlag, Berlin.

Frank, A. U., B. Palmer, and V. B. Robinson, 1986. *Formal Methods for Accurate Definitions of Some Fundamental Terms in Physical Geography*. Proceedings of First International Symposium on Spatial Data Handling, Zurich, Switzerland, pp. 544-571.

Franklin, S. E., and D. R. Peddle, 1990. *Classification of SPOT HRV Imagery and Texture Features*. International Journal of Remote Sensing, Vol. 11, No. 3, pp. 551-556.

Frost, R. M., 1995. *Improved Well Positions for Geoscientific Applications: Exploiting NAPP Photographs with Digitiser and PC-Based Bundle Adjustment Program*. Photogrammetric Engineering and Remote Sensing, Vol. 61, No. 7, pp. 927-934.

Fung, T., 1992. *Land Use and Land Cover Change Detection With Landsat MSS and SPOT HRV Data in Hong Kong*. Geocarto International: A Multi-Disciplinary Journal of Remote Sensing, Vol .3, pp. 33-41.

Gahegan, M., and J. Flack, 1996. *A Model to Support the Integration of Image Understanding Techniques within a GIS*. Photogrammetric Engineering and Remote Sensing, Vol. 62, No. 5, pp. 483-490.

- Geman, D., and B. Jedynek, 1996. *An Active Testing Model for Tracking Roads in Satellite Images*. IEEE Transactions on Pattern Analysis and Machine Intelligence, Vol. 18, No. 1, pp. 1-14.
- Gemello, R., F. Mana, and L. Sitta, 1991. *Rigel: An Inductive Learning System*. Machine Learning, Vol. 6, pp. 7-35.
- Giarrantano, J., and G. Riley, 1989. *Expert Systems: Principles and Programming*. PWS-Kent, Boston, Massachusetts, pp. 632.
- Gisolfi, A., and G. Nunez, 1993. *An Algebraic Approximation to the Classification with Fuzzy Attributes*. International Journal of Approximate Reasoning, Vol. 9, pp. 75-95.
- Gong, P., and B. Chen, 1988. *Remote Sensing Approaches Used in Chinese Urban Land Use Analysis*. 16th Congress of International Archives of Photogrammetry and Remote Sensing, Kyoto, Japan, Commissions I, II, III, IV, V, VI, VII, Vol. 27, pp. 271-276.
- Gong, P., and P. J. Howarth, 1990. *An Assessment of Some Factors Influencing Multispectral Land-Cover Classification*. Photogrammetric Engineering and Remote Sensing, Vol. 56, No. 5, pp. 597-603.
- Gong, P., D. J. Marceau, and P. J. Howarth, 1992. *A Comparison of Spatial Feature Extraction Algorithms for Land-Use Classification With SPOT HRV Data*. Remote Sensing of Environment, Vol. 40, pp. 137-151.
- Gonzalez, R. C., and P. A. Wintz, 1987. *Digital Image Processing: 2nd Edition*. Addison-Wesley Publishing Company, Reading, Massachusetts.
- Gopal, S., and C. Woodcock, 1994. *Theory and Methods for Accuracy Assessment of Thematic Maps Using Fuzzy Sets*. Photogrammetric Engineering and Remote Sensing, Vol. 60, No. 2, pp. 181-188.
- Goshtasby, A., 1987. *Geometric Correction of Satellite Images Using Composite Transformation Functions*. Proceedings of the Twenty-First Symposium on Remote Sensing of Environment, Vol. II, October, Ann Arbor, Michigan, pp. 825-834.
- Goshtasby, A., 1988. *Registration of Images with Geometric Distortions*. IEEE Transactions on Geoscience and Remote Sensing, Vol. 26, pp. 60-64.
- Goshtasby, A., G. C. Stockman, and C. V. Page, 1986. *A Region-Based Approach to Digital Image Registration with Subpixel Accuracy*. IEEE Transactions on Geoscience and Remote Sensing, Vol. 24, No. 3, pp. 390-399.
- Gray, N. A. B., 1990. *Capturing Knowledge through Top-Down Induction of Decision Trees*. IEEE Expert Intelligent Systems and their Applications, pp. 41-50.

Gruen, A., and H. Li, 1995. *Road Extraction from Aerial and Satellite Images by Dynamic Programming*. ISPRS Journal of Photogrammetry and Remote Sensing, Vol. 50, No. 4, pp. 11-21.

Guestari, S., 1996. *Personal Communication*.

Gugan, D. J., 1988. *Satellite Imagery as an Integrated GIS Component*. GIS/LIS'88 Proceedings Accessing the World, San Antonio, Vol. 1, pp. 174-180.

Gurney, C. M., 1981. *The Use of Contextual Information to Improve Land Cover Classification of Digital Remotely Sensed Data*. International Journal of Remote Sensing, Vol. 2, No. 4, pp. 379-388.

Gurney, C. M., and J. R. Townshend, 1983. *The Use of Contextual Information in the Classification of Remotely Sensed Data*. Photogrammetric Engineering and Remote Sensing, Vol. 49, pp. 55-64.

Haack, B. N., 1985. *Multisensor Data Analysis of Urban Environments*. Photogrammetric Engineering and Remote Sensing, Vol. 50, No. 10, pp. 1471-1477.

Harlow, C. A., M. M. Trividi, and R. W. Connors, 1986. *Use of Texture Operators in Segmentation*. Optical Engineering, Vol. 25, No. 11, pp. 1200-1207.

Haralick, R. M., 1979. *Statistical and Structural Approaches to Texture*. Proceedings of the IEEE, Vol. 67, No. 5, pp. 786-804.

Haralick, R. M., and L. G. Shapiro, 1985. *Survey: Image Segmentation Techniques*. Computer Vision, Graphic, and Image Processing, Vol. 29, pp. 100-132.

Harris, R., 1985. *Contextual Classification Post-Processing of Landsat Data Using a Probabilistic Relaxation Model*. International Journal of Remote Sensing, Vol. 6, No. 6, pp. 847-866.

Harris, P. M., and S. J. Ventura, 1995. *The Integration of Remotely Sensed Imagery to Improve Classification in an Urban Area*. Photogrammetric Engineering and Remote Sensing, Vol. 61, No. 8, pp. 993-998.

Hartog J. E. D., T. K. T. Kate, and J. J. Gerbrands, 1996. *Knowledge-Based Interpretation of Utility Maps*. Computer Vision and Image Understanding, Vol. 63, No. 1, pp. 105-117.

Hathout, S., 1988. *Land Use Change Analysis and Prediction of Suburban Corridor of Winnipeg, Manitoba*. Journal of Environmental Management, Vol. 27, pp. 325-335.

He, D. C., and L. Wang, 1990. *Texture Unit, Texture Spectrum, and Texture Analysis*. IEEE Transactions on Geoscience and Remote Sensing, Vol. 28, No. 4, pp. 509-512.

Henery, R. J., 1994. *Machine Learning, Neural and Statistical Classification* (Edited by Michie, D., D. J. Spiegelhalter, and C. C. Taylor). Department of Computer Science, University College, London, pp. 96-130.

Hepner, G. F., 1990. *Artificial Neural Network Classification Using a Minimal Training Set: Comparison to Conventional Supervised Classification*. Photogrammetric Engineering and Remote Sensing, Vol. 56, No. 4, pp. 469-473.

Holyer, R. J., and S. Peckinpaugh, 1989. *Edge Detection Applied to Satellite Imagery of Oceans*. IEEE Transaction on Geoscience and Remote Sensing, Vol. 27, No. 1, pp. 46-56.

Hsu, P. S., and C. H. Wu, 1990. *Using Scanned Digital Aerial Photographic Images to Describe the Perceptual Spaces of Urban Spatial Structure: An Analysis of Transportation Network and its Adjacent Land Use*. ISPRS Commission II/VII International Extraction and Analysis for Remote Sensing, University of Maine, USA, pp. 49-58.

Hunt, E. B., 1962. *Concept Learning: An Information Processing Problem*. Wiley, New York.

Hunter, G. J., and M. Goodchild, 1995. *Dealing with Error in Spatial Databases: A Simple Case Study*. Photogrammetric Engineering and Remote Sensing, Vol. 61, No. 5, pp. 529-537.

Hyde, R. F., and N. J. Vesper, 1983. *Some Effects of Resolution Cell Size on Image Quality*. LANDSAT Users Notes, No. 29, pp. 9-12.

Jackson, M. J., and P. A. Woodsford, 1991. *GIS Data Capture: Hardware and Software, Geographical Information Systems: Principles and Applications* (Edited by D. J. Maguire, M. Goodchild, and D. W. Rhind), Longman Scientific & Technical, John Wiley & Son, Inc., New York, pp. 239-249.

Jazouli, R., D. L. Verbyla, and D. L. Murphy, 1994. *Evaluation of SPOT Panchromatic Digital Imagery for Updating Road Locations in a Harvested Forest Area*. Photogrammetric Engineering and Remote Sensing. Vol. 60, No. 12, December, pp. 1449-1452.

Jensen, J. R., 1986. *Introductory Digital Image Processing*, Prentice-Hall, Englewood Cliffs, N.J., PP 569.

Jensen, J. R., 1995. *Issues Involving the Creation of Digital Elevation Models and Terrain Corrected Orthoimagery Using Soft-Copy Photogrammetry*. Geocarto International, Vol. 10, NO. 1, pp. 5-21.

Jensen, J. R., and D. L. Toll, 1982. *Detection Residential Land-Use Development at the Urban Fringe*. Photogrammetric Engineering and Remote Sensing, Vol. 19, pp. 629-643.

Johnson, J. H., 1989. *Pixel Parts and Picture Wholes*. From Pixels to Features (Edited by J. C. Simon), Elsevier Science Publishers B.V, North-Holland, pp. 347-372.

Johnsson, K., 1991. *Rule Based Extraction of Spectrally Heterogeneous Land Use Categories from SPOT Multispectral Data*. Licentiate Thesis, Royal Institute of Technology, Department of Photogrammetry, Stockholm, Sweden.

Johnsson, K., 1994. *Segment-Based Land-Use Classification from SPOT Satellite Data*. Photogrammetric Engineering and Remote Sensing, Vol. 60, No. 1, pp. 61-66.

Julien, B., 1992. *Experience with Four Probability-Based Induction Methods*. AI Applications, Vol. 6, pp. 51-56.

Karimi, H. A., and G. D. Lodwick, 1987. *A Simple Rule-Based System for Selection of Remote Sensing Imagery*. Proceedings of Eleventh Canadian Symposium on Remote Sensing, Waterloo, Ontario, Vol. II, pp. 591-598.

Kass, G. V., 1975. *Significant Testing in Automatic Interaction Detection*. Applied Statistics, Vol. 24, No. 2, pp. 178-189.

Kass, G. V., 1980. *An Exploratory Technique for Investigating Large Quantities of Categorical Data*. Applied Statistics, Vol. 29, No. 2, pp. 119-127.

Kepuska, V. Z., and S. O. Mason, 1995. *A Hierarchical Neural Network System for Signalised Point Recognition in Aerial Photographs*. Photogrammetric Engineering and Remote Sensing, Vol. 61, No. 7, pp. 917-925.

Khoshnevis, B., and S. Parisay, 1993. *Machine Learning and Simulation: Application in Queuing Systems*. Simulation, pp. 294-302.

Ko, K. T., 1995. *A Hybrid Road Identification System Using Image Processing Techniques and Back-Propagation Neural Networks*. Technical Report No. MSU-950607, June, Department of Computer Science, College of Engineering, Mississippi State University.

Konecny, G., 1990. *Review of Latest Technology in Satellite Mapping. Interim Representation International Mapping Remote Sensing Satellite Systems*. Institute of Photogrammetry, University of Hannover, pp. 11-22.

Koza, J. R., 1992. *Genetic Programming: on the Programming of Computers by Means of Natural Selection*, Imprint Cambridge, Mass.: MIT Press, c1992.

Labovtiz, M. L., and J. W. Marvin, 1986. *Precision in Geodetic Correction of TM Data as a Function of Number, Spatial Distribution, and Success in Matching of Control Points: A Simulation*. Remote Sensing of Environment, Vol. 20, pp. 237-252.

Lee, J., 1994. *Digital Analysis of Viewshed Inclusion and Topographic Features on Digital Elevation Models*. Photogrammetric Engineering and Remote Sensing, Vol. 60, No. 4, pp. 451-456.

Lees, B. G., 1994. *Decision Trees, Artificial Neural Networks and Genetic Algorithms for Classification of Remotely Sensed and Ancillary Data*. 7th Australian Remote Sensing Conference Proceedings, Melbourne, Australia, pp. 51-60.

Lees, B. G., and K. Ritman, 1991. *Decision Tree and Rule Induction Approach to Integration of Remotely Sensed and GIS Data in Mapping Vegetation in Disturbed or Hilly Environments*. Environmental Management, Vol. 15, pp. 828-831.

Li, L. G., Deecker, K. Yurach, and J. Seguin, 1989. *Updating Urban Street Network Files with High Resolution Satellite Imagery*. Proceedings of Auto-Carto IX Symposium, ASPRS/ACSM, Baltimore, Maryland, USA, pp. 21-30.

Li, Z. S., J. Kitter, and M. Petrou, 1993. *Automatic Registration of Aerial Photographs and Digitized Maps*. Optical Engineering, Vol. 32, No. 6, June, pp. 1213-1221.

Liepins, G., R. Goeltz, and R. Rush, 1990. *Machine Learning Techniques for Natural Resource Data Analysis*. AI Application, Vol. 4, No. 3, pp. 9-18.

Light, D. L., 1990. *Characteristics of Remote Sensors for Mapping and Earth Science Applications*. Photogrammetric Engineering and Remote Sensing, Vol. 56, No. 12, pp. 1613-1623.

Lincolne, R., 1995. *Personal Communication*. Space Image Unit, Central Science Laboratory, University of Tasmania, Hobart, Tasmania, Australia.

Lillesand, T., and R. Kiefer, 1987. *Remote Sensing and Image Interpretation: 2nd Edition*. John Wiley and Sons. PP. 721.

Lo, C. P., 1992. *A GIS Approach to Population Estimation in a Complex Environment Using SPOT Multispectral Images*. XVIIth Congress of International Archives of Photogrammetry and Remote Sensing Washington, D. C., Commission VII, Vol. XXIX, pp. 935-941.

Lodwick, G. D., and S. H. Paine, 1986. *Remote Sensing and Image Interpretation*. Publication No. 10009, Surveying Engineering, The University of Calgary, Calgary, Alberta, pp. 240-242.

Lowell, K. E., 1994. *Probabilistic Temporal GIS Modelling Involving More than Two Map Classes*. International Journal of Geographic Information Systems, Vol. 8, No. 1, pp. 73-93.

Lucas, P., and L. Van Der Gaag, 1991. *Principles of Expert Systems*. Addison-Wesley Publishing Company, Wokingham, UK, pp. 518.

- Lunetta, R. S., R. G. Congalton, L. K. Frenstermaker, J. R. Jensen, K. C. McGwire, and L. R. Tinney, 1991. *Remote Sensing and Geographic Information System Data Integration: Error Sources and Research Issues*. Photogrammetric Engineering & Remote Sensing, Vol. 57, No. 6, pp. 677-687.
- Mack, C., E. E. Marsh, and C. F. Hutchinson, 1995. *Application of Aerial Photography and GIS Techniques in the Development of a Historical Perspective of Environmental Hazards at the Rural-Urban Fringe*. Photogrammetric Engineering and Remote Sensing, Vol. 61, No. 8, pp. 1015-1020.
- Marshall, G., 1990. *Advanced Students' Guide to Expert Systems*. Heinemann Newnes, Oxford, UK, pp. 176.
- Marr, D., and E. Hildreth, 1980. *Theory of Edge Detection*. Proceedings of the Royal Society of London, B 207, pp. 187-217.
- Marr, D., 1982. *Vision*. W. H. Freeman and Company, San Francisco. PP. 397.
- Marvin, J. W., M. Labovitz, and R. E. Wolf, 1987. *Derivation of Fast Algorithm to Account for Distortions Due to the Terrain in Earth-Viewing Satellite Sensor Images*. IEEE Transactions on Geoscience and Remote Sensing, Vol. 25, No. 2, March, pp. 244-251.
- Mather, P. M., 1985. *Remote Sensing Letters: A Computationally-Efficient Maximum-Likelihood Classifier Employing Prior Probabilities for Remotely-Sensed Data*. International Journal of Remote Sensing. Vol. 6, No. 2, pp. 369-376.
- Mather, P. M., 1987. *Computer Processing of Remotely Sensed Images*. John Wiley and Sons, Chichester, UK, pp. 352.
- Mather, P. M., 1995. *Map-Image Registration Accuracy Using Least-Squares Polynomials*. International Journal of Geographic Information Systems, Vol. 9, No. 5, pp. 543-554.
- Martin, L. R. G., P. J. Howarth, and G. H. Holder, 1988. *Multispectral Classification of Land Use at the Rural-Urban Fringe Using SPOT Data*. Canadian Journal of Remote Sensing. Vol. 14, No. 2, pp. 72-79.
- Mathworks., 1995. *MATLAB High-Performance Numeric Computation and Visualisation Software*. Reference Guide: Version 4.0, The MATHWORKS Inc.
- Mathworks., 1995. *Image Processing TOOLBOX for Use with MATLAB*. Reference Guide: Version 4.0, The MATHWORKS Inc.
- Mason, S. O., and K. W. Wong, 1992. *Image Alignment by Line Triples*. Photogrammetric Engineering and Remote Sensing, Vol. 58, No. 9, pp. 1329-1334.

Mason, D. C., M. A. O'Conail, and S. B. Bell, 1994. *Handling Four-Dimensional Geo-Referenced Data*. International Journal of Geographic Information Systems, Vol. 8, No. 2, pp. 191-215.

Mason, S., 1995. *Expert System-Based Design of Close-Range Photogrammetric Networks*. ISPRS Journal of Photogrammetry and Remote Sensing, Vol. 50, No. 5, pp. 13-25.

McKeown, D. M., W. A. Harvey, and J. McDermott, 1985. *Rule-Based Interpretation of Aerial Imagery*. IEEE Transactions on Pattern Analysis and Machine Intelligence PAMI, Vol. 8, pp. 532-542.

McKeown, D. M., 1987. *The Role of Artificial Intelligence in the Integration of Remotely Sensed Data with GIS*. IEEE Transactions on Geoscience and Remote Sensing, Vol. GE-25, No. 3, pp. 330-348.

McKeown, D. M., and A. Zlotnick, 1990. *Built-Up Area Feature Extraction: First Year Report*. Technical Report AD-A220-005, School of Computer Science, Carnegie Mellon University, Pennsylvania, USA.

Michaelis, M., 1988. *Incorporation of Texture Information as an Aid to the Feature Extraction and Classification with SPOT Data*. 16th Congress of International Archives of Photogrammetry and Remote Sensing, Kyoto, Japan, Commissions I, II, III, IV, V, VI, VII, Vol. 27, Vol. 27, pp. 139-148.

Michie, D., 1991. *Methodologies from Machine Learning in Data Analysis and Software*. The Computer Journal, Vol. 34, No. 6, pp. 559-565.

Michie, D., D. J. Spiegelhalter, and C. C. Taylor, 1994. *Machine Learning, Neural and Statistical Classification (Edited by Michie, D., D. J. Spiegelhalter, and C. C. Taylor)*. Department of Computer Science, University College, London, pp. 1-15.

Milne, A. K., 1988. *Change Detection Analysis Using Landsat Imagery: A Review of Methodology*. Proceedings of IGARSS'88 Symposium, Edinburgh, Scotland, pp. 541-544.

Mirsa, P., 1986. *Small Format Aerial Photography-A New Planning and Administrative Tool for Town Planners in India*. Proceeding of the 7th International Symposium Remote Sensing for Resources Development and Environment Management, Enschede, Netherlands, pp. 853-864.

Moller-Jensen, L., 1990. *Knowledge-Based Classification of an Urban Area Using Texture and Context Information in Landsat-TM Imagery*. Photogrammetric Engineering and Remote Sensing, Vol. 56, No. 6, pp. 899-904.

Monga, O., R. Deriche, and J. M. Rocchisani, 1991. *3D Edge Detection Using Recursive Filtering: Application to Scanner Images*. Image Understanding, Vol. 53, No. 1, pp. 76-87.

- Moore, D. M., B. G. Lees, S. M. Davey, 1991. *A New Method for Predicting Vegetation Distributions Using Decision Tree Analysis in a Geographic Information System*. Environmental Management, Vol. 15, pp. 59-71.
- Muller, J. C., 1991. *Generalization of Spatial Databases* (Edited by D. J. Maguire, M. F. Goodchild, D. W. Rhind). Longman Scientific & Technical, John Wiley & Son Inc., New York, Vol. 1, pp. 457-475.
- Nagarathinam, V., K. Jayagobi, M. Maruthachalam, S. Panchanathan and R. Palanivelu, 1988. *Urban Monitoring Using SPOT Imagery - A Case Study*. 16th Congress of International Archives of Photogrammetry and Remote Sensing, Kyoto, Japan, Commissions I, II, III, IV, V, VI, VII, Vol. 27, pp. 322-328.
- Nalwa, V. S., and T. O. Binford, 1986. *On Detecting Edges*. IEEE Transactions on Geoscience and Remote Sensing, Vol. PAMI-8, No. 6, pp. 699-714.
- Nevatia, R., and K. R. Babu, 1980. *Linear Feature Extraction and Description*. Computer Graphics and Image Processing, Vol. 13, pp. 257-269.
- Numan, N. M. S., J. Ghasson, and H. A. Thannoon, 1992. *Topographic Map Revision in Northern Iraq Using DTMs and Orthophotos*. ITC Journal, Vol. 3, pp. 244-248.
- O'Brien, D., 1987. *Road Network Extraction from SPOT Panchromatic Data*. Proceedings, International Symposium on Topographic Applications of SPOT Data. Canadian Institute of Surveying and Mapping, Sherbrooke, Quebec, Canada, pp. 273-287.
- O'Brien, D., 1991. *Computer Assisted Feature Extraction (InterEx)*. Proceedings of the 14th Canadian Symposium on Remote Sensing, Calgary, Alberta, May, 199, Canada, pp. 423-428.
- Oliveira, M. D. L. N. D., 1986. *Visual Aerial Photograph Texture Discrimination for Delineation Homogeneous Residential Sectors: An Instrument for Urban Planners*. Proceedings of the 7th International Symposium Remote Sensing for Resources Development and Environment Management, Enschede, Netherlands, pp. 809-811.
- Pai, M. L., J. C. Bezdek, R. L. Cannon, and W. L. Cameron, 1986. *Terrain Mapping with MMW Radar: An Approach Using Sensor Fusion and Knowledge-Based Heuristics*. SPIE, Vol. 726 Mobile Robots, pp. 289-295.
- Patmios, E., 1986. *Photointerpretation and Orthophotograph at the Study of Monuments in Urban Areas*. Proceedings of the 7th International Symposium of Remote Sensing for Resources Development and Environmental Management, Enschede, Netherlands, pp. 865-866.
- Peddle, D. R., 1995. *Knowledge Formulation Supervised Evidential Classification*. Photogrammetric Engineering and Remote Sensing, Vol. 61, No. 4, pp. 409-417.

Petrou, M., 1993. *Optimal Convolution Filters and an Algorithm for the Detection of Wide Linear Features*. IEEE Processing-1, Vol. 140, No. 5, pp. 331-339.

Peuquet, D., 1981a. *An Examination of Techniques for Reformatting Digital Cartographic Data/Part 1: the Raster-to-Vector Process*. Cartographica, Vol. 18, No. 1, pp. 34-48.

Peuquet, D., 1981b. *An Examination of Techniques for Reformatting Digital Cartographic Data/Part 2: The Vector-to-Raster Process*. Cartographic, Vol. 18, No. 3, pp. 21-33.

Peuquet, D., 1983. *A Hybrid Structure for the Storage and Manipulation of Very Large Spatial Data Sets*. Computer Vision, Graphics, and Image Processing, No. 24, pp. 14-27.

Peuquet, D., 1979. *Raster Processing: an Alternative Approach to Automated Cartographic Data Handling*. American Cartographer, No. 6, pp. 129-139.

PhotoGIS Documentation., 1994. *PhotoGIS User's Guide, Direct from Aerial Photographs to Geographic Information Systems: Version 2*. Salamanca Software, Hobart, Tasmania, Australia.

Piwowar, J. M., E. F. LeDrew, and D. J. Dudycha, 1990. *Integration of Spatial Data in Vector and Raster Formats in a Geographic Information System Environment*. International Journal of Geographical Information Systems, Vol. 4, No. 4, pp. 429-444.

Polidori, L., and J. Chorowicz, 1993. *Comparison of Bilinear and Brownian Interpolation for Digital Elevation Models*. ISPRS Journal of Photogrammetry and Remote Sensing, Vol. 48, No. 2, pp. 18-23.

Pratt, R. K., 1978. *Digital Image Processing*. New York, John Wiley and Sons.

Pries, R. A., 1995. *A System for Large-Scale Image Mapping and GIS Data Collection*. Photogrammetric Engineering and Remote Sensing, Vol. 61, No. 5, pp. 503-511.

Quinlan, J. R., 1983. *Learning Efficient Classification Procedures and their Application to Chess and Games*. Machine Learning (Edited by R. S. Michalski, J. G. Carbonell, and T. M. Mitchell), Tioga, Palo Alto, C. A.

Quinlan, J. R., 1986. *Induction of Decision Trees*. Machine Learning, Vol. 1, pp. 81-106.

Quinlan, J. R., 1990. *Learning Logical Definition from Relations*. Machine Learning, Vol. 5, pp. 239-266.

Quarmby, N. A., and Townshend, J. R. G., 1988. *Preliminary Analyses of SPOT HRV Multispectral Products for an Arid and a Temperate Environment*. Proceedings of the International Symposium on SPOT-1 Image Utilisation, Assessment, Results, Paris, France, pp. 583-612.

Reddy, R. K. T., and G. F. Bonham-Carter, 1991. *A Decision-Tree Approach to Mineral Potential Mapping in Snow Lake Area Manitoba*. Canadian Journal of Remote Sensing, Vol. 17, No. 2, pp. 191-200.

Reed, T. R., and H. J. M. Du-Bois, 1993. *A Review of Recent Texture Segmentation and Feature Extraction Techniques*. CVGIP:-Image-Understanding, 57(3), pp. 359-372.

Richards, J. A., 1986. *Remote Sensing Digital Image Processing: An Introduction*. Springer-Verlag, Berlin.

Richards, J. A., 1993. *Digital Image Processing in Remote Sensing Advances and Future Trends*. Proceedings of Advanced Remote Sensing Conference, University of New South Wales, Sydney, New South Wales, July, pp. 291-297.

Robinson, V. B., and A. V. Frank, 1987. *Expert Systems for Geographic Information Systems*. Photogrammetric Engineering and Remote Sensing, Vol. 33, No. 10, pp. 1435-1441.

Rohwer, R., M. Wynne-Jones, and F. W. Wysotzki, 1994. *Machine Learning, Neural and Statistical Classification* (Edited by Michie, D., D. J. Spiegelhalter, and C. C. Taylor). Department of Computer Science, University College, London, pp. 84-105.

Rosenfeld, A., and A. Kak, 1982. *Digital Picture Processing: Second Edition*. Academic Press, New York, New Jersey.

Ryan, T. W., P. J. Sementilli, P. Yuen, and B. R. Hun, 1991. *Extracting of Shoreline Features by Neural Nets and Image Processing*. Photogrammetric Engineering and Remote Sensing, Vol. 57, No. 7, pp. 947-955.

Schanzer, D. L., G. W. Plunkett, and D. Wall, 1990. *Filters for Residential Road Delineation from SPOT PLA Imagery*. Proceedings of GIS for the 1990s, Second National Conference on GIS, Ottawa, Canada, pp. 801-813.

Serra, J., 1988. *Image Analysis and Mathematical Morphology*. Vol. 2: Theoretical Advances, Academic Press.

Serra, J., 1996. *Course on Mathematical Morphology*. 1996 Sydney International Statistical Congress, Sydney, New South Wales, Australia.

Shafer, G., 1976. *A Mathematical Theory of Evidence*. Princeton University Press, Princeton.

Shimoda, H., Y. Kasai, R. Yamaguchi, K. Fukue, and T. Sakata, 1988. *Effects of Spatial Resolution to Land Cover Classification Accuracies for SPOT HRV and Landsat TM Data*. 16th Congress of International Archives of Photogrammetry and Remote Sensing, Kyoto, Japan, Commissions I, II, III, IV, V, VI, VII, Vol. 27, Vol. 27, pp. 544-553.

Silfer, A. T., 1988. *Generating GIS Coverages for Satellite Imagery*. Proceedings of GIS/LIS'88, San Antonio, Vol. 1, pp. 52-57.

Skidmore, A. K., 1990. *Terrain Position as Mapped from Gridded Digital Elevation Model*. International Journal of Geographic Information Systems, Vol. 4, No. 1, pp. 33-49.

Skidmore, A. K., F. Watford, P. Luckananurug, and P. J. Ryan, 1996a. *An Operational GIS Expert System for Mapping Forest Soils*. Photogrammetric Engineering and Remote Sensing, Vol. 62, No. 5, pp. 501-511.

Skidmore, A. K., A. Gauld, and P. Walker, 1996b. *Classification of Kangaroo Habitat Distribution Using Three GIS Models*. International Journal of Geographic Information Systems, Vol. 10, No. 4, pp. 441-454.

Smith, T. R., and J. E. Yiang, 1991. *Knowledge-Based Approaches in GIS*. Geographical Information Systems: Principles and Applications, (Edited by D. J. Maguire, M. Goodchild, and D. W. Rhind), Longman Scientific & Technical, John Wiley & Son Inc., New York, pp. 413-525.

Solberg, R., S. Fiskum, and M. C. Giffen, 1990. *Detection of Urban Areas by Interference Filtering*. IGARSS'90-10th Annual, International Geoscience and Remote Sensing, College Park, May. PP. 1995-99.

Sirinivinsan, A., and J. A. Richards, 1993. *Analysis of GIS Spatial Data Using Knowledge-Based Methods*. International Journal of Geographical Information Systems, Vol. 7, No. 6, pp. 479-500.

Stadelmann, M., and G. D. Lodwick, 1993. *A Rule-Based System for Extraction of Cartographic Features from Landsat TM Imagery*. Cartography, Vol. 22, No. 2, pp. 1-9.

Steiner, D. R., 1992. *The Integration of Digital Orthophotographs with GISs in a Microcomputer Environment*. ITC Journal, Vol. 1, pp. 65-71.

Stilla, U., 1995. *Map-Aided Structural Analysis of Aerial Images*. ISPRS Journal of Photogrammetry and Remote Sensing, Vol. 50, No. 4, pp. 2-10.

Stockwell, D. R. B., 1993. *LBS: Bayesian Learning System for Rapid Expert System Development*. Expert Systems with Applications, Vol. 6, pp. 137-147.

Stone, M., 1974. *Cross-Validatory Choice and Assessment of Statistical Predictions*. Journal of Royal Statistical Society, No. 2, pp. 111-147.

Strobl, J., 1993. *Detecting and Documenting Change: Integrated Resource Map Revision by Aerial Surveying*. Proceedings of GIS'93 Symposium, Vancouver, British Columbia, Canada, PP977-982.

Swaan, R., D. Hawkins, A. Westwell-Proper, and W. Johnstone, 1988. *The Potential for Automated Mapping from Geocoded Digital Image Data*. Photogrammetric Engineering and Remote Sensing, Vol. 54, No. 2, pp. 187-193.

Swain, P. H., H. J. Siegel, and B. W. Smith, 1980. *Cotextual Classification of Multispectral Remote Sensing Data Using a Multiprocessor System*. IEEE Transactions on Geoscience and Remote Sensing. Vol. 18, No. 2, pp. 197-203.

Taib, A. K., and J. C. Trinder, 1992. *An Object-Oriented Approach to the Design of Knowledge-Bases and Geographic Information Systems*. Proceedings of Twentieth Australian Conference on Urban and Regional Information Systems, Gold Coast, Qld, pp. 149-156.

Tavakoli, M., and R. Bajcsy, 1976. *Computer Recognition of Roads from Satellite Pictures*. IEEE Transactions on Geoscience and Remote Sensing, Vol. 6, No. 9, pp. 623-636.

Thirlwall, S. L., C. Galipeau, S. D. Melvin, and H. D. Moore, 1988. *Comprehensive Evaluation of High Resolution Satellite Imagery for Map Revision and Change Detection*. Surveys and Mapping Branch, Energy, Mines and Resources and Supply and Services Canada. Contract No. 23232-6-1326/SQ, Ottawa, Canada by Gregory Geoscience Ltd., Ottawa, Ontario, pp. 1-70.

Toll, D. L., and J. A. Kennard, 1984. *Investigation of SPOT Spectral and Spatial Characteristics for Discriminating Land Use and Cover in Prince George's Country, Maryland*. SPOT Simulation Application Handbook. American Society of Photogrammetry, Falls Church, Virginia, pp. 165-170.

Toll, D. L., 1985. *Landsat-4 Thematic Mapper Scene Characteristics of a Suburban and Rural Area*. Photogrammetric Engineering and Remote Sensing. Vol. 51, No. 9, pp. 1471-1482.

Ton, J., 1989. *A Knowledge-Based Approach to Landsat Image Interpretation*. Ph.D Dissertation, Department of Computer Science, Michigan State University, pp. 15-46.

Ton, J., J. Sticken, and A. Jain, 1991. *Knowledge-Based Segmentation of Landsat Images*. IEEE Transactions on Geoscience and Remote Sensing, Vol. 29, No. 2, pp. 222-232.

Torlegard, K., 1992. *Sensors for Photogrammetric Mapping: Review and Prospects*. ISPRS Journal of Photogrammetry and Remote Sensing, Vol. 47, pp. 241-262.

Townsend, F. E., 1981. *Feature Extraction and Planimetric Mapping by Computer Processing of Digital Stereopair*, Ph.D Thesis, University of Wisconsin, Ann Arbor, Michigan, USA.

Treitz, P. M., P. Howarth, and P. Gong, 1992. *Applications of Satellite and GIS Technologies for Land-Cover and Land-Use Mapping at the Rural-Urban Fringe: A Case Study*. Photogrammetric Engineering and Remote Sensing, Vol. 58, No. 4, pp. 439-448.

Tsai, V. J. D., 1993. *Delaunay Triangulations in TIN Creation: an Overview and a Linear-Time Algorithm*. International Journal of Geographic Information Systems, Vol. 7, No. 6, pp. 501-524.

Tudor, G. S., and L. J. Sugarbaker, 1993. *GIS Orthographic Digitising of Aerial Photographs by Terrain Modelling*. Photogrammetric Engineering and Remote Sensing, Vol. 59, No. 4, pp. 499-503.

Turner, D., 1994. *Detection of Sea Ice in Antarctic AVHRR Imagery with an Artificial Neural Network*. Honours Thesis, Institute of Antarctic and Southern Ocean Studies, University of Tasmania, Australia.

Usery, E. L., and R. Welch, 1989. *A Raster Approach to Topographic Map Revision*. Photogrammetric Engineering and Remote Sensing, Vol. 55, No. 1, pp. 55-59.

Ungar, S. G., C. J. Merry, R. Irish, H. L. McKim, and M. S. Miller, 1988. *Extraction of Topography from Side-Looking Satellite System - A Case Study with SPOT Simulation Data*. Remote Sensing of Environment, Vol. 26, pp. 26-51.

Van Cleynebregel, J., F. Fierens, P. Suetens, and A. Oosterlinck, 1990. *Delineating Road Structures on Satellite Imagery by a GIS-Guided Technique*. Photogrammetric Engineering and Remote Sensing, Vol. 56, No. 6, pp. 893-898.

Vanderberug, G. J., and A. Rozefeld, 1978. *Linear Feature Mapping*. IEEE Transactions on Systems, Man, and Cybernetic, Vol. 8, No. 10, pp. 768-774.

Van Der Heijen, F., 1995. *Edge and Line Feature Extraction Based on Covariance Models*. IEEE Transactions on Pattern Analysis and Machine Intelligence, Vol. 17, No. 1, pp. 16-33.

Van Gool, L., P. Dewaele, and A. Oosterlinck, 1985. *Texture Analysis*. Computer Vision, Graphics, and Image Processing, Vol. 29, pp. 336-357.

Van Heist, M., W. Van Wijnggarden, and H. Huizing, 1988. *Monitoring Tunisia's Steppes with SPOT*. ITC Journal, Vol. 3, pp. 232-237.

Van Wie, P., and M. Stein, 1977. *A Landsat Digital Image Rectification System*. IEEE Transactions on Geoscience and Electronics, Vol. 15, No. 3, pp. 130-137.

Vanzuella, L., and S. Cabay, 1988. *Hybrid Spatial Data Structures*. GIS/LIS'88 Proceedings Accessing the World. San Antonio, Vol. 1, pp. 360-372.

Van Zuylen, L., 1980. *Map Revision*. ITC Journal, Vol. 1, pp. 130-139.

Veregin, H., 1994. *Integration of Simulation Modelling and Error Propagation for the Buffer Operation in GIS*. Photogrammetric Engineering and Remote Sensing, Vol. 60, No. 4, PP. 427-435.

Veregin, H., 1996. *Error Propagation through the Buffer Operation for Probability Surfaces*. Photogrammetric Engineering and Remote Sensing, Vol. 62, No. 4, pp. 419-428.

Walker, P. A., and D. M. Moore, 1988. *SIMPLE: An Inductive Modelling and Mapping Tool for Spatially-Oriented Data*. International Journal of Geographical Information Systems, Vol. 2, No. 4, pp. 347-363.

Walker, P. A., and L. Belbin, 1990. *The Identification of Spatial Associations and their Incorporation in Geographic Information Systems*. Proceedings of the 4th International Symposium Spatial Data Handling, Vol. 1, Zurich, Switzerland, pp. 522-530.

Walker, P. A., 1990. *Modelling Wildlife Distributions Using a Geographic Information System: Kangaroos in Relation to Climate*. Journal of Biogeography, Vol. 17, pp. 279-289.

Walker, P. A., 1991. *Habitat: A Procedure for Modelling a Disjoint Environmental Envelope for Plant and Animal Species*. Global Ecology and Biogeography Letters, Vol. 1, pp. 108-118.

Walsh, S. J., J. W. Cooper, I. E. Van Essen, and K. R. Gakkager, 1990. *Practical Paper: Image Enhancement of Landsat Thematic Mapper Data and GIS Data Interpretation for Evaluation of Resource Characteristics*. Photogrammetric Engineering and Remote Sensing. Vol. 65, No. 8, pp. 1135-1141.

Wang, F., and R. Newkirk, 1987. *Design and Implementation of a Knowledge Based System for Remotely Sensed Change Detection*. Journal of Imaging Technology, Vol. 13, No. 4, pp. 116-122.

Wang, F., and R. Newkirk, 1988. *A Knowledge-Based System for Highway Network Extraction*. IEEE Transactions on Geoscience and Remote Sensing, Vol. 26, No. 5, pp. 525-531.

Wang, L., and D. C. He, 1990. *A New Statistical Approach for Texture Analysis*. Photogrammetric Engineering and Remote Sensing, Vol. 56, No. 1, pp. 61-66.

Wang .G., P. M. Treitz, and P. J. Howarth, 1992. *Road Network Detection from SPOT Imagery for Updating Geographical Information Systems in the Rural-Urban Fringe*. International Journal of Geographical Information Systems, Vol. 6 ,No. 2, PP . 141-157.

Wang, J., and W. Liu, 1994. *Road Extraction from Multispectral Satellite Imagery*. Canadian Journal of Remote Sensing, Vol. 20, No. 2, pp. 180-191.

Wehenkel, L., and M. Pavella, 1991. *Decision Tree and Transient Stability of Electric Power Systems*. Automatica, Vol. 27, No. 1, pp. 115-134.

Welch, R., 1982. *Spatial Resolution Requirements for Urban Studies*. International Journal of Remote Sensing, Vol. 3, No. 3, pp. 139-146.

Welch, R., and E. L. Usery, 1984. *Cartographic Accuracy of Landsat-4 MSS and TM Image Data*. IEEE Transactions on Geoscience and Remote Sensing, Vol. GE-22, No. 3, pp. 281-288.

Welch, R., 1985. *Cartographic Potential of SPOT Image Data*. Photogrammetric Engineering and Remote Sensing, Vol. 51, No. 8, pp. 1085-1091.

Wilkinson, G. G., and J. Megier, 1990. *Evidential Reasoning in a Pixel Classification Hierarchy - a Potential Method for Integrating Image Classifiers and Expert System Rules Based on Geographic Context*. International Journal of Remote Sensing, Vol. 11, No. 10, pp. 1963-1968.

Williams, G. J., 1987. *Some Experiments in Decision Tree Induction*. The Australian Computer Journal, Vol. 19, No. 2, pp. 84-91.

Wolf, P. R., 1988. *Elements of Photogrammetry (With Air Photo Interpretation and Remote Sensing): Second Edition*. McGraw-Hill Kogakusha, Ltd. PP. 100-350.

Wolfer, J., J. Roberge, and T. Grace, 1994. *Robust Multispectral Road Classification in Landsat Thematic Mapper Imagery*. Proceedings of the World Congress on Neural Networks, San Diego, CA, 1994, pp. I-260-I-268.

Yee, B., 1987. *An Expert System for Planimetric Feature Extraction*. Proceedings IEEE International Geoscience and Remote Sensing, Vol. 1, Ann Arbor, Michigan, USA, pp. 321-325.

Zelek, J. S., 1990. *Computer-Aided Linear Planimetric Feature Extraction*. IEEE Transactions on Geoscience and Remote Sensing, Vol. 28, No. 4, pp. 567-572.

Zhizhuo, W., 1990. *Principles of Photogrammetry (With Remote Sensing)*. Press of Wuhan Technical University of Surveying and Mapping, Publishing House of Surveying and Mapping, Beijing, China. PP. 462-484.

Zhu, M. L., and P. S. Yeh, 1986. *Automatic Road Detection on Aerial Photographs*. Proceedings of IEEE 1986 Computer Vision and Pattern Recognition, Miami Beach, Florida, June 22-26, IEEE Computer Society Press, pp. 34-40.

Zhou, Q., 1991. *A Method for Integrating Remote Sensing and Geographic Information Systems*. Photogrammetric Engineering and Remote Sensing, Vol. 55, No. 5, pp. 591-596.

Zhou, X. J., and T. S. Dillon, 1991. *A Statistical-Heuristic Feature Selection Criterion for Decision Tree Induction*. IEEE Transactions on Pattern Analysis and Machine Intelligence, Vol. 13, No. 8, pp. 834-841.

Zlotnick, A., and P. D. Carnine Jr, 1993. *Finding Road Seeds in Aerial Images*. CVGIP: Image Understanding, Vol. 57, No. 2, pp. 243-260.

APPENDIX

APPENDIX A

APPENDIX A: Data Sets Information

a) Air Photo Prints	1) 1:42,000 B and W, Film No. 7176, Negative No. 62, Date: 2/12/1991
	2) 1:42,000 B and W, Film No. 906, Negative No. 188, Date: 10/2/1982
	3) 1:12,500 Colour, Film No. 1234, Negative No. 101, Date: 11/3/95
	4) 1:22,500 Colour, Film No. 934, Negative No. 183, Date: 11/1/84
b) Flat Hardcopy	1) Blackmans Bay 1:25,000
	2) Tarroona 1:25,000
c) Digital Data (Contours, Roads, Streams)	1) 5223 Blackmans Bay 1:25,000
	2) 5224 Tarroona 1:25,000

Table 1 Data sets information

APPENDIX B

Appendix B: MATLAB Code for Plotting the Components of Relief Displacement.

```
% Ali Forghani, September 1996
% This is the relief.m
% This program plots the components of relief displacement.

%*****

% Opening data file
dir1='/gis/students/alif/relief/';
fid1=fopen([dir1 'relief.txt'],'r');
data=fscanf(fid1,"%f",[inf,5]);
[m,n]=size(data);
for i=1:m
j=data(i,1);
k=data(i,2);
dX(j,k)=data(i,4);
dY(j,k)=data(i,5);
end;
hold on;
quiver(dX,dY);
hold off;

%*****
```

Table 1 Shows the components of relief displacement for 1982 imagery.

X	Y	r(cm)	H(M)	h(M)	d(cm)	d(mm)	(M) ground	d(pixels)	dX (pixels)	dY(pixels)	Extra Points
11.00	1	5.523	6858	15	0.012	0.121	5.073	2.537	2.526	0.230	
11	2	5.590	6858	1	0.001	0.008	0.342	0.171	0.168	0.031	
11	3	5.701	6858	2	0.002	0.017	0.698	0.349	0.337	0.092	
11	4	5.852	6858	10	0.009	0.085	3.584	1.792	1.684	0.612	
11	5	6.042	6858	80	0.070	0.705	29.600	14.800	13.473	6.124	
11	6	6.265	6858	90	0.082	0.822	34.531	17.266	15.157	8.268	
10	1	5.025	6858	55	0.040	0.403	16.926	8.463	8.421	0.842	
10	2	5.099	6858	10	0.007	0.074	3.123	1.561	1.531	0.306	
10	3	5.220	6858	3	0.002	0.023	0.959	0.480	0.459	0.138	
10	4	5.385	6858	3.5	0.003	0.027	1.154	0.577	0.536	0.214	
10	5	5.590	6858	30	0.024	0.245	10.271	5.135	4.593	2.297	
10	6	5.831	6858	60	0.051	0.510	21.426	10.713	9.186	5.512	
9	1	4.528	6858	120	0.079	0.792	33.274	16.637	16.535	1.837	
9	2	4.610	6858	60	0.040	0.403	16.939	8.469	8.268	1.837	
9	3	4.743	6858	30	0.021	0.207	8.715	4.357	4.134	1.378	
9	4	4.924	6858	5	0.004	0.036	1.508	0.754	0.689	0.306	
9	5	5.148	6858	20	0.015	0.150	6.305	3.153	2.756	1.531	
9	6	5.408	6858	12	0.009	0.095	3.975	1.987	1.654	1.102	
8	1	4.031	6858	128	0.075	0.752	31.600	15.800	15.678	1.960	
8	2	4.123	6858	50	0.030	0.301	12.625	6.313	6.124	1.531	
8	3	4.272	6858	40	0.025	0.249	10.465	5.233	4.899	1.837	
8	4	4.472	6858	10	0.007	0.065	2.739	1.369	1.225	0.612	
8	5	4.717	6858	24	0.017	0.165	6.933	3.467	2.940	1.837	
8	6	5.000	6858	40	0.029	0.292	12.248	6.124	4.899	3.675	
7	1	3.536	6858	95	0.049	0.490	20.570	10.285	10.182	1.455	
7	2	3.640	6858	70	0.037	0.372	15.605	7.802	7.502	2.143	
7	3	3.808	6858	50	0.028	0.278	11.660	5.830	5.359	2.297	
7	4	4.031	6858	15	0.009	0.088	3.703	1.852	1.608	0.919	
7	5	4.301	6858	20	0.013	0.125	5.268	2.634	2.143	1.531	
7	6	4.610	6858	45	0.030	0.302	12.704	6.352	4.823	4.134	
6	1	3.041	6858	90	0.040	0.399	16.764	8.382	8.268	1.378	
6	2	3.162	6858	80	0.037	0.369	15.493	7.747	7.349	2.450	
6	3	3.354	6858	50	0.024	0.245	10.271	5.135	4.593	2.297	
6	4	3.606	6858	15	0.008	0.079	3.312	1.656	1.378	0.919	
6	5	3.905	6858	45	0.026	0.256	10.762	5.381	4.134	3.445	
6	6	4.243	6858	50	0.031	0.309	12.991	6.496	4.593	4.593	
5	1	2.550	6858	80	0.030	0.297	12.491	6.246	6.124	1.225	
5	2	2.693	6858	75	0.029	0.294	12.368	6.184	5.741	2.297	
5	3	2.915	6858	65	0.028	0.276	11.606	5.803	4.976	2.986	
5	4	3.202	6858	40	0.019	0.187	7.843	3.921	3.062	2.450	
5	5	3.536	6858	57	0.029	0.294	12.342	6.171	4.364	4.364	
6	6	4.243	6858	64	0.040	0.396	16.629	8.315	5.879	5.879	
4	1	2.062	6858	65	0.020	0.195	8.207	4.103	3.981	0.995	
4	2	2.236	6858	70	0.023	0.228	9.586	4.793	4.287	2.143	

4	3	2.500	6858	65	0.024	0.237	9.952	4.976	3.981	2.986	
4	4	2.828	6858	63	0.026	0.260	10.913	5.456	3.858	3.858	
4	5	3.202	6858	56	0.026	0.261	10.980	5.490	3.430	4.287	
4	6	3.606	6858	60	0.032	0.315	13.249	6.624	3.675	5.512	
3	1	1.581	6858	70	0.016	0.161	6.778	3.389	3.215	1.072	
3	2	1.803	6858	55	0.014	0.145	6.072	3.036	2.526	1.684	
3	3	2.121	6858	60	0.019	0.186	7.795	3.897	2.756	2.756	
3	4	2.500	6858	55	0.020	0.200	8.421	4.210	2.526	3.368	
3	5	2.915	6858	70	0.030	0.298	12.499	6.249	3.215	5.359	
3	6	3.354	6858	45	0.022	0.220	9.244	4.622	2.067	4.134	
2	1	1.118	6858	80	0.013	0.130	5.478	2.739	2.450	1.225	
2	2	1.414	6858	57	0.012	0.118	4.937	2.468	1.745	1.745	
2	3	1.803	6858	55	0.014	0.145	6.072	3.036	1.684	2.526	
2	4	2.236	6858	95	0.031	0.310	13.009	6.505	2.909	5.818	
2	5	2.693	6858	102	0.040	0.400	16.820	8.410	3.123	7.808	
2	6	3.162	6858	30	0.014	0.138	5.810	2.905	0.919	2.756	
1	1	0.707	6858	110	0.011	0.113	4.764	2.382	1.684	1.684	
1	2	1.118	6858	70	0.011	0.114	4.793	2.396	1.072	2.143	
1	3	1.581	6858	60	0.014	0.138	5.810	2.905	0.919	2.756	
1	4	2.062	6858	110	0.033	0.331	13.888	6.944	1.684	6.737	
1	5	2.550	6858	90	0.033	0.335	14.052	7.026	1.378	6.890	
1	6	3.041	6858	25	0.011	0.111	4.657	2.328	0.383	2.297	
Extra Points											
9.5	1.4	4.801	6858	130	0.091	0.910	38.226	19.113	18.909	2.787	A
0.7	0.85	0.551	6858	120	0.010	0.096	4.046	2.023	1.286	1.562	B
10.2	7.3	6.272	6858	125	0.114	1.143	48.011	24.005	19.521	13.971	C

APPENDIX C

Appendix C: MATLAB Code for Building Data for a Knowledge-Based System, Using Edge Enhancement Operators, Edge Detection Filters and Morphological Operations Methods.

% Interactive Linear Feature Detection Algorithm (ILFDA)

% Ali Forghani, December 1996

%A Program for semi-automatic linear feature detection (field boundaries, rivers, roads) using different
% edge detectors, in which the process is followed by morphological operation. The ILFDA is a Unix
% based program that performs the concept of interactive linear feature delineation. By specifying
% different edge enhancement, noise removing filters, edge detectors, thresholds, filters, morphological
% tools the operator can gain different results. This program is connected to four sub programs
% (edge_det.m, canny2d.m, fcanny2d.m, bmpwrit2.m). The program was written in MATLAB code at
% the Department of Surveying & Spatial Information Science, University
% of Tasmania, Australia.

%*****

%This is the ilfda.m

```
clear
clc
clf
bbb = 1;
filename = input(' INPUT YOUR BITMAP IMAGE FILE (.BMP): ','s');
[x1,map] = bmpread(filename);
imagesc(x1); colormap gray
imzoom on
NOTE=input(['You should first go to option 5, and then to the other options!'],'s');
while bbb == 1
    clc
    disp(' 1. Noise filtering')
    disp(' 2. Edge detection or using a M-file')
    disp(' 3. Morphological operations')
    disp(' 4. Saving the result in bmp format')
    disp(' 5. Stretching ')
    disp(' 0. quit')
    option = input('Choice');
    if option == 5
        answer = 1;
        while answer == 1
            clf
            x = ind2gray(x1,map);
            a1 = input('Lower graylevel');
            b1 = input('Upper graylevel');
            x = imadjust(x,[a1 b1],[[]]);
            x = gray2ind(x,256);
            imagesc(x); colormap gray(256)
            answer = input('Do you want to change the graylevel ?[1/0] ');
        end;
    elseif option == 1
        clc
```



```

disp(' 1. Wiener')
disp(' 2. Median')
option1 = input(' Which filter do you want ?');
if option1 == 1
    clf
    x = wiener2(x);
    imshow(x,map), xlabel('Wiener noise removing filter')
    bbb = 1;
elseif option1 == 2
    clf
    x = medfilt2(x);
    imshow(x,map), xlabel('Median smoothing filter')
    bbb = 1;
end;
elseif option == 2
    clc
    disp(' 1. Sobel')
    disp(' 2. Marr-Hildreth')
    disp(' 3. M-file With Many Edge Detector Options')
    disp(' 4. 2D Canny')
    disp(' 5. 2D Canny Edge with an Approximation of Canny's Filter')
% Option for edge detection algorithms
    option2 = input(' Which edge detector do you want ?');
    if option2 == 1,
        clf
        [bw,tol] = edge(x,'sobel');
        fprintf('the tolerance is set to : %2.3f,tol);
        imshow(bw), xlabel('Sobel edge detection filter'),
        title('threshold level');
% Option for the level of thresholding
        tolerance = input('CHANGE THE TOLERANCE ?', 's');
        if tolerance == 'y'
            while tolerance == 'y'
                ans2 = input(' NEW TOLERANCE ?');
                [bw,tol]=edge(x,ans2,'sobel');
                imshow(bw);
                tolerance = input ('CHANGE TOLERANCE ? yes/no','s');
            end;
        elseif tolerance == 'n'
            end;
    elseif option2 == 2
        clf
        [bw,tol] = edge(x,'marr');
        fprintf('the tolerance is set to : %2.3f,tol);
        imshow(bw); xlabel('Marr edge detection filter'),title('threshold level');
% Option for the level of thresholding
        tolerance = input('CHANGE THE TOLERANCE ?', 's');
        if tolerance == 'y'
            while tolerance == 'y'
                ans2 = input(' NEW TOLERANCE ?');
                [bw,tol]=edge(x,ans2,'marr');
                imshow(bw), xlabel('Marr edge detection filter'), title('threshold level');
                tolerance = input ('CHANGE TOLERANCE ?','s');
            end;
        elseif tolerance == 'n'
            end;
    elseif option2 == 3

```

```

% Option for a M-file of Edge Detection
clf
EdgeDetector=input(['HAVE YOU SELECTED YOUR EDGE DETECTOR FORM MODE ? ','s']);
% if yes (an edge detector has already been selected in the M-file) please continue, otherwise you should go
% back the M-file to select your desired edge detector by editing of the M-file. In the edge_det.m file, there
% are five options or modes that the user can put for the mode. These modes are Sobel edge detector,
% Differential operator 4 masks, Nagao & differential 3 points, and the Deriche's operator
% (alpha = 2, alpha = 1, alpha = 0.5).
    Edgeoutput = edge_det(x,'de1');
    imagesc(Edgeoutput);colormap gray
    mini=min(Edgeoutput(:)); maxi=max(Edgeoutput(:));
threshold = input(['INPUT THE THRESHOLD TO GET A BINARY IMAGE ', mini, '->', maxi, ': ']);
    imagesc(Edgeoutput); colormap gray; colorbar
% We should have an image with 0 and 1(binary image). So the image must be thresholded.
    bw = Edgeoutput > threshold;
    imshow(bw),
elseif option2 == 4
    N = input('INPUT THE FILTER SIZE IN PIXELS (7,9, 11, 13 etc): ');
    Edgeoutput = canny2d(x, N);
    imagesc(Edgeoutput);colormap gray;colorbar
    mini=num2str(min(Edgeoutput(:))); maxi=num2str(max(Edgeoutput(:)));
threshold = input(['INPUT THE THRESHOLD TO GET A BINARY IMAGE ', mini, '->', maxi, ': ']);
    bw = Edgeoutput > threshold;
    imshow(bw), xlabel(' 2D Canny Edge Detector')
elseif option2 == 5
    N = input('INPUT THE FILTER SIZE IN PIXELS (7,9 or 13): ');
    Edgeoutput = fcanny2d(x, N);
    imagesc(Edgeoutput);colormap gray;colorbar
    mini=num2str(min(Edgeoutput(:)));
    maxi=num2str(max(Edgeoutput(:)));
threshold = input(['INPUT THE THRESHOLD TO GET A BINARY IMAGE ', mini, '->', maxi, ': ']);
    bw = Edgeoutput > threshold;
    imshow(bw), xlabel(' An Approximation of the 2D Canny Edge Detector')
end;
% if option2
elseif option == 3
% Option for types of hit and miss operations
% If the user wishes to put some explanation or titles on the graphic, he/she has % to edit the graphic line eg
% imshow(bw), xlabel(' 2D Canny Edge Detector'),
% ylabel('Morphological Operation'), or imshow(bw), xlabel('2D Deriche Operator % If Alpha = 0.5'),
% ylabel('Morphological Operation').
clf, clc
    opt = 1;
    while opt == 1
    disp(' 1/close 2/bridge 3/fill 4/skeleton 5/dilation 6/erosion')
    option3 = input(' Which morphological operation do you want?');
    if option3 == 1
        num = input(' Closing Tolerance? ');
        bw = bwmorph(bw,'close',num);
        imshow(bw),
        opt = 1;
    elseif option3 == 2
        num = input(' Bridging Tolerance? ');
        bw = bwmorph(bw,'bridge',num);
        imshow(bw),
        opt = 1;
    elseif option3 == 3

```

```

    num = input(' Filling Tolerance? ');
    bw = bwmorph(bw,'fill',num);
    imshow(bw),
    opt = 1;
elseif option3 == 4
    num = input(' Skeleton Tolerance? ');
    bw = bwmorph(bw,'skel',num);
    imshow(bw),
    opt = 1;
elseif option3 == 5
    num = input(' Dilation Tolerance? ');
    bw = bwmorph(bw,'dilate',num);
    imshow(bw),
    opt = 1;
elseif option3 == 6
    num = input(' Erosion Tolerance? ');
    bw = bwmorph(bw,'erode',num);
    imshow(bw),
    opt = 1;
else opt = 0;
end;
bbb = 1;
end;
elseif option == 4
    outputfile = input('INPUT YOUR IMAGE OUTPUT FILE USING EXTENSION: ','s');
    bmpwrit2(~bw,map,outputfile)
elseif option == 0
    bbb = 0;
end;
end;
end;

%*****

% This is the edge_detect.m

% This M-file contains many edge detection operators including Sobel, Differential Operator 4 Masks,
% Nagao & Differential 3 points, and 2D Deriche with different filter sizes.
% (C) Parc, 1995 J. Devars & S. Guetari
% Updated by A. Forghani, May 1996
function ImGrd=edge_detect(ImSrc,Mode,Snul,Lc);
% IG=edge_detect(IS,MODE,S0,LC) ==> Create an edge image IG from a source image IS,
% images are gray level image coded on 8 bits (0...255).
% - if threshold S0 is specified then the pixels of IG < S0 are equal to
% - if LC is specified and non zero, IG is the image of transition of lines
% - MODE='sob' : Sobel's operator
%   'd4m' : differential operator 4 masks
%   'ngd' : Nagao & differential 3 points
%   'de2' : Deriche's operator alpha=2
%   'de1' :      alpha=1
%   'de0' :      alpha=.5
ImDst=[]; Smin=0; Cret=0;
if nargin < 2,    error('Problem with the number of arguments'),
elseif ~isstr(Mode),  error('Problem with the argument mode format'),
else,
    Mode=lower(Mode);
    Sob=all(Mode == 'sob');

```

```

D4m=all(Mode == 'd4m');
Ngd=all(Mode == 'ngd');
De2=all(Mode == 'de2');
De1=all(Mode == 'de1');
De0=all(Mode == 'de0');
if ~(Sob|D4m|Ngd|De2|De1|De0), error('Pb codage mode'),
elseif nargin >= 3,
    Smin=Snul;
    if nargin == 4, Cret=(Lc ~= 0); end
end;
end;
[Ny,Nx]=size(ImSrc);
if Sob, % Operateur de Sobel, norme euclidienne
MskH=[-1 0 1;-2 0 2;-1 0 1]/4;
IgH=conv2(ImSrc,MskH,'same');
MskV=[1 2 1;0 0 0;-1 -2 -1]/4;
IgV=conv2(ImSrc,MskV,'same');
Grd=sqrt(IgV.*IgV+IgH.*IgH);
Grd([1 Ny],:)=zeros(2,Nx);
Grd(:,[1 Nx])=zeros(Ny,2);
elseif D4m, % Operateur differentiel 4 masques
Msk0=[1 2 1;0 0 0;-1 -2 -1]/4;
Grd=abs(conv2(ImSrc,Msk0,'same'));
Msk1=[0 1 2;-1 0 1;-2 -1 0]/4;
Grd=max(Grd,abs(conv2(ImSrc,Msk1,'same')));
Msk2=[-1 0 1;-2 0 2;-1 0 1]/4;
Grd=max(Grd,abs(conv2(ImSrc,Msk2,'same')));
Msk3=[-2 -1 0;-1 0 1;0 1 2]/4;
Grd=max(Grd,abs(conv2(ImSrc,Msk3,'same')));
Grd([1 Ny],:)=zeros(2,Nx);
Grd(:,[1 Nx])=zeros(Ny,2);
elseif Ngd, % Nagao puis differentiel 3 points
Msk=[1 1 1;1 1 1;1 1 1]/9;
Ia=conv2(ImSrc,Msk,'same');
Ib=conv2(ImSrc.*ImSrc,Msk,'same')-Ia.*Ia;
for Y=2:Ny-3
    V3yV=Ib(Y:Y+2,:); V3yV=V3yV(:);
    V3yM=Ia(Y:Y+2,:); V3yM=V3yM(:); Xlin=4;
    for X=3:Nx-2
        [Vmin,Pos]=min(V3yV(Xlin:Xlin+8));
        ImSrc(Y+1,X)=round(V3yM(Xlin-1+Pos));
        Xlin=Xlin+3;
    end;
end;
Ia=abs(conv2(ImSrc,[-1 1],'same'));
Ib=abs(conv2(ImSrc,[1;-1],'same'));
Grd=max(max(Ia,Ib),.75*(Ia+Ib));
Grd([1 2 Ny-1 Ny],:)=zeros(4,Nx);
Grd(:,[1 2 Nx-1 Nx])=zeros(Ny,4);
elseif (De2|De1|De0), % Operateur de Deriche alpha = 2, 1 ou .5
if De2,
    F=[-0.0074;-0.0411;-0.2027;-0.7488; 0; 0.7488; 0.2027; 0.0411; 0.0074];
    H=[ 0.0085; 0.0451; 0.2000; 0.4926; 0.2000; 0.0451; 0.0085];
elseif De1,
    F=[-0.0070;-0.0162;-0.0368;-0.0800;-0.1630;-0.2955;-0.4016; 0;...
        0.4016; 0.2955; 0.1630; 0.0800; 0.0368; 0.0162; 0.0070];
    H=[ 0.0044; 0.0102; 0.0230; 0.0500; 0.1020; 0.1848; 0.2512;...

```

```

    0.1848; 0.1020; 0.0500; 0.0230; 0.0102; 0.0044];
else
F=[-0.0033;-0.0050;-0.0076;-0.0115;-0.0173;-0.0257;-0.0376;...
-0.0543;-0.0767;-0.1054;-0.1390;-0.1719;-0.1889;-0.1557; 0;...
0.1557; 0.1889; 0.1719; 0.1390; 0.1054; 0.0767; 0.0543;...
0.0376; 0.0257; 0.0173; 0.0115; 0.0076; 0.0050; 0.0033];
H=[ 0.0014; 0.0022; 0.0033; 0.0051; 0.0077; 0.0115; 0.0171;...
0.0250; 0.0361; 0.0510; 0.0701; 0.0924; 0.1143; 0.1256;...
0.1143; 0.0924; 0.0701; 0.0510; 0.0361; 0.0250; 0.0171;...
0.0115; 0.0077; 0.0051; 0.0033; 0.0022; 0.0014];
end;
ILcol=ImSrc; ILcol=reshape(conv2(ILcol(:),H,'same'),Ny,Nx);
ILlgn=ImSrc; ILlgn=reshape(conv2(ILlgn(:),H,'same'),Nx,Ny);
ILcol=ILcol'; ILcol=reshape(conv2(ILcol(:),F,'same'),Nx,Ny);
ILcol=abs(ILcol');
ILlgn=ILlgn'; ILlgn=reshape(conv2(ILlgn(:),F,'same'),Ny,Nx);
ILlgn=abs(ILlgn);
Grd=max(max(ILcol,ILlgn),.75*(ILcol+ILlgn));
Grd([1 2 3 4 Ny-3 Ny-2 Ny-1 Ny],:)=zeros(8,Nx);
Grd(:,[1 2 3 4 Nx-3 Nx-2 Nx-1 Nx])=zeros(Ny,8);
end;
% Image of gradient with pixels < Smin put to 0
if Smin > 0,
Nuls=find(Grd < Smin); Grd(Nuls)=zeros(size(Nuls));
end;
if ~Cret, ImGrd=round(Grd);
% Determination of edges in 4 connectivity.
else,
Grd=reshape(Grd',Nx*Ny,1);
ImGrd=zeros(Nx*Ny,1);
V4=[1 Nx -1 -Nx];
Sequence=[Nx+2:Nx*(Ny-1)-1]; % Sequential Tests
for Indx=Sequence, % of profil ^ or /=
Pix=Grd(Indx);
if Pix,
Sgn=sign(Grd(V4+Indx)-Pix)+1;
Profil=Sgn(1:2)+4*Sgn(3:4);
if any(Profil <= 1), ImGrd(Indx)=Pix; end
end;
end;
ImGrd=(reshape(round(ImGrd),Nx,Ny));
end;

%*****

% This is the Canny2D.m

function [out, H] = canny2D(in,N)
% Computes Canny's edge detector
% in is the edge input
% N=7,9,11, 13, etc..
% N is the filter size
% H is the filter coefficients
N = 1/floor(N/2);%N is the step
x = [-1:N:0]';
a1 = 0.1486768717;
a2 = -0.2087553476;

```

```

a3 = -1.244653939;
a4 = -0.7912446531;
alpha = 2.0522;
w = 1.56939;
lambda1=-2;
sx=sin(w*x); cx=cos(w*x);
h = exp(-alpha*x) .* (a1*sx + a2*cx);
h = h + exp(alpha*x) .* (a3*sx + a4*cx);
h = h - lambda1/2;
l=length(h);
H = [h ;-flipud(h(2:l-1));h(1)]/max(h);
out = max(abs(filter2(H,in)),abs(filter2(H',in)));
out = floor(255*out/max(out(:)));

```

%*****

% This is the fcanny2d.m

```

function out=fcanny2d(in,N)
% Performs an approximation of the Canny's filter
% N = 7, 9 or 13 pixels
% N is the size of the filter transfer function
if nargin <2,
    N = 7;
end;
if N==7
H =[0,0.5814,1.0000,0,-1.0000,-0.5814,0]';
elseif N==9
H =[0,0.2292,0.9070,0.7276,0,-0.7276, -0.9070,-0.2292,0]';
elseif N==13
H =[0,0.2292,0.5814,0.9070,1.0000,0.7276,0,-0.7276, ...
-1.0000,-0.9070,-0.5814,-0.2292,0]';
end;
out = filter2(H,in);
out = (abs(out) + abs(filter2(H',in)))/2;
out = floor(255*out/max(out(:)));

```

%*****

% This is the bmpwrite.m

```

function bmpwrite(X,map, filename);
% BMPWRITE Write a BMP (Microsoft Windows Bitmap) file to disk.
% BMPWRITE(X,MAP,'filename') writes a BMP file containing the
% indexed image X and colormap MAP to a disk file called 'filename'.
% If no file extension is given with the filename, the extension
% '.bmp' is assumed.
% See also: BMPREAD, GIFWRITE, HDFWRITE, PCXWRITE, TIFFWRITE,
% XWDWRITE.
% Mounil Patel 7/20/93
% Copyright (c) 1993 by The MathWorks, Inc.
% Updated 12/22/94, Jean Devars
if (nargin~=3)
    error('Requires three arguments.');
```

```

end;
if (isstr(filename)~=1)
    error('Requires a string filename as the third argument.');
```

```

end;
if (isempty(findstr(filename, '.'))==1)
    filename=[filename, '.bmp'];
end;
fid=fopen(filename, 'wb', 'l');
if (fid==-1)
    error(['Error opening ', filename, ' for output.']);
end;
% Header 54 bytes + Colormap 4*256 bytes = 1078 bytes
fwrite(fid, ['B'; 'M'], 'char');
[biHeight, biWidth]=size(X);
bfSize=biHeight*(biWidth+rem(biWidth,4))+1078;
fwrite(fid, bfSize, 'long');
bfReserved1=0;
fwrite(fid, bfReserved1, 'short');
bfReserved2=0;
fwrite(fid, bfReserved2, 'short');
bfOffBits=1078;
fwrite(fid, bfOffBits, 'long');
biSize=40;
fwrite(fid, biSize, 'long');
fwrite(fid, biWidth, 'long');
fwrite(fid, biHeight, 'long');
biPlanes=1;
fwrite(fid, biPlanes, 'short');
biBitCount=8;
fwrite(fid, biBitCount, 'short');
% Unused values : all zeros
biCompression=0;
fwrite(fid, biCompression, 'long');
biSizeImage=0;
fwrite(fid, biSizeImage, 'long');
biXPels=0;
fwrite(fid, biXPels, 'long');
biYPels=0;
fwrite(fid, biYPels, 'long');
biClrUsed=0;
fwrite(fid, biClrUsed, 'long');
biClrImportant=0;
fwrite(fid, biClrImportant, 'long');
[m, n]=size(map);
if (m>256)
    error('Colormap exceeds 256 colors!');
elseif (m~=256)
    map=[map; zeros(256-m, 3)];
end;
map=[fliplr(map*255), zeros(256, 1)'];
fwrite(fid, map(:), 'uchar');
X=(X-1);
if (rem(biWidth, 4)~=0)
    X=[X, zeros(biHeight, rem(biWidth, 4))];
end;
X=rot90(X, 3);
fwrite(fid, X(:), 'uchar');
fclose(fid);

```

%*****


```
% Ali Forghani, Februray 1997
```

```
% This is the accuracy.m
```

```
% This code computes the overall classification accuracy, omission errors, and commission errors for the  
output of edge detectors and morphological operations (Chapter 6), and supervised classification (Chapter  
9).
```

```
load I;
```

```
% I is the output data in ASCII format.
```

```
load roads;
```

```
% roads are the reference road map in ASCII format.
```

```
load roads;
```

```
[m,n]=size(roads);
```

```
number_correct_road=0;
```

```
number_correct_non_road=0;
```

```
for i=1:m
```

```
for j=1:n
```

```
if roads(i,j)==1 % if sample's pixel is in road % roads is the reference map
```

```
if I(i,j)==1 % if results'pixel is in road % I is edge detection
```

```
number_correct_road=number_correct_road+1;
```

```
end;
```

```
else
```

```
if I(i,j)==0 %if results'pixel is in non-road
```

```
number_correct_non_road=number_correct_non_road+1;
```

```
end;
```

```
end;
```

```
end;
```

```
end;
```

```
number_total_pixel=m*n;
```

```
acc_road=number_correct_road/number_total_pixel;
```

```
Omission_error_road=1-acc_road;
```

```
Commission_error_road=1-number_correct_non_road/number_total_pixel;
```

```
disp(Omission_error_road);
```

```
disp(Commission_error_road);
```

```
disp(acc_road);
```

```
%*****
```

APPENDIX D

Appendix D: FORTRAN 77 Code for Generating a Tabular ASCII File from the ARC/INFO Grid ASCII Files.

c.....Ali Forghani, March 1997

- c A FORTRAN 77 routine was written to preprocess the ARC/INFO grid ASCII files in order to
- c generate a tabular ASCII file to be interfaced with a decision tree software (KnowledgeSEEKER).
- c To use this routine:
- c Firstly, an ASCII file called eg names has to be created. It contains the names of variables .
- c Secondly, the number of variables (data files), and the number of rows and columns has to be
- c specified in the code by editing the program, eg parameter(nfiles=7,nrows=180,ncols=162). It
- c should be noted that the variables (grid ASCII files) must not contain headings or other texts.
- c Thirdly, the program must be compiled and then the compiled file can be used to generate a tabular
- c ASCII data file by using columns>data command at the UNIX prompt.

* *****

```
program columns
  parameter(nfiles=7,nrows=180,ncols=162)
  real*4 x(nfiles,nrows,ncols)
  character*8 datafile(nfiles)

  open(5,file='names',status='unknown')
  do 100 i = 1,nfiles
    read(5,1000) datafile(i)
1000 format(A8)
100 continue

  do 10 i = 1,nfiles
    open(5,file=datafile(i),status='unknown')
    do 20 j = 1,nrows
      read(5,*) (x(i,j,k),k=1,ncols)
20    continue
    close(5)
10  continue
  do 30 j = 1,nrows
    do 40 k = 1,ncols
      write(*,*) (x(i,j,k), i=1,nfiles)
40  continue
30  continue
end
```

APPENDIX E

Appendix E: MATLAB Code for Development of a Decision Tree Processing Expert System (DTPES) to Map Out the Spatial Distribution of Roads and their Background from the GIS Database.

% Ali Forghani, May 1997

% Decision Tree Processing Expert System (DTPES).

% DTPES is a Knowledge_Based system that performs image classification using multi-source data.

% This program is composed of three sub-routines namely ks2mat.m, matrules.m, and dtpes.m.

% The ks2mat.m code automatically converts generic rules into specified MATLAB rules. The

% generic rules were generated from a classification tree which was built in knowledge-based

% software (KnowledgeSEEKER algorithm).

% The matrules.m stores the MATLAB formatted rules for the dtpes.m.

% The dtpes.m calls the multi-source data and evaluates all rules for a given pixel with a forward

% chaining process. After execution of rules against the datasets, the output of the DTPES is plotted as

% an image, and the overall classification accuracy based on the reference data is computed and

% printed.

% The DTPES is a Unix based program that was written in MATLAB code at the Department of

% Surveying & Spatial Information Science, and the CODES Centre, University of Tasmania,

% Australia.

DTPES=input(['This program is a Decision Tree Processing Expert System (DTPES) that predicts the roads probability (presence of roads) from remote sensing imagery and a GIS dataset via using generated rules by a decision tree algorithm (KnowledgeSEEKER) for the purpose of image classification in context of feature detection, please hit return'],'s');

clear

clc

clf

% loading the datasets for execution of rules.

load roads

load edge

load photo82

load streams

load fieldb

load landuse

load dem

% The matrules function located the rules to be called by the dtpes.m.

roads_probability=matrules(roads,edge,photo82,streams,fieldb,landuse,dem);

% plotting the image

I = roads_probability;

map = gray(100);

I = ind2gray(roads_probability, map);

J = histeq(I,256);

subplot(2,2,1), imshow(I, 100), title('Original');

```

subplot(2,2,2), imshow(J,100), title('Equalized');
subplot(2,2,3), imhist(I,100), title('Original');
subplot(2,2,4), imhist(J,100), title('Equalized');
% estimating of the overall accuracy
[m,n]=size(roads);
sigma=0;sweight=0;
for i=1:m
    for j=1:n
        if roads(i,j)==-9999
            road=0;weight=0.5;
        else
            road=100;weight=1.0;
        end;
        uncertainty=abs(roads_probability(i,j)-road)/100;
        probability=(1-uncertainty)*weight;
        sigma =sigma+probability;
        sweight=sweight+weight;
    end;
end;
probability=sigma/sweight;
disp(probability);
% saving the image in a file
outputfile = input('INPUT YOUR IMAGE OUTPUT FILE USING EXTENSION: ','s');
bmpwrite(roads_probability,map,'outputfile');

%*****

% This is the ks2mat.m.

% The ks2mat.m program converts a text file which contains KnowledgeSEEKER generic rules into
% MATLAB rules for the DTPES program. The MATLAB rules are printed in a file called matrules.m.

% Opening result file
dir1='/gis/students/alif/s2/s2old/';
fid1=fopen([dir1 '99rules.txt'],'r');
fid2 = fopen([dir1 'matrules.m'], 'w');
fprintf(fid2,'%s\n','function roads_probability=matrules(roads,edge,photo82,streams,fieldb,landuse,dem)');
fprintf(fid2,'%s\n','[m,n]=size(roads);');
fprintf(fid2,'%s\n','for i=1:m');
fprintf(fid2,'%s\n','for j=1:n');
fprintf(fid2,'%s\n','roads_probability(i,j)=0;');
escape=0;str1(1)='a';
while 1==1
    %Passing empty lines
    while str1(1)~='R'
        str1=fgets(fid1);
        if str1==''
            escape=1;
            break;
        end;
    end;
    if escape==1
        break;
    end;
    % writing to the result file
    i=1;

```

```

while str1(i)~= 'T'
    i=i+1;
end;
fprintf(fid2,'%s\n',['%' str1(1:i-1)]);
% Getting next line
str1=fgets(fid1);
fprintf(fid2,'%s','if ');
count=0;
while str1(1)~= 'T'
    % Passing blank characters
    i=1;
    while str1(i)==blanks(1)
        i=i+1;
    end;
    % Getting name of variable 1
    j=i;
    while str1(j)~='='
        j=j+1;
    end;
    name1=str1(i+1:j-2);
    ss=size(str1);
    % Finding the kind of rule
    k=j+1;case=1;
    while k<=ss(2)
        if (str1(k)==' ')(str1(k)=='(')
            case=2;break;
        end;
        if str1(k-1:k)=='or'
            case=3;break;
        end;
        k=k+1;
    end;
    count=count+1;
    if count~=1
        fprintf(fid2,'%s','&');
    end;
    if case==2
        % Getting values
        while (str1(j)~='[')&(str1(j)~='(')
            j=j+1;
        end;
        if str1(j)=='['
            marker1='>=';
        else
            marker1='>';
        end;
        i=j+1;
        while str1(i)~='='
            i=i+1;
        end;
        value1=str1(j+1:i-1);
        j=i+1;
        while (str1(j)~=')')&(str1(j)~=']')
            j=j+1;
        end;
        if str1(j)==']'
            marker2='<=';

```

```

else
    marker2='<';
end;
value2=str1(i+1:j-1);
% writing to the result file
fprintf(fid2,'%s\n',['(' name1 '(i,j)' marker1 value1 ')&(' name1 ...
    '(i,j)' marker2 value2 ') ...']);
end; % case 2
if case==1
    % Getting value
    value=str2num(str1(j+1:ss(2)-1));
    % Writing to result file
    fprintf(fid2,'%s\n',['(' name1 '(i,j)=' num2str(value) ') ...']);
end; % case 1
if case==3
    k1=j+1;k2=j;i=0;
    % Getting value
    while (str1(k1)~= 'r')
        if (str1(k1)==' ')|(str1(k1)=='o')
            i=i+1;
            value3(i)=str2num(str1(k2+1:k1-1));
            k2=k1;
        end;
        k1=k1+1;
    end;
    i=i+1;
    value3(i)=str2num(str1(k1+1:ss(2)));
    % writing to the result file
    for k1=1:i
        fprintf(fid2,'%s',['(' name1 '(i,j)=' num2str(value3(k1)) ')']);
        if k1==i
            fprintf(fid2,'%s\n','...');
        else
            fprintf(fid2,'%s',' ');
        end;
    end;
end; % case3
% Getting next line
str1=fgets(fid1);
end; % while
i=1;
str1=fgets(fid1);str2=fgets(fid1);
str3=fgets(fid1);
while str3(1)~='R'
    i=i+1;
    str3=fgets(fid1);
    if str3==''
        break;
    end;
end;
if i==2
    str2=str1;
end;
str1=str3;
k=i-1;
i=1;
% Passing blank characters

```

```

while str2(i)==blanks(1)
    i=i+1;
end;
% Getting name of variable 1
j=i;
while str2(j)~=' '
    j=j+1;
end;
name1=str2(i+1:j-2);
% Getting value1
i=j+3;
while str2(i)~=blanks(1)
    i=i+1;
end;
value1=str2num(str2(j+1:i));
ss=size(str2);
value2=str2num(str2(i:ss(2)-2));
if k==1
    if value1==-9999.00
        value=0;
    elseif value1==1
        value=100;
    end;
else
    value=value2;
end;
fprintf(fid2,'%s\n',[ name1 '_probability(i,j)=' name1 '_probability(i,j)+' num2str(value) ']);
fprintf(fid2,'%s\n','end;');
end; % While
fprintf(fid2,'%s\n','end;');
fprintf(fid2,'%s\n','end;');
fclose(fid1);
fclose(fid2);

%*****

% This is the matrules.m

% The matrules.m contains the rules to be executed against the database.
function roads_probability=matrules(roads,edge,photo82,streams,fieldb,landuse,dem)
[m,n]=size(roads);
for i=1:m
    for j=1:n
        roads_probability(i,j)=0;
        %RULE_1
        if (photo82(i,j)>=12)&(photo82(i,j)<20) ...
            &(edge(i,j)==1) ...
            roads_probability(i,j)=roads_probability(i,j)+20.3;
        end;
        %RULE_2
        if (photo82(i,j)>=12)&(photo82(i,j)<20) ...
            &(edge(i,j)==-9999) ...
            roads_probability(i,j)=roads_probability(i,j)+0.3;
        end;
        %RULE_3
        if (photo82(i,j)>=20)&(photo82(i,j)<22) ...
            &(edge(i,j)==1) ...

```



```

&(dem(i,j)>=1)&(dem(i,j)<91) ...
roads_probability(i,j)=roads_probability(i,j)+4.3;
end;
%RULE_4
if (photo82(i,j)>=20)&(photo82(i,j)<22) ...
&(edge(i,j)==1) ...
&(dem(i,j)>=91)&(dem(i,j)<110) ...
roads_probability(i,j)=roads_probability(i,j)+75;
end;
%RULE_5
if (photo82(i,j)>=20)&(photo82(i,j)<22) ...
&(edge(i,j)==1) ...
&(dem(i,j)>=110)&(dem(i,j)<=139) ...
roads_probability(i,j)=roads_probability(i,j)+1.3;
end;
%RULE_6
if (photo82(i,j)>=20)&(photo82(i,j)<22) ...
&(edge(i,j)==-9999) ...
roads_probability(i,j)=roads_probability(i,j)+0.6;
end;
%RULE_7
if (photo82(i,j)>=22)&(photo82(i,j)<24) ...
&(dem(i,j)>=1)&(dem(i,j)<91) ...
roads_probability(i,j)=roads_probability(i,j)+0;
end;
%RULE_8
if (photo82(i,j)>=22)&(photo82(i,j)<24) ...
&(dem(i,j)>=91)&(dem(i,j)<115) ...
roads_probability(i,j)=roads_probability(i,j)+2.6;
end;
%RULE_9
if (photo82(i,j)>=22)&(photo82(i,j)<24) ...
&(dem(i,j)>=115)&(dem(i,j)<119) ...
roads_probability(i,j)=roads_probability(i,j)+0.9;
end;
%RULE_10
if (photo82(i,j)>=22)&(photo82(i,j)<24) ...
&(dem(i,j)>=119)&(dem(i,j)<122) ...
roads_probability(i,j)=roads_probability(i,j)+3.3;
end;
%RULE_11
if (photo82(i,j)>=22)&(photo82(i,j)<24) ...
&(dem(i,j)>=122)&(dem(i,j)<128) ...
&(edge(i,j)==1) ...
roads_probability(i,j)=roads_probability(i,j)+14.3;
end;
%RULE_12
if (photo82(i,j)>=22)&(photo82(i,j)<24) ...
&(dem(i,j)>=122)&(dem(i,j)<128) ...
&(edge(i,j)==-9999) ...
roads_probability(i,j)=roads_probability(i,j)+0.7;
end;
%RULE_13
if (photo82(i,j)>=22)&(photo82(i,j)<24) ...
&(dem(i,j)>=128)&(dem(i,j)<131) ...
roads_probability(i,j)=roads_probability(i,j)+5.5;
end;

```

```

%RULE_14
if (photo82(i,j)>=22)&(photo82(i,j)<24) ...
&(dem(i,j)>=131)&(dem(i,j)<=139) ...
roads_probability(i,j)=roads_probability(i,j)+0;
end;
%RULE_15
if (photo82(i,j)>=24)&(photo82(i,j)<26) ...
&(edge(i,j)==1) ...
roads_probability(i,j)=roads_probability(i,j)+11.4;
end;
%RULE_16
if (photo82(i,j)>=24)&(photo82(i,j)<26) ...
&(edge(i,j)==-9999) ...
&(dem(i,j)>=1)&(dem(i,j)<110) ...
&(landuse(i,j)==7)|(landuse(i,j)==9)|(landuse(i,j)==11)|(landuse(i,j)==1)...
roads_probability(i,j)=roads_probability(i,j)+25;
end;
%RULE_17
if (photo82(i,j)>=24)&(photo82(i,j)<26) ...
&(edge(i,j)==-9999) ...
&(dem(i,j)>=1)&(dem(i,j)<110) ...
&(landuse(i,j)==8) ...
roads_probability(i,j)=roads_probability(i,j)+0.4;
end;
%RULE_18
if (photo82(i,j)>=24)&(photo82(i,j)<26) ...
&(edge(i,j)==-9999) ...
&(dem(i,j)>=110)&(dem(i,j)<115) ...
roads_probability(i,j)=roads_probability(i,j)+3;
end;
%RULE_19
if (photo82(i,j)>=24)&(photo82(i,j)<26) ...
&(edge(i,j)==-9999) ...
&(dem(i,j)>=115)&(dem(i,j)<119) ...
roads_probability(i,j)=roads_probability(i,j)+0.3;
end;
%RULE_20
if (photo82(i,j)>=24)&(photo82(i,j)<26) ...
&(edge(i,j)==-9999) ...
&(dem(i,j)>=119)&(dem(i,j)<122) ...
roads_probability(i,j)=roads_probability(i,j)+7.1;
end;
%RULE_21
if (photo82(i,j)>=24)&(photo82(i,j)<26) ...
&(edge(i,j)==-9999) ...
&(dem(i,j)>=122)&(dem(i,j)<128) ...
roads_probability(i,j)=roads_probability(i,j)+2.2;
end;
%RULE_22
if (photo82(i,j)>=24)&(photo82(i,j)<26) ...
&(edge(i,j)==-9999) ...
&(dem(i,j)>=128)&(dem(i,j)<131) ...
roads_probability(i,j)=roads_probability(i,j)+6.5;
end;
%RULE_23
if (photo82(i,j)>=24)&(photo82(i,j)<26) ...
&(edge(i,j)==-9999) ...

```

```

&(dem(i,j)>=131)&(dem(i,j)<=139) ...
roads_probability(i,j)=roads_probability(i,j)+0;
end;
%RULE_24
if (photo82(i,j)>=26)&(photo82(i,j)<29) ...
&(edge(i,j)==1) ...
&(dem(i,j)>=1)&(dem(i,j)<131) ...
roads_probability(i,j)=roads_probability(i,j)+10.2;
end;
%RULE_25
if (photo82(i,j)>=26)&(photo82(i,j)<29) ...
&(edge(i,j)==1) ...
&(dem(i,j)>=131)&(dem(i,j)<=139) ...
roads_probability(i,j)=roads_probability(i,j)+100;
end;
%RULE_26
if (photo82(i,j)>=26)&(photo82(i,j)<29) ...
&(edge(i,j)==-9999) ...
&(dem(i,j)>=1)&(dem(i,j)<110) ...
roads_probability(i,j)=roads_probability(i,j)+0.4;
end;
%RULE_27
if (photo82(i,j)>=26)&(photo82(i,j)<29) ...
&(edge(i,j)==-9999) ...
&(dem(i,j)>=110)&(dem(i,j)<115) ...
roads_probability(i,j)=roads_probability(i,j)+3.8;
end;
%RULE_28
if (photo82(i,j)>=26)&(photo82(i,j)<29) ...
&(edge(i,j)==-9999) ...
&(dem(i,j)>=115)&(dem(i,j)<119) ...
roads_probability(i,j)=roads_probability(i,j)+1.4;
end;
%RULE_29
if (photo82(i,j)>=26)&(photo82(i,j)<29) ...
&(edge(i,j)==-9999) ...
&(dem(i,j)>=119)&(dem(i,j)<122) ...
roads_probability(i,j)=roads_probability(i,j)+6.2;
end;
%RULE_30
if (photo82(i,j)>=26)&(photo82(i,j)<29) ...
&(edge(i,j)==-9999) ...
&(dem(i,j)>=122)&(dem(i,j)<131) ...
roads_probability(i,j)=roads_probability(i,j)+2.7;
end;
%RULE_31
if (photo82(i,j)>=26)&(photo82(i,j)<29) ...
&(edge(i,j)==-9999) ...
&(dem(i,j)>=131)&(dem(i,j)<=139) ...
roads_probability(i,j)=roads_probability(i,j)+0;
end;
%RULE_32
if (photo82(i,j)>=29)&(photo82(i,j)<33) ...
&(edge(i,j)==1) ...
roads_probability(i,j)=roads_probability(i,j)+9.6;
end;
%RULE_33

```

```

if (photo82(i,j)>=29)&(photo82(i,j)<33) ...
&(edge(i,j)=-9999) ...
&(dem(i,j)>=1)&(dem(i,j)<115) ...
&(landuse(i,j)=7)|(landuse(i,j)=1)|(landuse(i,j)=11)...
roads_probability(i,j)=roads_probability(i,j)+9.7;
end;
%RULE_34
if (photo82(i,j)>=29)&(photo82(i,j)<33) ...
&(edge(i,j)=-9999) ...
&(dem(i,j)>=1)&(dem(i,j)<115) ...
&(landuse(i,j)=8)|(landuse(i,j)=9)...
roads_probability(i,j)=roads_probability(i,j)+0.8;
end;
%RULE_35
if (photo82(i,j)>=29)&(photo82(i,j)<33) ...
&(edge(i,j)=-9999) ...
&(dem(i,j)>=115)&(dem(i,j)<119) ...
roads_probability(i,j)=roads_probability(i,j)+8.1;
end;
%RULE_36
if (photo82(i,j)>=29)&(photo82(i,j)<33) ...
&(edge(i,j)=-9999) ...
&(dem(i,j)>=119)&(dem(i,j)<125) ...
roads_probability(i,j)=roads_probability(i,j)+5.6;
end;
%RULE_37
if (photo82(i,j)>=29)&(photo82(i,j)<33) ...
&(edge(i,j)=-9999) ...
&(dem(i,j)>=125)&(dem(i,j)<=139) ...
roads_probability(i,j)=roads_probability(i,j)+1.1;
end;
%RULE_38
if (photo82(i,j)>=33)&(photo82(i,j)<38) ...
&(edge(i,j)=1) ...
roads_probability(i,j)=roads_probability(i,j)+10.9;
end;
%RULE_39
if (photo82(i,j)>=33)&(photo82(i,j)<38) ...
&(edge(i,j)=-9999) ...
&(dem(i,j)>=1)&(dem(i,j)<128) ...
roads_probability(i,j)=roads_probability(i,j)+7.7;
end;
%RULE_40
if (photo82(i,j)>=33)&(photo82(i,j)<38) ...
&(edge(i,j)=-9999) ...
&(dem(i,j)>=128)&(dem(i,j)<=139) ...
roads_probability(i,j)=roads_probability(i,j)+2.4;
end;
%RULE_41
if (photo82(i,j)>=38)&(photo82(i,j)<51) ...
&(landuse(i,j)=8)|(landuse(i,j)=7)...
&(edge(i,j)=1) ...
roads_probability(i,j)=roads_probability(i,j)+17.5;
end;
%RULE_42
if (photo82(i,j)>=38)&(photo82(i,j)<51) ...
&(landuse(i,j)=8)|(landuse(i,j)=7)...

```

```

&(edge(i,j)=-9999) ...
&(dem(i,j)>=1)&(dem(i,j)<91) ...
roads_probability(i,j)=roads_probability(i,j)+5;
end;
%RULE_43
if (photo82(i,j)>=38)&(photo82(i,j)<51) ...
&(landuse(i,j)==8)|(landuse(i,j)==7)...
&(edge(i,j)=-9999) ...
&(dem(i,j)>=91)&(dem(i,j)<115) ...
roads_probability(i,j)=roads_probability(i,j)+11.7;
end;
%RULE_44
if (photo82(i,j)>=38)&(photo82(i,j)<51) ...
&(landuse(i,j)==8)|(landuse(i,j)==7)...
&(edge(i,j)=-9999) ...
&(dem(i,j)>=115)&(dem(i,j)<122) ...
roads_probability(i,j)=roads_probability(i,j)+17.4;
end;
%RULE_45
if (photo82(i,j)>=38)&(photo82(i,j)<51) ...
&(landuse(i,j)==8)|(landuse(i,j)==7)...
&(edge(i,j)=-9999) ...
&(dem(i,j)>=122)&(dem(i,j)<131) ...
roads_probability(i,j)=roads_probability(i,j)+9.3;
end;
%RULE_46
if (photo82(i,j)>=38)&(photo82(i,j)<51) ...
&(landuse(i,j)==8)|(landuse(i,j)==7)...
&(edge(i,j)=-9999) ...
&(dem(i,j)>=131)&(dem(i,j)<=139) ...
roads_probability(i,j)=roads_probability(i,j)+4.7;
end;
%RULE_47
if (photo82(i,j)>=38)&(photo82(i,j)<51) ...
&(landuse(i,j)==9)|(landuse(i,j)==11)|(landuse(i,j)==1)...
roads_probability(i,j)=roads_probability(i,j)+0;
end;
%RULE_48
if (photo82(i,j)>=51)&(photo82(i,j)<102) ...
&(landuse(i,j)==8) ...
&(dem(i,j)>=1)&(dem(i,j)<110) ...
roads_probability(i,j)=roads_probability(i,j)+53.4;
end;
%RULE_49
if (photo82(i,j)>=51)&(photo82(i,j)<102) ...
&(landuse(i,j)==8) ...
&(dem(i,j)>=110)&(dem(i,j)<115) ...
&(edge(i,j)==1) ...
roads_probability(i,j)=roads_probability(i,j)+52.6;
end;
%RULE_50
if (photo82(i,j)>=51)&(photo82(i,j)<102) ...
&(landuse(i,j)==8) ...
&(dem(i,j)>=110)&(dem(i,j)<115) ...
&(edge(i,j)=-9999) ...
roads_probability(i,j)=roads_probability(i,j)+22.2;
end;

```

```

%RULE_51
if (photo82(i,j)>=51)&(photo82(i,j)<102) ...
&(landuse(i,j)==8) ...
&(dem(i,j)>=115)&(dem(i,j)<119) ...
roads_probability(i,j)=roads_probability(i,j)+31.5;
end;
%RULE_52
if (photo82(i,j)>=51)&(photo82(i,j)<102) ...
&(landuse(i,j)==8) ...
&(dem(i,j)>=119)&(dem(i,j)<128) ...
roads_probability(i,j)=roads_probability(i,j)+25.4;
end;
%RULE_53
if (photo82(i,j)>=51)&(photo82(i,j)<102) ...
&(landuse(i,j)==8) ...
&(dem(i,j)>=128)&(dem(i,j)<131) ...
&(edge(i,j)==1) ...
roads_probability(i,j)=roads_probability(i,j)+45.8;
end;
%RULE_54
if (photo82(i,j)>=51)&(photo82(i,j)<102) ...
&(landuse(i,j)==8) ...
&(dem(i,j)>=128)&(dem(i,j)<131) ...
&(edge(i,j)==-9999) ...
roads_probability(i,j)=roads_probability(i,j)+18.8;
end;
%RULE_55
if (photo82(i,j)>=51)&(photo82(i,j)<102) ...
&(landuse(i,j)==8) ...
&(dem(i,j)>=131)&(dem(i,j)<=139) ...
&(edge(i,j)==1) ...
roads_probability(i,j)=roads_probability(i,j)+48.6;
end;
%RULE_56
if (photo82(i,j)>=51)&(photo82(i,j)<102) ...
&(landuse(i,j)==8) ...
&(dem(i,j)>=131)&(dem(i,j)<=139) ...
&(edge(i,j)==-9999) ...
roads_probability(i,j)=roads_probability(i,j)+13.9;
end;
%RULE_57
if (photo82(i,j)>=51)&(photo82(i,j)<102) ...
&(landuse(i,j)==1) ...
roads_probability(i,j)=roads_probability(i,j)+33.3;
end;
%RULE_58
if (photo82(i,j)>=51)&(photo82(i,j)<102) ...
&(landuse(i,j)==7) ...
roads_probability(i,j)=roads_probability(i,j)+28;
end;
%RULE_59
if (photo82(i,j)>=51)&(photo82(i,j)<102) ...
&(landuse(i,j)==11) ...
roads_probability(i,j)=roads_probability(i,j)+18.8;
end;
%RULE_60
if (photo82(i,j)>=51)&(photo82(i,j)<102) ...

```

```

&(landuse(i,j)==9) ...
roads_probability(i,j)=roads_probability(i,j)+0.5;
end;
%RULE_61
if (photo82(i,j)>=102)&(photo82(i,j)<=157) ...
&(landuse(i,j)==1)&(landuse(i,j)==11)...
roads_probability(i,j)=roads_probability(i,j)+100;
end;
%RULE_62
if (photo82(i,j)>=102)&(photo82(i,j)<=157) ...
&(landuse(i,j)==8) ...
&(dem(i,j)>=1)&(dem(i,j)<115) ...
roads_probability(i,j)=roads_probability(i,j)+71.2;
end;
%RULE_63
if (photo82(i,j)>=102)&(photo82(i,j)<=157) ...
&(landuse(i,j)==8) ...
&(dem(i,j)>=115)&(dem(i,j)<125) ...
roads_probability(i,j)=roads_probability(i,j)+56.8;
end;
%RULE_64
if (photo82(i,j)>=102)&(photo82(i,j)<=157) ...
&(landuse(i,j)==8) ...
&(dem(i,j)>=125)&(dem(i,j)<=139) ...
roads_probability(i,j)=roads_probability(i,j)+95.5;
end;
%RULE_65
if (photo82(i,j)>=102)&(photo82(i,j)<=157) ...
&(landuse(i,j)==7) ...
&(dem(i,j)>=1)&(dem(i,j)<128) ...
roads_probability(i,j)=roads_probability(i,j)+19.5;
end;
%RULE_66
if (photo82(i,j)>=102)&(photo82(i,j)<=157) ...
&(landuse(i,j)==7) ...
&(dem(i,j)>=128)&(dem(i,j)<=139) ...
roads_probability(i,j)=roads_probability(i,j)+68.5;
end;
%RULE_67
if (photo82(i,j)>=102)&(photo82(i,j)<=157) ...
&(landuse(i,j)==9) ...
roads_probability(i,j)=roads_probability(i,j)+0;
end;
end;
end;

```

```

%*****

```


APPENDIC F

Appendix F: Cross-Tabulation of the Classification Trees

Cross-Tabulation shows the generated decision trees as a table. It allows the user to view the contents of the nodes of a decision tree (Case 1) in as follows:

***** SPLIT TABLE *****

photo82 split below root node.

Independent Var: photo82
Variable Type: Continuous
Cluster Type: Monotonic
Missing Values: OFF
Nulls Included: ON
Cluster signif: 0.050000

Clusters:

- 1) [12,20)
- 2) [20,22)
- 3) [22,24)
- 4) [24,26)
- 5) [26,29)
- 6) [29,33)
- 7) [33,38)
- 8) [38,51)
- 9) [51,102)
- 10) [102,157]

Cross Tabulation +----- photo82 -----+										
	1	2	3	4	5	6	7	8	9	10
roads	[12,20)	[20,22)	[22,24)	[24,26)	[26,29)	[29,33)	[33,38)	[38,51)	[51,102)	[102,157]
-9999.00	3246	3134	2926	2934	3678	3438	2760	2561	2108	339
12.0	11.6	10.8	10.8	13.6	12.7	10.2	9.4	7.8	1.2	92.5
99.4	99.2	97.8	96.7	96.8	96.0	92.4	86.5	71.2	58.5	
1.00000	21	25	66	100	123	145	226	399	853	240
1.0	1.1	3.0	4.5	5.6	6.6	10.3	18.2	38.8	10.9	7.5
0.6	0.8	2.2	3.3	3.2	4.0	7.6	13.5	28.8	41.5	
Total	3267	3159	2992	3034	3801	3583	2986	2960	2961	579
	11.1	10.8	10.2	10.3	13.0	12.2	10.2	10.1	10.1	2.0

CHI: 3839.99 (df = 9)
P: 0.000000

***** SPLIT TABLE *****

edge split below photo82 - [12,20).

Independent Var: edge
Variable Type: Categorical
Cluster Type: Free

Missing Values: OFF
Nulls Included: ON
Cluster signif: 0.050000

Clusters:
1) 1.00000
2) -9999.00

Cross Tabulation +--- edge ----+				
	1	2	Row	
roads	1.00000	-9999.00	edge	Total

-9999.00	47	3199	3246	
	1.4	98.6	99.4	
	79.7	99.7		

1.00000	12	9	21	
	57.1	42.9	0.6	
	20.3	0.3		
=====				
Total	59	3208	3267	
	1.8	98.2	100.0	

CHI: 364.97 (df = 1)
P: 0.000000

***** SPLIT TABLE *****
Leaf edge - 1.00000 below photo82 - [12,20).

Independent Var: edge
Variable Type: Categorical
Cluster Type: Free
Missing Values: OFF
Nulls Included: ON
Cluster signif: 0.050000

Cross Tabulation		
	Row	
roads	edge	Total

-9999.00	47	
	79.7	

1.00000	12	
	20.3	

Total	59	
	100.0	

***** SPLIT TABLE *****
Leaf edge - -9999.00 below photo82 - [12,20).

Independent Var: edge
Variable Type: Categorical
Cluster Type: Free
Missing Values: OFF
Nulls Included: ON
Cluster signif: 0.050000

Cross Tabulation
Row
roads edge Total

-9999.00 3199
99.7

1.00000 9
0.3

Total 3208
100.0

***** SPLIT TABLE *****
edge split below photo82 - [20,22).

Independent Var: edge
Variable Type: Categorical
Cluster Type: Free
Missing Values: OFF
Nulls Included: ON
Cluster signif: 0.050000

Clusters:
1) 1.00000
2) -9999.00

Cross Tabulation +---- edge ----+
1 2 Row
roads 1.00000 -9999.00 edge Total

-9999.00 120 3014 3134
3.8 96.2 99.2
95.2 99.4

1.00000 6 19 25
24.0 76.0 0.8
4.8 0.6
=====

Total 126 3033 3159
4.0 96.0 100.0

CHI: 26.35 (df = 1)
P: 0.000015

***** SPLIT TABLE *****
dem split below edge - 1.00000.

Independent Var: dem
Variable Type: Continuous
Cluster Type: Monotonic
Missing Values: OFF
Nulls Included: ON
Cluster signif: 0.050000

Clusters:
1) [1,91)
2) [91,110)
3) [110,139]

Cross Tabulation +----- dem -----+

	1	2	3	Row	
roads	[1,91)	[91,110)	[110,139	dem	Total
-9999.00	45	1	74	120	
	37.5	0.8	61.7	95.2	
	95.7	25.0	98.7		
1.00000	2	3	1	6	
	33.3	50.0	16.7	4.8	
	4.3	75.0	1.3		
Total	47	4	75	126	
	37.3	3.2	59.5	100.0	

CHI: 45.48 (df = 2)
P: 0.000010

***** SPLIT TABLE *****
Leaf dem - [1,91) below edge - 1.00000.

Independent Var: dem
Variable Type: Continuous
Cluster Type: Monotonic
Missing Values: OFF
Nulls Included: ON
Cluster signif: 0.050000

Cross Tabulation

	Row	
roads	dem	Total
-9999.00	45	
	95.7	
1.00000	2	
	4.3	

Total 47
100.0

***** SPLIT TABLE *****

Leaf dem - [91,110) below edge - 1.00000.

Independent Var: dem
Variable Type: Continuous
Cluster Type: Monotonic
Missing Values: OFF
Nulls Included: ON
Cluster signif: 0.050000

Cross Tabulation

Row		
roads	dem	Total

-9999.00	1	
	25.0	

1.00000 3
75.0

Total 4
100.0

***** SPLIT TABLE *****

Leaf dem - [110,139] below edge - 1.00000.

Independent Var: dem
Variable Type: Continuous
Cluster Type: Monotonic
Missing Values: OFF
Nulls Included: ON
Cluster signif: 0.050000

Cross Tabulation

Row		
roads	dem	Total

-9999.00	74	
	98.7	

1.00000 1
1.3

Total 75
100.0

***** SPLIT TABLE *****

Leaf edge - -9999.00 below photo82 - [20,22).

Independent Var: edge
 Variable Type: Categorical
 Cluster Type: Free
 Missing Values: OFF
 Nulls Included: ON
 Cluster signif: 0.050000

Cross Tabulation

	Row	
roads	edge	Total
-9999.00	3014	
	99.4	
1.00000	19	
	0.6	
Total	3033	
	100.0	

***** SPLIT TABLE *****

dem split below photo82 - [22,24).

Independent Var: dem
 Variable Type: Continuous
 Cluster Type: Monotonic
 Missing Values: OFF
 Nulls Included: ON
 Cluster signif: 0.050000

Clusters:

- 1) [1,91)
- 2) [91,115)
- 3) [115,119)
- 4) [119,122)
- 5) [122,128)
- 6) [128,131)
- 7) [131,139]

Cross Tabulation	+----- dem -----+							
	1	2	3	4	5	6	7	Row
roads	[1,91)	[91,115)	[115,119)	[119,122)	[122,128)	[128,131)	[131,139]	dem Total
-9999.00	289	787	421	323	688	358	60	2926
	9.9	26.9	14.4	11.0	23.5	12.2	2.1	97.8
	100.0	97.4	99.1	96.7	98.7	94.5	100.0	
1.00000	0	21	4	11	9	21	0	66

	0.0	31.8	6.1	16.7	13.6	31.8	0.0	2.2
	0.0	2.6	0.9	3.3	1.3	5.5	0.0	
<hr/>								
Total	289	808	425	334	697	379	60	2992
	9.7	27.0	14.2	11.2	23.3	12.7	2.0	100.0

CHI: 35.68 (df = 6)
P: 0.000090

***** SPLIT TABLE *****
Leaf dem - [1,91) below photo82 - [22,24).

Independent Var: dem
Variable Type: Continuous
Cluster Type: Monotonic
Missing Values: OFF
Nulls Included: ON
Cluster signif: 0.050000

Cross Tabulation

	Row	
roads	dem	Total
<hr/>		
-9999.00	289	
	100.0	
1.00000	0	
	0.0	
Total	289	
	100.0	

***** SPLIT TABLE *****
Leaf dem - [91,115) below photo82 - [22,24).

Independent Var: dem
Variable Type: Continuous
Cluster Type: Monotonic
Missing Values: OFF
Nulls Included: ON
Cluster signif: 0.050000

Cross Tabulation

	Row	
roads	dem	Total
<hr/>		
-9999.00	787	
	97.4	
1.00000	21	
	2.6	

Total 808
100.0

***** SPLIT TABLE *****
Leaf dem - [115,119) below photo82 - [22,24).

Independent Var: dem
Variable Type: Continuous
Cluster Type: Monotonic
Missing Values: OFF
Nulls Included: ON
Cluster signif: 0.050000

Cross Tabulation

Row		
roads	dem	Total

-9999.00	421	
99.1		

1.00000 4
0.9

Total 425
100.0

***** SPLIT TABLE *****
Leaf dem - [119,122) below photo82 - [22,24).

Independent Var: dem
Variable Type: Continuous
Cluster Type: Monotonic
Missing Values: OFF
Nulls Included: ON
Cluster signif: 0.050000

Cross Tabulation

Row		
roads	dem	Total

-9999.00	323	
96.7		

1.00000 11
3.3

Total 334

100.0

***** SPLIT TABLE *****
edge split below dem - [122,128).

Independent Var: edge
Variable Type: Categorical
Cluster Type: Free
Missing Values: OFF
Nulls Included: ON
Cluster signif: 0.050000

Clusters:
1) 1.00000
2) -9999.00

Cross Tabulation +---- edge ----+

	1	2	Row	
roads	1.00000	-9999.00	edge	Total
-9999.00	24	664	688	
	3.5	96.5	98.7	
	85.7	99.3		
1.00000	4	5	9	
	44.4	55.6	1.3	
	14.3	0.7		
Total	28	669	697	
	4.0	96.0	100.0	

CHI: 38.65 (df = 1)
P: 0.000002

***** SPLIT TABLE *****
Leaf edge - 1.00000 below dem - [122,128).

Independent Var: edge
Variable Type: Categorical
Cluster Type: Free
Missing Values: OFF
Nulls Included: ON
Cluster signif: 0.050000

Cross Tabulation

	Row	
roads	edge	Total
-9999.00	24	
	85.7	
1.00000	4	
	14.3	

Total 28
100.0

***** SPLIT TABLE *****
Leaf edge - -9999.00 below dem - [122,128).

Independent Var: edge
Variable Type: Categorical
Cluster Type: Free
Missing Values: OFF
Nulls Included: ON
Cluster signif: 0.050000

Cross Tabulation

Row		
roads	edge	Total

-9999.00	664	
	99.3	

1.00000 5
0.7

Total 669
100.0

***** SPLIT TABLE *****
Leaf dem - [128,131) below photo82 - [22,24).

Independent Var: dem
Variable Type: Continuous
Cluster Type: Monotonic
Missing Values: OFF
Nulls Included: ON
Cluster signif: 0.050000

Cross Tabulation

Row		
roads	dem	Total

-9999.00	358	
	94.5	

1.00000 21
5.5

Total 379

100.0

***** SPLIT TABLE *****

Leaf dem - [131,139] below photo82 - [22,24).

Independent Var: dem
Variable Type: Continuous
Cluster Type: Monotonic
Missing Values: OFF
Nulls Included: ON
Cluster signif: 0.050000

Cross Tabulation

Row
roads dem Total

-9999.00 60
100.0

1.00000 0
0.0

Total 60
100.0

***** SPLIT TABLE *****

edge split below photo82 - [24,26).

Independent Var: edge
Variable Type: Categorical
Cluster Type: Free
Missing Values: OFF
Nulls Included: ON
Cluster signif: 0.050000

Clusters:

- 1) 1.00000
- 2) -9999.00

Cross Tabulation +--- edge ----+

1 2 Row
roads 1.00000 -9999.00 edge Total

-9999.00 195 2739 2934
6.6 93.4 96.7
88.6 97.3

1.00000 25 75 100
25.0 75.0 3.3
11.4 2.7
=====

Total 220 2814 3034
 7.3 92.7 100.0

CHI: 48.44 (df = 1)
P: 0.000000

***** SPLIT TABLE *****
Leaf edge - 1.00000 below photo82 - [24,26).

Independent Var: edge
Variable Type: Categorical
Cluster Type: Free
Missing Values: OFF
Nulls Included: ON
Cluster signif: 0.050000

Cross Tabulation

Row	
roads	edge Total

-9999.00	195
88.6	
1.00000	25
11.4	
Total	220
100.0	

***** SPLIT TABLE *****
dem split below edge - -9999.00.

Independent Var: dem
Variable Type: Continuous
Cluster Type: Monotonic
Missing Values: OFF
Nulls Included: ON
Cluster signif: 0.050000

- Clusters:
- 1) [1,110)
 - 2) [110,115)
 - 3) [115,119)
 - 4) [119,122)
 - 5) [122,128)
 - 6) [128,131)
 - 7) [131,139]

Cross Tabulation

+----- dem -----+							
1	2	3	4	5	6	7	Row
roads	[1,110)	[110,115	[115,119	[119,122	[122,128	[128,131	[131,139 dem Total

-9999.00	669	350	377	286	669	314	74	2739
	24.4	12.8	13.8	10.4	24.4	11.5	2.7	97.3
	99.4	97.0	99.7	92.9	97.8	93.5	100.0	

1.00000	4	11	1	22	15	22	0	75
	5.3	14.7	1.3	29.3	20.0	29.3	0.0	2.7
	0.6	3.0	0.3	7.1	2.2	6.5	0.0	

Total	673	361	378	308	684	336	74	2814
	23.9	12.8	13.4	10.9	24.3	11.9	2.6	100.0

CHI: 65.67 (df = 6)
P: 0.000000

***** SPLIT TABLE *****

landuse split below dem - [1,110).

Independent Var: landuse
Variable Type: Categorical
Cluster Type: Free
Missing Values: OFF
Nulls Included: ON
Cluster signif: 0.050000

Clusters:

- 1) 7.00000, 9.00000, 11.0000, 1.00000
- 2) 8.00000

Cross Tabulation +--- landuse ---+

	1	2	Row
roads	7.00000	8.00000	landuse Total

-9999.00	3	666	669
	0.4	99.6	99.4
	75.0	99.6	

1.00000	1	3	4
	25.0	75.0	0.6
	25.0	0.4	

Total	4	669	673
	0.6	99.4	100.0

CHI: 40.57 (df = 1)
P: 0.000004

***** SPLIT TABLE *****

Leaf landuse - 7.00000... below dem - [1,110).

Independent Var: landuse
Variable Type: Categorical
Cluster Type: Free
Missing Values: OFF
Nulls Included: ON
Cluster signif: 0.050000

Cross Tabulation

	Row	
roads	landuse	Total
-9999.00	3	
	75.0	
1.00000	1	
	25.0	
Total	4	
	100.0	

***** SPLIT TABLE *****

Leaf landuse - 8.00000 below dem - [1,110).

Independent Var: landuse
 Variable Type: Categorical
 Cluster Type: Free
 Missing Values: OFF
 Nulls Included: ON
 Cluster signif: 0.050000

Cross Tabulation

	Row	
roads	landuse	Total
-9999.00	666	
	99.6	
1.00000	3	
	0.4	
Total	669	
	100.0	

***** SPLIT TABLE *****

Leaf dem - [110,115) below edge - -9999.00.

Independent Var: dem
 Variable Type: Continuous
 Cluster Type: Monotonic
 Missing Values: OFF
 Nulls Included: ON
 Cluster signif: 0.050000

Cross Tabulation

	Row	
--	-----	--

roads	dem	Total
-9999.00	350	97.0

1.00000	11	3.0
---------	----	-----

Total	361	100.0
-------	-----	-------

***** SPLIT TABLE *****
 Leaf dem - [115,119) below edge - -9999.00.

Independent Var: dem
 Variable Type: Continuous
 Cluster Type: Monotonic
 Missing Values: OFF
 Nulls Included: ON
 Cluster signif: 0.050000

Cross Tabulation

roads	dem	Total
-9999.00	377	99.7
1.00000	1	0.3
Total	378	100.0

***** SPLIT TABLE *****
 Leaf dem - [119,122) below edge - -9999.00.

Independent Var: dem
 Variable Type: Continuous
 Cluster Type: Monotonic
 Missing Values: OFF
 Nulls Included: ON
 Cluster signif: 0.050000

Cross Tabulation

roads	dem	Total
-9999.00	286	

92.9

1.00000 22
7.1

Total 308
100.0

***** SPLIT TABLE *****

Leaf dem - [122,128) below edge - -9999.00.

Independent Var: dem
Variable Type: Continuous
Cluster Type: Monotonic
Missing Values: OFF
Nulls Included: ON
Cluster signif: 0.050000

Cross Tabulation

roads	dem	Total

-9999.00		669
		97.8

1.00000 15
2.2

Total 684
100.0

***** SPLIT TABLE *****

Leaf dem - [128,131) below edge - -9999.00.

Independent Var: dem
Variable Type: Continuous
Cluster Type: Monotonic
Missing Values: OFF
Nulls Included: ON
Cluster signif: 0.050000

Cross Tabulation

roads	dem	Total

-9999.00		314
		93.5

1.00000 22
6.5

Total 336
100.0

***** SPLIT TABLE *****
Leaf dem - [131,139] below edge - -9999.00.

Independent Var: dem
Variable Type: Continuous
Cluster Type: Monotonic
Missing Values: OFF
Nulls Included: ON
Cluster signif: 0.050000

Cross Tabulation
Row
roads dem Total

-9999.00 74
100.0

1.00000 0
0.0

Total 74
100.0

***** SPLIT TABLE *****
edge split below photo82 - [26,29).

Independent Var: edge
Variable Type: Categorical
Cluster Type: Free
Missing Values: OFF
Nulls Included: ON
Cluster signif: 0.050000

Clusters:
1) 1.00000
2) -9999.00

Cross Tabulation +--- edge -----+
1 2 Row
roads 1.00000 -9999.00 edge Total

-9999.00 326 3352 3678
8.9 91.1 96.8
89.1 97.6

```

-----
1.00000    40  83 123
          32.5 67.5 3.2
          10.9 2.4
-----
Total      366 3435 3801
          9.6 90.4 100.0

```

CHI: 76.55 (df = 1)
P: 0.000000

***** SPLIT TABLE *****
dem split below edge - 1.00000.

Independent Var: dem
Variable Type: Continuous
Cluster Type: Monotonic
Missing Values: OFF
Nulls Included: ON
Cluster signif: 0.050000

Clusters:
1) [1,131)
2) [131,139]

```

Cross Tabulation  +---- dem ----+
                   1  2  Row
roads  [1,131) [131,139 dem Total
-----
-9999.00    326  0  326
          100.0 0.0 89.1
          89.8 0.0
-----
1.00000     37  3  40
          92.5 7.5 10.9
          10.2 100.0
-----
Total      363  3  366
          99.2 0.8 100.0

```

CHI: 24.65 (df = 1)
P: 0.000790

***** SPLIT TABLE *****
Leaf dem - [1,131) below edge - 1.00000.

Independent Var: dem
Variable Type: Continuous
Cluster Type: Monotonic
Missing Values: OFF
Nulls Included: ON
Cluster signif: 0.050000

Cross Tabulation
Row

roads dem Total

-9999.00 326
 89.8

1.00000 37
 10.2

Total 363
 100.0

***** SPLIT TABLE *****

Leaf dem - [131,139] below edge - 1.00000.

Independent Var: dem
Variable Type: Continuous
Cluster Type: Monotonic
Missing Values: OFF
Nulls Included: ON
Cluster signif: 0.050000

Cross Tabulation

Row
roads dem Total

-9999.00 0
 0.0

1.00000 3
 100.0

Total 3
 100.0

***** SPLIT TABLE *****

dem split below edge - -9999.00.

Independent Var: dem
Variable Type: Continuous
Cluster Type: Monotonic
Missing Values: OFF
Nulls Included: ON
Cluster signif: 0.050000

Clusters:

- 1) [1,110)
- 2) [110,115)
- 3) [115,119)
- 4) [119,122)
- 5) [122,131)

6) [131,139]

Cross Tabulation +----- dem -----+

	1	2	3	4	5	6	Row
roads	[1,110)	[110,115	[115,119	[119,122	[122,131	[131,139	dem Total
-9999.00	760	329	430	320	1415	98	3352
	22.7	9.8	12.8	9.5	42.2	2.9	97.6
	99.6	96.2	98.6	93.8	97.3	100.0	
1.00000	3	13	6	21	40	0	83
	3.6	15.7	7.2	25.3	48.2	0.0	2.4
	0.4	3.8	1.4	6.2	2.7	0.0	
Total	763	342	436	341	1455	98	3435
	22.2	10.0	12.7	9.9	42.4	2.9	100.0

CHI: 41.39 (df = 5)
P: 0.000023

***** SPLIT TABLE *****
Leaf dem - [1,110) below edge - -9999.00.

Independent Var: dem
Variable Type: Continuous
Cluster Type: Monotonic
Missing Values: OFF
Nulls Included: ON
Cluster signif: 0.050000

Cross Tabulation

	Row
roads	dem Total
-9999.00	760
	99.6
1.00000	3
	0.4
Total	763
	100.0

***** SPLIT TABLE *****
Leaf dem - [110,115) below edge - -9999.00.

Independent Var: dem
Variable Type: Continuous
Cluster Type: Monotonic
Missing Values: OFF
Nulls Included: ON
Cluster signif: 0.050000

Cross Tabulation		
Row		
roads	dem	Total

-9999.00	329	
	96.2	
1.00000	13	
	3.8	
Total	342	
	100.0	

***** SPLIT TABLE *****

Leaf dem - [115,119) below edge - -9999.00.

Independent Var: dem
Variable Type: Continuous
Cluster Type: Monotonic
Missing Values: OFF
Nulls Included: ON
Cluster signif: 0.050000

Cross Tabulation		
Row		
roads	dem	Total

-9999.00	430	
	98.6	
1.00000	6	
	1.4	
Total	436	
	100.0	

***** SPLIT TABLE *****

Leaf dem - [119,122) below edge - -9999.00.

Independent Var: dem
Variable Type: Continuous
Cluster Type: Monotonic
Missing Values: OFF
Nulls Included: ON
Cluster signif: 0.050000

Cross Tabulation

	Row	
roads	dem	Total
-9999.00		320
	93.8	

1.00000	21
6.2	

Total	341
100.0	

***** SPLIT TABLE *****
 Leaf dem - [122,131) below edge - -9999.00.

Independent Var: dem
 Variable Type: Continuous
 Cluster Type: Monotonic
 Missing Values: OFF
 Nulls Included: ON
 Cluster signif: 0.050000

Cross Tabulation

	Row	
roads	dem	Total
-9999.00		1415
	97.3	
1.00000	40	
2.7		
Total	1455	
100.0		

***** SPLIT TABLE *****
 Leaf dem - [131,139] below edge - -9999.00.

Independent Var: dem
 Variable Type: Continuous
 Cluster Type: Monotonic
 Missing Values: OFF
 Nulls Included: ON
 Cluster signif: 0.050000

Cross Tabulation

	Row	
roads	dem	Total

-9999.00 98
100.0

1.00000 0
0.0

Total 98
100.0

***** SPLIT TABLE *****

edge split below photo82 - [29,33).

Independent Var: edge
Variable Type: Categorical
Cluster Type: Free
Missing Values: OFF
Nulls Included: ON
Cluster signif: 0.050000

Clusters:

- 1) 1.00000
- 2) -9999.00

Cross Tabulation +--- edge ----+

1 2 Row
roads 1.00000 -9999.00 edge Total

-9999.00 546 2892 3438
15.9 84.1 96.0
90.4 97.1

1.00000 58 87 145
40.0 60.0 4.0
9.6 2.9

=====

Total	604	2979	3583
	16.9	83.1	100.0

CHI: 57.75 (df = 1)
P: 0.000000

***** SPLIT TABLE *****

Leaf edge - 1.00000 below photo82 - [29,33).

Independent Var: edge
Variable Type: Categorical
Cluster Type: Free
Missing Values: OFF
Nulls Included: ON
Cluster signif: 0.050000

Cross Tabulation

roads	Row edge Total
-9999.00	546
90.4	

1.00000	58
9.6	

Total	604
100.0	

***** SPLIT TABLE *****
dem split below edge - -9999.00.

Independent Var: dem
Variable Type: Continuous
Cluster Type: Monotonic
Missing Values: OFF
Nulls Included: ON
Cluster signif: 0.050000

Clusters:
1) [1,115)
2) [115,119)
3) [119,125)
4) [125,139]

Cross Tabulation		+----- dem -----+				
roads		1	2	3	4	Row
		[1,115)	[115,119)	[119,125)	[125,139)	dem Total
-9999.00		771	307	646	1168	2892
		26.7	10.6	22.3	40.4	97.1
		98.8	91.9	94.4	98.9	
1.00000		9	27	38	13	87
		10.3	31.0	43.7	14.9	2.9
		1.2	8.1	5.6	1.1	
Total		780	334	684	1181	2979
		26.2	11.2	23.0	39.6	100.0

CHI: 70.54 (df = 3)
P: 0.000000

***** SPLIT TABLE *****
landuse split below dem - [1,115).

Independent Var: landuse
Variable Type: Categorical
Cluster Type: Free
Missing Values: OFF

Nulls Included: ON
Cluster signif: 0.050000

Clusters:
1) 7.00000, 1.00000, 11.0000
2) 8.00000, 9.00000

Cross Tabulation +--- landuse ---+

	1	2	Row
roads	7.00000	8.00000	landuse Total
-9999.00	28	743	771
	3.6	96.4	98.8
	90.3	99.2	
1.00000	3	6	9
	33.3	66.7	1.2
	9.7	0.8	
Total	31	749	780
	4.0	96.0	100.0

CHI: 20.56 (df = 1)
P: 0.000678

***** SPLIT TABLE *****
Leaf landuse - 7.00000... below dem - [1,115).

Independent Var: landuse
Variable Type: Categorical
Cluster Type: Free
Missing Values: OFF
Nulls Included: ON
Cluster signif: 0.050000

Cross Tabulation

	Row
roads	landuse Total
-9999.00	28
	90.3
1.00000	3
	9.7
Total	31
	100.0

***** SPLIT TABLE *****
Leaf landuse - 8.00000... below dem - [1,115).

Independent Var: landuse

Variable Type: Categorical
Cluster Type: Free
Missing Values: OFF
Nulls Included: ON
Cluster signif: 0.050000

Cross Tabulation

Row		
roads	landuse	Total
<hr/>		
-9999.00	743	
	99.2	

1.00000 6
0.8

Total 749
100.0

***** SPLIT TABLE *****
Leaf dem - [115,119) below edge - -9999.00.

Independent Var: dem
Variable Type: Continuous
Cluster Type: Monotonic
Missing Values: OFF
Nulls Included: ON
Cluster signif: 0.050000

Cross Tabulation

Row		
roads	dem	Total
<hr/>		
-9999.00	307	
	91.9	

1.00000 27
8.1

Total 334
100.0

***** SPLIT TABLE *****
Leaf dem - [119,125) below edge - -9999.00.

Independent Var: dem
Variable Type: Continuous
Cluster Type: Monotonic
Missing Values: OFF

Nulls Included: ON
Cluster signif: 0.050000

Cross Tabulation

	Row	
roads	dem	Total

-9999.00	646	
	94.4	
1.00000	38	
	5.6	
Total	684	
	100.0	

***** SPLIT TABLE *****
Leaf dem - [125,139] below edge - -9999.00.

Independent Var: dem
Variable Type: Continuous
Cluster Type: Monotonic
Missing Values: OFF
Nulls Included: ON
Cluster signif: 0.050000

Cross Tabulation

	Row	
roads	dem	Total

-9999.00	1168	
	98.9	
1.00000	13	
	1.1	
Total	1181	
	100.0	

***** SPLIT TABLE *****
edge split below photo82 - [33,38).

Independent Var: edge
Variable Type: Categorical
Cluster Type: Free
Missing Values: OFF
Nulls Included: ON
Cluster signif: 0.050000

Clusters:
1) 1.00000
2) -9999.00

Cross Tabulation +---- edge ----+

	1	2	Row	
roads	1.00000	-9999.00	edge	Total

-9999.00	829	1931	2760	
	30.0	70.0	92.4	
	89.1	93.9		

1.00000	101	125	226	
	44.7	55.3	7.6	
	10.9	6.1		
=====				
Total	930	2056	2986	
	31.1	68.9	100.0	

CHI: 20.92 (df = 1)
P: 0.000054

***** SPLIT TABLE *****
Leaf edge - 1.00000 below photo82 - [33,38).

Independent Var: edge
Variable Type: Categorical
Cluster Type: Free
Missing Values: OFF
Nulls Included: ON
Cluster signif: 0.050000

Cross Tabulation

	Row	
roads	edge	Total

-9999.00	829	
	89.1	

1.00000	101	
	10.9	

Total	930	
	100.0	

***** SPLIT TABLE *****
dem split below edge - -9999.00.

Independent Var: dem
Variable Type: Continuous
Cluster Type: Monotonic
Missing Values: OFF

Nulls Included: ON
Cluster signif: 0.050000

Clusters:
1) [1,128)
2) [128,139]

Cross Tabulation +---- dem ----+				
	1	2	Row	
roads	[1,128)	[128,139	dem	Total

-9999.00	1317	614	1931	
	68.2	31.8	93.9	
	92.3	97.6		

1.00000	110	15	125	
	88.0	12.0	6.1	
	7.7	2.4		
=====				
Total	1427	629	2056	
	69.4	30.6	100.0	

CHI: 21.67 (df = 1)
P: 0.001607

***** SPLIT TABLE *****
Leaf dem - [1,128) below edge - -9999.00.

Independent Var: dem
Variable Type: Continuous
Cluster Type: Monotonic
Missing Values: OFF
Nulls Included: ON
Cluster signif: 0.050000

Cross Tabulation		
	Row	
roads	dem	Total

-9999.00	1317	
	92.3	
1.00000	110	
	7.7	
Total	1427	
	100.0	

***** SPLIT TABLE *****
Leaf dem - [128,139] below edge - -9999.00.

Independent Var: dem

Variable Type: Continuous
Cluster Type: Monotonic
Missing Values: OFF
Nulls Included: ON
Cluster signif: 0.050000

Cross Tabulation

Row
roads dem Total

-9999.00 614
97.6

1.00000 15
2.4

Total 629
100.0

***** SPLIT TABLE *****
landuse split below photo82 - [38,51).

Independent Var: landuse
Variable Type: Categorical
Cluster Type: Free
Missing Values: OFF
Nulls Included: ON
Cluster signif: 0.050000

Clusters:

- 1) 8.00000, 7.00000
- 2) 9.00000, 11.0000, 1.00000

Cross Tabulation +--- landuse ---+

1 2 Row
roads 8.00000. 9.00000. landuse Total

-9999.00 2377 184 2561
92.8 7.2 86.5
85.6 100.0

1.00000 399 0 399
100.0 0.0 13.5
14.4 0.0

Total 2776 184 2960
93.8 6.2 100.0

CHI: 30.57 (df = 1)
P: 0.000037

***** SPLIT TABLE *****

edge split below landuse - 8.00000....

Independent Var: edge
Variable Type: Categorical
Cluster Type: Free
Missing Values: OFF
Nulls Included: ON
Cluster signif: 0.050000

Clusters:

- 1) 1.00000
- 2) -9999.00

Cross Tabulation +---- edge -----+

1 2 Row
roads 1.00000 -9999.00 edge Total

-9999.00 1224 1153 2377
51.5 48.5 85.6
82.5 89.2

1.00000 259 140 399
64.9 35.1 14.4
17.5 10.8

=====

Total	1483	1293	2776
	53.4	46.6	100.0

CHI: 24.72 (df = 1)
P: 0.000022

***** SPLIT TABLE *****

Leaf edge - 1.00000 below landuse - 8.00000....

Independent Var: edge
Variable Type: Categorical
Cluster Type: Free
Missing Values: OFF
Nulls Included: ON
Cluster signif: 0.050000

Cross Tabulation

Row
roads edge Total

-9999.00 1224
82.5

1.00000 259
17.5

Total 1483
100.0

***** SPLIT TABLE *****

dem split below edge - -9999.00.

Independent Var: dem
Variable Type: Continuous
Cluster Type: Monotonic
Missing Values: OFF
Nulls Included: ON
Cluster signif: 0.050000

Clusters:

- 1) [1,91)
- 2) [91,115)
- 3) [115,122)
- 4) [122,131)
- 5) [131,139]

Cross Tabulation		+----- dem -----+					
		1	2	3	4	5	Row
roads		[1,91)	[91,115)	[115,122	[122,131	[131,139	dem Total
-9999.00		114	128	289	480	142	1153
		9.9	11.1	25.1	41.6	12.3	89.2
		95.0	88.3	82.6	90.7	95.3	
1.00000		6	17	61	49	7	140
		4.3	12.1	43.6	35.0	5.0	10.8
		5.0	11.7	17.4	9.3	4.7	
Total		120	145	350	529	149	1293
		9.3	11.2	27.1	40.9	11.5	100.0

CHI: 27.28 (df = 4)
P: 0.000980

***** SPLIT TABLE *****

Leaf dem - [1,91) below edge - -9999.00.

Independent Var: dem
Variable Type: Continuous
Cluster Type: Monotonic
Missing Values: OFF
Nulls Included: ON
Cluster signif: 0.050000

Cross Tabulation	
	Row
roads	dem Total
-9999.00	114
	95.0

1.00000 6
5.0

Total 120
100.0

***** SPLIT TABLE *****

Leaf dem - [91,115) below edge - -9999.00.

Independent Var: dem
Variable Type: Continuous
Cluster Type: Monotonic
Missing Values: OFF
Nulls Included: ON
Cluster signif: 0.050000

Cross Tabulation
Row
roads dem Total

-9999.00 128
88.3

1.00000 17
11.7

Total 145
100.0

***** SPLIT TABLE *****

Leaf dem - [115,122) below edge - -9999.00.

Independent Var: dem
Variable Type: Continuous
Cluster Type: Monotonic
Missing Values: OFF
Nulls Included: ON
Cluster signif: 0.050000

Cross Tabulation
Row
roads dem Total

-9999.00 289
82.6

1.00000 61
17.4

Total 350
100.0

***** SPLIT TABLE *****

Leaf dem - [122,131) below edge - -9999.00.

Independent Var: dem
Variable Type: Continuous
Cluster Type: Monotonic
Missing Values: OFF
Nulls Included: ON
Cluster signif: 0.050000

Cross Tabulation

Row		
roads	dem	Total

-9999.00		480
		90.7

1.00000 49
9.3

Total 529
100.0

***** SPLIT TABLE *****

Leaf dem - [131,139] below edge - -9999.00.

Independent Var: dem
Variable Type: Continuous
Cluster Type: Monotonic
Missing Values: OFF
Nulls Included: ON
Cluster signif: 0.050000

Cross Tabulation

Row		
roads	dem	Total

-9999.00		142
		95.3

1.00000 7
4.7

Total 149
100.0

***** SPLIT TABLE *****

Leaf landuse - 9.00000... below photo82 - [38,51).

Independent Var: landuse
Variable Type: Categorical
Cluster Type: Free
Missing Values: OFF
Nulls Included: ON
Cluster signif: 0.050000

Cross Tabulation

Row
roads landuse Total

-9999.00 184
100.0

1.00000 0
0.0

Total 184
100.0

***** SPLIT TABLE *****

landuse split below photo82 - [51,102).

Independent Var: landuse
Variable Type: Categorical
Cluster Type: Free
Missing Values: OFF
Nulls Included: ON
Cluster signif: 0.050000

Clusters:

- 1) 8.00000
- 2) 1.00000
- 3) 7.00000
- 4) 11.0000
- 5) 9.00000

Cross Tabulation +----- landuse -----+

1 2 3 4 5 Row
roads 8.00000 1.00000 7.00000 11.0000 9.00000 landuse Total

-9999.00 1157 2 508 13 428 2108
54.9 0.1 24.1 0.6 20.3 71.2
64.1 66.7 72.0 81.2 99.5

1.00000 649 1 198 3 2 853
76.1 0.1 23.2 0.4 0.2 28.8

35.9 33.3 28.0 18.8 0.5

Total	1806	3	706	16	430	2961
	61.0	0.1	23.8	0.5	14.5	100.0

CHI: 214.19 (df = 4)

P: 0.000000

***** SPLIT TABLE *****

dem split below landuse - 8.00000.

Independent Var: dem

Variable Type: Continuous

Cluster Type: Monotonic

Missing Values: OFF

Nulls Included: ON

Cluster signif: 0.050000

Clusters:

- 1) [1,110)
- 2) [110,115)
- 3) [115,119)
- 4) [119,128)
- 5) [128,131)
- 6) [131,139]

Cross Tabulation +----- dem -----+

	1	2	3	4	5	6	Row
roads	[1,110)	[110,115	[115,119	[119,128	[128,131	[131,139	dem Total

-9999.00	75	165	178	424	266	49	1157
	6.5	14.3	15.4	36.6	23.0	4.2	64.1
	46.6	59.1	68.5	74.6	57.0	69.0	

1.00000	86	114	82	144	201	22	649
	13.3	17.6	12.6	22.2	31.0	3.4	35.9
	53.4	40.9	31.5	25.4	43.0	31.0	

Total	161	279	260	568	467	71	1806
	8.9	15.4	14.4	31.5	25.9	3.9	100.0

CHI: 65.12 (df = 5)

P: 0.000000

***** SPLIT TABLE *****

Leaf dem - [1,110) below landuse - 8.00000.

Independent Var: dem

Variable Type: Continuous

Cluster Type: Monotonic

Missing Values: OFF

Nulls Included: ON

Cluster signif: 0.050000

Cross Tabulation

roads	dem	Total
-9999.00	75	
	46.6	
1.00000	86	
	53.4	
Total	161	
	100.0	

***** SPLIT TABLE *****
edge split below dem - [110,115).

Independent Var: edge
Variable Type: Categorical
Cluster Type: Free
Missing Values: OFF
Nulls Included: ON
Cluster signif: 0.050000

Clusters:
1) 1.00000
2) -9999.00

Cross Tabulation		+---- edge ----+	
roads	1 2 Row	1.00000 -9999.00	edge Total
-9999.00	81 84 165		
	49.1 50.9 59.1		
	47.4 77.8		
1.00000	90 24 114		
	78.9 21.1 40.9		
	52.6 22.2		
Total	171 108 279		
	61.3 38.7 100.0		

CHI: 25.33 (df = 1)
P: 0.000019

***** SPLIT TABLE *****
Leaf edge - 1.00000 below dem - [110,115).

Independent Var: edge
Variable Type: Categorical
Cluster Type: Free
Missing Values: OFF
Nulls Included: ON
Cluster signif: 0.050000

Cross Tabulation

	Row	
roads	edge	Total

-9999.00	81
47.4	

1.00000	90
52.6	

Total	171
100.0	

***** SPLIT TABLE *****

Leaf edge - -9999.00 below dem - [110,115).

Independent Var: edge
Variable Type: Categorical
Cluster Type: Free
Missing Values: OFF
Nulls Included: ON
Cluster signif: 0.050000

Cross Tabulation

	Row	
roads	edge	Total

-9999.00	84
77.8	

1.00000	24
22.2	

Total	108
100.0	

***** SPLIT TABLE *****

Leaf dem - [115,119) below landuse - 8.00000.

Independent Var: dem
Variable Type: Continuous
Cluster Type: Monotonic
Missing Values: OFF
Nulls Included: ON
Cluster signif: 0.050000

Cross Tabulation

Row		
roads	dem	Total

-9999.00		178
	68.5	
1.00000		82
	31.5	
Total		260
	100.0	

***** SPLIT TABLE *****
 Leaf dem - [119,128) below landuse - 8.00000.

Independent Var: dem
 Variable Type: Continuous
 Cluster Type: Monotonic
 Missing Values: OFF
 Nulls Included: ON
 Cluster signif: 0.050000

Cross Tabulation

Row		
roads	dem	Total

-9999.00		424
	74.6	
1.00000		144
	25.4	
Total		568
	100.0	

***** SPLIT TABLE *****
 edge split below dem - [128,131).

Independent Var: edge
 Variable Type: Categorical
 Cluster Type: Free
 Missing Values: OFF
 Nulls Included: ON
 Cluster signif: 0.050000

- Clusters:
- 1) 1.00000
 - 2) -9999.00

Cross Tabulation +--- edge -----+
 1 2 Row
 roads 1.00000 -9999.00 edge Total

-9999.00	227	39	266
	85.3	14.7	57.0
	54.2	81.2	

1.00000	192	9	201
	95.5	4.5	43.0
	45.8	18.8	

Total	419	48	467
	89.7	10.3	100.0

CHI: 12.88 (df = 1)
 P: 0.000645

***** SPLIT TABLE *****
 Leaf edge - 1.00000 below dem - [128,131).

Independent Var: edge
 Variable Type: Categorical
 Cluster Type: Free
 Missing Values: OFF
 Nulls Included: ON
 Cluster signif: 0.050000

Cross Tabulation
 Row
 roads edge Total

-9999.00	227
	54.2

1.00000	192
	45.8

Total	419
	100.0

***** SPLIT TABLE *****
 Leaf edge - -9999.00 below dem - [128,131).

Independent Var: edge
 Variable Type: Categorical
 Cluster Type: Free
 Missing Values: OFF
 Nulls Included: ON
 Cluster signif: 0.050000

Cross Tabulation

roads	edge	Total
-9999.00	39	81.2

1.00000	9	18.8
---------	---	------

Total	48	100.0
-------	----	-------

***** SPLIT TABLE *****
edge split below dem - [131,139].

Independent Var: edge
Variable Type: Categorical
Cluster Type: Free
Missing Values: OFF
Nulls Included: ON
Cluster signif: 0.050000

Clusters:
1) 1.00000
2) -9999.00

Cross Tabulation +---- edge ----+				
roads	1.00000	-9999.00	edge	Total
-9999.00	18	31	49	
	36.7	63.3	69.0	
	51.4	86.1		
1.00000	17	5	22	
	77.3	22.7	31.0	
	48.6	13.9		
Total	35	36	71	
	49.3	50.7	100.0	

CHI: 9.98 (df = 1)
P: 0.002040

***** SPLIT TABLE *****
Leaf edge - 1.00000 below dem - [131,139].

Independent Var: edge
Variable Type: Categorical
Cluster Type: Free
Missing Values: OFF
Nulls Included: ON
Cluster signif: 0.050000

Cross Tabulation

Row
roads edge Total

-9999.00 18
51.4

1.00000 17
48.6

Total 35
100.0

***** SPLIT TABLE *****

Leaf edge - -9999.00 below dem - [131,139].

Independent Var: edge
Variable Type: Categorical
Cluster Type: Free
Missing Values: OFF
Nulls Included: ON
Cluster signif: 0.050000

Cross Tabulation

Row
roads edge Total

-9999.00 31
86.1

1.00000 5
13.9

Total 36
100.0

***** SPLIT TABLE *****

Leaf landuse - 1.00000 below photo82 - [51,102).

Independent Var: landuse
Variable Type: Categorical
Cluster Type: Free
Missing Values: OFF
Nulls Included: ON
Cluster signif: 0.050000

Cross Tabulation

roads	landuse	Total
-9999.00	2	66.7

1.00000	1	33.3
---------	---	------

Total	3	100.0
-------	---	-------

***** SPLIT TABLE *****
 Leaf landuse - 7.00000 below photo82 - [51,102).

Independent Var: landuse
 Variable Type: Categorical
 Cluster Type: Free
 Missing Values: OFF
 Nulls Included: ON
 Cluster signif: 0.050000

roads	landuse	Total
-9999.00	508	72.0

1.00000	198	28.0
---------	-----	------

Total	706	100.0
-------	-----	-------

***** SPLIT TABLE *****
 Leaf landuse - 11.0000 below photo82 - [51,102).

Independent Var: landuse
 Variable Type: Categorical
 Cluster Type: Free
 Missing Values: OFF
 Nulls Included: ON
 Cluster signif: 0.050000

roads	landuse	Total
-------	---------	-------

-9999.00 13
81.2

1.00000 3
18.8

Total 16
100.0

***** SPLIT TABLE *****

Leaf landuse - 9.00000 below photo82 - [51,102).

Independent Var: landuse
Variable Type: Categorical
Cluster Type: Free
Missing Values: OFF
Nulls Included: ON
Cluster signif: 0.050000

Cross Tabulation
Row
roads landuse Total

-9999.00 428
99.5

1.00000 2
0.5

Total 430
100.0

***** SPLIT TABLE *****

landuse split below photo82 - [102,157].

Independent Var: landuse
Variable Type: Categorical
Cluster Type: Free
Missing Values: OFF
Nulls Included: ON
Cluster signif: 0.050000

Clusters:
1) 1.00000, 11.0000
2) 8.00000
3) 7.00000
4) 9.00000

Cross Tabulation +----- landuse -----+

	1	2	3	4	Row
roads	1.00000	8.00000	7.00000	9.00000	landuse Total
-9999.00	0	86	120	133	339
	0.0	25.4	35.4	39.2	58.5
	0.0	32.7	65.9	100.0	
1.00000	1	177	62	0	240
	0.4	73.8	25.8	0.0	41.5
	100.0	67.3	34.1	0.0	
Total	1	263	182	133	579
	0.2	45.4	31.4	23.0	100.0

CHI: 172.07 (df = 3)

P: 0.000000

***** SPLIT TABLE *****

Leaf landuse - 1.00000... below photo82 - [102,157].

Independent Var: landuse

Variable Type: Categorical

Cluster Type: Free

Missing Values: OFF

Nulls Included: ON

Cluster signif: 0.050000

Cross Tabulation

	Row	
roads	landuse	Total
-9999.00	0	
	0.0	
1.00000	1	
	100.0	
Total	1	
	100.0	

***** SPLIT TABLE *****

dem split below landuse - 8.00000.

Independent Var: dem

Variable Type: Continuous

Cluster Type: Monotonic

Missing Values: OFF

Nulls Included: ON

Cluster signif: 0.050000

Clusters:

1) [1,115)

2) [115,125)

3) [125,139]

Cross Tabulation		+----- dem -----+			
		1	2	3	Row
roads		[1,115)	[115,125	[125,139	dem Total
-9999.00		21	63	2	86
		24.4	73.3	2.3	32.7
		28.8	43.2	4.5	
1.00000		52	83	42	177
		29.4	46.9	23.7	67.3
		71.2	56.8	95.5	
Total		73	146	44	263
		27.8	55.5	16.7	100.0

CHI: 23.61 (df = 2)

P: 0.002158

***** SPLIT TABLE *****

Leaf dem - [1,115) below landuse - 8.00000.

Independent Var: dem
Variable Type: Continuous
Cluster Type: Monotonic
Missing Values: OFF
Nulls Included: ON
Cluster signif: 0.050000

Cross Tabulation		Row	
		dem	Total
-9999.00		21	
		28.8	
1.00000		52	
		71.2	
Total		73	
		100.0	

***** SPLIT TABLE *****

Leaf dem - [115,125) below landuse - 8.00000.

Independent Var: dem
Variable Type: Continuous
Cluster Type: Monotonic
Missing Values: OFF
Nulls Included: ON
Cluster signif: 0.050000

Cross Tabulation

roads	Row dem	Total
-9999.00	63 43.2	
1.00000	83 56.8	
Total	146 100.0	

***** SPLIT TABLE *****

Leaf dem - [125,139] below landuse - 8.00000.

Independent Var: dem
Variable Type: Continuous
Cluster Type: Monotonic
Missing Values: OFF
Nulls Included: ON
Cluster signif: 0.050000

Cross Tabulation

roads	Row dem	Total
-9999.00	2 4.5	
1.00000	42 95.5	
Total	44 100.0	

***** SPLIT TABLE *****

dem split below landuse - 7.00000.

Independent Var: dem
Variable Type: Continuous
Cluster Type: Monotonic
Missing Values: OFF
Nulls Included: ON
Cluster signif: 0.050000

Clusters:

1) [1,128)

2) [128,139]

Cross Tabulation		+---- dem ----+		
	1	2	Row	
roads	[1,128)	[128,139	dem	Total

-9999.00	103	17	120	
	85.8	14.2	65.9	
	80.5	31.5		

1.00000	25	37	62	
	40.3	59.7	34.1	
	19.5	68.5		
=====				
Total	128	54	182	
	70.3	29.7	100.0	

CHI: 40.58 (df = 1)

P: 0.000027

***** SPLIT TABLE *****

Leaf dem - [1,128) below landuse - 7.00000.

Independent Var: dem
Variable Type: Continuous
Cluster Type: Monotonic
Missing Values: OFF
Nulls Included: ON
Cluster signif: 0.050000

Cross Tabulation		Row	
roads	dem	Total	

-9999.00	103		
	80.5		

1.00000	25		
	19.5		

Total	128		
	100.0		

***** SPLIT TABLE *****

Leaf dem - [128,139] below landuse - 7.00000.

Independent Var: dem
Variable Type: Continuous
Cluster Type: Monotonic
Missing Values: OFF
Nulls Included: ON
Cluster signif: 0.050000

Cross Tabulation

roads	Row dem	Total
-9999.00	17 31.5	
1.00000	37 68.5	
Total	54 100.0	

***** SPLIT TABLE *****

Leaf landuse - 9.00000 below photo82 - [102,157].

Independent Var: landuse
Variable Type: Categorical
Cluster Type: Free
Missing Values: OFF
Nulls Included: ON
Cluster signif: 0.050000

Cross Tabulation

roads	Row landuse	Total
-9999.00	133 100.0	
1.00000	0 0.0	
Total	133 100.0	

%*****

APPENDIX G

Appendix G: Generated Classification Decision Tree

Figure 1 Shows a generated classification decision tree using clustering method.